FUNCTION AND REGULATION OF FISH CYP3 GENES

CHARACTERIZING THE FUNCTION AND REGULATION OF ORPHAN CYP3 GENES IN ZEBRAFISH (DANIO RERIO)

By LANA SHAYA, H.B.Sc., M.Sc.

A Thesis Submitted to the School of Graduate Studies in Partial Fulfillment of the

Requirements for the Degree Doctor of Philosophy

McMaster University DOCTOR OF PHILOSOPHY (2019) Hamilton, Ontario (Biology)

TITLE: Characterizing the Function and Regulation of Orphan CYP3C Genes in Zebrafish (*Danio rerio)* AUTHOR: Lana Shaya, Hon B.Sc. (University of Toronto Mississauga); M.Sc. (McMaster University) SUPERVISOR: Dr. Joanna Y. Wilson NUMBER OF PAGES: xxi, 235

LAY ABSTRACT

Cytochrome P450 (CYP) enzymes break down compounds such as hormones and pharmaceuticals. While mammals have genes in the CYP3A subfamily, fish have unique subfamilies not found in mammals. The function and regulation of the CYP3 family in fish is unknown, but commonly assumed to be like human CYP3. The purpose of this thesis was to identify what receptors and compounds regulate CYP3C enzymes in zebrafish. We found that regulation of CYP3C enzymes in zebrafish is different than humans. Zebrafish CYP3C genes are regulated by the aryl hydrocarbon receptor and estrogen receptor, while human CYP3A is regulated by the pregnane-x-receptor. I used a high throughput approach to screen thousands of compounds to identify the function of CYP3A65 and CYP3C1 from zebrafish. CYP3A65 and CYP3C1 metabolize several plant-based and pharmaceutical compounds. CYP3A65 and CYP3C1 are more functionally similar to each other than to CYP3A in humans.

ABSTRACT

Genome sequencing has resulted in the identification of >55,000 cytochrome P450 enzymes, many of which have an unknown function and regulation. In mammals, CYP3 genes appear in only one subfamily (CYP3A), which metabolize >50% of pharmaceuticals and some steroids in humans. Unlike mammals, fish contain genes in the CYP3A, CYP3B, CYP3C and CYP3D subfamilies. While it is commonly assumed that fish and mammalian CYP3A are functional similar, the function and regulation of fish CYP3 remains largely unknown. In this thesis, the receptors and compounds that regulate CYP3C genes in zebrafish were assessed. The induction of CYP3C genes in response to the aryl hydrocarbon (AHR) and estrogen receptor (ER) ligands, β-naphthoflavone and 17β-estradiol, was measured using quantitative PCR in intestine, liver and gonads. Zebrafish CYP3C genes were inducible by β-naphthoflavone and 17β-estradiol, implicating the aryl hydrocarbon and estrogen receptor in CYP3C gene regulation and suggesting that regulation of CYP3 genes in fish differs from that in mammals. To define the function of zebrafish CYP3A65 and CYP3C1, fluorogenic compounds which are specific markers of CYP1 and CYP3A activity in humans, were screened for metabolism by CYP3A65 and CYP3C1. Both CYP3A65 and CYP3C1 had the capacity to metabolize several of these compounds and the substrate profile overlapped with zebrafish CYP1A, suggesting that these compounds are not specific in fish. A high throughput approach was employed to screen ~4000 small biologically and pharmacologically active compounds for metabolism by CYP3A65 and CYP3C1, using NADPH consumption to assess catalytic activity. The substrate profiles of CYP3A65 and CYP3C1 largely overlapped and were different than mammalian CYP3A4. CYP3A65 and CYP3C1 appeared to have a bias for quinone-based compounds but further studies are required to confirm quinones as substrates and to assess a strong structure-activity relationship. Overall, this study provides insight on the regulation, function and evolution on CYP3 genes in fish.

ACKNOWLEDGEMENT

During graduate school, I was blessed with great mentorship, supportive colleagues, friends and family, making my experience one I will never forget. I offer sincere thanks to the people who provided me with everything I needed to succeed!

Joanna is EVERYTHING a mentor should be. I started in her lab as a shy, know-nothing student who shutdown every time things were not easy. Thanks to her mentorship, I am a strong, confident scientist who can do anything. Joanna, your patience is unmatched! I will never forget the times you willingly made yourself available to listen to a practice presentation for a millionth time or address an unwarranted, panic-inducing science concern. Thank you for taking the time to get to know me as a scientist and a person, and to always selflessly push me towards the path that would get me to where I wanted to be. Thank you for being an amazing mentor and my strongest advocate. I could not have done this with any other supervisor. You will forever be my lab family.

At the front and center of my success are my amazing and loving parents, Aadl and Walaa Shaya Gulla. Mom and Dad, thank you for the financial and emotional support you always so willingly provided. There had been countless nights when I felt I could not continue but I took comfort in knowing that you believed in me when I did not believe in myself. No matter how tired you were, you always tried to learn about what I did (even when I was terrible at explaining), and continued to ask for updates throughout the years, and motivated me to work hard. Sometimes the stress of work would cause me to be a less than ideal daughter to ideal parents, and for that I apologize, but thank you for loving and supporting me regardless. I hope that this makes you proud, and that you feel I did justice to your sacrifices for and investments in me. I love you guys so much and I am so lucky to have you in my corner. I am invincible with you by my side.

Of course, I must acknowledge the support of my sister and 2 little brothers. They are here because I appreciate their patience during the times I yelled at them when I was PhDlife-level-stressed. To my sister, thank you for being just as PhDlife-level-stressed, so I always had someone at home who got it (and who sometimes was even more stressed and could yell louder than me, making me look like an angel to mom and dad ;)). To my baby brothers, thanks for taking advantage of my no-time-for-anything-PhDlife and washing my car for an exuberant monetary value; it was worth it! I enjoyed having a spotless looking car. Love you guys. Xo.

I would like to thank my fiancé, Michal Galus. The last few months have been the most challenging of my life and I know it made me a challenging person to love. Who decides to buy a house, get a job, write a Ph.D. and plan a wedding all at once? Crazy people, that's who! Michal, I could not imagine making it through all this craziness without you. Amidst our massive list of responsibilities, you let me prioritize my degree and career, and stepped up to handle everything that I could not. You encouraged me to go after what I wanted and put my needs above yours. The good news is, now that the thesis is done, there will not be anymore unprovoked anger towards you for having free time when I did not, but the bad news is I have free time now to bother you during yours.

A huge thanks to all the past and present members of the Wilson Lab who have provided their technical and emotional support to this project. A special thank you to Shumaila Fraz and Derek Alsop for always being so willing when I needed experimental advice and support. To James and Andrea, for keeping me sane and making the last couple of years of my Ph.D. some of the most enjoyable. Thank you especially for all the anxiety-attack-panic-calming compression hugs that were better than any coping mechanism ever described and for the late nights spent figuring out plasmid orientations or arguing about tip racking. Truly, I could not imagine a better duo to contemplate why on earth my gene construct would not do what it did two days ago.

Thank you to my committee members, Ben Evans and Bhagwati Gupta, for always being available to read my drafts and answer any questions. It has been a pleasure learning from you.

Thank you to the administrative staff at Biology whom have worked tirelessly to ensure the success of their students. To name a few that have made me life so much easier at Mac: Barb Reuter, Kathy Greaves and Karen Haines. The passion with which you do your job is one I can only aspire to have. Thank you for not making me feel like another number in the system.

These are only a few of the many people that had an impact on me during my graduate life, and there is not enough room here to name all the others whom I appreciate and will miss immensely. I am very sad that this chapter of my life has ended but I will forever remember my time at McMaster University and the wonderful people that shaped my experience.

TABLE OF CONTENTS

LAY ABSTRACT iii
ABSTRACT iv
ACKNOWLEDGEMENT vi
TABLE OF CONTENTS viii
LIST OF TABLES xii
LIST OF FIGURES xiv
LIST OF ABBREVIATIONS AND SYMBOLS xvi
DECLARATION OF ACADEMIC ACHIEVEMENT xx

CHAPTER 1
GENERAL INTRODUCTION

CYTOCHROME P450 SUPERFAMILY 1
NOMENCLATURE OF CYTOCHROME P450 GENES 5
EVOLUTION OF CYTOCHROME P450 FAMILY 3 7
CYTOCHROME P450 FAMILY 3 EXPRESSION 8
CYTOCHROME P450 FAMILY 3 REGULATION 10
CYTOCHROME P450 FAMILY 3 FUNCTION 14
CYTOCHROME P450 HETEROLOGOUS EXPRESSION SYSTEMS 16
ZEBRAFISH AS A MODEL ORGANISM FOR CYP3 RESEARCH 18
THESIS GOALS 20
CHAPTER SUMMARY 21
REFERENCES 24

CHAPTER 2
CYP3C GENE REGULATION BY THE ARYL HYDROCARBON AND ESTROGEN RECEPTORS IN ZEBRAFISH

ABSTRACT 33
INTRODUCTION 35
MATERIALS AND METHODS 38

Animals 38
Chemicals 38
Exposure 39
Dose-Response of CYP3C Induction by Exposure to βNF and E_2 39
Time-course for induction of CYP3Cs 40
Tissue Collection and RNA Extractions 40
Quantitative PCR 41
Data and Statistical Analysis 42
RESULTS 43
Effects of Increasing Concentrations of β-naphthoflavone on CYP3C and CYP1A Expression 43
Time-Course of mRNA Induction by Exposure to β-naphthoflavone 44
Effects of Increasing Concentrations of 17β-estradiol on Male CYP3C and VTG Expression 45
Effects of Increasing Concentrations of 17β-estradiol on Female CYP3C and VTG Expression 46
Time-Course of mRNA Induction by Exposure to a Single Dose of 17β-estradiol 47
DISCUSSION 47
The Role of the AhR in Regulation of CYP3Cs 48
The Role of ER in CYP3C Regulation 50
Functional Implications from the Involvement of the AhR and ER in Regulation 52
ACKNOWLEDGEMENTS 54
TABLES 55
FIGURES 60
REFERENCES 76

CHAPTER 3
HIGH THROUGHPUT SCREENING OF SMALL BIOACTIVE COMPOUNDS FOR SUBSTRATES OF ZEBRAFISH (*DANIO RERIO*) CYP3C1

ABSTRACT 81
INTRODUCTION 83

MATERIALS AND METHODS 86
CYP3C1 Heterologous Expression 86
Total P450 Analysis and Cytochrome P450 Reductase Activity 88
High Throughput Screening Assay Design: NADPH Depletion 89
Reactive Oxygen Species (ROS) 2’7’ Dichlorofluorescin Probe Assay 92
Determining K_M and IC_{50} in the top hits 93
RESULTS 94
Expression of CYP3C1 Protein and Catalytic Activity 94
High Throughput Screening for NADPH Depletion with and Without Enzyme 95
Reactive Oxygen Species (ROS) 2’7’Dichlorofluorescin Probe Assay, K_m and IC_{50} ... 96
DISCUSSION 98
Functional Testing with Fluorogenic Probe Substrates 99
High Throughput Screening for CYP3C1 Catalytic Activity 101
Metabolism of Natural Plant Products 101
Metabolism of Pharmacologically Active Compounds 102
Metabolism of Structurally Diverse Compounds 103
Metabolism of Structurally Diverse Quinone Based Substrates 103
Developing a Profile of CYP3C1 Substrates 106
ACKNOWLEDGEMENT 108
TABLES 109
FIGURES 131
REFERENCES 138

CHAPTER 4
HIGH THROUGHPUT SCREENING OF SMALL BIOACTIVE COMPOUNDS FOR SUBSTRATES OF ZEBRAFISH (*DANIO RERIO*) CYP3A65

ABSTRACT 145
INTRODUCTION 147
MATERIALS AND METHODS 151
Total P450 Analysis and Cytochrome P450 Reductase Activity 152
Fluorescent Catalytic Assays 152

High Throughput Screening Assay Design: NADPH Depletion 153
Reacting Oxygen Species (ROS) 2'7' Dichlorofluorescin Probe Assay 156
Determining K_M and IC_{50} in the top hits 157
RESULTS 158
High Throughput Screening for NADPH Depletion With and Without Enzyme........ 159
Reactive Oxygen Species (ROS) 2'7'Dichlorofluorescin Probe Assay, K_m and IC_{50} . 160
DISCUSSION 162
Zebrafish CYP3A65 and Mammalian CYP3A4 Substrate Profiles............................ 163
Overlap between CYP3A65 and CYP3C1 Substrate Profiles 167
Developing a Profile of CYP3A65 Substrates 169
ACKNOWLEDGEMENT 171
TABLES 172
FIGURES 191
REFERENCES 198

CHAPTER 5
GENERAL DISCUSSION

ORPHAN CYTOCHROME P450 GENES 204
REGULATORY CONTROL OF CYP3C ENZYMES IN ZEBRAFISH 210
CHARACTERIZING THE FUNCTION OF CYP3C1 AND CYP3A65 216
EVOLUTION OF CYTOCHROME P450 FAMILY 3 223
REFERENCES 226

LIST OF TABLES

CHAPTER 2
CYP3C GENE REGULATION BY THE ARYL HYDROCARBON AND ESTROGEN RECEPTORS IN ZEBRAFISH

1. **TABLE 2.1** qPCR primers for CYP3C, housekeeping and positive control genes in zebrafish……………………………………………………………………….55

2. **SUPPLEMENTARY TABLE 2.1.** Fold Induction with standard error of the mean (SEM) of CYP3Cs, CYP1A in female zebrafish exposed to β-naphthoflavone (βNF) and CYP3Cs and Vitellogenin (VTG) in male and female zebrafish exposed to 17β-estradiol (E2)……………………………………….56

3. **SUPPLEMENTARY TABLE 2.2** Maximum fold induction (Mean ± standard error of the mean), maximum fold concentration (Max-fold concentrations, μM) and EC50 of CYP3C1-4, CYP1A and vitellogenin (VTG) gene expression in liver, intestine and gonads of zebrafish exposed to β-naphthoflavone (βNF) and 17β-estradiol (E_2)…………………………………………………………...58

CHAPTER 3
HIGH THROUGHPUT SCREENING OF SMALL BIOACTIVE COMPOUNDS FOR SUBSTRATES OF ZEBRAFISH (*DANIO RERIO*) CYP3C1

1. **TABLE 3.1** K_M and V_{max} of the metabolism of alkyloxy-resorufin substrates, BFC and DBF by heterologously expressed zebrafish CYP3C1…………………………………………………………………………109

2. **TABLE 3.2** NADPH depletion, reactive oxygen species (ROS) formation, and NADPH depletion in the absence of enzyme for the 132 top hit compounds of heterologously expression zebrafish CYP3C1…………………………………………………………………………111

3. **TABLE 3.3** K_M and IC_{50} of the top 48 hit substrates of CYP3C1. Compound name and structure are given. K_M was determined for rates of NADPH depletion and IC_{50} was based on the inhibition of BFC metabolism…………………………………………………………………...124

CHAPTER 4
HIGH THROUGHPUT SCREENING OF SMALL BIOACTIVE COMPOUNDS FOR SUBSTRATES OF ZEBRAFISH (*DANIO RERIO*) CYP3A65

1. **TABLE 4.1** K_M and V_{max} of the metabolism of alkyloxy-resorufin substrates, BFC and DBF by heterologously expressed zebrafish CYP3A65……………………………………………………………………….172

2. **TABLE 4.2** NADPH depletion, reactive oxygen species (ROS) formation, and NADPH depletion in the absence of enzyme for the 139 top hit compounds of heterologously expression zebrafish CYP3A65…………………………………………………………………….174

3. **TABLE 4.3** K_M and IC_{50} of the top 32 hit substrates of CYP3A65. Compound name and structure are given. K_M was determined for rates of NADPH depletion and IC_{50} was based on the inhibition of BFC metabolism…………………………………………………………………...187

LIST OF FIGURES

CHAPTER 2
CYP3C GENE REGULATION BY THE ARYL HYDROCARBON AND ESTROGEN RECEPTORS IN ZEBRAFISH

1. **FIGURE 2.1** The induction of CYP1A and CYP3C genes in female zebrafish intestine (A), liver (B) and gonads (C) following β-naphthoflavone (βNF) exposure. …………………………………………………………………60

2. **FIGURE 2.2** The time-course of CYP1A, CYP3C1 and CYP3C3 gene induction in female zebrafish liver (A) and intestine (B) by 1 μM β-naphthoflavone (βNF)……………………………………………………………………..64

3. **FIGURE 2.3** Induction of Vitellogenin (VTG) and CYP3C genes in male zebrafish liver (A) and induction of CYP3C genes in intestine (B) and gonads (C) following 17 β-estradiol (E_2) exposure………………………………………………………………….…66

4. **FIGURE 2.4** Induction of Vitellogenin (VTG) and CYP3C genes in female zebrafish liver (A) and induction of CYP3C genes in intestine (B) and gonads (C) following 17 β-estradiol (E_2) exposure……………………………………………………………………..70

5. **FIGURE 2.5** The time-course of Vitellogenin (VTG) and CYP3C gene induction in male zebrafish liver (A) and intestine (B) by 0.1 μM 17β-estradiol (E_2)……………………………………………………………………………..74

CHAPTER 3
HIGH THROUGHPUT SCREENING OF SMALL BIOACTIVE COMPOUNDS FOR SUBSTRATES OF ZEBRAFISH (*DANIO RERIO*) CYP3C1

1. **FIGURE 3.1** The effects of increasing concentrations of DMSO (%v/v) on the rates of CYP3C1 mediated **A)** NADPH depletion with 20 μM 7-methoxyresorufin (7-MR) and **B)** 7-hydroxy-4-(trifluoromethyl)coumarin (HFC) formation at 20 μM 7-benxyloxy-4-(trifluoromethyl) coumarin (BFC)……………………………………………………………………………131

2. **FIGURE 3.2** The maximum catalytic activity of CYP3C1 mediated metabolism for alkyloxy-resorufin substrates……………………………………………..132

3. **FIGURE 3.3** The maximum catalytic activity of CYP3C1 mediated metabolism of 7-benxyloxy-4-(trifluoromethyl) coumarin (BFC) and dibenzylfluorescein (DBF)…………………………………………………………………………133

4. **FIGURE 3.4** Michaelis-Menten curves of 7-methoyxresorufin (7-MR) and B) 7-benxyloxy-4-(trifluoromethyl)coumarin (BFC) metabolism……………………………………………………………….…134

5. **FIGURE 3.5** Rate of NADPH depletion for ~4000 compounds, reported as a percent of the positive control (CYP3C1 + 7-methoxyresorufin; 7-MR)……………………………………………………………………………..136

CHAPTER 4
HIGH THROUGHPUT SCREENING OF SMALL BIOACTIVE COMPOUNDS FOR SUBSTRATES OF ZEBRAFISH (*DANIO RERIO*) CYP3A65

1. **FIGURE 4.1** The effects of increasing concentrations of DMSO (%v/v) on the rates of CYP3A65 mediated **A)** NADPH depletion with 20 µM 7-methoxyresorufin (7-MR) and **B)** 7-hydroxy-4-(trifluoromethyl) coumarin (HFC) formation from 100 µM 7-benxyloxy-4-(trifluoromethyl)coumarin (BFC)………………………………………………………………………….191

2. **FIGURE 4.2 A)** Michaelis-Menten curves of 7-methoyxresorufin (7-MR) and **B)** 7-benxyloxy-4-(trifluoromethyl)coumarin (BFC) metabolism……………………………………………………………….…192

3. **FIGURE 4.3** The maximum catalytic activity of CYP3A65 mediated metabolism for alkyloxy-resorufin substrates……………………………………………..194

4. **FIGURE 4.4** The maximum catalytic activity of CYP3A65 mediated metabolism of 7-benxyloxy-4-(trifluoromethyl) coumarin (BFC) and dibenzylfluorescein (DBF)…………………………………………………………………………195

5. **FIGURE 4.5** Rate of NADPH depletion for ~4000 compounds, reported as a percent of the positive control (CYP3A65 + 7-methoxyresorufin; 7-MR)………………………………………………………………………..…196

LIST OF ABBREVIATIONS AND SYMBOLS

μM	Micromolar
μL	Microlitres
μg	Micrograms
μg mL^{-1}	Microgram per Litre
°C	Degrees Celsius
%v/v	Percent volume to volume ratio
7-BR	7-benzyloxyresorufin
7-ER	7-ethyoxyresorufin
7-MR	7-methyoxyresorufin
7-PR	7-pentoxyresorufin
AHR	Aryl hydrocarbon receptor
ALA	δ-aminolevulinic acid
AMMC	3-[2-(N,N-diethyl-Nmethylamino)ethyl]-7-methoxy-4-methylcoumarin
ANOVA	Analysis of variance
AR	Androgen receptor
ARE	Androgen response element
ARNT	Arylhydrocarbon nuclear translocator
AROD	Alkyloxy-resorufin-O-deethylase
BaP	Benzo[a]pyrene
BFC	7-benzyloxy-4-trifluoromethylcoumarin
BFCOD	7-benzyloxy-4-trifluoromethylcoumarin O-debenzylase
Bp	Base pairs
BQ	7-benxyloxyquinoline

CAR	Constitutive androstane receptor
CO	Carbon monoxide
CPR	Cytochrome P450 reductase
CYP	Cytochrome P450
CYP3	Cytochrome P450 family 3
CYP3A	Cytochrome p450 family 3 subfamily A
DBF	Dibenzylfluorescein
DCF	Dichlorofluorescin
DCFH-DA	2'7'-dichlorofluorescin diacetate
DEX	Dexamethasone
DMSO	Dimethylsulfoxide
E.coli	*Escherichia coli*
E_2	17β-estradiol
EC_{50}	Half maximum effective concentration
ER	Estrogen receptor
ERE	Estrogen response element
EROD	Ethoxyresorufin-O-deethylase
EtOH	Ethanol
GC/MS	Gas chromatography mass spectrometry
GR	Glucocorticoid receptor
h	Hours
HCl	Hydrochloric acid
HFC	7-hydroxy-4-trifluoromethylcoumarin
hpf	Hours post fertilization
HTS	High throughput screen

IC_{50}	Half maximal inhibitory concentration
K_M	Menton constant
KPO_4	Potassium phosphate
LB	Luria-Bertani
LC/MS	Liquid chromatography mass spectrometry
LOD	Lowest limit of detection
M	Molar
mM	Millimolar
MAMC	7-methoxy-4-(aminomethyl)-coumarin
MFC	7-methyoxy-trifluoromethylcoumarin
MO	Morpholinos
NaCl	Sodium Chloride
NADPH	Nicotinamide adenine dinucleotide phosphate hydrogen
nm	Nanometres
nmol	nanomoles
OmpA	Outer membrane protein A gene
PAHs	Poly cyclic aromatic hydrocarbons
PCBs	Polychlorinated biphenyls
PCN	Pregnenolone-16a-carbonitrile
pmol	Picomoles
PN	Pregnenolone
PPAR	Peroxisome proliferator-activated receptor
PXR	Pregnane-x-receptor
RH	Substrate
RIF	Rifampicin

ROH	Hydrozylated substrate
ROS	Reactive oxygen species
RXR	Retinoid-x-receptor
SEM	Standard error of the mean
TB	Terrific Broth
TCDD	2,3,7,8 tetrachlorodibenzo-*p*-dioxin
Temp	Temperature
VDR	Vitamin D receptor
V_{max}	Maximum velocity
VTG	Vitellogenin
XRE	Xenobiotic response element
Z’	Z-prime
βNF	β-naphthoflavone

DECLARATION OF ACADEMIC ACHIEVEMENT

This thesis is organized in a sandwich format as recommended by the supervisory committee and approved by McMaster University and contains 5 chapters. Chapter 1 is an introduction to cytochrome P450 literature, with a special focus on cytochrome P450 family 3. Chapter 2 to 4 are manuscripts that are either published (Chapter 2) or ready to submit in peer reviewed journals (Chapter 3 and 4). Chapter 5 is a general discussion of the major findings, the contribution of this thesis to the overall field of orphan cytochrome P450s and outlines some future research.

CHAPTER 1 **GENERAL INTRODUCTION**

CHAPTER 2 **CYP3C GENE REGULATION BY THE ARYL HYDROCARBON AND ESTROGEN RECEPTORS IN ZEBRAFISH**

Authors: Lana Shaya, Devon E. Jones and Joanna Y. Wilson

Date Accepted: October 24, 2018

Journal: *Toxicology and Applied Pharmacology*

Comments: L.S. conducted most of the study and wrote the manuscript under the supervision of J.Y.W. The experiments relating to the time course of CYP3C induction by 17β-estradiol were performed by D.E.J. under L.S. and J.Y.W.'s supervision.

CHAPTER 3 **HIGH THROUGHPUT SCREENING OF SMALL BIOACTIVE COMPOUNDS FOR SUBSTRATES OF ZEBRAFISH (*DANIO RERIO*) CYP3C1**

Authors: Lana Shaya, Taylor Wiseman and Joanna Y. Wilson

Status: To be submitted

Journal: *TBA*

Comments: L.S. conducted most of the study and wrote the manuscript under the supervision of J.Y.W. Work relating to K_M and V_{max} of fluorogenic substrates, and general support was provided by T.W.

CHAPTER 4 **HIGH THROUGHPUT SCREENING OF SMALL BIOACTIVE COMPOUNDS FOR SUBSTRATES OF ZEBRAFISH (*DANIO RERIO*) CYP3A65**

Authors: Lana Shaya, Taylor Wiseman and Joanna Y. Wilson

Status: To be submitted

Journal: *TBA*

Comments: L.S. conducted most of the study and wrote the manuscript under the supervision of J.Y.W. Work relating to K_M and V_{max} of fluorogenic substrates, and general support during screening was provided by T.W.

CHAPTER 5 **GENERAL DISCUSSION**

CHAPTER 1

GENERAL INTRODUCTION

CYTOCHROME P450 SUPERFAMILY

Cytochrome P450 (CYP) enzymes are a large group of membrane bound, heme proteins found in bacteria, archaea and eukaryotes. CYP enzymes are responsible for the metabolism of steroids, fatty acids, prostaglandins, bile acids and play a critical role in biosynthesis of signaling molecules such as hormones (as reviewed by Denisov et al 2005). Most notably, CYPs are critical members of the defensome, a suite of genes that encode for nuclear receptors, transporters, and enzymes critical in the defence of an animal from various toxicants (Goldstone et al 2006). CYPs mediate the biotransformation of compounds to more polar compounds; for xenobiotics these are typically more soluble metabolites that can be readily excreted (as reviewed by Denisov et al 2005). In some cases, CYPs metabolically activate chemical procarcinogens, pharmaceuticals and other foreign and endogenous compounds (as reviewed by Guengerich & Shimada 1998).

Cytochrome P450 enzymes were initially identified as carbon monoxide binding pigments in pig liver microsomes (Klingenberg 1958, Garfinkle 1958) and later identified to be hemeoproteins that were a b-type cytochrome (Omura & Sato 1962). Later studies established that the proteins could incorporate an O_2 into organic substrates (Estabrook et al 1963) and were established as monooxygenase enzymes with a heme-iron active site (Omura & Sato 1964a, 1964b). A substrate (RH) binds to the active site containing the ferric state (Fe_3+) iron, which is reduced to the ferrous (Fe_2^+) state (Sligar 1976). This reduction from the ferric to ferrous state of the iron results in a conformational change and promotes an electron donation from the reduction of the cofactor nicotinamide adenine dinucleotide phosphate hydrogen (NADPH) to $NADP^+$. In vertebrates and some bacteria, the reduction of NADPH is catalyzed by a flavoprotein cytochrome P450 reductase (CPR; Masters et al 1971). This electron donation results in the recruitment of an oxygen molecule to bind to the substrate bound complex (Fe^{2+}-O_2(RH); as reviewed by Denisov et al 2005). This complex is reduced following the recruitment of a second electron, through the reduction of NADPH by either CPR or cytochrome b5 (Hildebrant & Estabrook, 1971), and two protons from the surrounding environment. As a result, the oxygen bond is broken, and a new complex is formed ($(Fe\text{-}O)^{3+}$) with the RH, known as the P450 compound 1 complex (Loew et al 2000). This process results in the production of one molecule of water (Raag & Poulos 1989; Haines et al 2001). Finally, the oxygen on the P450 compound 1 complex is transferred to the substrate, resulting in a hydroxylated product (ROH; Loew et al 2000). The product is released, and the enzyme returns to its resting state. In some cases, the substrate binds to the active site, triggering the catalytic cycle but only to result in the consumption of NADPH, yielding reactive oxygen species (ROS; Kahl et al 1989, Persson et al 1990, Scholz et al 1990) but limited metabolism. The consumption of NADPH without product formation is termed an uncoupled reaction. There are multiple points in the catalytic cycle where uncoupled reactions may occur. Firstly, superoxide anions may be produced when the first unstable complex (Fe^{2+}-O_2) is broken down (As reviewed by Denisov et al 2005). Secondly, peroxides occur through the protonation of the cytochrome complex 1. Finally, NADPH may be consumed and the catalytic cycle proceeds until the formation of the $(Fe\text{-}O)^{3+}RH$ complex which is then reduced to water instead of a hydroxylated product. The abundance of reactive oxygen species is an indication of a high level of uncoupled reactions.

There are multiple approaches and methods of measuring CYP activity, some which may be specific for each CYP and its unique substrate(s). Measuring rate of substrate loss or product formation is an effective way to confirm metabolism by different CYP isoform, however this requires specific analytical approaches (e.g. gas chromatography mass spectrometry, liquid chromatography mass spectrometry) that differ for each analyte. The data from these approaches provides very specific information how well an individual substrate is metabolized and, in the case of product detection, defines the exact metabolites formed. Utilizing these approaches for screening several substrates is problematic and expensive as the assay must be designed and optimized for each unique CYP and substrate or product being detected.

In the case of the major human xenobiotic metabolizing CYP enzymes, a fluorogenic catalytic assay is commonly used to directly measure CYP activity (Crespi et al 1997). In this approach, synthetic, fluorogenic probe substrates have been designed with a certain specificity to one or more CYP isoforms. Probe substrates are metabolized by CYP enzymes to produce an easily measured florescent product (Murray et al 2001, Stresser et al 2002). This assay is limited by what fluorogenic substrates are available and the specificity of an individual CYP enzyme for that probe. Most fluorogenic substrates are designed for mammalian CYP1A (7-ethyoxyresorufin), CYP2 (dibenzylfluorescein) and CYP3A (7-benzyloxy-4-trifluoromethylcoumarin) enzymes and little data is available on the specificity of fluorogenic substrates for non-mammalian CYP enzymes. More recently, commercially developed fluorogenic probes have been developed for a wider range of mammalian CYPs and luminogenic probes (Promega P450-Glo^{TM}; Cali et al 2006, Bosetti et al 2005, Auld et al 2013) have been developed for a similar purpose.

Measurement of NADPH depletion or NADP+ formation is an alternative and effective method of measuring CYP activity (Harskamp et al 2012) that is independent of the specific CYP and substrate combination. In this approach, microsomes, cells, or membrane fractions containing CYP enzymes may be incubated with any substrate and a known amount of NADPH, the concentration of which can be monitored over time using spectrophotometry (Gorsky et al 1984, Harskamp et al 2012). The versatility of this approach is its strength, yet, NADPH depletion is an indirect measure of CYP mediated metabolism. Though this method is excellent for measuring CYP metabolism of many substrates, there is a potential that NADPH depletion is not a result of product formation but instead a result of uncoupled reactions. Thus, monitoring NADPH or NADP+ in CYP mediated reactions requires careful follow up to determine whether reactive oxygen species, metabolites, or a combination has been produced.

NOMENCLATURE OF CYTOCHROME P450 GENES

With each genome sequenced, many cytochrome P450 genes are discovered. To date there are approximately 55 000 named cytochrome P450 genes (Nelson & Nebert 2018) but only a small fraction of these are extensively studied. A nomenclature system was described to differentiate CYPs and allow for adequate communication within and between research fields. Cytochrome P450s were first named due to their placement in cytoplasmic membrane (cyto) and their unique ability to produce a soret peak at 450nm (chrome) when the reduced form of the enzyme is complexed with carbon monoxide; for gene nomenclature cytochrome P450 is abbreviated to CYP. The remainder of the naming convention is based on the amino acid sequence similarity (Nelson 2006). Genes that are more than 40% identical in amino acid sequence are placed in the same family and denoted by an Arabic numeral. Genes that are 55% or more similar in their amino acid sequence are placed in the same subfamily and denoted by a capital letter. Finally, each gene within a subfamily is given a unique number in order of discovery.

The standard nomenclature rules typically allow for the inference of evolutionary information about each unique family and subfamily, as genes within the same subfamily are expected to be derived from a common ancestor and all subfamilies should cluster together to form a family clade (Nelson 1999). In most cases, phylogenetic studies support the nomenclature system with at least one important exception (Goldstone et al 2010, Yan & Cai 2010). In the CYP3 family, fish CYP3 genes were assigned to the

CYP3A subfamily based on sequence similarity to mammalian sequences and available phylogenies. Yet, CYP3A65 in zebrafish was only 54% identical to the mammalian CYP3A (Goldstone et al 2010), suggesting that the inclusion of this gene in the CYP3A family was near the cut off for standard nomenclature rules. As new genomic data became available, it has become clear that the fish CYP3A genes likely co-orthologs of mammalian CYP3A genes and are incorrectly named (Goldstone et al 2010, Yan & Cai 2010). This, and other cases of incorrect nomenclature assignment, demonstrate that cytochrome P450 nomenclature is dependent on the sampling size of the sequences used in sequence similarity comparisons and tree building methods. More sequence sampling in bioinformatic tree analyses allow for a better determination of evolutionary relationship and more accurate gene nomenclature.

With increasing numbers of identified genes from the different domains of life, large phylogenies have identified the evolutionary relationships across CYP subfamilies. CYP families that commonly and regularly cluster together across phylogenetic analyses have been placed into clans and are hypothesized to arise from a common ancestral gene; this portrays higher order evolutionary relationship between CYP families (Nelson 1999). Clans are typically named for the dominant gene family (e.g. Clan 2 contains CYP families 1, 2, 17, 18, 21 and others; the largest of which is CYP2 genes) or the gene family with the lowest number (e.g. Clan 3 contains CYP families 3, 5, 6, 9 and others).

EVOLUTION OF CYTOCHROME P450 FAMILY 3

Cytochrome P450 enzymes are ancient enzymes that may date back to 3.5 billion years ago (as reviewed by Danielson 2002, Nebert et al 1989, Nelson et al 1993,). Early function of cytochrome P450s likely involved the detoxification of oxygen, as it was introduced into the environment (Nebert & Feyereisen et al 1994). The most conserved, ancestral gene is hypothesized to be CYP51, which is involved in the synthesis of sterols (as reviewed by Lepesheva & Waterman 2007). To date 19 CYP families have been identified in vertebrates (Nelson et al 2013). CYP1-4 are the most diversified of the enzyme superfamily and well known for their involvement in chemical defense. Specifically, CYP3A genes in humans are pharmacologically important enzymes, particularly CYP3A4 which can metabolize over 50% of all pharmaceutical drugs (Zanger & Schwab 2013). The CYP3 family likely diverged approximately ~800 million years ago from a common vertebrate ancestor (McArthur et al 2003). Interestingly, mammals, birds, reptiles and amphibians have only a single subfamily (CYP3A) within the CYP3 family (McArthur et al 2003, Qiu et al 2008) while 4 additional subfamilies have been identified in the teleost lineage (CYP3A, CYP3B, CYP3C and CYP3D) (Corley-Smith et al 2006, Yan & Cai 2010). While all fish have 1 or more CYP3A genes, CYP3B, CYP3C and CYP3D have been identified in some (but not all) fish genomes and the distribution of each subfamily across different teleost lineages is not yet clear. 7 CYP3B genes have been identified: CYP3B1 and CYP3B2 were identified in the green spotted and the Japanese pufferfish (*T. nigroviridis; F. rubripes*, respectively*)*, CYP3B3-

CYP3B6 in medaka (*O. latipes*), and CYP3B7 in stickleback (*G. aculeatus*; Yan & Cai 2010). There were 5 CYP3C genes identified: CYP3C1, CYP3C2, CYP3C3 and CYP3C4 were found in tandem on the zebrafish chromosome 3 (*D. rerio*; Goldstone et al 2010). CYP3C1-CYP3C4 have a shared synteny with mammalian CYP3A (Goldstone et al 2010). CYP3C5 was identified in channel catfish (*I. punctatus*; (Zhang et al 2014). CYP3D genes appear in sablefish (*A. fimbri*), gilt-head sea bream (*S. aurata*), Atlantic Halibut (*H. hippoglossus*), stickleback, largemouth bass *(M. salmoides),* green spotted and Japanese pufferfish (Yan & Cai 2010).

CYP3A genes from mammals, birds and reptiles cluster together (Qiu et al 2008) in phylogenetic analyses, while CYP3A in fish clusters more closely with fish CYP3B, CYP3C and CYP3D genes (Yan & Cai 2010). Within the teleost CYP3 clade, CYP3A and CYP3D have undergone a tandem duplication event and diverged from a common ancestor while CYP3B and CYP3C split from CYP3A due to chromosome duplication (Goldstone et al 2010). The split of CYP3B/C cluster from CYP3A/D cluster is estimated to have occurred ~370 million years ago, corresponding to the teleost-specific whole genome duplication event (Yan & Cai 2010). The gene duplication events that led to the diversification of the CYP3 subfamilies is suggestive of new functions acquired to accommodate the changing environment (McArthur et al 2003).

CYTOCHROME P450 FAMILY 3 EXPRESSION

In general, CYP enzymes are ubiquitously expressed in all animals and likely have a site-specific function. Mammalian CYP3A genes are predominately expressed in organs that are important for the absorption, distribution, metabolism and excretion of compounds. Generally, the highest expression of CYP3A is in the liver, intestine and kidney (as reviewed by Zanger & Schwab 2013). Mammalian CYP3A genes are highly expressed in extrahepatic tissues such as gonads and brain (as reviewed by Zanger & Schwab 2013). Expression of CYP3A in these tissues is an indication for a role in the biosynthesis and/or breakdown of hormones and other signaling molecules (Meyer et al 2007). Indeed, mammalian CYP3As are known to metabolize steroid hormones (as reviewed by Tsuchiya et al 2005).

Fish CYP3A was first identified in rainbow trout, scup and Atlantic Cod and like mammalian CYP3A, high expression was observed in the liver, kidney and intestine (as reviewed by Schlenk et al 2008). Since then, several other fish CYP3As have been identified and all appear to be highly expressed in detoxification organs (Celander & Stegeman 1997, Christen et al 2010, Kullman & Hinton 2001, Lee & Buhler 2003, Tseng et al 2005). Expression of CYP3A in hepatic tissue was indicative of a potential role for CYP3A in biotransformation of xenobiotics in fish. However, some fish CYP3A genes are also expressed in extrahepatic tissues such as brain and gonads (Lee et al 1998, Celander and Stegeman 1997, Hegelund and Celander 2003).

There is little data for the expression of other CYP3 subfamilies in fish. Quantitative expression analysis of zebrafish CYP3C1-CYP3C4 and medaka CYP3B3-CYP3B6 indicated that these genes are widely expressed in developing and adult fish (Shaya et al 2014). There was significant expression of CYP3C and CYP3B genes in detoxification organs like the liver, intestine and kidney. There was notably high expression of several CYP3C and CYP3B genes in extrahepatic organs such as the brain, gonad and heart. High expression of CYP3C and CYP3B was found in sensory organs such as the eye and olfactory rosette. Additionally, CYP3C and CYP3B were differentially expressed between male and female fish which suggests that CYP3C and CYP3B genes may serve sex specific functions in these animals or be regulated in a sex specific manner. Currently no data exists for the tissue distribution of CYP3D genes in any fish species.

CYTOCHROME P450 FAMILY 3 REGULATION

In mammals, the regulation of CYPs is mediated by various receptors in the nuclear receptor and the basic-helix-loop-helix per ARNT sim (bHLH PAS) protein families. For CYP1-4 family genes, the most common receptors involved in gene regulation are the aryl hydrocarbon receptor (AHR), constitutive androstane receptor (CAR), peroxisome proliferator-activated receptor (PPAR), pregnane-x-receptor (PXR) and vitamin D receptor (VDR; as reviewed by Waxman 1999). Once a ligand binds a certain receptor, the receptor recruits a heterodimerization partner. Generally, the heterodimerization partners are the aryl hydrocarbon nuclear translocator (ARNT; for AHR) and the retinoid-x-receptor (RXR; for PXR, PPAR, CAR and VDR). Following heterodimerization, the receptor/heterodimer complex, along with other co-factors, binds a response element in the promoter region of responsive genes and activates transcription (Goodwin et al 1999). The regulation of mammalian CYP3A is predominately mediated by the PXR and CAR nuclear receptors (Goodwin et al 1999). Mammalian CYP3A is inducible by ligands of the PXR and CAR such as rifampicin (RIF), dexamethasone (DEX), pregnenolone-16α-carbonitrile (PCN), phenobarbital, and ortho-PCBs (as reviewed by Hahn et al 2005, Kliewer et al 2002). In mammals, the PXR is also activated by bile acids and steroids to induce CYP3A genes (Goodwin et al., 2002).

The regulation of fish CYP3A genes is not well characterized. To date, CAR homologs have not been identified in fish genomes and current opinion is that fish lack CAR. Though a PXR homolog has been cloned from zebrafish (Bainy et al 2013), the response element required for PXR gene activation in CYP3 genes is not well conserved across vertebrates (Wassmur et al 2010). In mammals, the response element is characterized by a unique left and right half sites separated by 6 nucleotides (Kliewer et al 2002); in fish, the left half site is not found in most fish species while the right, more conserved half site, is only found in some fish species (Wassmur et al 2010). Additionally, the response to PXR ligands in fish is species dependent and the level of induction of CYP genes by PXR ligands is not as large as that seen in mammals exposed to the same ligands (Corcoran et al 2012, Tseng et al 2005, Wassmur et al 2013). While some known mammalian PXR ligands successfully activated zebrafish PXR, RIF, PCN, and DEX surprisingly did not (Moore et al 2002). Further research is required to determine the PXR response element in fish, appropriate PXR ligands in fish, and the involvement of the PXR in regulating members of the CYP3 family in fish.

The AHR is a member of the bHLH PAS transcription factor family. Ligands of the AHR are mostly xenobiotics that are planar and polycyclic such as poly cyclic aromatic hydrocarbons (PAHs), polychlorinated biphenyls (PCBs) and dioxins (as reviewed by Hahn et al 2005). Following ligand binding, the AHR heterodimerizes with the aryl hydrocarbon nuclear translocator (For reviews see: Gu et al 2000, Hahn 2001). The heterodimer then binds to the xenobiotic response element (XREs) in the promoter site of the target gene and induces transcription. The piscine AHR is highly diversified in fish lineages and include three AHR clades: AHR1, AHR2 and AHR3 (Hahn et al 2005). Zebrafish have 3 AHRs; AHR1a, AHR1b and AHR2 (Andreasen et al 2002a, Karchner et al 2005, Tanguay et al 1999). AHR2 is widely expressed and highly inducible by 2,3,7,8 tetrachlorodibenzo-*p*-dioxin (TCDD) and other AHR ligands and is the main receptor involved in CYP1A induction (Andreasen et al 2002b, Prasch et al 2003, Van Tiem & Di Giulio 2011).

Fish CYP3A genes generally have multiple XREs in the promoter region which may indicate the involvement of AHR in CYP3 regulation (Kubota et al, 2015 Shaya et al 2014). Larval zebrafish CYP3A65 was inducible by TCDD (Chang et al 2013, Tseng et al 2005) and PCB126 (Kubuto et al 2015). Suppression of AHR2 translation and a morpholino knockdown of the receptor significantly reduced the expression of CYP3A65 in larval zebrafish (Tseng et al 2005). These studies suggest that AHR is involved in the regulation of zebrafish CYP3A65 and that AHR2 is specifically involved in regulation of CYP3A65 in larval tissues. There is some evidence to suggest that CYP3A65 in zebrafish is also regulated by PXR. Zebrafish larval CYP3A65 was inducible by the prototypical PXR ligands, pregnenolone (PN; Kubota et al 2015), RIF and DEX (Tseng et al 2005). Morpholino knockdown of the PXR receptor resulted in decreased expression of CYP3A65 (Kubota et al 2015). This data suggests that PXR may also be involved in regulating CYP3A in fish.

Overall, there is little data on regulation of CYP3C, CYP3B and CYP3D genes in fish. *In silico* analysis of the 10kb region upstream of CYP3C and CYP3B promoter site identified several XREs in the promoter region (Kubuto et al 2015, Shaya et al 2014). CYP3C1 was inducible by PCB126 in larval zebrafish suggesting a role for AHR in CYP3C1 regulation (Kubuto et al 2015). However, larval CYP3C1 was not inducible by TCDD (Corely-Smith et al 2006) which suggest that AHR regulation may be ligand specific. Additionally, CYP3C1 was inducible by PN (Kubota et al 2015) but not DEX or RIF (Corley-Smith et al 2006). PN mediated induction of CYP3C1 was abolished following morpholino knockdown of the PXR (Kubota et al 2015). This may suggest a role for PXR in regulating CYP3C1 but better characterized PXR ligands for fish species will aid in understanding the involvement of the PXR in fish CYP3 family regulation. To date, there are no data on the involvement of the AHR or PXR in CYP3B or CYP3D regulation.

The identification of several estrogen response elements and androgen response elements in the promoter region of CYP3C and CYP3B suggest a role for estrogen (ER) and androgen receptors (AR) in the regulation of fish CYP3 family (Shaya et al 2014).

The involvement of the ER and AR would not be surprising as differential expression of CYP3C and CYP3B genes in zebrafish males and females suggests that steroids impact the level of expression (Shaya et al 2014). There is also some evidence to suggest CYP3A4 in humans may be regulated in part by the estrogen receptor (Williams et al 2004). Further investigating the involvement of the nuclear receptors and AHR may help delineate the mechanism of regulation of CYP3 in fish.

CYTOCHROME P450 FAMILY 3 FUNCTION

In general, CYP enzymes are functionally versatile and play a critical role in the metabolism of both exogenous and endogenous compounds. CYP1-4 are highly involved in xenobiotic metabolism and are well studied in mammals. Unlike other CYPs, the CYP3 family is characterized by a promiscuous active site that allows for the docking of many structurally unrelated substrates of various classes (as reviewed by Ekroos & Sjogren 2006). In humans, the CYP3 family has high clinical value for the ability of the enzyme to metabolize more than 50% of pharmaceuticals, many environmental contaminants, and other xenobiotics (Zanger & Schwab 2013). There is some evidence to suggest that CYP3A enzymes can metabolize mycotoxins (Delaforge et al 1997, Shimada et al 1989) and bioactivate environmental procarcinogens, such as polycyclic aromatic hydrocarbons (PAH; Shimada et al 1989). The metabolism of steroids in mammals is an important process that is well established and mediated by several CYP enzymes including CYP3A (as reviewed by Tsuchiya et al 2005). Mammalian CYP3A enzymes in the brain and liver are important for the hydroxylation of testosterone, androstenedione, progesterone, dehydroepiandrosterone (Wang et al 2000) and estradiol (Lee et al 2001). Overall, the physiological role of CYP3A in mammals is to detoxify exogenous compounds and metabolize important signalling molecules like hormones.

To date, the function of fish CYP3 genes are largely unknown. There is some experimental evidence to suggest that fish CYP3As can hydroxylate steroids, such as estradiol and testosterone (as reviewed by Schlenk et al 2008), and PAHs, such as benzo[a]pyrene (Scornaienchi et al 2010b). It is commonly assumed that fish CYP3A metabolize mammalian CYP3A substrates and play an overall similar role however, some functional data challenges this hypothesis. Heterologously expressed zebrafish CYP3A65 was tested against specific mammalian CYP3A substrates: 7-benzyloxy-5-(trifluoromethyl) coumarin (BFC), 7-benxyloxyquinoline (BQ), dibenzylfourescein (DBF; Scornaienchi et al 2010a). Surprisingly CYP3A65 was not able to metabolise the specific mammalian CYP3A substrates BQ. CYP3A65 was able to metabolize BFC and DBF but at rates that are much lower than mammalian CYP3A. Unexpectedly, zebrafish CYP1A metabolized BFC more efficiently than CYP3A65 and purified liver microsomes from fish exposed to a potent CYP1A inducer, β-naphthoflavone, had increased capacity for BQ metabolism (Smith & Wilson 2010). These data, together, suggest that mammalian CYP3A specific substrates are not specific for zebrafish CYP3A65 and it is likely there is differences amongst CYP3A enzyme function between mammals and fish.

There is no data on CYP3C, CYP3B or CYP3D function. Some hypotheses can be made for CYP3C and CYP3B function based on gene expression profiles. The notable expression in defense organs, such as liver and intestine, is indicative of a role for CYP3C and CYP3B in xenobiotic detoxification (Shaya et al 2014). This is further supported by the implication of the PXR in CYP3C regulation (Kubota et al 2015). It is common that ligands of the AHR and PXR are also substrates of the enzymes the receptors regulate. Perhaps the PXR is activated by xenobiotic that are also metabolized by CYP3C1, indicating a role for CYP3C in detoxification of PXR ligands to prevent bioaccumulation. The expression of CYP3C and CYP3B in sensory organs like the eye and olfactory rosette (Shaya et al 2014) may imply a role for CYP3C and CYP3B in metabolism of signalling molecules that are important for behaviours mediated through sensory organs such as feeding, breeding and predatory avoidance. Expression in organs like the brain and gonad could imply a role for zebrafish CYP3C and medaka CYP3B in steroid metabolism (Shaya et al 2014); this may be partially supported by the differential expression of these genes in male and female fish. The presence of EREs in the promoter region of these genes further supports this hypothesis. Functional testing is required to test to better understand CYP3B, CYP3C and CYP3D function.

CYTOCHROME P450 HETEROLOGOUS EXPRESSION SYSTEMS

Studying the function of individual CYPs *in vivo* or whole tissue systems is very difficult. Any given tissue will express several different CYPs (as reviewed by Di Giulio et al 2008); there was significant overlap in tissue expression of CYP3Cs in zebrafish (Shaya et al 2014) and between the CYP3Cs and CYP3A65 (Corley-Smith et al 2006, Shaya et al 2014, Tseng et al 2005). Heterologous expression systems provide a valuable approach to express individual CYP enzymes in isolation and produce significant quantities of protein in a cheap and efficient manner. CYPs have previously been heterologously expressed in mammalian (Crespi et al 1993), insect (Lu et al 2010), yeast (Corley-Smith et al 2006; Stegeman et al 2015) and bacteria (Pritchard et al 1997) systems. Because cytochrome P450s are often found in the endoplasmic reticulum (ER), organisms that contain an ER, such as insects and yeast, offer some advantage to heterologously express vertebrate cytochrome P450s. However, yeast expression requires fermentation, which can have poorer protein yield, and can produce compounds that interfere with CO difference spectra, resulting in a need to normalize catalytic activity to total protein instead of total P450 content (Stegeman et al 2015). This latter is a significant disadvantage if comparing across proteins or across batches of the same enzyme. While insect expression systems have good yield and CO difference spectra, designing vectors for insect expression systems are more challenging than bacterial systems, where many commercial vectors are available. Despite the lack of ER, *Escherichia coli* (*E.coli)* is often used for heterologous CYP expression as it is easy to manipulate and there are several available vectors that are compatible (Friedberg et al 1999). A significant disadvantage of bacterial expression systems is the typical modification the 5' end of the gene, producing a modified protein product that may not be functionally identical to the original sequence (as reviewed by Gonzalez & Korzekwa 1995, Pritchard et al 1997). Previous studies, comparing the quantity of protein produced in *E.coli*, Sf9 insect, bovine adrenal, yeast and COS cell microsomes found that *E.coli* produced relatively more functional protein than the other systems and 50% more than Sf9 (insect) cells (Waterman et al 1995).

In most cases, the modification of the 5'prime end of the gene is necessary for heterologous expression of metazoan CYP genes in bacteria; CYP proteins are membrane proteins and must be appropriately targeted to a membrane to properly fold. Modification of the 5'prime end may be problematic as it may alter the native function of the protein. However, fusing a native bacterial leader sequence, for example from the outer membrane protein A gene (ompA), to the 5'prime end of the CYP cDNA allows for the recruitment of the CYP to bacterial membrane where it may be folded with no change to the gene sequence (Pritchard et al 1997). The additional modification of the OmpA leader sequence to include an alanine and proline amino acids to the 3'prime region of the leader sequence (ompA2+) allows for better cleavage by the bacterial signal peptidase (Friedberg et al 1999, Pritchard et al 1997). This method has previously been used to express a number of vertebrate CYP enzymes (Pritchard et al 1997, Scornaienchi et al 2010a, Scornaienchi et al 2010b).

ZEBRAFISH AS A MODEL ORGANISM FOR CYP3 RESEARCH

Zebrafish are a commonly used tool in biomedical, physiology, pharmacology and toxicology research (MacRae & Peterson 2015). The zebrafish is a tropical fish originating from India (Arunachalam et al 2013). The small size of zebrafish fish (2 – 4 cm) makes it a cheap and easy to culture in the laboratory (Hill et al 2005). The zebrafish is an asynchronous breeder that can produce 100s of transparent embryos, that hatch within 9 days and are reproductively mature by 3 months (Hill et al 2005). These attributes make the zebrafish an excellent tool for studying development and reproduction. There are some disadvantages associated with the zebrafish as a model organism. The small size can be problematic for research requiring large quantities of tissue (ie. protein) and in most cases leads to an increase in the number of animals needed.

The zebrafish is an important model system for the study of human health and other fish species, many of which are difficult to culture in the laboratory. In fact, many genetic markers of human disorders appear in the zebrafish genome (Dooley & Zon 2000). Though the molecular pathways between zebrafish and other vertebrates are highly conserved, it is important to note that zebrafish lack organs that appear in other vertebrates such as the lung and may not be a suitable model for all research questions. The teleost specific gene duplication makes it difficult to extrapolate gene data to humans and other vertebrates (Hill et al 2005) as many genes in zebrafish have multiple copies which would have subfunctionalized or neofunctionalized functionality.

For this thesis, the zebrafish is especially beneficial due to having a fully sequenced genome that allows us to more easily identify, clone, quantify and express CYP genes/proteins. Zebrafish allow us to study a teleost specific CYP3 family (CYP3C) and CYP3A genes to better understand the function and regulation of the CYP3 family in fish. From mammalian studies, it is understood that the CYP3 family is important for the metabolism of xenobiotic compounds, some of which are aquatic contaminates and pharmaceuticals. Additionally, the CYP3 family is very important in the metabolism of endogenous compounds like steroids and play a critical role in homeostasis. Understanding CYP3s in zebrafish will contribute to understanding what the fish CYP3 family contributes to the defensome. Understanding the capacity of the CYP3 family in fish for metabolism of pharmaceuticals will be critical information for developing the zebrafish as a biomedical model species and for understanding the effects of human pharmaceuticals in the environment.

THESIS GOALS

CYPs are important for detoxification of environmental contaminants and for the biosynthesis and activation of biological signaling molecules and other endogenous compounds. In vertebrates, including fish, there are 19 CYP gene families identified to date (Nelson et al 2013). Amongst those, the CYP3 family is highly expressed in detoxification organs like the liver and intestine and is especially relevant for the metabolism of endogenous and exogenous compounds, making it an interesting target to study. Unlike mammals, fish provide a unique avenue to study multiple CYP3 subfamilies. The function of CYP3A in fish is commonly thought to be like the function of mammalian CYP3A, but data suggest that there may be important functional differences. It is likely that other CYP3 subfamilies, such CYP3C, contribute to xenobiotic metabolism. CYP3Cs are more widely expressed in zebrafish than CYP3A but the regulation and function of the CYP3C subfamily is largely unknown. Its not yet clear if CYP3 subfamily duplications resulted in new or redundant functions. In this thesis, I characterized the substrates metabolized by zebrafish CYP3A65 and CYP3C1 to provide functional data that can be used to determine metabolic capacity of CYP3A65 and CYP3C1. I characterized the regulatory pathways of CYP3C1 to understand the condition in which CYP3C1 is expressed to perform its function. This data will further contribute to understanding what CYP3As and CYP3Cs contribute to the chemical defense pathways in zebrafish. Despite the lack of characterization of the fish CYP3s involvement in xenobiotic and endogenous compound metabolism, this model organism is commonly used tool in drug discovery, environmental toxicology, and fish biology (Dai et al 2014). Determining the metabolic capacity of this important model organism allows for a better use of this species in health and environmental research. Overall this study will provide data that will significantly contribute to understanding function of the CYP3 family in fish.

CHAPTER SUMMARY

Chapter 2 examines the involvement of the ER and AHR in the regulation of CYP3C1, CYP3C2, CYP3C3 and CYP3C4 genes in adult zebrafish. The presence of several estrogen receptor elements (EREs) and xenobiotic response elements (XREs) in the promoter region of the CYP3C genes (Shaya et al 2014, Kubota et al 2015) suggested a regulatory role for both endogenous (e.g. estrogens) and exogenous (e.g. planar polycyclic contaminants) compounds in CYP3C gene regulation. To assess ER and AHR receptor regulation, adult male and female fish were exposed to 17β-estradiol or β-naphthoflavone and the dose response and time response relationships for each ligand were determined in multiple tissues. Determining how CYPs are regulated provides important information to understand when and where the enzyme is expressed to perform its physiological function. The content of this chapter provides robust data on the regulation of CYP3Cs in zebrafish.

Chapter 3 focuses on the heterologous expression and functional assessment of CYP3C1 in *E.coli* utilizing the OmpA2+ system. CYP3C1 protein was assessed for the metabolism of 11 synthetic fluorogenic substrates with known mammalian specificity and in a high through put screen (HTS). CYP3C1 was tested for NADPH consumption with ~4000 small bioactive compounds compiled from a variety of commercially available libraries that contain approved, drugs, drug-like compounds and natural products. Unlike mammals, CYP3 in zebrafish includes four subfamilies with unknown function. Identifying what substrates are metabolized by CYP3Cs provided functional data to characterize how these widely expressed genes contribute to exogenous compounds metabolism.

Chapter 4 focuses on the HTS screening assay to assess the metabolism of a library of compounds by zebrafish CYP3A65. CYP3A65 was expressed, purified and tested for NADPH consumption with ~4000 small bioactive compounds compiled from a variety of commercially available libraries that contain approved, drugs, drug-like compounds and natural products. The function of CYP3A in fish is poorly characterized and the conservation of function across fish and mammalian CYP3A genes is not clear. An HTS approach was important to assess CYP3A65 function because it is evident that mammalian CYP3A accommodates 100s of structurally unrelated compounds and screening a small number of compounds will not provide adequate information on CYP3A65 function. The HTS of zebrafish CYP3A65 provides significant data to infer the functional role of CYP3A65 and how the function compares to mammalian CYP3A.

Chapter 5 discusses the major findings presented in chapters 2-4 and the relevance of the thesis.

REFERENCES

Andreasen EA, Hahn ME, Heideman W, Peterson RE, Tanguay RL. 2002a. The zebrafish (*Danio rer*io) aryl hydrocarbon receptor type 1 is a novel vertebrate receptor. *Molecular Pharmacology* 62: 234-49

Andreasen EA, Spitsbergen JM, Tanguay RL, Stegeman JJ, Heideman W. et al. 2002b. Tissue-specific expression of AHR2, ARNT2, and CYP1A in zebrafish embryos and larvae: effects of developmental stage and 2, 3, 7, 8-tetrachlorodibenzo-p-dioxin exposure. *Toxicological Sciences* 68: 403-19

Arunachalam M, Raja M, Vijayakumar C, Malaiammal P, Mayden RL. 2013. Natural history of zebrafish (*Danio rerio*) in India. *Zebrafish* 10: 1-14

Auld DS, Veith H, Cali JJ. 2013. Bioluminescent assays for cytochrome P450 enzymes. *Methods in Molecular Biology (Clifton, N.J.)* 987: 1-9

Bainy AC, Kubota A, Goldstone JV, Lille-Langoy R, Karchner SI, et al. 2013. Functional characterization of a full length pregnane X receptor, expression in vivo, and identification of PXR alleles, in zebrafish (*Danio rerio*). *Aquatic Toxicology* 142-143: 447-57

Bosetti A, Sobol M, Ma D, Good T, Liu D, Cali JJ. 2005. Bioluminescent cytochrome P450 assays. *Pharmacology* 3: 9-18

Cali JJ, Ma D, Sobol M, Simpson DJ, Frackman S, et al. 2006. Luminogenic cytochrome P450 assays. *Expert Opinion on Drug Metabolism & Toxicology* 2: 629-45

Celander M, Stegeman JJ. 1997. Isolation of a cytochrome P450 3A cDNA sequence (CYP3A30) from the marine teleost Fundulus heteroclitus and phylogenetic analyses of CYP3A genes. *Biochemical and Biophysical Research Communications* 236: 306-12

Chang CT, Chung HY, Su HT, Tseng HP, Tzou WS, Hu CH. 2013. Regulation of zebrafish CYP3A65 transcription by AHR2. *Toxicology and Applied Pharmacology* 270: 174-84

Christen V, Caminada D, Arand M, Fent K. 2010. Identification of a CYP3A form (CYP3A126) in fathead minnow (*Pimephales promelas*) and characterisation of putative CYP3A enzyme activity. *Analytical and Bioanalytical Chemistry* 396: 585-95

Corcoran J, Lange A, Winter MJ, Tyler CR. 2012. Effects of pharmaceuticals on the expression of genes involved in detoxification in a carp primary hepatocyte model. *Environmental Science and Technology* 46: 6306-14

Corley-Smith GE, Su HT, Wang-Buhler JL, Tseng HP, Hu CH, et al. 2006. CYP3C1, the first member of a new cytochrome P450 subfamily found in zebrafish (*Danio rerio*). *Biochemical and Biophysical Research Communications* 340: 1039-46

Crespi CL, Langenbach R, Penman BW. 1993. Human cell lines, derived from AHH-1 TK+/- human lymphoblasts, genetically engineered for expression of cytochromes P450. *Toxicology* 82: 89-104

Crespi CL, Miller VP, Penman BW. 1997. Microtiter Plate Assays for Inhibition of Human, Drug-Metabolizing Cytochromes P450. *Analytical Biochemistry* 248: 188-90

Dai YJ, Jia YF, Chen N, Bian WP, Li QK, et al. 2014a. Zebrafish as a model system to study toxicology. *Environmental Toxicology and Chemistry* 33: 11-7

Danielson PB. 2002. The cytochrome P450 superfamily: biochemistry, evolution and drug metabolism in humans. *Current Drug Metabolism* 3: 561-97

Delaforge M, Andre F, Jaouen M, Dolgos H, Benech H, et al. 1997. Metabolism of tentoxin by hepatic cytochrome P-450 3A isozymes. *European Journal of Biochemistry* 250: 150-7

Denisov IG, Makris TM, Sligar SG, Schlichting I. 2005. Structure and chemistry of cytochrome P450. *Chemical reviews* 105: 2253-77

Dooley K, Zon LI. 2000. Zebrafish: a model system for the study of human disease. *Current Opinion in Genetics and Development* 10: 252-6

Ekroos M, Sjogren T. 2006. Structural basis for ligand promiscuity in cytochrome P450 3A4. *Proceedings of the National Academy of Sciences of the United States of America* 103: 13682-7

Estabrook RW, Cooper DY, Rosenthal O. 1963. The light reversible carbon monozide inhibition of the steroid c21-hydroxylase system of the adrenal cortex. *Biochemische Zeitschrift* 338: 741-55

Friedberg T, Pritchard MP, Bandera M, Hanlon SP, Yao D, et al. 1999. Merits and limitations of recombinant models for the study of human P450-mediated drug metabolism and toxicity: an intralaboratory comparison. *Drug Metabolism Reviews* 31: 523-44

Garfinkel D. 1958. Studies on pig liver microsomes. I. Enzymic and pigment composition of different microsomal fractions. *Archives of Biochemistry and Biophysics* 77: 493-5090

Goldstone JV, Hamdoun A, Cole BJ, Howard-Ashby M, Nebert DW, et al. 2006. The chemical defensome: environmental sensing and response genes in the Strongylocentrotus purpuratus genome. *Developmental Biology* 300: 366-84

Goldstone JV, McArthur AG, Kubota A, Zanette J, Parente T, et al. 2010. Identification and developmental expression of the full complement of Cytochrome P450 genes in Zebrafish. *BMC Genomics* 11: 643

Gonzalez FJ, Korzekwa KR. 1995. Cytochromes P450 Expression Systems. *Annual Review of Pharmacology and Toxicology* 35: 369-90

Goodwin B, Hodgson E, Liddle C. 1999. The orphan human pregnane X receptor mediates the transcriptional activation of CYP3A4 by rifampicin through a distal enhancer module. *Molecular Pharmacology* 56: 1329-39

Goodwin B, Redinbo MR, Kliewer SA. 2002. Regulation of cyp3a gene transcription by the pregnane x receptor. *Annual Review of Pharmacology and Toxicology* 42: 1-23

Gorsky LD, Koop DR, Coon MJ. 1984. On the stoichiometry of the oxidase and monooxygenase reactions catalyzed by liver microsomal cytochrome P-450. Products of oxygen reduction. *The Journal of Biological Chemistry* 259: 6812-7

Gu Y-Z, Hogenesch JB, Bradfield CA. 2000. The PAS superfamily: sensors of environmental and developmental signals. *Annual Review of Pharmacology and Roxicology* 40: 519-61

Guengerich FP, Shimada T. 1998. Activation of procarcinogens by human cytochrome P450 enzymes. *Mutation Research* 400: 201-13

Hahn ME. 2001. Dioxin toxicology and the aryl hydrocarbon receptor: insights from fish and other non-traditional models. *Marine Biotechnology* 3: S224-S238

Hahn ME, Merson RR, Karchner SI. 2005. Chapter 7 Xenobiotic receptors in fish: Structural and functional diversity and evolutionary insights In *Biochemistry and Molecular Biology of Fishes*, ed. TP Mommsen, TW Moon, pp. 191-228: ElsevierHaines DC, Tomchick DR, Machius M, Peterson JA. 2001. Pivotal role of water in the mechanism of P450BM-3. *Biochemistry* 40: 13456-65

Harskamp J, Britz-McKibbin P, Wilson JY. 2012. Functional screening of cytochrome P450 activity and uncoupling by capillary electrophoresis. *Analytical Chemistry* 84: 862-6

Hegelund T, Celander MC. 2003. Hepatic versus extrahepatic expression of CYP3A30 and CYP3A56 in adult killifish (*Fundulus heteroclitus*). *Aquatic Toxicology* 64: 277-91

Hildebrandt A, Estabrook RW. 1971. Evidence for the participation of cytochrome b5 in hepatic microsomal mixed-function oxidation reactions. *Archives of Biochemistry and Biophysics* 143: 66-79

Hill AJ, Teraoka H, Heideman W, Peterson RE. 2005. Zebrafish as a Model Vertebrate for Investigating Chemical Toxicity. *Toxicological Sciences* 86: 6-19

Kahl R, Weinke S, Kappus H. 1989. Production of reactive oxygen species due to metabolic activation of butylated hydroxyanisole. *Toxicology* 59: 179-94

Karchner SI, Franks DG, Hahn ME. 2005b. AHR1B, a new functional aryl hydrocarbon receptor in zebrafish: tandem arrangement of AHR1b and AHR2 genes. *The Biochemical Journal* 392: 153-61

Kliewer SA, Goodwin B, Willson TM. 2002. The nuclear pregnane X receptor: a key regulator of xenobiotic metabolism. *Endocrine Reviews* 23: 687-702

Klingenberg M. 1958. Pigments of rat liver microsomes. Archives of Biochemistry and Biophysics 75: 376-86 Kubota A, Goldstone JV, Lemaire B, Takata M, Woodin BR, Stegeman JJ. 2015. Role of pregnane X receptor and aryl hydrocarbon receptor in transcriptional regulation of pxr, CYP2, and CYP3 genes in developing zebrafish. *Toxicological Sciences* 143: 398-407

Kullman SW, Hinton DE. 2001. Identification, characterization, and ontogeny of a second cytochrome P450 3A gene from the fresh water teleost medaka (*Oryzias latipes*). *Molecular Reproduction and Development* 58: 149-58

Lee AJ, Kosh JW, Conney AH, Zhu BT. 2001. Characterization of the NADPH-Dependent Metabolism of 17β-Estradiol to Multiple Metabolites by Human Liver Microsomes and Selectively Expressed Human Cytochrome P450 3A4 and 3A5. *Journal of Pharmacology and Experimental Therapeutics* 298: 420-32

Lee SJ, Wang-Buhler JL, Cok I, Yu TS, Yang YH, et al. 1998. Cloning, sequencing, and tissue expression of CYP3A27, a new member of the CYP3A subfamily from embryonic and adult rainbow trout livers. *Archives Biochemistry Biophysics* 360: 53-61

Lee SJ, Buhler DR. 2003. Cloning, tissue distribution, and functional studies of a new cytochrome P450 3A subfamily member, CYP3A45, from rainbow trout (*Oncorhynchus mykiss*) intestinal ceca. *Archives of Biochemistry and Biophysics* 412: 77-89

Lepesheva GI, Waterman MR. 2007. Sterol 14α-Demethylase Cytochrome P450 (CYP51), a P450 in all Biological Kingdoms. *Biochimica et Biophysica Acta* 1770: 467-77

Loew GH, Harris DL. 2000. Role of the heme active site and protein environment in structure, spectra, and function of the cytochrome p450s. *Chemical Reviews* 100: 407-20

Lu H, Ma J, Liu N, Wang S. 2010. Effects of heme precursors on CYP1A2 and POR expression in the baculovirus/Spodoptera frugiperda system. *Journal of Biomedical Research* 24: 242-49

MacRae CA, Peterson RT. 2015. Zebrafish as tools for drug discovery. *Nature Reviews. Drug Discovery* 14: 721-31

Masters BSS, Baron J, Taylor WE, Isaacson EL, LoSpalluto J. 1971. Immunochemical Studies on Electron Transport Chains Involving Cytochrome P-450: I. effects of antibodies to pig liver microsomal reduced triphosphopyridine nucleotide-cytochrome-c reductase and the non-heme iron protein from bovine adrenocortical mitochondria *Journal of Biological Chemistry* 246: 4143-50

McArthur AG, Hegelund T, Cox RL, Stegeman JJ, Liljenberg M, et al. 2003. Phylogenetic analysis of the cytochrome P450 3 (CYP3) gene family. *Journal of Molecular Evolution* 57: 200-11

Meyer RP, Gehlhaus M, Knoth R, Volk B. 2007. Expression and function of cytochrome p450 in brain drug metabolism. *Current Drug Metabolism* 8: 297-306

Murray GI, Melvin WT, Greenlee WF, Burke MD. 2001. Regulation, function, and tissue-specific expression of cytochrome P450 CYP1B1. *Annual Review of Pharmacology and Toxicology* 41: 297-316

Nebert DW, Nelson DR, Feyereisen R. 1989. Evolution of the cytochrome P450 genes. *Xenobiotica; the Fate of Foreign Compounds in Biological Systems* 19: 1149-60

Nebert DW and Feyereisen R. 1994, Evolutionar argument for a connection between drug metabolism and signal transduction, in Cytochrome P450 Biochemistery, Biophysics and Molecular Biology Letcher, M. C. (Ed,), Paris: Libbey, 3-13

Nelson DR and Nebert DW. 2018. Cytochrome P450 (*CYP*) Gene Superfamily. In eLS, John Wiley & Sons, Ltd (Ed.). doi:10.1002/9780470015902.a0005667.pub3

Nelson DR. 1999. Cytochrome P450 and the Individuality of Species. *Archives of Biochemistry and Biophysics* 369: 1-10

Nelson DR. 2006. Cytochrome P450 nomenclature, 2004. *Methods in Molecular Biology* 320: 1-10

Nelson DR, Goldstone JV, Stegeman JJ. 2013. The cytochrome P450 genesis locus: the origin and evolution of animal cytochrome P450s. *Philosophical Transactions of the Royal Society B: Biological Sciences* 368: 20120474

Nelson DR, Kamataki T, Waxman DJ, Guengerich FP, Estabrook RW, et al. 1993. The P450 superfamily: update on new sequences, gene mapping, accession numbers, early trivial names of enzymes, and nomenclature. *DNA and Cell Biology* 12: 1-51

Persson JO, Terelius Y, Ingelman-Sundberg M. 1990. Cytochrome P-450-dependent formation of reactive oxygen radicals: isozyme-specific inhibition of P-450-mediated reduction of oxygen and carbon tetrachloride. *Xenobiotica* 20: 887-900

Omura T, Sato R. 1962. A new cytochrome in liver microsomes. *The Journal of Biological Chemistry* 237: 1375-6

Omura T, Sato R. 1964a. The carbon monoxide-binding pigment of liver microsomes. I. evidence for its hemoprotein nature. *The Journal of Biological Chemistry* 239: 2370-8

Omura T, Sato R. 1964b. The carbon-monoxide binding pigment of liver microsomes. II. Solubilization, purification, and properties. *The Journal of Biological Chemistry* 239: 2379-85 Prasch AL, Teraoka H, Carney SA, Dong W, Hiraga T, et al. 2003. Aryl hydrocarbon receptor 2 mediates 2,3,7,8-tetrachlorodibenzo-p-dioxin developmental toxicity in zebrafish. *Toxicological Sciences* 76: 138-50

Pritchard MP, Ossetian R, Li DN, Henderson CJ, Burchell B, et al. 1997. A general strategy for the expression of recombinant human cytochrome P450s in Escherichia coli using bacterial signal peptides: expression of CYP3A4, CYP2A6, and CYP2E1. *Archives of Biochemistry and Biophysics* 345: 342-54

Qiu H, Taudien S, Herlyn H, Schmitz J, Zhou Y, et al. 2008. CYP3 phylogenomics: evidence for positive selection of CYP3A4 and CYP3A7. *Pharmacogenetics and Genomics* 18: 53-66

Raag R, Poulos TL. 1989. The structural basis for substrate-induced changes in redox potential and spin equilibrium in cytochrome P-450CAM. *Biochemistry* 28: 917-22

Schlenk D, Celander M, Gallagher E, George S, James M, et al. 2008. Biotransformation in Fishes In *Toxicology of Fishes*, ed. R Di Giulio, D DHinton, pp. 153-234. Boca Raton: Taylor and Francis Group

Scholz W, Schutze K, Kunz W, Schwarz M. 1990. Phenobarbital enhances the formation of reactive oxygen in neoplastic rat liver nodules. *Cancer Research* 50: 7015-22

Scornaienchi ML, Thornton C, Willett KL, Wilson JY. 2010a. Cytochrome P450-mediated 17beta-estradiol metabolism in zebrafish (*Danio rerio*). *The Journal of Endocrinology* 206: 317-25

Scornaienchi ML, Thornton C, Willett KL, Wilson JY. 2010b. Functional differences in the cytochrome P450 1 family enzymes from zebrafish (*Danio rerio*) using heterologously expressed proteins. *Archives of Biochemistry and Biophysics* 502: 17-22

Shaya L, Dejong C, Wilson JY. 2014. Expression patterns of cytochrome P450 3B and 3C genes in model fish species. *Comparative Biochemistry and Physiology Part C: Toxicology and Pharmacology* 166: 115-25

Shimada T, Iwasaki M, Martin MV, Guengerich FP. 1989. Human liver microsomal cytochrome P-450 enzymes involved in the bioactivation of procarcinogens detected by umu gene response in Salmonella typhimurium TA 1535/pSK1002. *Cancer Research* 49: 3218-28

Sligar SG. 1976. Coupling of spin, substrate, and redox equilibria in cytochrome P450. *Biochemistry* 15: 5399-406

Smith EM, Wilson JY. 2010. Assessment of cytochrome P450 fluorometric substrates with rainbow trout and killifish exposed to dexamethasone, pregnenolone-16alpha-carbonitrile, rifampicin, and beta-naphthoflavone. *Aquatic Toxicology* 97: 324-33

Stegeman JJ, Behrendt L, Woodin BR, Kubota A, Lemaire B, et al. 2015. Functional characterization of zebrafish cytochrome P450 1 family proteins expressed in yeast. *Biochimica et Biophysica Acta* 1850: 2340-52

Stresser DM, Turner SD, Blanchard AP, Miller VP, Crespi CL. 2002. Cytochrome P450 fluorometric substrates: identification of isoform-selective probes for rat CYP2D2 and human CYP3A4. *Drug Metabolism and Disposition: the Biological Fate of Chemicals* 30: 845-52

Tanguay RL, Abnet CC, Heideman W, Peterson RE. 1999. Cloning and characterization of the zebrafish (*Danio rerio*) aryl hydrocarbon receptor. *Biochimica et Biophysica Acta (BBA)-Gene Structure and Expression* 1444: 35-48

Tseng HP, Hseu TH, Buhler DR, Wang WD, Hu CH. 2005b. Constitutive and xenobiotics-induced expression of a novel CYP3A gene from zebrafish larva. *Toxicology and Applied Pharmacology* 205: 247-58

Tsuchiya Y, Nakajima M, Yokoi T. 2005. Cytochrome P450-mediated metabolism of estrogens and its regulation in human. *Cancer Letters* 227: 115-24

Van Tiem LA, Di Giulio RT. 2011. AHR2 knockdown prevents PAH-mediated cardiac toxicity and XRE- and ARE-associated gene induction in zebrafish (*Danio rerio*). *Toxicology and Applied Pharmacology* 254: 280-7

Wang H, Napoli KL, Strobel HW. 2000. Cytochrome P450 3A9 catalyzes the metabolism of progesterone and other steroid hormones. *Molecular and Cellular Biochemistry* 213: 127-35

Wassmur B, Gräns J, Kling P, Celander MC. 2010. Interactions of pharmaceuticals and other xenobiotics on hepatic pregnane X receptor and cytochrome P450 3A signaling pathway in rainbow trout (*Oncorhynchus mykiss*). *Aquatic Toxicology (Amsterdam, Netherlands)* 100: 91-100

Wassmur B, Grans J, Norstrom E, Wallin M, Celander MC. 2013. Interactions of pharmaceuticals and other xenobiotics on key detoxification mechanisms and cytoskeleton in *Poeciliopsis lucida* hepatocellular carcinoma, PLHC-1 cell line. *Toxicology in Vitro* 27: 111-20

Waterman MR, Jenkins CM, Pikuleva I. 1995. Genetically engineered bacterial cells and applications. *Toxicology Letters* 82-83: 807-13

Waxman DJ. 1999. P450 gene induction by structurally diverse xenochemicals: central role of nuclear receptors CAR, PXR, and PPAR. *Archives of Biochemistry and Biophysics* 369: 11-23

Williams ET, Leyk M, Wrighton SA, Davies PJ, Loose DS, et al. 2004. Estrogen regulation of the cytochrome P450 3A subfamily in humans. *The Journal of Pharmacology and Experimental Therapeutics* 311: 728-35

Yan J, Cai Z. 2010. Molecular evolution and functional divergence of the cytochrome P450 3 (CYP3) Family in Actinopterygii (ray-finned fish). *PLoS One* 5: e14276

Zanger UM, Schwab M. 2013. Cytochrome P450 enzymes in drug metabolism: regulation of gene expression, enzyme activities, and impact of genetic variation. *Pharmacology and Therapeutics* 138: 103-41

Zhang J, Yao J, Wang R, Zhang Y, Liu S, et al. 2014. The cytochrome P450 genes of channel catfish: their involvement in disease defense responses as revealed by meta-analysis of RNA-Seq datasets. *Biochimica et biophysica acta* 1840: 2813-28

CHAPTER 2

CYP3C GENE REGULATION BY THE ARYL HYDROCARBON AND ESTROGEN RECEPTORS IN ZEBRAFISH

Reproduced with permission from Toxicology and Applied Pharmacology

[Shaya L, Jones DE, Wilson JY. 2019. CYP3C gene regulation by the aryl hydrocarbon and estrogen receptors in zebrafish. *Toxicol Appl Pharmacol* 362: 77-85] © 2019

ABSTRACT

Cytochrome P450 (CYPs) enzymes are critical for the metabolism of exogenous and endogenous compounds. In mammals, the CYP3s are arguably the most important xenobiotic metabolizing enzymes and are all contained within the CYP3A subfamily. In fish, CYP3s include CYP3A and multiple subfamilies unique to the teleost lineage. The goal of this study was to provide insight on the regulation of genes in the CYP3C subfamily. Zebrafish, which have 4 CYP3C genes, were exposed to 17β-estradiol (E_2; 0.001-10μM) or β-naphthoflavone (βNF; 0.005-1μM), prototypical ligands of the estrogen receptor (ER) and the aryl hydrocarbon receptor (AhR), respectively. Gene expression was measured in the liver, intestine and gonads using quantitative PCR. CYP1A and vitellogenin (VTG) gene expression were used as positive controls for AhR and ER regulation, respectively. Exposure to βNF resulted in the dose-dependant induction of CYP1A and CYP3C genes in the female intestine but not in the liver. E_2 exposure resulted in the induction of all CYP3Cs in the male intestine and in the female liver. VTG was induced in both female and male livers. CYP3C3 and CYP3C4 were induced in the testis; CYP3C1 and CYP3C4 were slightly induced in the ovary. The time-course of gene induction was investigated in the liver and intestine after exposure to βNF

(0.5μM) and E_2 (0.1μM). Inducible genes were up-regulated within 12 hours after exposure. These data support a role for the AhR and ER in the regulation of CYP3Cs. Overall, the induction of CYP3Cs by AhR and ER ligands is different from mammalian CYP3A and may suggest a functional role for CYP3Cs that involves planar aromatic hydrocarbons and steroids.

INTRODUCTION

Cytochrome P450s (CYPs) are a superfamily of membrane bound, heme-enzymes that are critical for the metabolism and biotransformation of many endogenous and exogenous compounds. Most of the substrates metabolized by CYPs are pharmaceuticals, environmental contaminants and plant by-products (As reviewed by Uno et al 2012, Zanger & Schwab 2013) but CYPs are also critical in the biosynthesis of endogenous compounds such as steroids, fatty acids, and prostaglandins (as reviewed by Nebert & Russell 2002, Pinot & Beisson 2011, Zanger & Schwab 2013).

Technological advances in whole genome sequencing have helped identify ~55 000 named CYPs (Nelson & Nebert 2018) but only a handful of these genes are extensively studied. As such, most CYPs are labelled "orphans," with unknown function and regulation (as reviewed by Guengerich et al 2010, Nelson & Nebert 2018). Mammalian CYP3s are extensively studied due to their important role in xenobiotic metabolism. Specifically, mammalian CYP3As metabolizes more than 50% of all known drugs (Guengerich 1999, Zanger & Schwab 2013). The CYP3 family in fish contains CYP3A, CYP3B, CYP3C and CYP3D subfamilies. While all fish species have at least one CYP3A; CYP3B, CYP3C, and CYP3D appear in only some fish species (Yan & Cai 2010). Zebrafish (*D. rerio*) have CYP3A65 and 4 CYP3Cs genes (Yan & Cai 2010). Of the fish CYP3s, only the CYP3As have been studied in multiple species. This study focuses on better understanding the regulation of CYP3Cs.

In mammals, CYP3As dominate as the most highly expressed CYPs in detoxification organs like the liver and intestine (as reviewed by Zanger & Schwab 2013). Some expression has been detected in sexually dimorphic organs such as the brain and gonads, where they may play critical roles in metabolizing endogenous compounds like steroids (Finnström et al 2001, Rosenbrock et al 2001, Williams et al 2004). Like mammals, CYP3As in fish were highly expressed in the liver and small intestine (Husoy et al 1994, Tseng et al 2005). Two studies have found that CYP3Cs in zebrafish were highly expressed in organs important for detoxification but expression was also high in organs like gonads and brain (Corley-Smith et al 2006, Shaya et al 2014). The expression of each CYP3C gene varied between male and female fish in both zebrafish and medaka (Shaya et al 2014). It is not clear whether CYP3Cs contribute to pharmaceutical or xenobiotic metabolism.

Regulation of fish CYP3 genes is very poorly understood but the available data indicates that fish CYP3s are regulated by pathways that differ from mammalian CYP3s (Chang et al 2013, Corley-Smith et al 2006, Kubota et al 2015). The aryl hydrocarbon receptor (AhR) has been implicated in regulating the CYP3 genes in fish (Chang et al 2013, Kubota et al 2015, Tseng et al 2005). The AhR is an important transcription factor that binds planar aromatic xenobiotics such as dioxins, polychlorinated biphenyls (PCBs) and polycyclic aromatic hydrocarbons (PAHs) to induce the expression of detoxification enzymes (as reviewed by Hahn et al 2005). Ligand activated AhR binds its heterodimerization partner, the aryl hydrocarbon nuclear translocator (ARNT) protein, prior to interaction with a xenobiotic response element (XRE) in the promoter site of the target gene to induce transcription (as reviewed by Gu et al 2000, Hahn et al 2005). XREs have been identified upstream of CYP3C1 (Shaya et al 2014, Kubota et al 2015), CYP3C2, and CYP3C4 (Shaya et al 2014) genes. Yet, CYP3C1 was not induced by the AhR ligand 2,3,7,8 tetrachlorodibenzo-*p*-dioxin (TCDD) in embryonic and larval zebrafish (Corley-Smith et al 2006) but inducible by the AhR ligand PCB 126 (Kubota et al 2015). Regulation of CYP3Cs have not yet been experimentally investigated in the context of adult animals.

Several (EREs) were found in 10kb promoter region of all the CYP3C genes, which implicates the ER in regulation of CYP3C (Shaya et al 2014). CYP3Cs were constitutively expressed in the gonads and brain and expression was generally higher in female organs than in males, further suggesting a role for estrogen hormone involvement in CYP3C gene regulation (Shaya et al 2014).

Despite the lack of data to determine function and regulation of fish CYP3s, zebrafish and the CYP3 gene family play an important role in biomedical research, drug development and screening, developmental biology, toxicology and fish biology (as reviewed by Dai et al 2014 , Zon & Peterson 2005). However, studies suggest that the function of CYP3A may not be conserved between mammals and fish (Scornaienchi et al 2010a) and even less is known about the function of the other CYP3 subfamilies. It is unknown if CYP3B, CYP3C or CYP3D have an overlap in function with CYP3A or if they contribute to pharmaceutical or xenobiotic metabolism.

This study determined the up-regulation of CYP3C genes by AhR and ER ligands in adult zebrafish, an important model organism. This information is important because the CYP3C genes are orphan CYPs in a gene family that is critical for pharmaceutical and other xenobiotic metabolism and are expressed in detoxification organs. Understanding the regulation of CYP3 genes may provide insight on function. Receptor ligands which regulate CYP genes are often substrates; compounds which induce their own metabolism. For example, AhR ligands are commonly CYP1A substrates (ie. polycyclic aromatic hydrocarbons). We hypothesize that the AhR and ER regulate zebrafish CYP3Cs. Understanding regulation may provide a starting point for functional studies to better characterize orphan CYPs with unknown function.

MATERIALS AND METHODS

Animals

Wild-type zebrafish were maintained in a semi-recirculating housing system that allowed for a 10% daily water change-out. Temperature was maintained at 28.5^{o}C, pH at 7-8 and conductivity at 450-470µS. Fish were kept at a 14:10 light, dark cycle and were fed with commercial tropical fish flakes (twice per day; Tetramin Tropical Flakes, Tetra, USA) and live brine shrimp (once per day; *A. salina;* GLS Brine Shrimp, USA). All experiments involving animals were conducted in accordance to McMaster University approved animal use and standard operating protocols.

Chemicals

β-naphthoflavone (βNF) and 17β-estradiol (E_2) were purchased from Sigma-Aldrich (Saint Louis, MO). Dimethysulfoxide (DMSO) was purchased from Caledon Laboratories (Georgetown, ON). βNF was dissolved in dimethysulfoxide (DMSO) and prepared fresh before each exposure day. E_2 was dissolved in ethanol (EtOH), in glass vials, protected from light and stored at -20°C.

Exposure

Dose-Response of CYP3C Induction by Exposure to βNF and E_2

Wild-type zebrafish were exposed in 2-litre tanks containing 12 fish each (6 fish per L). We expected a large difference in responsiveness to E_2 between male and female zebrafish due to variable levels of endogenous $E_{2;}$ both sexes were exposed to E_2 to investigate sex-specific response. Only female zebrafish were exposed to βNF. Tanks were set up in a water table, heated to 28.5°C, to maintain appropriate water temperature. Fish were acclimated for 1 day in the 2-litre tanks prior to the start of the exposure. Three replicate tanks (control) were subjected to a waterborne exposure to 0.01% DMSO vehicle (βNF exposure) or 0.01% ethanol (E_2 exposure). The remaining tanks were exposed in triplicates to βNF and E_2 at various concentrations (βNF; 0.005, 0.05, 0.2, 0.5 and 1µM; E_2: 0.001, 0.01, 0.1. 1, 5 and 10µM). βNF concentrations included those that were previously effective in induced CYP1A in zebrafish embryos (Timme-Laragy et al 2007) and adults (Jönsson et al 2007) . E_2 concentrations included those that were previously effective in inducing VTG in zebrafish embryos (Hao et al 2013) and adults (Rose et al 2002). Tanks were continuously aerated and partially covered with parafilm to minimize evaporation between water change-outs. 90% water renewals were completed daily throughout the exposure. Fish remained unfed for the duration of the exposure. After 96 hours of exposure (h), animals were weighed and dissected for gonads, intestine and liver. Organs were selected to include those involved in endogenous and exogenous compound metabolism but also organs that had both high and moderate basal expression of CYP3C genes (Shaya et al 2014)

Time-course for induction of CYP3Cs

Triplicate 9-litre tanks containing 50 female fish were exposed to 0.5µM βNF or 0.01% DMSO. The concentration of exposure was based on βNF dose-response data from the intestine (Figure 1A). Triplicate 9-litre tanks containing 50 male fish were exposed to 0.1µM E_2 or 0.01% EtOH. The concentration and sex of fish was based on dose-response data (Figure 1, 3). Exposure conditions were maintained as described above for the dose response study. 12 fish were sampled from each tank at 6h, 12h, 48h and 96h post exposure. The tank volume was adjusted after sampling to maintain consistent fish density (6 fish/liter). Sampled fish were weighed and dissected for liver, intestine and gonads. Tissue was flash frozen in liquid nitrogen and stored at -80^{o}C.

<u>Tissue Collection and RNA Extractions</u>

A single biological replicate consisted of tissue pooled from 3 fish, for every treatment, to provide sufficient tissue for quantitative PCR (qPCR); 9-12 pools were collected per treatment. RNA was extracted using Invitrogen's TRrizol (Carlsbad, CA) method with two 75% ethanol rinses to ensure purity of samples. RNA purity was assessed for all samples using a Thermo Scientific Nanodrop 2000c (Wilmington, DE). Samples with 260/280 ratios below 1.8 were not used in further applications. 100% of RNA samples for male livers were assessed for RNA quality and integrity using for RNA integrity using Agilent's 2100 BioAnalyzer (Santa Clara, CA) in the Farncombe Metagenomics Facility at McMaster University. Samples with an RNA integrity number (RIN) that was below 5 were not included in analysis for the male E_2 exposed livers. 25% of the remaining samples were also assessed for RNA integrity. The RIN was typically above the cut off for 82%-100% of samples. Samples that did not meet the standard RIN cut off were further assessed for quality. Integrity of these samples was further assessed by looking at housekeeping gene variation in these samples and with stringent cDNA and qPCR controls. Housekeeping gene expression level was consistent within these samples and all controls were negative for genomic contamination. Finally, samples were treated with Invitrogen DNAse Amplification Grade (Carlsbad, CA) prior to cDNA synthesis using Invitrogen Superscript II (Carlsbad, CA).

Quantitative PCR

Quantitative PCR (qPCR) was utilized to measure the expression of CYP3C1, CYP3C2, CYP3C3, CYP3C4, CYP1A, VTG and β-actin genes. All samples were run in technical duplicates using a BioRad CFX Connect Real-Time PCR Detection System (Ontario, CAN) and Sigma Aldrich LuminoCT SYBR Green qPCR Ready Mix (St Louis, MO). A 5-8-point standard curve was generated for each gene tested. The template used for the standard curves were from pooled cDNA from highest expressing organs. The R^2 values for all standard curves were >0.97% and the efficiency ranged from 90-110%. All primer sets were previously designed (Alsop & Vijayan 2008, Evans et al 2008, Sahoo & Oikari 2014, Shaya et al 2014) and summarized in Table 1 but re-optimized for annealing temperature using temperature gradients on the BioRad CFX Connect (Hamilton, ON). All plates included no template (NTC) and no reverse transcriptase (NRT) controls and samples were run for 40 cycles, followed by a melt curve analysis to assess primer specificity. NTC controls showed no amplification for all runs. Amplification was not seen for most NRTs; in places were amplification was seen, the cycle threshold value was more than 7 cycles greater than target gene amplification. Because some amplification was seen in NRTs, samples with a 35 cycle threshold or more were not included in the data analysis to ensure the quantification of only target genes, unbiased by non-specific amplification.

Data and Statistical Analysis

A box and whisker plot based on the Tukey method was utilized to identify outliers in raw CT values for β-Actin. Outliers were omitted from further analysis. Box and whisker plots were also used to assess outliers within each treatment for all genes of interest. Data analysis was performed using NORMA-Gene (Heckmann et al 2011). NORMA-Gene is a data-driven normalization algorithm that does not require a housekeeping gene to robustly analyze qPCR data. NORMA-Gene is an excel based macro that is designed to reduce the variation within treatments and normalize data across

5 or more genes. Systat Software SigmaStat Version 12.2 (San Jose, CA) and GraphPad Prism Version 5 (San Diego, CA) were used to statistically analyze gene expression. For the dose-response data, all samples were analyzed relative to the vehicle control and a One-Way ANOVA followed by an LSD Fischer Test ($p<0.050$) was used to test the difference in expression between each dose and control. For the time-course experiments, a two-tailed t-test ($p<0.050$) was used to test the level of expression relative to control within each time point. A log transformation was utilized to normalize data for analysis. If normalization was not obtained following transformation, a One-way ANOVA on ranks, followed by a Dunn's test was utilized to test significance

RESULTS

<u>Effects of Increasing Concentrations of β-naphthoflavone on CYP3C and CYP1A Expression</u>

In the intestine, expression of CYP1A, CYP3C1, CYP3C2, CYP3C3 followed a typical dose-response curve (Figure 1A); induction increased with increasing concentrations of βNF while CYP3C4 induction was only significant at the highest tested dose. Levels of CYP3C1, CYP3C3 and CYP3C4 induction was similar, ranging from a 2-3-fold maximal induction. CYP1A and CYP3C2 were more highly induced by βNF. Maximal induction of CYP1A and CYP3C2 was approximately 20 and 30 folds greater than control, respectively.

In the liver, CYP3C1 and CYP3C4 expression was only slightly induced at the intermediate doses with ~1.5-fold induction but expression returned to control levels at the higher concentrations of βNF (Figure 1B). Expression of CYP3C2, CYP3C3 and CYP1A were not induced in the zebrafish liver. In the case of CYP3C3, higher concentrations of βNF resulted in expression levels that were significantly less than controls.

In the ovary, slight induction of CYP3C1, CYP3C2 and CYP3C4 was observed (Figure 1C). CYP3C1 had the smallest fold induction of the three CYP3C genes and expression was similar to control levels at the higher concentrations of βNF. CYP3C2 and CYP3C4 had the highest induction of gene expression at 4-5-fold greater than control.

Overall, expression was dose-dependent and tissue specific. CYP3C2 was the most highly induced in the intestine; this induction was higher than any other CYP3C gene in any of the organs. CYP3C1 and CYP3C4 were induced in all organs, but induction was typically ≤2 fold.

Time-Course of mRNA Induction by Exposure to β-naphthoflavone

The time-course for CYP1A and CYP3C induction was investigated in liver and intestine (Figure 2). Induction of CYP1A mRNA expression was 42-fold greater than control at 6h post exposure in the liver (Figure 2A). The mRNA levels began to decrease following 12h and were not significantly different than controls at 96h. The maximal induction of CYP1A in the intestine was 36-fold more than control at 6h but unlike liver, expression remained high and was 20-fold greater than control at 96h (Figure 2B).

CYP3C1 expression in the liver was 2-fold greater than control at 12h post exposure and remained elevated for the duration of the experiment (Figure 2A). CYP3C1 was up-regulated at 6h and 96h in the intestine (Figure 2B). Unexpectedly, CYP3C2 was not inducible in the intestine through-out time (Figure 2B).

Effects of Increasing Concentrations of 17β-estradiol on Male CYP3C and VTG Expression

In the liver, expression of VTG in males exposed to E_2 was maximally induced at 1μM; the CYP3Cs were much less inducible than VTG (Figure 3A). CYP3C1, CYP3C2 and CYP3C3 were down-regulated with at least some doses of E_2. Interestingly, CYP3C2 and CYP3C3 had a U- shape dose-response with mRNA levels decreasing at 0.01μM (CYP3C2) or 1μM (CYP3C3) and increasing back to basal levels at 5μM or higher.

In intestine, all CYP3C genes were induced in a dose-dependent manner (Figure 3B). CYP3C3 had a multiphasic dose-response where small induction was seen in a dose-dependent manner to 0.1μM, followed by significant decrease in expression and a final maximal induction at 10μM dose. CYP3C2 expression was 1.5-fold greater than controls but expression decreased by 50% between 1μM-10μM. CYP3C1 and CYP3C4 induction in the intestine was represented by a relatively linear dose-response with a maximum induction at 10μM. Overall, levels of induction were similar between all CYP3C genes in the intestine.

In testis, induction of CYP3Cs was variable across treatments (Figure 3C). CYP3C1 and CYP3C2 were not inducible whereas CYP3C3 and CYP3C4 were slightly up-regulated in a dose-dependent manner. Interestingly, CYP3C1, CYP3C3 and CYP3C4 were down-regulated by exposure to 1uM E_2 but the down-regulation was attenuated at 5μM. CYP3C3 and CYP3C4 were slightly more inducible in the testis than CYP3C1 and CYP3C2.

Overall, the expression of all CYP3C genes varied amongst the tissues tested in males exposed to E_2. CYP3C1 and CYP3C2 expression was not inducible in the liver and testis but inducible in the intestine (Figure 3A, 3B). CYP3C3 and CYP3C4 were only inducible in the intestine and testis (Figure 3B, 3C). Maximal induction was never greater than 3-fold for any CYP3C gene in any organ.

Effects of Increasing Concentrations of 17β-estradiol on Female CYP3C and VTG Expression

Unlike in the male liver, all CYP3C genes and VTG were induced to some extent in the female liver (Figure 4A). VTG was more inducible in the male liver than in the female liver (Figure 3A, Figure 4A). Maximum induction for all CYP3Cs was observed at the 10μM concentration. Interestingly, CYP3C3 and CYP3C4 expression increased in a dose-dependent manner and the maximal mRNA levels were an average 7-fold greater than maximal VTG mRNA levels. CYP3C3 and CYP3C4 were more highly inducible in the female liver than CYP3C1 and CYP3C2.

Unlike in male zebrafish, CYP3Cs were not strongly induced in the female intestine (Figure 4B) or in the ovary (Figure 4C). CYP3C1 and CYP3C4 were very slightly induced (1.3-1.6-fold) in both the intestine and ovary but only CYP3C4 expression increased in a dose-dependent manner in the intestine (Figure 4B). Both CYP3C1 and CYP3C4 expression decreased in the ovary between 1µM-10µM (Figure 4C).

Overall, CYP3C1 and CYP3C2 were more inducible in the female liver than in the intestine or ovary (Figure 4). CYP3C3 was only inducible in the female liver and CYP3C4 was inducible in all organs but maximum induction in the liver was ~ 4-fold more than in intestine or ovary. CYP3C expression was more inducible in male intestine (Figure 3B), testis (Figure 3C) and female liver (Figure 4A).

Time-Course of mRNA Induction by Exposure to a Single Dose of 17β-estradiol

Time-course of VTG and CYP3C induction by E_2 was investigated in male liver (Figure 5A) and intestine (Figure 5B). VTG expression in male liver was time-dependent and several folds greater than control at 96h (Figure 5A). CYP3C1 was slightly down-regulated at 96h. CYP3C2 and CYP3C4 induction was detected at 6h; CYP3C2 expression was abolished after 12h and CYP3C4 remained up-regulated between 6-96h. No induction of CYP3Cs was observed at any of the time points in intestine (Figure 5B). In fact, slight down-regulation of CYP3C1, CYP3C2 and CYP3C3 at 48h was observed.

DISCUSSION

The presence of many XREs and EREs in the promoter region of CYP3C genes suggest a role for AhR and ER, respectively, in CYP3C regulation (Shaya et al 2014). In this study, we utilized prototypical ligands of the AhR (βNF) and ER (E_2) to test the role of these receptors in the regulation of zebrafish CYP3C1, CYP3C2, CYP3C3, CYP3C4. Expression of the CYP3C genes was compared to genes highly inducible by AhR (CYP1A) and ER (VTG). Induction after exposure to these compounds suggests that both the AhR and ER are involved in regulating CYP3Cs but in a manner that is tissue specific, gene specific, sex specific and dependent on time of exposure.

The Role of the AhR in Regulation of CYP3Cs

In fish, CYP1A is a prototypical AhR regulated gene that is highly inducible by βNF (Husoy et al 1994, Chung-Davidson et al 2004, Jönsson et al 2007, Timme-Laragy et al 2007). The induction of CYP1A is a strong indication that βNF uptake resulted in activation of AhR and CYP3C gene induction. In support of our study, Kubota et al. (2015) found that CYP3C1 was up-regulated by the AhR agonist PCB126 in zebrafish at 72 hours post fertilization (hpf) with embryonic exposure. The induction was successfully blocked following the knockdown of AhR2 expression by an AhR2 morpholino (Kubota et al 2015), supporting our findings that AhR ligands can induce CYP3C gene expression in adults.

Our study, taken with the findings of Kubota et al (2015) and Corley-Smith et al (2005), suggests that AhR regulation of CYP3Cs is dependent on the specific ligand. In adult zebrafish, Jönsson et al (2007) showed that expression of CYP1A, CYP1B1 and CYP1C1 was not inducible in the liver of animals treated with βNF while PCB126 was able to induce all three genes. This data suggest that it is important to consider the ligand when looking at the involvement of ligand-activated transcription factors in regulation of cytochrome P450s. Overall, the use of different AhR ligands may contribute to the differences seen in AhR regulation of CYP3Cs between Corley-Smith et al (2005), Kubota et al (2015) and this study.

The dose-response data generally showed little induction of CYP3Cs in liver at 96hrs but expression of CYP3C1 was upregulated by 12 hours post exposure in both liver and intestine (Figure 2). It is likely that regulation of CYP3C1 by the AhR is time dependent, as is true for CYP1A. The lack of induction of CYP1A in zebrafish liver at 96h (Figure 1B) was similar to prior studies in this species (Jönsson et al 2007). The time-course of induction of CYP1A in the liver (Figure 2B) supports our dose response data and that of Jönsson et al (2007); CYP1A expression was abolished in the liver following 12h (Figure 2A). The half-life of zebrafish CYP1A transcript is unknown but in mammals, CYP1A transcript half-life is very short (Dalton et al 2000). In killifish (*F. heteroclitus*) it appears that CYP1A protein half-life is much longer than mRNA half-life, lasting 48h (Kloepper-Sams & Stegeman 1994). It is possible that CYP1A mRNA was already degraded in the liver at 96h or no longer induced due to an extended half-life of the CYP1A protein. Jönsson et al (2007) suggested that since βNF is very highly metabolized by CYP1A and that organs of first contact, such as gills, can induce CYP1A, sufficient gill metabolism of βNF may occur before sufficient βNF reached all organs to induce detectible levels of CYP1A gene. Either of these, or a combination, may have contributed to the lack of CYP1A and CYP3C1 induction in the liver.

CYP3C gene induction by βNF was organ specific. Organ specificity is commonly seen in the induction of fish CYP3As and CYP1As. Induction of zebrafish CYP3A65 was several-fold greater in the intestine than in the liver (Tseng et al 2005). Similarly, induction of zebrafish (Jönsson et al 2007) and killifish (*F. heteroclitus*; Zanette et al 2010) CYP1A was several folds greater in brain and testis than in liver and intestine. The differences in induction observed in various organs is most likely due to the tissue distribution of AhR and its heterodimerization partner, ARNT, as well as the interaction between different AhR subtypes to different target genes.

One exciting finding in this study is that CYP3C2 was more highly inducible than CYP1A in the intestine in animals exposed to a range of βNF concentrations (Figure 1) but this finding was not confirmed in animals exposed to 0.5µM in the time course experiment (Figure 4B). The constitutive level of CYP3C2 expression in the wild-type fish for the time-course was almost 1.5 folds greater than in the animals used for the time-course experiment (data not shown). This data suggest that the level of induction may be dependent on the amount of constitutively expressed gene. Previous studied have reported variability in gene regulation pathways between different strains of zebrafish (Van den Bos 2017) and mice (Kraus et al 2012). The wildtype fish in this study were not genotyped. In the future, this may be better controlled for by utilizing genetically similar zebrafish for all exposures.

<u>The Role of ER in CYP3C Regulation</u>

Zebrafish VTG is an egg yolk precursor gene that is ER regulated and highly inducible by a wide range of E_2 concentrations (Rose et al 2002, Brion et al 2004, Levi et al 2009, Hoa et al 2013). VTG is a biomarker of estrogenic exposure in both male and female zebrafish. The induction of VTG in the male (Figure 3) and female liver (Figure 4) confirms the uptake of E_2 and the activation of ER with exposure to E_2. In this study, E_2 exposure resulted in the induction of CYP3Cs in male and female zebrafish in a tissue and sex-specific manner. The presence of several EREs in the promoter region of CYP3Cs (Shaya et al 2014) along with data we present here support a role for ER in the regulation of CYP3Cs. There is limited information concerning the role of E_2 in fish CYP3 regulation but like CYP3C1, CYP3A expression varies with sex and reproductive cycles, suggesting a role for estrogen in the regulation of other fish CYP3 (as reviewed by Di Giulio & Hinton 2008).

Many steroid regulated genes are differentially regulated in male and female liver, such as VTGs (Wang et al 2005). In our study, we found that exposure of male and female fish to E_2 resulted in unique regulatory patterns. Generally, we expect genes regulated by E_2 through the ER pathway to have higher constitutive expression in females in comparison to males due to the higher level of endogenous estradiol in female. Constitutive expression of VTG in the male zebrafish liver is less than in female liver (Wang et al 2005) and in our study VTG was more inducible in males (Figure 3), than in female zebrafish (Figure 4). Like VTG and some fish CYP3As (as reviewed by Di Giulio & Hinton 2008), CYP3Cs were generally more highly constitutively expressed in the female intestine and ovary than in male intestine and testis (Shaya et al 2014). This basal expression data support our finding that CYP3Cs are generally more inducible in male than female for intestine and gonads. It is also possible other steroids may be involved in regulation of CYP3C gene expression in liver. Along with ERE's, CYP3Cs have multiple androgen response elements in the promoter region that suggests a possible role for both estrogen and androgen receptors in gene regulation (Shaya et al 2014). This is true for other CYPs involved in hormone systems; CYP3A27 in juvenile rainbow trout was slightly induced with exposure to testosterone (Buhler et al 2000). Overall, differential expression of CYP3s between sexes has been seen in mammals (reviewed by Waxman and Holloway 2009) and fish (Lee et al 1998, Shaya et al 2014) and suggests a sex specific role for CYP3s.

We observed an overall tissue-specific regulation of CYP3Cs in E_2 induced zebrafish. This is not uncommon for CYPs; for example, in fish, there are two CYP19 genes which are expressed differently in the brain and ovary. CYP19a is predominately expressed in ovary, while CYP19b is expressed in the brain (as reviewed by Callard et al 2001). In many fish species, CYP19b is highly inducible by E_2 but CYP19a is not (Callard et al 2001, Cheshenko et al 2007). Perhaps the concentration of E_2 in these tissues would contribute to the differences observed in expression.

<u>Functional Implications from the Involvement of the AhR and ER in Regulation</u>

Zebrafish is a model organism frequently utilized for physiology, pharmacology, drug screening, drug development, biomedical sciences and toxicology. Yet, we have limited understanding of the capacity of this species for pharmaceutical and other xenobiotic metabolism, nor the specific genes involved. Clearly, we expect that CYP3 family will be relevant but the exact isoforms that are most important remains unclear. As illustrated in this study, zebrafish CYP3Cs are distinctive from mammalian CYP3As in their regulatory mechanisms and appear to involve at least AhR and ER. It is likely that CYP3Cs play a role in endogenous and exogenous compound metabolism in the organism that is determined by the tissue distribution, developmental stage, and sex. Understanding the regulation and function of CYP3Cs will allow for better understanding of the zebrafish as a biomedical and toxicological model.

Sites of expression and regulation of gene expression may provide some insight on the functional roles of the orphan CYP3s. This study supports the involvement of both the AhR and ER in regulating CYP3Cs in adult zebrafish liver, intestine and gonads. The AhR ligand binding domain is rather conservative and accommodates structurally similar compounds that are commonly metabolized by the AhR target defensome genes. In this study, the AhR dependent induction of CYP3Cs in the intestine of zebrafish may suggest a role in detoxification of AhR ligands that could be introduced through diet or environmental exposure. It is interesting to speculate that this may include the planar aromatic hydrocarbons, which are well known ligands for AhR and substrates for CYP1s. Yet, gene induction after βNF exposure was modest for all but CYP3C2, where maximal induction was 30-fold over basal expression, suggesting that phenotypic changes in drug metabolism would be more likely with CYP3C2 induction.

The ER has many CYP gene targets; most of which are involved in the production and metabolism of steroids such zebrafish CYP19a (as reviewed by Callard et al 2001). In mammals, it is also well established that CYP3As are involved in metabolism of estrogens (as reviewed by Tsuchiya et al 2005). The involvement of fish CYP3As in steroid metabolism is limited but some data suggest that fish CYP3A27 and 3A45, 3A38 and 3A40 (as reviewed by Di Giulio et al 2008) and CYP3A65 (Scornaienchi et al 2010a) metabolize estrogens. Though the regulation of these enzymes is not well understood, it is apparent that, like CYP3Cs, CYP3A expression is to some extend dependent on sex (as reviewed by Di Giulio et al 2008). E_2 mediated regulation of CYP3Cs in a sex specific manner suggest that CYP3Cs are regulated by estrogens. Determining whether CYP3Cs can metabolize male and female specific steroids or steroid-like substances might be beneficial in understanding the function of CYP3Cs. Significant work would be required to test functional hypotheses regarding the CYP3C enzymes.

ACKNOWLEDGEMENTS

This research was supported by the Natural Sciences and Engineering Council of Canada (NSERC). We thank Aman Amin and Carl Lindo for their involvement with exposures and RNA extractions and all the members of the Wilson Laboratory at McMaster University for animal husbandry support.

TABLES

TABLE 2.1 qPCR primers for CYP3C, housekeeping and positive control genes in zebrafish. CYP3C, β-actin, vitellogenin, and CYP1A primers were from Shaya et al (2014), Alsop and Vijayan, (2008), Sahoo et al (2013), and Evans et al (2008), respectively. Primer sequences are shown for both forward (F) and reverse (R) strands and arranged alphabetically. The optimal annealing temperatures are given in degrees Celsius (◦C) and product length is given in base pairs (bp).

Gene	**Primer Sequence (5'-3')**	**Temp (◦C)**	**Length (bp)**
β-actin	F: TGTCCCTGTATGCCTCTGGT R: AAGTCCAGACGGAGGATGG	60	121
CYP1A	F: GCATTACGATACGTTCGATTAACCAC R: GCTCCGAATAGGTCATTGACGAT	62	120
CYP3C1	F: TCCAGACCTCTGGGAGTCTCCTAAT R: GCATGAAGGCACACTGGTTGATCT	60	89
CYP3C2	F: TAAGCATGTTTTCAAAGCCGACTGTGG R: GGTTGTTCACTTGTAGTGTCCTTCAC	62	160
CYP3C3	F: GGGAATAAGTGTGTTTTCAAGGTCAATTATGA R: GGTTGTTCACTTGTGGTGTCTTTCGC	60	165
CYP3C4	F: TGGTCGCTGACCTGGAAGTGA R: AAGGGGCCAGCCAGTCCTGT	62	100
Vitellogenin	F: GCTTTGCCTATTCCCCACATC R: GCTCTGCTGTAACGGTAGT	60	108

SUPPLEMENTARY TABLE 2.1. Fold Induction with standard error of the mean (SEM) of CYP3Cs, CYP1A in female zebrafish exposed to β-naphthoflavone (βNF) and CYP3Cs and Vitellogenin (VTG) in male and female zebrafish exposed to 17β-estradiol (E2)

		(µM)	CYP3C1		CYP3C2		CYP3C3		CYP3C4		CYP1A	
BNF Exposure	**Liver**		FOLD	SEM	FOLD	SEM	FOLD	SEM	FOLD	SEM	FOLD	SEM
		0	1.00	0.09	1.00	0.16	1.00	0.39	1.00	0.05	1.00	0.11
		0.005	1.25	0.11	1.39	0.19	1.10	0.17	1.08	0.10	1.07	0.07
		0.05	1.44	0.10	1.30	0.27	1.80	0.65	1.14	0.20	1.43	0.22
		0.2	1.32	0.17	1.38	0.19	0.97	0.18	1.52	0.16	1.06	0.12
		0.4	1.07	0.14	1.00	0.14	0.43	0.06	0.97	0.13	0.85	0.09
		0.5	0.87	0.11	1.36	0.18	0.31	0.09	0.89	0.08	0.85	0.15
		1	1.75	0.78	1.26	0.37	0.45	0.27	1.45	0.28	2.14	1.24
	Intestine											
		0	1.00	0.05	1.00	0.20	1.00	0.18	1.00	0.08	1.00	0.10
		0.005	0.95	0.11	1.11	0.24	1.39	0.31	0.82	0.05	0.85	0.15
		0.05	0.83	0.08	0.79	0.16	0.90	0.12	0.63	0.09	0.76	0.09
		0.2	1.36	0.11	7.05	1.48	1.66	0.24	1.41	0.11	1.50	0.13
		0.4	1.61	0.10	13.73	2.07	2.31	0.38	1.35	0.09	2.34	0.28
		0.5	2.33	0.19	29.39	5.37	2.33	0.28	1.54	0.11	3.38	0.32
		1	2.37	0.14	26.84	3.41	3.21	0.46	1.87	0.12	16.83	2.49
	Gonads											
		0	1.00	0.10	1.00	0.18	1.00	0.30	1.00	0.11	NA	NA
		0.005	1.96	0.19	2.29	0.26	0.84	0.11	3.62	0.60	NA	NA
		0.05	2.08	0.23	2.08	0.29	1.36	0.35	2.33	0.29	NA	NA
		0.2	2.05	0.15	2.11	0.24	1.45	0.34	3.27	0.38	NA	NA
		0.4	1.74	0.23	2.21	0.36	1.23	0.28	2.64	0.48	NA	NA
		0.5	1.56	0.37	3.23	0.68	2.10	0.39	2.76	0.52	NA	NA
		1	0.90	0.20	3.71	0.50	1.74	0.55	5.30	1.51	NA	NA
E_2 Male Exposure	**Liver**		FOLD	SEM	FOLD	SEM	FOLD	SEM	FOLD	SEM	FOLD	SEM
		0	1.00	0.62	1.00	0.46	1.00	0.45	1.00	0.40	1.00	0.92
		0.001	0.54	0.09	0.69	0.16	0.57	0.12	0.86	0.21	2.99	0.72
		0.01	0.25	0.08	0.15	0.02	1.39	1.05	0.75	0.29	3.61	1.26
		0.1	0.19	0.02	0.24	0.04	0.31	0.11	0.59	0.07	4.91	1.10
		1	0.17	0.02	0.71	0.17	0.12	0.04	0.72	0.07	7.97	1.35
		5	0.28	0.04	1.75	0.28	0.46	0.22	1.41	0.13	5.65	1.32
		10	0.18	0.04	0.48	0.24	1.05	0.62	0.86	0.22	2.73	0.51
	Intestine											
		0	1.00	0.04	1.00	0.09	1.00	0.13	1.00	0.06	NA	NA
		0.001	1.18	0.06	1.15	0.06	1.46	0.09	1.41	0.08	NA	NA
		0.01	1.39	0.08	1.28	0.10	1.37	0.15	1.48	0.09	NA	NA
		0.1	1.89	0.11	1.58	0.10	1.67	0.16	1.59	0.09	NA	NA

		1	1.79	0.20	0.41	0.05	1.01	0.11	1.74	0.14	NA	NA
		5	2.02	0.19	0.49	0.05	0.98	0.15	1.78	0.12	NA	NA
		10	2.63	0.26	0.38	0.07	2.63	0.26	3.13	0.35	NA	NA
	Gonads											
		0	1.00	0.08	1.00	0.06	1.00	0.09	1.00	0.10	NA	NA
		0.001	1.51	0.35	0.70	0.12	1.55	0.37	1.20	0.11	NA	NA
		0.01	1.37	0.16	0.77	0.13	1.88	0.38	1.48	0.13	NA	NA
		0.1	1.02	0.26	0.83	0.13	1.10	0.24	1.56	0.11	NA	NA
		1	0.32	0.05	0.63	0.04	0.47	0.05	0.99	0.05	NA	NA
		5	0.70	0.14	1.19	0.15	1.12	0.20	2.57	0.24	NA	NA
		10	0.50	0.08	0.56	0.08	0.56	0.05	1.58	0.22	NA	NA
E_2 Female Exposure	**Liver**		FOLD	SEM	FOLD	SEM	FOLD	SEM	FOLD	SEM	FOLD	SEM
		0	1.00	0.11	1.00	0.13	1.00	0.20	1.00	0.07	1.00	0.14
		0.001	1.06	0.09	0.94	0.08	1.07	0.20	1.03	0.11	2.27	0.36
		0.01	1.06	0.07	1.08	0.11	0.89	0.26	1.27	0.09	2.87	0.36
		0.1	1.12	0.18	0.86	0.09	5.50	2.64	1.98	0.19	3.07	0.65
		1	0.91	0.10	1.31	0.16	4.77	0.92	1.44	0.16	2.12	0.24
		5	1.11	0.14	1.46	0.23	2.04	0.67	3.12	0.48	2.33	0.26
		10	2.41	0.17	3.12	0.54	14.59	3.68	6.34	0.65	2.60	0.28
	Intestine											
		0	1.00	0.06	1.00	0.07	1.00	0.07	1.00	0.05	NA	NA
		0.001	0.92	0.04	1.06	0.07	0.65	0.03	1.08	0.06	NA	NA
		0.01	0.99	0.05	1.27	0.05	1.12	0.11	1.45	0.07	NA	NA
		0.1	1.31	0.06	1.30	0.11	0.85	0.09	1.58	0.10	NA	NA
		1	0.90	0.06	0.66	0.06	0.73	0.07	1.09	0.08	NA	NA
		5	1.04	0.03	0.70	0.04	0.84	0.09	1.39	0.21	NA	NA
		10	1.05	0.05	0.88	0.09	1.11	0.20	1.78	0.11	NA	NA
	Gonads											
		0	1.00	0.08	1.00	0.11	1.00	0.27	1.00	0.11	NA	NA
		0.001	0.87	0.05	0.91	0.06	1.03	0.09	1.05	0.10	NA	NA
		0.01	0.95	0.09	1.19	0.10	0.57	0.08	0.99	0.11	NA	NA
		0.1	1.34	0.11	1.24	0.11	0.71	0.09	1.50	0.19	NA	NA
		1	0.90	0.10	0.74	0.11	1.09	0.16	1.25	0.12	NA	NA
		5	0.93	0.05	1.12	0.06	0.58	0.06	1.11	0.13	NA	NA
		10	0.74	0.05	0.94	0.18	1.05	0.18	0.76	0.06	NA	NA

SUPPLEMENTARY FIGURE 2.2 Maximum fold induction (Mean ± standard error of the mean), maximum fold concentration (Max-fold concentrations, µM) and EC50 of CYP3C1-4, CYP1A and vitellogenin (VTG) gene expression in liver, intestine and gonads of zebrafish exposed to β-naphthoflavone (βNF) and 17β-estradiol (E2). EC50s calculated using APPBioquest (https://www.aatbio.com/tools/ec50-calculator, retrieved October 10, 2018). "-" EC50s could not be computed due to lack of dose response

			CYP3C1	CYP3C2	CYP3C3	CYP3C4	CYP1A
βNF Exposure	Liver						
		Maximum Fold Induction	1.78 ± 0.78	1.39 ± 0.19	1.80 ± 0.65	1.52 ± 0.16	2.14 ± 1.24
		Max-Fold Concentration	1	0.005	0.05	0.2	1
		EC50	0.271	-	-	0.012	-
	Intestine						
		Maximum Fold Induction	2.37 ± 0.14	29.39 ± 5.374	3.21 ± 0.46	1.87 ± 0.12	16.83 ± 2.49
		Max-Fold Concentration	1	0.5	1	1	1
		EC50	0.347	0.402	0.51	0.378	3.148
	Gonads						
		Maximum Fold Induction	2.08 ± 0.233	3.71 ± 0.50	2.10 ± 0.39	5.30 ± 1.52	NA
		Max-Fold Concentration	0.05	1	0.5	1	NA
		EC50	-	1.7	0.188	0.508	NA

			CYP3C1	CYP3C2	CYP3C3	CYP3C4	VTG
E_2 Male Exposure	Liver						
		Maximum Fold Induction	1.00 ± 0.622	1.745 ± 0.282	1.387 ± 1.052	1.406 ± 0.132	7.967 ± 1.349
		Max-Fold Concentration	0	5	0.01	5	1
		EC50	-	-	-	-	0.002
	Intestine						
		Maximum Fold Induction	2.63 ± 0.256	1.58 ± 0.10	2.63 ± 0.260	3.13 ± 0.348	NA
		Max-Fold Concentration	10	0.1	10	10	NA
		EC50	2.03	0.405	36.148	5.811	NA
	Gonads						
		Maximum Fold Induction	1.51 ± 0.35	1.19 ± 0.13	1.88 ± 0.38	1.56 ± 0.11	NA
		Max-Fold Concentration	0.001	5	0.01	0.1	NA
		EC50	0.117	-	0.101	0.101	NA

E_2 Female Exposure	**Liver**						
		Maximum Fold Induction	2.41 ± 0.17	3.12 ± 0.54	14.59 ± 3.68	6.34 ± 0.65	3.07 ± 0.65
		Max-Fold Concentration	10	10	10	10	0.1
		EC50	-	15.38	13.04	14	-
	Intestine						
		Maximum Fold Induction	1.31 ± 0.06	1.30 ± 0.109	1.11 ± 0.113	1.78 ± 0.111	NA
		Max-Fold Concentration	0.1	0.1	0.01	10	NA
		EC50	-	-	-	0.137	NA
	Gonads						
		Maximum Fold Induction	1.34 ± 0.114	1.24 ± 0.109	1.09 ± 0.164	1.50 ± 0.191	NA
		Max-Fold Concentration	0.1	0.1	1	0.1	NA
		EC50	-	-	-	-	NA

FIGURES

FIGURE 2.1 The induction of CYP1A and CYP3C genes in female zebrafish intestine (A), liver (B) and gonads (C) following β-naphthoflavone (βNF) exposure. CYP1A expression was not determined in gonads. Gene expression is presented as a fold change relative to the vehicle control (0.01% DMSO). Different letters (a, b, c, d, etc) above the bars indicate significant differences between treatments as tested by a One-Way ANOVA ($p<0.05$). Statistical significance of the induction of CYP3C4 in the intestine and all CYP3Cs in the gonads was tested using a One-Way ANOVA run on ranks. Error bars depict standard error of the mean.

A)

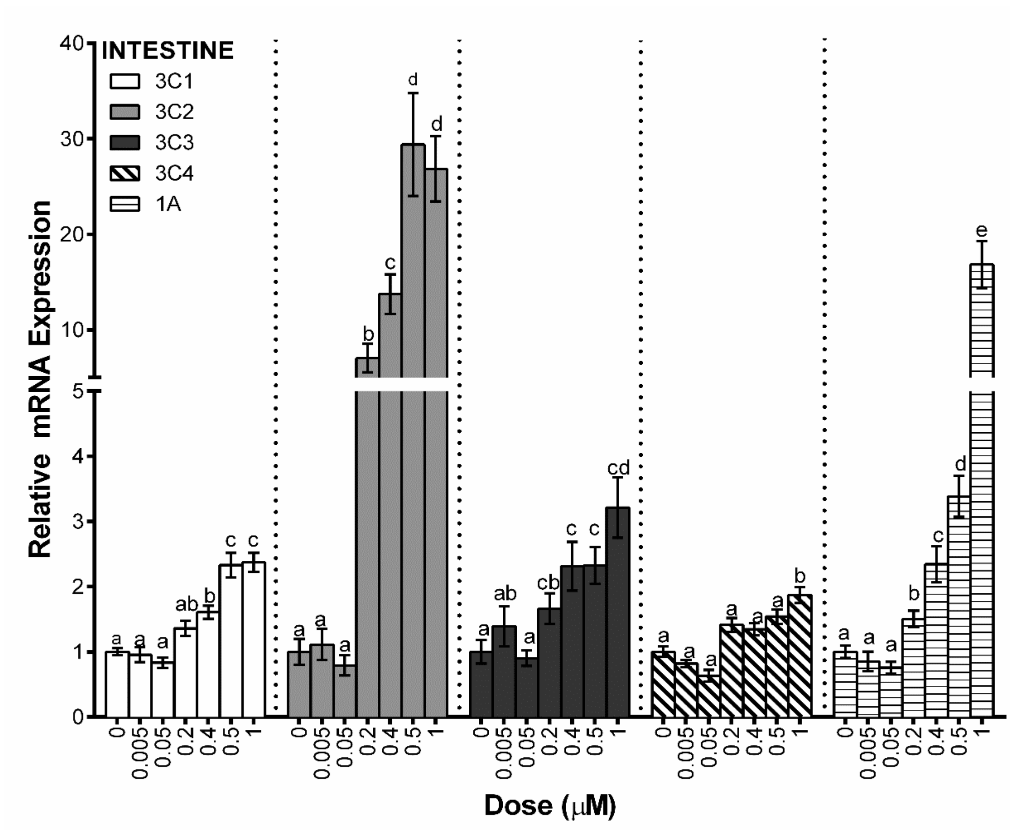
INTESTINE
3C1
3C2
3C3
3C4
1A
Relative mRNA Expression
Dose (μM)

B)

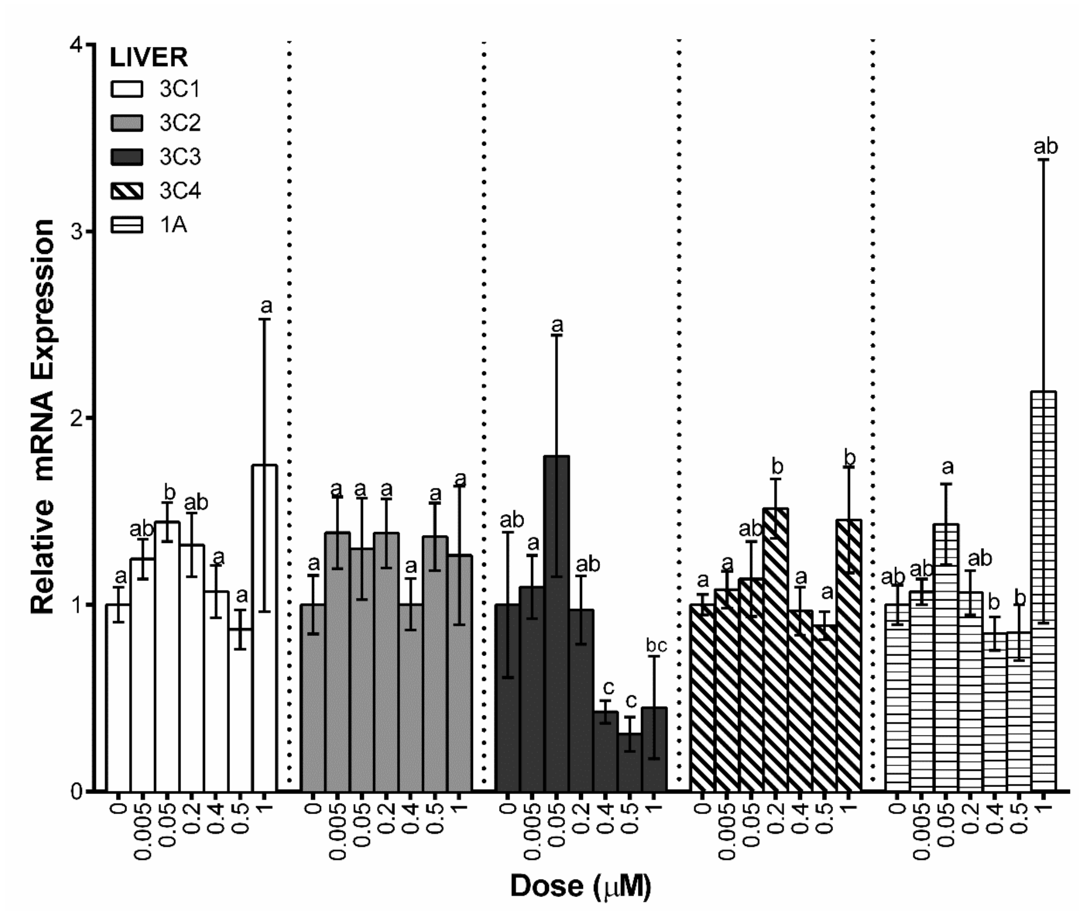
LIVER
3C1
3C2
3C3
3C4
1A
Relative mRNA Expression
Dose (μM)
0
0.005
0.05
0.2
0.4
0.5
1

C)

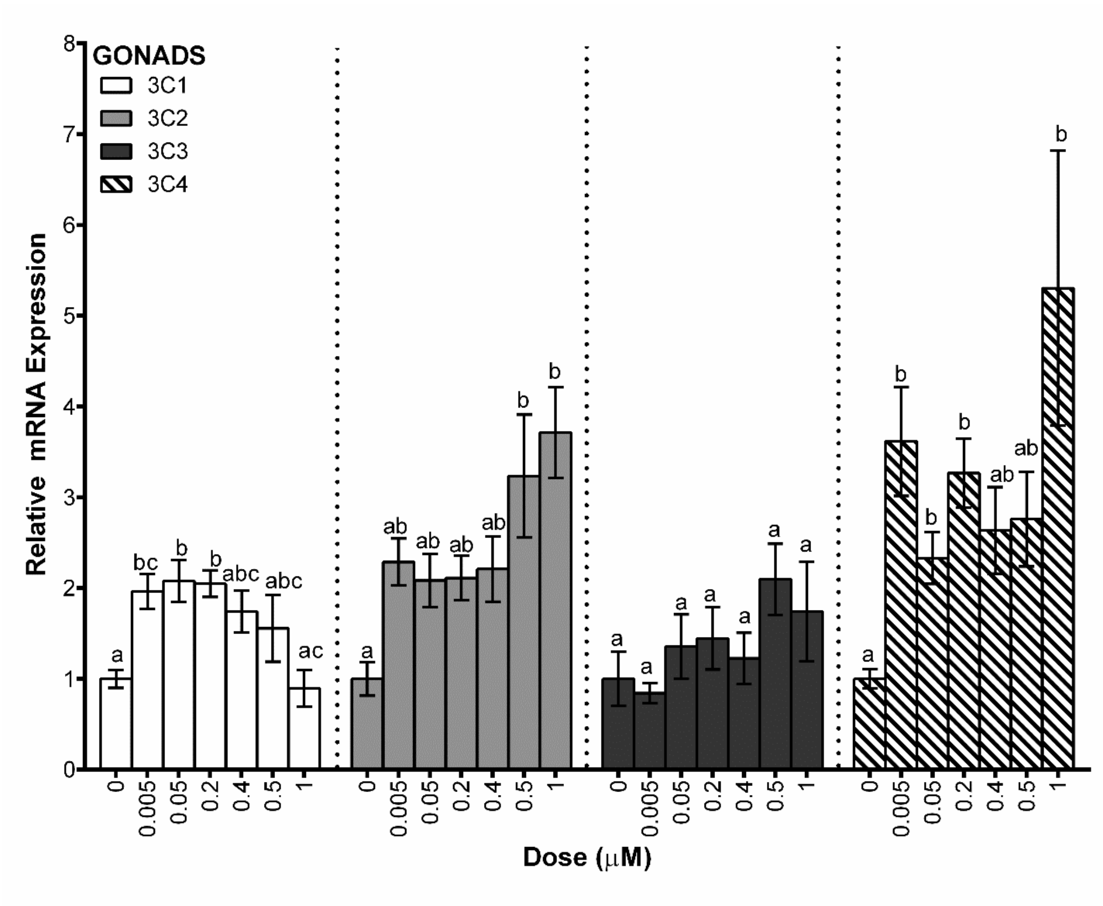

GONADS
3C1
3C2
3C3
3C4
Relative mRNA Expression
Dose (μM)
0
0.005
0.05
0.2
0.4
0.5
1
a
bc
b
b
abc
abc
ac
ab

FIGURE 2.2 The time-course of CYP1A, CYP3C1 and CYP3C3 gene induction in female zebrafish liver (A) and intestine (B) by 1 μM β-naphthoflavone (βNF). Gene expression is presented as a fold change compared to vehicle control (0.01% DMSO) for each time point. Asterisks indicate significant differences in fold induction for each time point relative to the 6-hour control as tested by a t-test ($P>0.050$).

A)

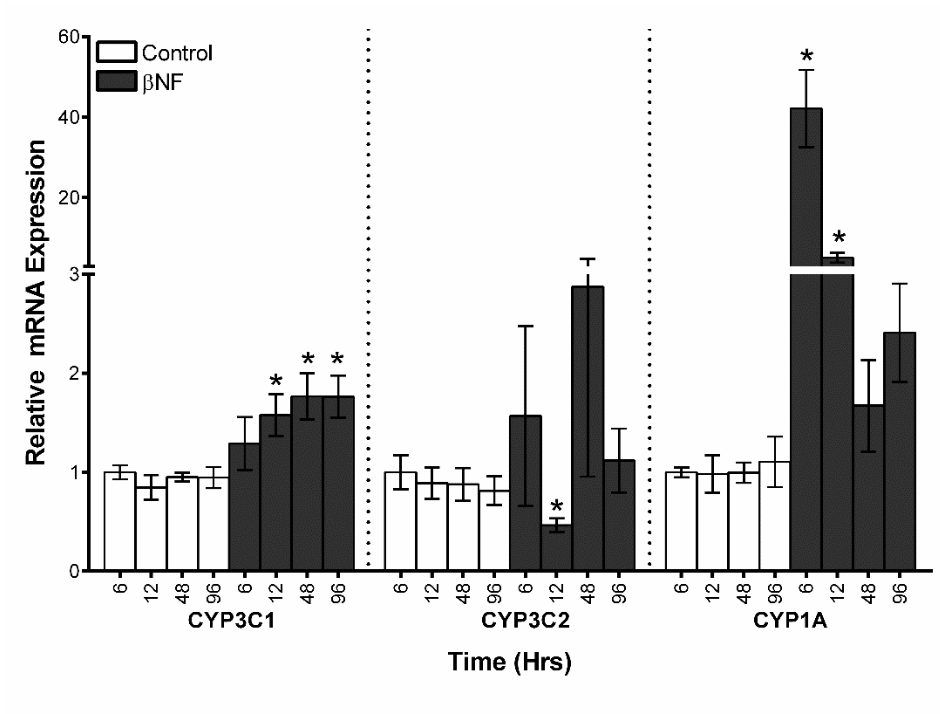
Control
βNF
Relative mRNA Expression
60
40
20
3
2
1
0
6
12
48
96
6
12
48
96
CYP3C1
CYP3C2
CYP1A
Time (Hrs)

B)

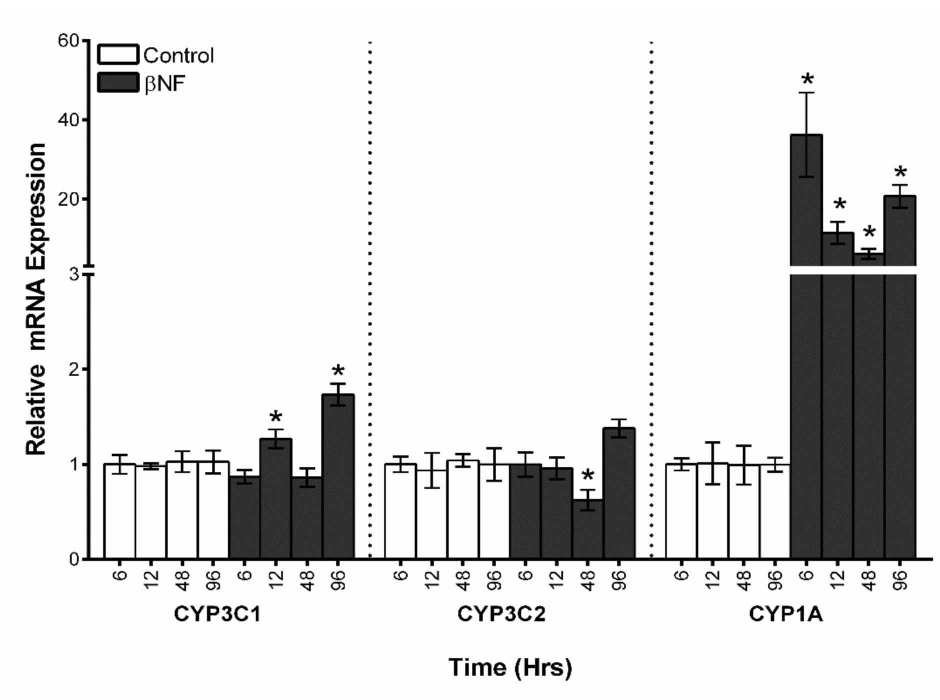
Control
βNF
Relative mRNA Expression
60
40
20
3
2
1
0
6
12
48
96
6
12
48
96
CYP3C1
CYP3C2
CYP1A
Time (Hrs)

FIGURE 2.3 Induction of Vitellogenin (VTG) and CYP3C genes in male zebrafish liver (A) and induction of CYP3C genes in intestine (B) and gonads (C) following 17 β-estradiol (E_2) exposure. Gene expression is presented as a fold change relative to the vehicle control (0.01% ethanol). Different letters (a, b, c, d, etc) above the bars indicate significant differences between treatments as tested by a One-Way ANOVA ($p<0.05$). Statistical induction of VTG and CYP3C4 in liver and CYP3C2 in gonad was tested using a One-Way ANOVA run on ranks. Error bars depict standard error of the mean. Asterisks (*) denotes treatments not included in analysis due to small sample size (n=2).

A)

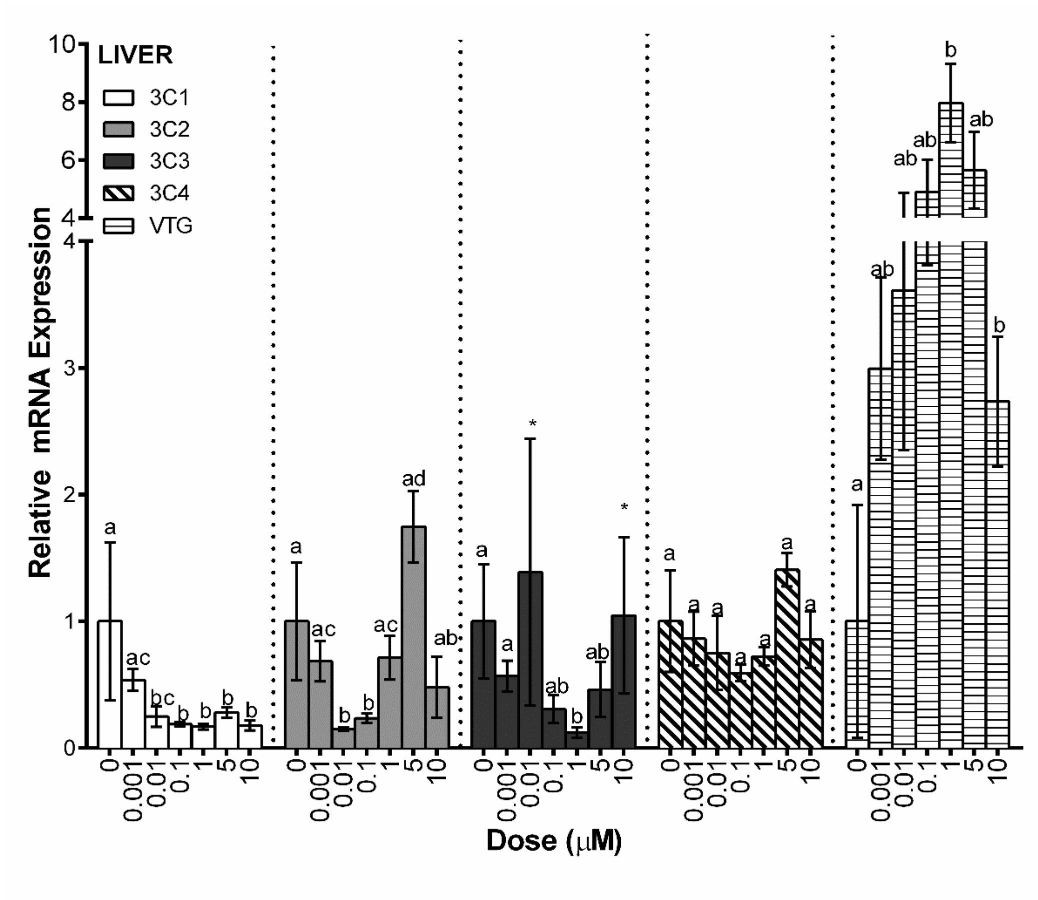

B)

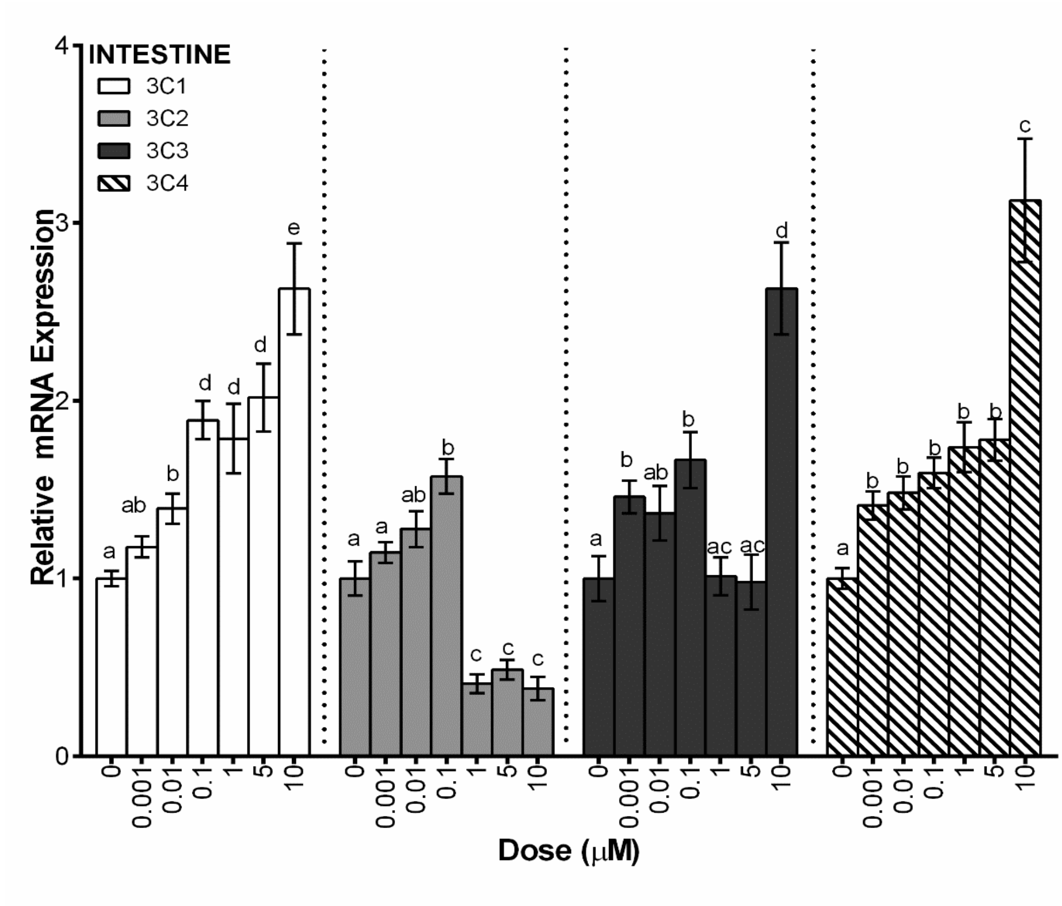

INTESTINE
3C1
3C2
3C3
3C4
Relative mRNA Expression
Dose (μM)
0
0.001
0.01
0.1
1
5
10
a
ab
b
c
d
e
ac

C)

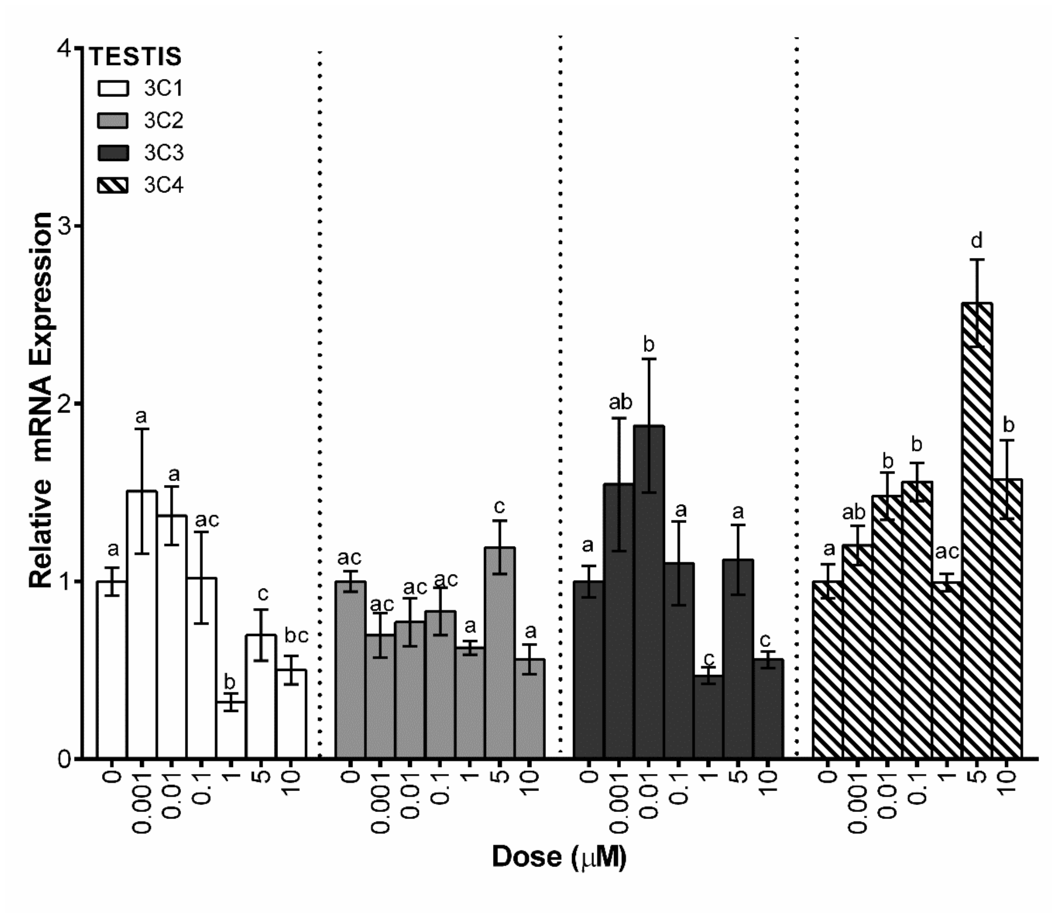
TESTIS
3C1
3C2
3C3
3C4
Relative mRNA Expression
0
1
2
3
4
a
a
a
ac
b
c
bc
ac
ac
ac
ac
a
c
a
a
ab
b
a
c
a
c
a
ab
b
b
ac
d
b
0
0.001
0.01
0.1
1
5
10
Dose (μM)

FIGURE 2.4 Induction of Vitellogenin (VTG) and CYP3C genes in female zebrafish liver (A) and induction of CYP3C genes in intestine (B) and gonads (C) following 17 β-estradiol (E_2) exposure. Different letters (a, b, c, d, etc) above the bars indicate significant differences between treatments as tested by a One-Way ANOVA ($p<0.05$) Statistical induction of CYP3C2 in intestine was tested using a One-Way ANOVA run on ranks. Error bars depict standard error of the mean.

A)

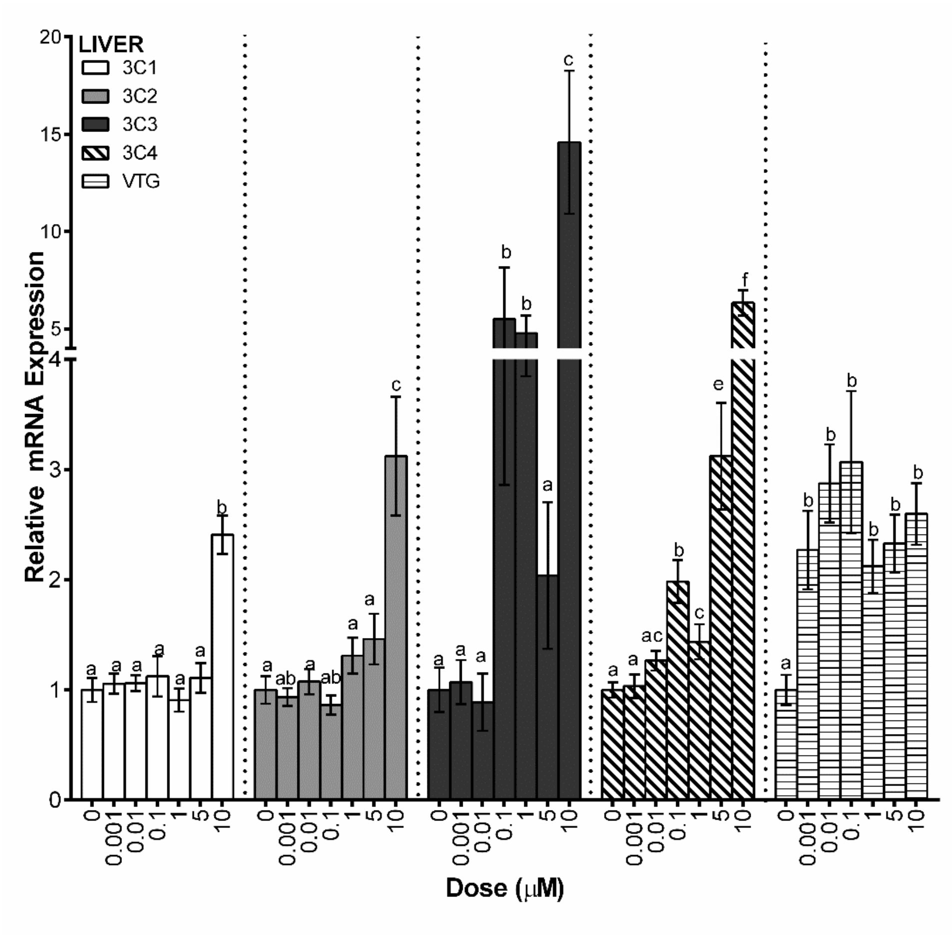
LIVER
3C1
3C2
3C3
3C4
VTG
Relative mRNA Expression
Dose (μM)
0
0.001
0.01
0.1
1
5
10

B)

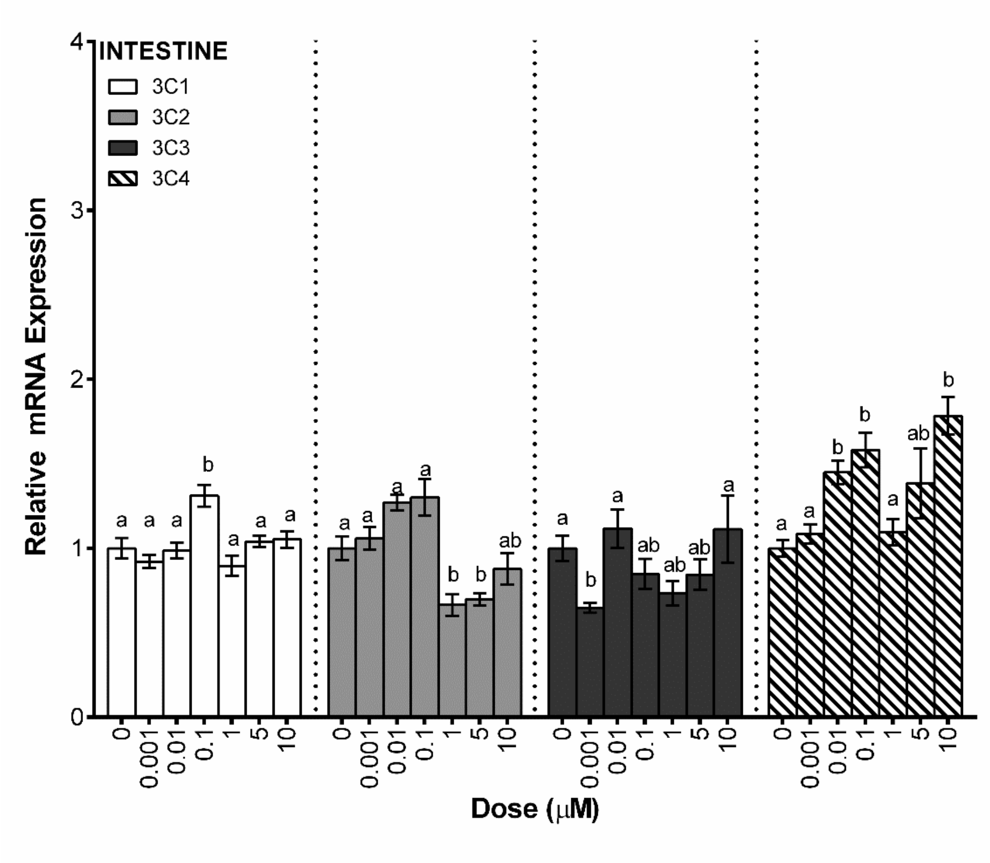
INTESTINE
3C1
3C2
3C3
3C4
Relative mRNA Expression
Dose (μM)
0
1
2
3
4
0.001
0.01
0.1
5
10
a
b
ab

C)

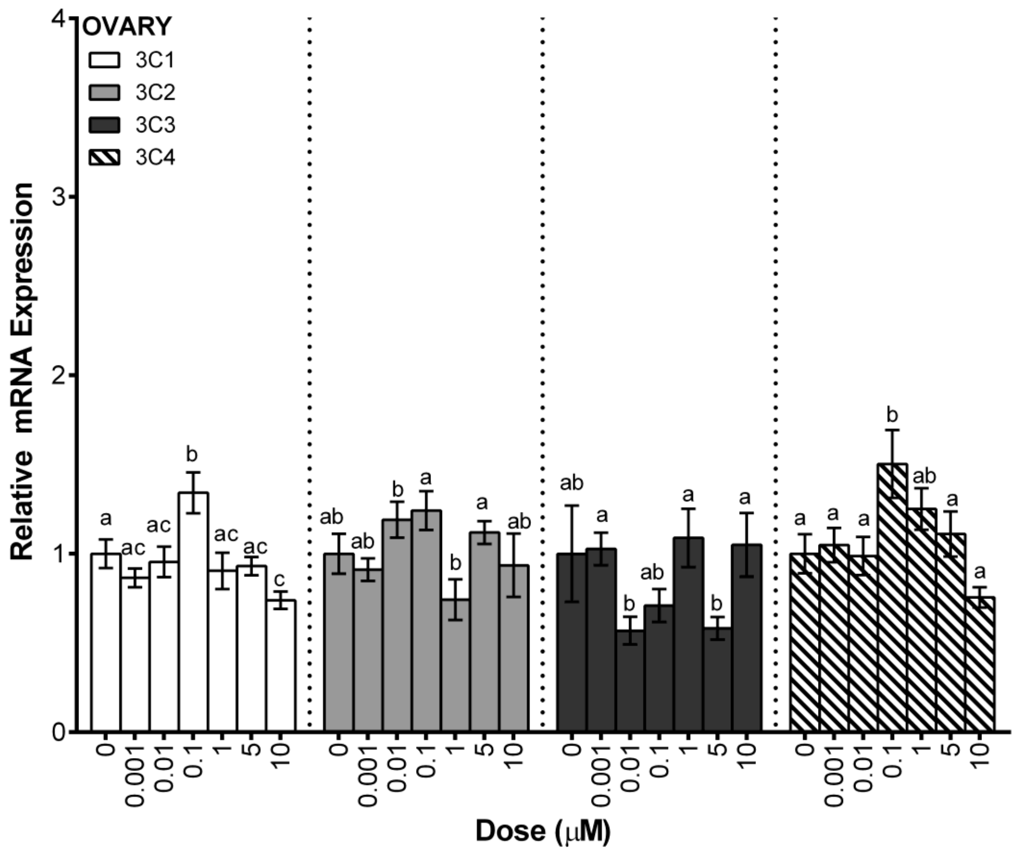
OVARY
3C1
3C2
3C3
3C4
Relative mRNA Expression
Dose (μM)
0
1
2
3
4
0.001
0.01
0.1
5
10
a
ac
b
c
ab

FIGURE 2.5 The time-course of Vitellogenin (VTG) and CYP3C gene induction in male zebrafish liver (A) and intestine (B) by 0.1 µM 17β-estradiol (E_2). Gene expression is presented as a fold change compared to vehicle control (0.01% ethanol) for each time point. Asterisks indicate significant differences in fold induction for each time point relative to the 6-hour control.

A)

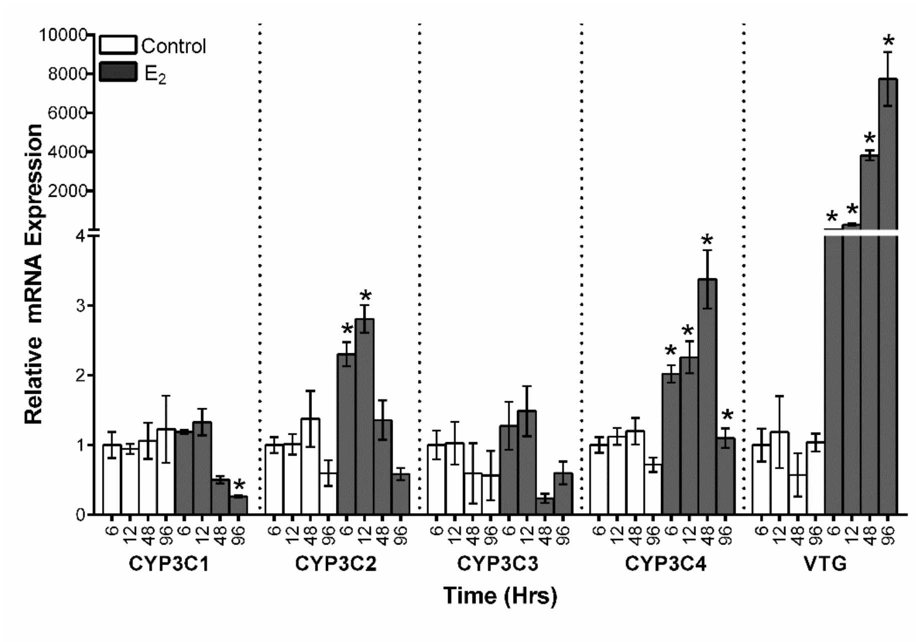
Control
E2
Relative mRNA Expression
10000
8000
6000
4000
2000
4
3
2
1
0
CYP3C1
CYP3C2
CYP3C3
CYP3C4
VTG
Time (Hrs)

B)

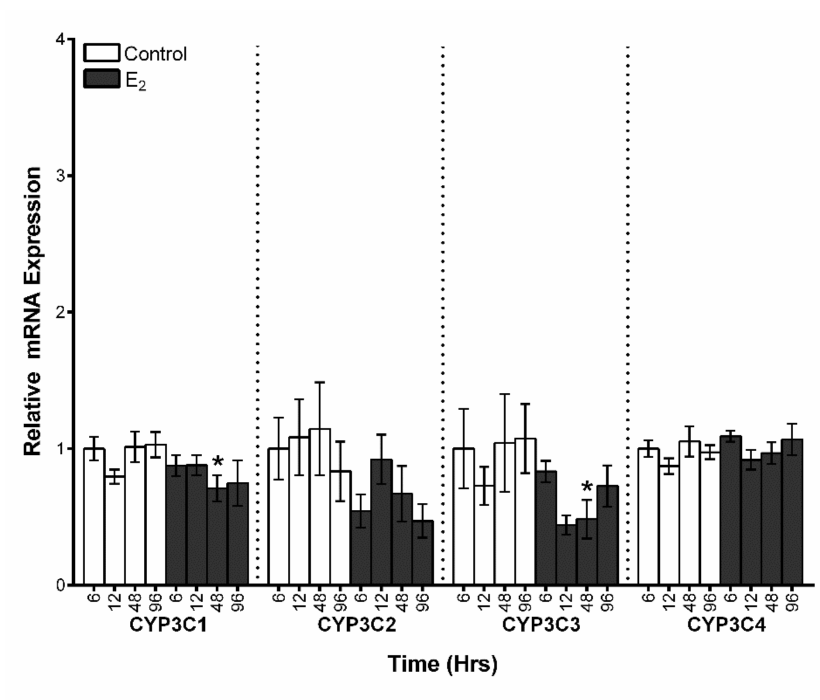
Control
E2
Relative mRNA Expression
4
3
2
1
0
CYP3C1
CYP3C2
CYP3C3
CYP3C4
Time (Hrs)

REFERENCES

Alsop D, Vijayan MM. 2008. Development of the corticosteroid stress axis and receptor expression in zebrafish. *American Journal of Physiology-Regulatory, Integrative and Comparative Physiology* 294: R711-R19

Brion F, Tyler CR, Palazzi X, Laillet B, Porcher JM, et al. 2004. Impacts of 17β-estradiol, including environmentally relevant concentrations, on reproduction after exposure during embryo-, larval-, juvenile- and adult-life stages in zebrafish (*Danio rerio*). *Aquatic Toxicology* 68: 193-217

Buhler DR, Miranda CL, Henderson MC, Yang Y-H, Lee S-J, Wang-Buhler J-L. 2000. Effects of 17β-estradiol and testosterone on hepatic mRNA/protein levels and catalytic activities of CYP2M1, CYP2K1, and CYP3A27 in rainbow trout (*Oncorhynchus mykiss*). *Toxicology and Applied Pharmacology* 168: 91-101

Callard GV, Tchoudakova AV, Kishida M, Wood E. 2001. Differential tissue distribution, developmental programming, estrogen regulation and promoter characteristics of cyp19 genes in teleost fish. *The Journal of Steroid Biochemistry and Molecular Biology* 79: 305-14

Chang C-T, Chung H-Y, Su H-T, Tseng H-P, Tzou W-S, Hu C-H. 2013. Regulation of zebrafish CYP3A65 transcription by AHR2. *Toxicology and Applied Pharmacology* 270: 174-84

Cheshenko K, Brion F, Le Page Y, Hinfray N, Pakdel F, et al. 2007. Expression of zebra fish aromatase cyp19a and cyp19b genes in response to the ligands of estrogen receptor and aryl hydrocarbon receptor. *Toxicological Sciences* 96: 255-67

Chung-Davidson Y-W, Rees CB, Wu H, Yun S-S, Li W. 2004. β-naphthoflavone induction of CYP1A in brain of juvenile lake trout (*Salvelinus namaycush* Walbaum). *Journal of Experimental Biology* 207: 1533-42

Corley-Smith GE, Su H-T, Wang-Buhler J-L, Tseng H-P, Hu C-H, et al. 2006. CYP3C1, the first member of a new cytochrome P450 subfamily found in zebrafish (*Danio rerio*). *Biochemical and Biophysical Research Communications* 340: 1039-46

Dai YJ, Jia YF, Chen N, Bian WP, Li QK, et al. 2014. Zebrafish as a model system to study toxicology. *Environmental Toxicology and Chemistry* 33: 11-17

Dalton TP, Dieter MZ, Matlib RS, Childs NL, Shertzer HG, et al. 2000. Targeted knockout of Cyp1a1 gene does not alter hepatic constitutive expression of other genes in the mouse [Ah] battery. *Biochemical and Biophysical Research Communications* 267: 184-9

Di Giulio RT, Hinton DE. 2008. *The Toxicology of Fishes*. Boca Raton: CRC Press, Taylor and Francis Group.

Evans BR, Karchner SI, Franks DG, Hahn ME. 2005. Duplicate aryl hydrocarbon receptor repressor genes (ahrr1 and ahrr2) in the zebrafish Danio rerio: structure, function, evolution, and AHR-dependent regulation in vivo. *Archives of Biochemistry Biophysics* 441: 151-670

Finnström N, Bjelfman C, Söderström T, Smith G, Egevad L, et al. 2001. Detection of cytochrome P450 mRNA transcripts in prostate samples by RT-PCR. *European Journal of Clinical Investigation* 31: 880-86

Gu Y-Z, Hogenesch JB, Bradfield CA. 2000. The PAS superfamily: sensors of environmental and developmental signals. *Annual Review of Pharmacology and Toxicology* 40: 519-61

Guengerich FP. 1999. Cytochrome P-450 3A4: regulation and role in drug metabolism. *Annual Review of Pharmacology and Toxicology* 39: 1-17

Guengerich FP, Tang Z, Salamanca-Pinzón SG, Cheng Q. 2010. Characterizing proteins of unknown function: orphan cytochrome p450 enzymes as a paradigm. *Molecular Interventions* 10: 153

Hahn ME, Merson RR, Karchner SI. 2005. Xenobiotic receptors in fish: Structural and functional diversity and evolutionary insights. *Biochemistry and Molecular Biology of Fishes* 6: 191-228

Hao R, Bondesson M, Singh AV, Riu A, McCollum CW, et al. 2013. Identification of estrogen target genes during zebrafish embryonic development through transcriptomic analysis. *PLOS ONE* 8: e79020

Heckmann L-H, Sørensen PB, Krogh PH, Sørensen JG. 2011. NORMA-Gene: A simple and robust method for qPCR normalization based on target gene data. *Bmc Bioinformatics* 12: 250

Husoy A-M, Myers MS, Willis ML, Collier TK, Celander M, Goksoyr A. 1994. Immunohistochemical localization of CYP1A-like and CYP3A-like isozymes in hepatic and extrahepatic tissues of Atlantic cod (*Gadus morhua L*), a marine fish. *Toxicology and Applied Pharmacology* 129: 294-308

Jönsson ME, Orrego R, Woodin BR, Goldstone JV, Stegeman JJ. 2007b. Basal and 3,3,'4,4',5-Pentachlorobiphenyl-Induced Expression of Cytochrome P450 1A, 1B and 1C Genes in Zebrafish. *Toxicology and Applied Pharmacology* 221: 29-41

Kloepper-Sams P, Stegeman J. 1994. Turnover of hepatic microsomal cytochrome P4501A protein and heme in beta-naphthoflavone-induced *Fundulus heteroclitus*. *Molecular Marine Biology and Biotechnology* 3: 171-83

Kraus P, Xing X, Lim SL, Fun ME, Sivakamasundari V, et al. 2012. Mouse strain specific gene expression differences for illumina microarray expression profiling in embryos. *BMC Research Notes* 5: 232

Kubota A, Goldstone JV, Lemaire B, Takata M, Woodin BR, Stegeman JJ. 2015. Role of pregnane X receptor and aryl hydrocarbon receptor in transcriptional regulation of pxr, CYP2, and CYP3 genes in developing zebrafish. *Toxicological Sciences* 143: 398-407

Lee S-J, Wang-Buhler J-L, Cok I, Yu T-S, Yang Y-H, et al. 1998. Cloning, sequencing, and tissue expression of CYP3A27, a new member of the CYP3A subfamily from embryonic and adult rainbow trout livers. *Archives of Biochemistry and Biophysics* 360: 53-61

Levi L, Pekarski I, Gutman E, Fortina P, Hyslop T, et al. 2009. Revealing genes associated with vitellogenesis in the liver of the zebrafish (*Danio rerio*) by transcriptome profiling. *BMC Genomics* 10: 141-41

Nebert DW, Russell DW. 2002. Clinical importance of the cytochromes P450. *The Lancet* 360: 1155-62

Nelson DR, Nebert DW. 2018. Cytochrome P450 (CYP) gene superfamily.In *eLS,* John Wiley & Sons, Ltd (Ed). doi:10.1002/9780470015902.a0005667.pub3

Pinot F, Beisson F. 2011. Cytochrome P450 metabolizing fatty acids in plants: characterization and physiological roles. *The FEBS Journal* 278: 195-205

Rose J, Holbech H, Lindholst C, Norum U, Povlsen A, et al. 2002. Vitellogenin induction by 17beta-estradiol and 17alpha-ethinylestradiol in male zebrafish (*Danio rerio*). *Comp Biochem Physiol C Toxicol Pharmacol* 131: 531-9

Rosenbrock H, Hagemeyer CE, Ditter M, Knoth R, Volk B. 2001. Identification, induction and localization of cytochrome P450s of the 3A-subfamily in mouse brain. *Neurotoxicity Research* 3: 339-49

Sahoo TP, Oikari A. 2014. Use of early juvenile zebrafish Danio rerio for in-vivo assessment of endocrine modulation by xenoestrogens. *Journal of Environmental and Analytical Toxicology* 4: 1-13

Scornaienchi ML, Thornton C, Willett KL, Wilson JY. 2010. Cytochrome P450-mediated 17β-estradiol metabolism in zebrafish *(Danio rerio*). *Journal of Endocrinology* 206: 317-25

Shaya L, Dejong C, Wilson JY. 2014. Expression patterns of cytochrome P450 3B and 3C genes in model fish species. *Comparative Biochemistry and Physiology Part C: Toxicology and Pharmacology* 166:115-125

Timme-Laragy AR, Cockman CJ, Matson CW, Di Giulio RT. 2007. Synergistic induction of AHR regulated genes in developmental toxicity from co-exposure to two model PAHs in zebrafish. *Aquatic Toxicology* 85: 241-50

Tseng H-P, Hseu T-H, Buhler DR, Wang W-D, Hu C-H. 2005. Constitutive and xenobiotics-induced expression of a novel CYP3A gene from zebrafish larva. *Toxicology and Applied Pharmacology* 205: 247-58

Tsuchiya Y, Nakajima M, Yokoi T. 2005. Cytochrome P450-mediated metabolism of estrogens and its regulation in human. *Cancer Letters* 227: 115-24

Uno T, Ishizuka M, Itakura T. 2012. Cytochrome P450 (CYP) in fish. *Environmental Toxicology and Pharmacology* 34: 1-13

Van den Bos R, Mes W, Galligani P, Heil A, Zethof J, et al. 2017. Further characterisation of differences between TL and AB zebrafish (*Danio rerio*): Gene expression, physiology and behaviour at day 5 of the larval stage. *PLOS ONE* 12: e0175420

Wang H, Tan JT, Emelyanov A, Korzh V, Gong Z. 2005. Hepatic and extrahepatic expression of vitellogenin genes in the zebrafish, *Danio rerio*. *Gene* 356: 91-100

Waxman DJ, Holloway MG. 2009. Sex differences in the expression of hepatic drug metabolizing enzymes. *Molecular Pharmacology* 76: 215-28

Williams ET, Leyk M, Wrighton SA, Davies PJA, Loose DS, et al. 2004. Estrogen regulation of the cytochrome P450 3A subfamily in humans. *Journal of Pharmacology and Experimental Therapeutics* 311: 728

Yan J, Cai Z. 2010. Molecular evolution and functional divergence of the cytochrome P450 3 (CYP3) family in Actinopterygii (ray-finned fish). *PLoS One* 5: e14276

Zanette J, Jenny MJ, Goldstone JV, Woodin BR, Watka LA, et al. 2009. New cytochrome P450 1B1, 1C2 and 1D1 genes in the killifish *Fundulus heteroclitus*: Basal expression and response of five killifish CYP1s to the AHR agonist PCB126. *Aquatic Toxicology* 93: 234-43

Zanger UM, Schwab M. 2013. Cytochrome P450 enzymes in drug metabolism: Regulation of gene expression, enzyme activities, and impact of genetic variation. *Pharmacology and Therapeutics* 138: 103-41

Zon LI, Peterson RT. 2005. In vivo drug discovery in the zebrafish. *Nature Reviews Drug Discovery* 4: 35-44

CHAPTER 3

HIGH THROUGHPUT SCREENING OF SMALL BIOACTIVE COMPOUNDS FOR SUBSTRATES OF ZEBRAFISH (*DANIO RERIO*) CYP3C1

ABSTRACT

The Cytochrome P450 family 3 (CYP3) enzymes are some of the most important detoxification enzymes in vertebrates. Mammalian CYP3 enzymes are responsible for metabolism of xenobiotic and endogenous compounds such as hormones, vitamins, fatty acids, eicosanoids and prostaglandins. Human CYP3s, all of which are from the CYP3A subfamily, are critical in the biotransformation of ≥ 50% of pharmaceuticals. Teleost fish have a diversified CYP3 family that includes the CYP3A, 3B, 3C, and 3D subfamilies; the zebrafish genome contains a single CYP3A and four CYP3C genes. The functions of fish CYP3s are very poorly characterized. In this study, zebrafish CYP3C1 has been heterologously expressed and the catalytic activity of the enzyme has been examined using synthetic fluorogenic compounds and a high throughput screen. CYP3C1 metabolized all the tested alkyloxy-resorufin substrates; the greatest and lowest catalytic activity was with 7-methoyxresorufin (7-MR; 1385±765 pmol nmol P450^{-1} min^{-1}) and 7-benzyloxyresorufin (7- BR; 96±19 pmol nmol P450^{-1} min^{-1}), respectively. 7-BR had the smallest K_M (0.38±0.17 pmol nmol P450^{-1} min^{-1}). CYP3C1 was capable of 7-benzyloxy-4-trifluoromethylcoumarin (BFC) and dibenzylfluorescein (DBF) metabolism but not other coumarin substrates. CYP3C1 had comparable activity for BFC and 7-MR but BFC had a higher affinity for CYP3C1 (K_M=9.25±2.18 µM). That CYP3C1 has significant overlap in activity with CYP1s and CYP3A65 for fluorogenic probe substrates, reinforces

the lack of specificity of these substrates for fish CYPs. The high throughput screen was based on measuring the rate of NADPH cofactor depletion by CYP3C1 for ~4000 small, bioactive compounds from commercially available libraries. The high throughput screen identified 200 compounds with NADPH depletion above background and 132 compounds with at least 20% of the activity found with MR. The top substrates, such as plumbagin, menadione, idebenone, NSC 95397 and β-lapachone, were predominantly pharmacologically active quinone compounds and all had high rates of NADPH depletion, low production of reactive oxygen species, low K_m for NADPH depletion, and low IC_{50} values for inhibition of BFC metabolism, possibly reflecting a high affinity for the CYP3C1 enzyme. The high throughput screen has identified the metabolism of pharmacologically active quinone compounds as potentially important for CYP3C1 enzyme function.

INTRODUCTION

Cytochrome P450 (CYP) enzymes are a superfamily of proteins that are critical for the metabolism of many endogenous and exogenous compounds. In vertebrates, CYP enzymes are involved in homeostatic functions like the break down of fatty acids, steroids and prostaglandins. In general, CYPs catalyze a monooxygenase reaction that results in a more hydrophilic metabolite that can be more easily eliminated in urine or feces. This property allows CYPs to play an important role in the detoxification processes of xenobiotics like pharmaceuticals.

The cytochrome P450 active site contains a heme moiety with an iron that is initially in the ferric state (Fe^{+3}). The binding of the substrate to the active site triggers the reduction of nicotinamide adenine dinucleotide phosphate hydrogen (NADPH) by cytochrome P450 reductase (CPR; as reviewed by Guengerich 2001) and two serial electron donations to the catalytic reaction that results in the formation of water and, primarily, hydroxylation of the substrate (as reviewed by Denisov et al 2005). If reactions are not tightly coupled, CYP reactions can consume NADPH but produce reactive oxygen species (ROS), such as superoxides and peroxides, with little to no product formation (as reviewed by Denisov et al 2005). The catalytic reactions that result in the formation of significant ROS are considered uncoupled reactions. Cytochrome P450s that are commonly involved in xenobiotic detoxification often undergo uncoupled reactions (as reviewed by Denisov et al 2005).

CYP nomenclature is based on amino acid identity; CYPs with a sequence similarity of ≥40% are grouped in the same family while CYP subfamilies share ≥55% similarity (Nelson 2006). Advances in genomic sequencing has resulted in the identification of >55,000 named cytochrome P450s (Nelson & Nebert 2018) many of whom are "orphans" with unknown function (Guengerich & Cheng 2011). Of the many CYP families, the CYP3 family garners attention for its critical role in xenobiotic metabolism. Specifically, the CYP3 family in humans is the most important enzyme family in xenobiotic metabolism and is well known for biotransformation of >50% of all pharmaceuticals, most of which are structurally unrelated (as reviewed by Zanger & Schwab 2013). All vertebrates contain one or more CYP3 enzymes and their critical role in defense and homeostasis makes this family very relevant and important in toxicology and biomedical research.

In mammals, CYP3 genes are in only one subfamily (CYP3A), but teleost fish are much more diversified. The CYP3A, CYP3B, CYP3C and CYP3D subfamilies are all found in various teleost species (Yan & Cai 2010). The zebrafish (*Danio rerio)* contain one CYP3A gene (CYP3A65) and four CYP3C genes (CYP3C1, CYP3C2, CYP3C3, CYP3C4; Yan & Cai 2010). Evolutionary studies suggest that teleost CYP3A genes are more closely related to other the genes in the other teleost CYP3 subfamilies and that CYP3A genes in fish are paralogous to each other and co-orthologs of mammalian CYP3A genes (Nelson et al 2013, Yan & Cai 2010). Collectively, this raises significant questions about the functions of teleost CYP3s, where multiple paralogs may have some shared and distinct functions from mammalian CYP3As. To date, the suite of CYP3 enzymes are very poorly understood in fish, yet they may provide important data to understand CYP3 family function and evolution. The zebrafish is important for pharmacology/toxicology, physiology, neuroscience/behaviour and developmental research with significant use as a model species for other fish and biomedical research. Characterizing the function of CYP3s in zebrafish will provide important data on CYP function and biotransformation in a critical model species.

To date only a small number of studies have investigated the expression (Corley-Smith et al 2006, Shaya et al 2014) and regulation (Corley-Smith et al 2006, Kubota et al 2015, Shaya et al 2014) of zebrafish CYP3Cs. Quantitative analysis of zebrafish CYP3C1 – CYP3C4 genes indicate the genes have wide expression across many organs (Shaya et al 2014) including detoxification organs like the liver and intestine (Corley-Smith et al 2006, Shaya et al 2014). Of the CYP3C genes, CYP3C1 was most highly constitutively expressed in liver (Shaya et al 2014). The regulation of fish CYP3 is not well characterized but data are emerging to implicate multiple transcription factors. There is evidence to suggest that zebrafish CYP3C1 is regulated by pregnane-x-receptor (Kubota et al 2015), the aryl hydrocarbon receptor (Kubota et al 2015, Shaya et al 2019) and the estrogen receptor (Shaya et al 2019). Collectively, this suggests a potential role for CYP3Cs in detoxification yet, functional testing is required to investigate this hypothesis and elucidate the function of CYP3Cs in zebrafish.

In this study, we heterologously expressed CYP3C1 in *Escherichia coli* (*E.coli*) and determined the catalytic activity of CYP3C1 for a suite of fluorogenic CYP probe substrates and in a high throughput screen with ~4000 bioactive compounds from commercially available compound libraries. A high throughput approach was thought to provide significant novel data toward determining a function for CYP3C1, in light of the fact that functional data was entirely lacking and substrates of mammalian CYP3A lack a structure activity relationship (Ekroos & Sjögren 2006). The commercial libraries consisted of steroids, natural products and pharmaceuticals. CYP3C1 was hypothesized to metabolize many compounds in the library, mostly likely favouring pharmaceutical compounds due to the close evolutionary relationship between mammalian CYP3A and fish CYP3 enzymes.

MATERIALS AND METHODS

CYP3C1 Heterologous Expression

To ensure appropriate targeting of the zebrafish CYP3C1 (NM_212673.1) protein in bacterial membranes, the outer membrane protein (NC_000913.3) signal sequence (OmpA(2+)), consisting of 69 nucleotides of the *E. coli* outer membrane gene, was placed 5' prime to the CYP3C1 sequence, as has been previously used to produce active CYP enzymes (Pritchard et al 1997, Scornaienchi et al 2010a, Scornaienchi et al 2010b). The OmpA(2+)-CYP3C1 construct was synthesized by Integrated DNA Technologies (IDT; Skokie, IL). Constructs included a *Nde*I and a *Sal*I enzyme restriction site on the 5'and 3' end, respectively. The construct (50ng) was tailed for T/A cloning using Platinum Taq Polymerase (Invitrogen, Carlsbad, CA) following IDT's protocol. Tailed constructs were cloned into pGEM-T Easy vectors (Promega, Madison, WI) and transformed into *E. coli* JM109 cells (Promega, Madison, WI) following manufacturer's protocol. Plasmids were purified by PureLink Quick Plasmid Miniprep Kit (Invitrogen, Carlsbad, CA) and sequenced by Mobix Lab (McMaster University, Hamilton, ON) to verify sequence.

pGEM-T plasmids containing the OmpA(2+)-CYP3C1 construct were digested using *Nde*I and *Sal*I restriction enzymes (Invitrogen, Waltham, MA), gel purified by PureLink Quick Plasmid Gel Extraction Kit (Invitrogen, Waltham, MA), and ligated into the pCW vector and co-transformed with the pACYC vector containing human cytochrome P450 reductase (CPR) into *E.coli* JM109 cells. A sample was grown overnight at 37°C on Luria-Bertani (LB) agar plates supplemented with ampicillin (50 μg mL^{-1}) and chloramphenicol (25 μg mL^{-1}). A single colony was grown overnight in supplemented LB-broth. The sample was purified by PureLink Quick Plasmid Miniprep Kit (Invitrogen, Carlsbad, CA) and successful co-transformations were confirmed using PCR and restriction enzyme digestions with gel electrophoresis (data not shown); gel electrophoresis showed bands of the size matching the empty pCW vector and the CYP3C1 construct, bands matching the pCW vector ligated to CYP3C1, as well as the pACYC vector containing human cytochrome P450 reductase (CPR).

Cultures of the co-transformed (CYP3C1 + CPR) bacteria were grown in Terrific Broth (TB) supplemented with ampicillin (50 μg^{-1}mL), chloramphenicol (25 μg^{-1}mL), and thiamine (1mM). Once the culture had reached an appropriate density (OD600 of ~0.8) it was supplemented with isopropyl B-D-1-thiogalactopyranoside (IPTG; 1mM; Fisher Scientific, Pittsburgh, PA) and δ-aminolevulinic acid (0.5mM ALA; MP Biomedicals, Solon, OH). ALA was used to maximize the incorporation of the heme to ensure active enzyme. The cultures were incubated for 22 hours before cells were harvested and the membranes were purified as previously described (Pritchard et al 2006). Total protein content was determined using a bicinchoninic acid protein assay kit as per manufacturer's protocol (Thermo Scientific, Rockford, IL).

Total P450 Analysis and Cytochrome P450 Reductase Activity

Total P450 content was measured using a carbon monoxide (CO) difference spectral assay (Pritchard et al 2006) and calculated based on the extinction coefficient of $92mM^{-1}cM^{-1}$ (Omura & Sato 1964). Cytochrome P450 reductase activity was measured using NADH (5 mg mL^{-1} ; Sigma Aldrich, St Louis, MO) and cytochrome c (1 mg mL^{-1} from bovine; Sigma Aldrich, St Louis, MO) in 0.2 M potassium phosphate buffer at 37°C by determining increasing absorbance at 550nM over time (Pritchard et al 2006). Cytochrome P450 reductase activity was normalized for total protein content and calculated based on the extinction coefficient of 21 $mM^{-1}cm^{-1}$ (Massey 1959).

Fluorescent Catalytic Assays

CYP3C1 catalytic activity, K_M and V_{max} was determined for 10 synthetic fluorogenic probe substrates with known specificity for mammalian CYPs (Table 1; Murray et al 2001, Scornaienchi et al 2010b, Stresser et al 2002). All fluorogenic substrates were purchased from Sigma Aldrich (St Louis, MO). 7-ethoxyresorufin (7-ER), 7-methyoxyresorufin (7-MR), 7-benzyloxyresorufin (7-BR) and 7-pentoxyresorufin (7-PR) substrates were resuspended in dimethysulfoxide (DMSO). 3-[2-(N,N-diethyl-Nmethylamino)ethyl]-7-methoxy-4-methylcoumarin (AMMC), 7-methoxy-4-

(aminomethyl)-coumarin (MAMC), 7-benzyloxy-4(trifluoromethyl)coumarin (BFC), 7-benzyoxyquinoline (BQ), dibenzylfluorescein (DBF), and 7-methyoxy-trifluoromethylcoumarin (MFC) were resuspended in acetonitrile and sonicated for 30 seconds, on ice. The resorufin substrates reactions were run at 30°C in 40mM Tris HCl, 80mM NaCl; pH 7.8. All other substrates were run at 30ºC in 0.4M $KP0_4$ buffer at pH 7.4. All reactions were initiated with 1.33mM NADPH. A Michaelis-Menten curve was generated by measuring the catalytic activity on a Synergy 2 fluorimeter (BioTek, Winooski, VT), at various concentrations of substrate, over 15 minutes, and at appropriate excitation and emission. Substrate concentrations for each assay are summarized in Table 1. Catalytic activity was normalized to the total P450 content in each reaction. K_M and V_{max} values and respective standard error values were generated from fitting the Michaelis-Menten curve using an online tool (http://www.ic50.tk/kmvmax.html).

High Throughput Screening Assay Design: NADPH Depletion

The rate of NADPH depletion by CYP3C1 was used to assess catalytic activity for bioactive substrates from commercially available libraries including Prestwick, Microsource Spectrum, Library of Pharmacologically Active Compounds (LOPAC) and BioMol Natural Products Library (BioMol). Screens were performed at the Centre for Microbial Chemical Biology (McMaster University, Hamilton, ON). Prior to high throughput screening, the NADPH depletion assay was optimized for CYP3C1 with 7-MR using 1-3% DMSO, various concentrations of enzyme, temperature, light sensitivity and miniaturization of reaction volume. The Michaelis-Menten curve was developed for

CYP3C1 catalytic activity with 7-MR (Figure 3A) to determine an appropriate substrate concentration for the high throughput reactions. 50 µL reactions were run in 384 well plates, containing 41.5mM Tris-HCL, 83mM NaCl, 20 µM substrate in DMSO (2% v/v), 150 µM NADPH, and initiated with 2.96 µg of purified CYP3C1 membranes. Prior to high throughput screening, a Z-prime (Z') was calculated to assess the quality of the assay conditions chosen. The Z' is a statistical tool that measures the signal window by taking into consideration the mean and standard deviations of the positive control and negative controls. In this case, the positive and negative controls were the rate of NADPH depletion for CYP3C1 and 2% DMSO, with or without 20µM 7-MR, respectively. An acceptable Z' for a high throughput assay must be between 0.5 – 1; the closer to 1, the better the quality of the assay. The Z' prime was calculated at 0.76 from a single 384 well plate where half the wells contained the positive control and the other half contained negative controls (data not shown).

For the primary high throughput screen, each reaction was run twice, on replicate plates. Reactions were plated by Biomek® FXP Integrated Liquid Handler (Beckman Coulter, Indianapolis, IN). All experimental plates contained 32 positive controls (7-MR) and 32 negative controls (DMSO only) to ensure assay quality throughout the duration of the screen. For all assay plates, the change in absorbance at 355 nM was measured, using EnVision Multilabel Plate Reader (Perkin Elmer, Hopkinton, MA), every 2 minutes for a 10-minute duration, providing an 8-point curve. A rate was obtained from the curve for each of the wells in the 384 well plate. Rates of NADPH depletion in each well were calculated and normalized for total P450. The background was measured from the negative control wells (no substrate) and hits were defined as those whose rate of NADPH depletion was 3 times the standard deviations above the mean rate of NADPH depletion of the negative control (lowest limit of detection; LOD). Data for NADPH depletion are presented as a percent rate of the positive control.

Due to a technical error, 2 compound plates (containing 640 compounds) had one of the replicate plates run with double the concentration of substrate and DMSO (40 μM; 4% v/v DMSO). To account for differences in NADPH depletion at different substrate and DMSO concentrations across replicates, compounds were considered a hit if the rate of NADPH in either replicate 1 or replicate 2 met the cut-off (>LOD). Both replicate values are reported separately (Table 2).

The top 132 hits, based on the highest rate of NADPH depletion, were selected for a secondary screen to determine if the catalytic activity was protein dependent and reactive oxygen species generation (described below) to detect highly uncoupled reactions. Reactions were assessed for enzyme independent NADPH depletion by repeating reactions as described above but in the absence of the enzyme; the enzyme was replaced with an equal volume of buffer. Those reactions with significant NADPH depletion in absence of protein were considered false positives.

Reactive Oxygen Species (ROS) 2’7’ Dichlorofluorescin Probe Assay

The top 132 hits were assessed for reactive oxygen species (ROS) generation using the fluorogenic probe dichlorofluorescin (DCF). In the presence of ROS, DCF is converted to the fluorescent product, fluorescein, and can be measured spectrophotometrically. The DCF assay was done following previously described methods (LeBel et al 1992) but optimized for a 50 µL reaction. In this assay, 1mM of 2’7’-dichlorofluorescin diacetate (DCFH-DA; Sigma Aldrich, St Louis, MO) underwent deesterification to DCFH. Deesterfication was performed daily for use in the ROS assay. Reactions were plated into 384 well plates by BiomekFXP Integrated Liquid Handler (Bechman Coulter, Indianapolis, IN) and all assay conditions were as previously described for NADPH depletion except that reactions were initiated with CYP3C1 purified membranes in buffer containing DCFH. Each 384 well plate contained 32 positive controls. The rate of ROS formation between CYP1A and 7-PR, reactions that have been established as highly uncoupled (Harskamp et al 2012), served as a positive control. Plates also contained negative controls of CYP1A with 2% DMSO to provide a measure of background rates of fluorescence. Fluorescent activity was monitored for 15 minutes using a Synergy 4 fluorimeter (Synergy4, BioTek, Winooski, VT) with excitation wavelength at 485/20 nm and emission at 528/20 nm. The rate of ROS production was normalized for the total P450 and expressed as a percent rate of the positive control. Reactions that had a rate of ROS formation more than 3 standard deviations above the mean rate of ROS formation in the negative control were considered above background. . These hits were not considered false positives because it is common to see some ROS production in CYP reactions that result in product. Reactions with ROS formation that were >50% of the positive control (CYP1A and 7-PR) and if the NADPH depletion was <30% of the positive control (CYP3A65 and 7-MR) were considered highly uncoupled and suggestive of a false positive.

Determining K_M and IC_{50} in the top hits

The top hits were defined as those with low ROS activity and high rate of NADPH depletion that was protein dependent. K_M values for NADPH depletion were determined for the top 48 hits. Each substrate was serially diluted half a log from the highest concentration giving 11 final concentrations, ranging from of 0 µM (no substrate control) to 100 µM. Each substrate concentration was run in duplicate in a 50 µL reactions as described above. NADPH depletion was monitored every 2 minutes for 10 minutes. The rate of NADPH depletion was normalized for total P450 content and a Michaelis-Menten curve was generated from the dilution series for each substrate. K_M values were obtained from curve fitting nonlinear regression models using on online tool (http://www.ic50.tk/kmvmax.html)

IC_{50} values were determined for the top 48 hits, assessing the inhibition of fluorescent product produced from the catalytic reaction between CYP3C1 purified membranes and 20 µM BFC. The inhibition assay was optimized for BFC concentration and DMSO (Figure 3B). The Michaelis-Menten curve for BFC was developed to determine appropriate BFC concentration (Figure 4B). Each substrate was serially diluted half a log from the highest concentration giving 11 final concentrations, ranging from of 0 μM (no substrate control) to 100 μM. Other reaction components were as described above, except each reaction was initiated with 2.96 mg mL^{-1} of purified membranes and 20 μM of BFC. Fluorescent activity was monitored every 2 minutes, for 15 minutes on a Synergy 4 fluorimeter (BioTek, Winooski, VT) with excitation wavelength/bandwidth at 400/30 nm and emission at 528/20 nm. The rate of inhibition was normalized for the total P450 content. IC_{50} values were obtained from curve fitting nonlinear regression models using Sigma Plot (Systat Software, San Jose, CA).

RESULTS

Expression of CYP3C1 Protein and Catalytic Activity

The CO-difference spectrum for CYP3C1 assessed the presence of functional P450; P450 content was 0.185nmol mg^{-1}. Cytochrome P450 reductase activity was 23.99 nmol mg^{-1} min^{-1} indicating appropriate incorporation of a functional reductase. CYP3C1 catalytic activity was confirmed by measuring the rate of reaction of CYP3C1 for 10 synthetic fluorogenic probe substrates: 7-ER, 7-MR, 7-PR, 7-BR, DBF, BFC, MFC AMMC, MAMC, and BQ. CYP3C1 metabolized all resorufin substrates to some extent but had the highest activity for 7-MR (Table 1; Figure 2). 7-BR had the lowest K_M and V_{max} (Table 1) and 7-MR had a higher K_M but the highest V_{max} (Table 1). Rates of resorufin production by CYP3C1 mediated 7-MR metabolism followed traditional Michaelis-Menten kinetics (Figure 4A).

CYP3C1 did not metabolize many of the coumarin and the one quinoline fluorogenic substrates (MFC, AMMC, MAMC and BQ) under the tested conditions (data not shown). CYP3C1 did metabolize both BFC and DBF (Figure 3). DBF had a low K_M and thus a high affinity for CYP3C1 (Table 1), but the maximum rate of reaction between CYP3C1 and BFC was 4 times greater than for DBF (Figure 3). Rates of fluorescent product formation by CYP3C1 mediated BFC metabolism followed Mechaelis-Menten kinetics up to 60 μM (Figure 4B). BFC and 7-MR had comparable V_{max} values but BFC had a lower K_M than 7-MR (Table1).

High Throughput Screening for NADPH Depletion with and Without Enzyme

The high throughput assay was optimized for NADPH depletion by CYP3C1 and 7-MR. BFC absorbs light at 340nM (data not shown), interfering with the ability to read the rate of NADPH depletion in this assay and so could not be used as a positive control or to optimize the high throughput assay. The effects of temperature and light had little effect on rate of NADPH depletion. There was a 1.5-fold decrease in the rate of resorufin formation in the presence of 3% DMSO (Figure 1A). As a result, DMSO was maintained at 2% for subsequent experiments. The limit of detection (LOD) for NADPH depletion was 207.5 nmol nmol $P450^{-1}$ min^{-1}, which is equivalent to the mean rate of NADPH depletion in the negative controls, plus three times the standard deviation of the mean. The LOD was 13% of the rate of NADPH depletion in the positive control (with 7-MR substrate). Following the primary screen, 200 compounds substrates had a rate of NADPH depletion that was greater than the limit of detection (Figure 5). Of those hits, 132 substrates had a rate of NADPH depletion that was 20% of the rate of NADPH depletion for the positive control. Uvaol, 2',6'-dihydroxy-4'methoyx-chalcone, plumbagin and menadione had the highest rate of NADPH depletion of all the tested compounds (Table 2).

A secondary screen assessed the 132 top hits for protein independent NADPH depletion. Uvaol, 2',6'-dihydroxy-4'methoyx-chalcone, plumbagin and menadione had an insignificant rate of NADPH depletion in the absence of enzyme compared to the rate of NADPH depletion in the presence of an enzyme, indicating that the reaction was enzyme dependent (Table 2). Overall, little NADPH depletion was detected in the absence of the enzyme for all the top substrates (Table 2) although the rate of NADPH depletion for myricetin in the absence of the enzyme was about half of the rate of NADPH depletion in the presence of the enzyme, suggesting myricetin a poor substrate of CYP3C1 and a false positive (Table 2).

Reactive Oxygen Species (ROS) 2'7'Dichlorofluorescin Probe Assay, K_m and IC_{50}

The 132 top hits were assessed for ROS formation. The rate of ROS formation between the positive control, CYP1A and 7-PR, was 5480±644 pmol nmol $P450^{-1}$ min^{-1}. There was a detectable amount of background fluorescence in wells containing CYP1A and 2% DMSO but no substrate (974±220 pmol nmol $P450^{-1}$ min^{-1}), equivalent to 30% of the positive control. Of the 132 hits, 122 substrates interacted with CYP3C1 to produce fluorescence equivalent to the negative control, suggesting low or insignificant ROS production (Table 2). The highest rate of ROS formation was seen for methylene blue (120% of the positive control) and coralyne chloride hydrate (63% of the positive control) suggesting a highly uncoupled reaction with CYP3C1 (Table 2). Compounds with a high rate of NADPH depletion, such plumbagin, menadione, NSC 95397 and primaquine diphosphate, also had higher rates of ROS formation but only slightly above background (Table 2). Uvaol and 2,6 – dihydroxy-4'-methoxy-chalcone had very low rates of ROS formation and the highest rate of NADPH depletion (Table 2), which suggests highly coupled reactions between CYP3C1 and the top hits.

48 compounds were selected from the top 132 hits to assess enzyme affinity via determination of the K_M for NADPH depletion and an IC50 for inhibition of BFC metabolism. 11 substrates had K_M and IC_{50} values that were less than 20 μM and closely followed Michaelis-Menten kinetics as tested by curve-fitting tools (Table 3). An additional 19 compounds had NADPH depletion and 7 had fluorescence inhibition, but curve fitting was not possible because the highest concentration tested was not high enough to successfully obtain maximum NADPH depletion or fluorescence inhibition, resulting in a large error associated with the calculated K_M and IC_{50} values (Table 3). Plumbagin, NSC95397, idebenone, menadione, GW2974, duloxetine hydrochloride and 3',4-dimethoxydalbergione had large rates of NADPH depletion (≥50% the rate of the positive control) along with the smallest K_M (7 - 16 μM), and IC_{50} (4 - 16 μM; Table 3) values. It is likely these compounds are high affinity CYP3C1 substrates. 2',6'–dihydroxy-4'-methoxy-chalcone and osthole had the smallest IC_{50}s of the 48 compounds but the K_M value for NADPH depletion was not computable (Table 3). Compounds such as β-lapachone and nitromide had IC_{50} values that were less than 10 μM but had higher K_M values (21 μM, 35 μM, respectively; Table 3); thus, the screen has identified at least 10-13 high affinity substrates for CYP3C1.

DISCUSSION

In this study, we isolated zebrafish CYP3C1 by heterologous expression in *E.coli* to remove the confounding effects of whole tissue analysis where multiple co-expressed CYPs, with varying expression levels, may contribute to substrate metabolism. The heterologously expressed CYP3C1 enzyme was co-expressed with cytochrome P450 reductase and both enzymes were shown to be functional. Assessment of catalytic function was achieved by fluorogenic probes that are commonly used to test CYP catalytic activity and via a high throughput screen of ~4000 biologically and pharmacology active compounds based on NADPH depletion. CYP3C1 had a high catalytic activity for various fluorogenic alkyloxy-resorufins (7-ER, 7-MR, and 7-BR), the coumarin BFC, and fluorescein-based DBF (Table 1). From the 4000 screened compounds, 200 compounds were positive hits with NADPH depletion rates above the limit of detection based on the negative control (Figure 5). 132 of the top hits were selected for follow up to remove false positives; based on assessing the rate of NADPH depletion in the absence of enzyme and highly uncoupled reactions via measurement of ROS production (Table 2). Lastly, we determined the K_M (for NADPH depletion) and IC_{50} (for BFC inhibition) values of the top 48 compounds and found that most of these substrates had pharmacological activity and were structurally diverse. Yet, 9 of the 48 top substrates were quinone based, suggesting that CYP3C1 may have a bias for substrates that contain a quinone moiety. To our knowledge, this is the first study that has heterologeously expressed and characterized the function of CYP3C1 enzyme, a CYP expressed in zebrafish liver and proposed to be important in detoxification. Indeed, this is the first functional data for any CYP3C enzyme. Since zebrafish are an important model species that is commonly used in toxicology (as reviewed by Dai et al 2014, and Hill et al 2005), disease research (as reviewed by Dooley & Zon 2000), drug research and development (reviewed by Zon & Peterson 2005), these data fill important gaps in our knowledge of xenobiotic biotransformation.

Functional Testing with Fluorogenic Probe Substrates

The 10 synthetic fluorogenic substrates included three resorufin (7-ER, 7-MR, 7-BR) substrates whose metabolism (alkyloxy-resorufin-O-deethylase; AROD) is commonly used biomarkers of CYP1 activity in fish (Scornaienchi et al 2010b, Whyte et al 2000) and mammals (Murray et al 2001). Specifically, 7-ER (EROD) and 7-MR (MROD) are commonly used to assess CYP1A activity (White et al 1997). Like CYP1 enzymes (Scornaienchi et al 2010b, Stegeman et al 2015), CYP3C1 had the capacity to metabolize the alkyloxy-resorufin substrates (Table 1; Figure 2). In zebrafish, CYP1A metabolizes 7-ER at a higher rate than the other resorufins, followed by 7-MR (Scornaienchi et al 2010b, Stegeman et al 2015), at rates that are about 1000-fold more (Scornaienchi et al 2010b) than the rate of CYP3C1 metabolism of 7-MR and 7-ER (Figure 2). CYP3C1 had the highest rate of metabolism for 7-MR, and at rates that were comparable to zebrafish CYP1B1 (Scornaienchi et al 2010b). 7-BR is a substrate for zebrafish CYP1A and CYP1B1 (Scornaienchi et al 2010b, Stegeman et al 2015), and mammalian CYP2 (Kobayashi et al 2002, Nerurkar et al 1993). 7-BR metabolism by CYP3C was minor relative to other resorufin substrates (Table 1). Previous work with heterologously expressed zebrafish CYP1 enzymes demonstrated that they were not highly involved in 7-PR metabolism relative to the other alkyloxy-resorufin substrates (Scornaienchi et at 2010b, Stegeman et al 2015). Zebrafish CYP1B1 did not metabolize 7-PR (Scornaienchi et al 2010b, Stegeman et al 2015); CYP1D1 metabolized 7-PR at a rate of 100 pmol nmol P450^{-1} min^{-1} while CYP1A, CYP1C1 and CYP1C2 metabolized 7-PR at a rate of ~ 1000 pmol nmol P450^{-1} min^{-1} (Scornaienchi et al 2010b). CYP3C1 metabolized 7-PR (Figure 2), approximately 2-fold less than CYP1A, CYP1C1 and CYP1C2. In mammals, 7-PR activity (PROD) is traditionally used to assess CYP2 activity (Burke et al 1994); while PROD activity is seen in fish (Hartl et al 2007, Scornaienchi et al 2010b, Stegeman et al 2015), it is not clear what enzymes are responsible for 7-PR metabolism in tissues. In fish, 7-PR may be metabolized to some extent by fish CYP1 enzymes and CYP3C1.

CYP3C1 metabolized only one of the coumarin substrates, BFC and the fluorescein-based substrate, DBF (Figure 3). DBF is a mammalian CYP2 and CYP3A specific substrate (Stresser et al 2002); DBF is a substrate of mammalian CYP2C8, CYP2C9 and CYP2C19 (Koenig et al 2012). Zebrafish CYP3C1 metabolized DBF (Figure 3) at approximately the same rate as zebrafish CYP3A65, but at rates that are ~2-fold less than zebrafish CYP1B1 (Scornaienchi et al 2010b), suggesting this substrate may be metabolized by CYP1 and CYP3 enzymes in zebrafish. BFC metabolism (BFCOD; 7-benzyloxy-4-trifluoromethylcoumarin O-debenzylase) is commonly thought to be a function of mammalian (Crespi & Stresser 2000) and fish CYP3A (Burkina et al 2013, Hegelund et al 2004). There was higher BFC catalytic activity with expressed

CYP1A than with CYP3A65 (Scornaienchi et al 2010a). Expressed CYP3C1 metabolized BFC (Figure 3) at rates that were ~7 fold more than rates observed for zebrafish CYP3A65 (Scornaienchi et al 2010a) but these rates were still ~ 4-fold less than rates of metabolism by CYP1A (Scornaienchi et al 2010a). BFC metabolism is commonly used to determine CYP3A induction and catalytic activity in mammals and fish; this data demonstrates that multiple CYP families are capable of BFC metabolism *in vitro*. Direct testing *in vivo* is clearly needed to assess the relative role of the various CYP1 and CYP3 enzymes for metabolism of these fluorogenic probe substrates under (Scornaienchi et al 2010a).

<u>High Throughput Screening for CYP3C1 Catalytic Activity</u>

Metabolism of Natural Plant Products

The commercial libraries contained ~4000 non-redundant compounds that include biologically and pharmacologically active small molecules, off patent and FDA approved pharmaceuticals, and natural plant products. While we have not done an exhaustive curation of compounds, we did preliminary curation and identified approximately 400 mammalian CYP3A substrates, supporting the usefulness of these libraries in screening CYP3 enzymes. These libraries contained a diversity of substrates, providing rich information to infer overlap between fish and mammalian CYP3 enzymes and examine any potential structural similarities amongst top hits. CYP3C1 appears to metabolize ~200 of the compounds in the libraries, based on detectable NADPH depletion rates and overall low rates of protein independent NADPH depletion rates and ROS production in the follow up. 16 compounds were known mammalian CYP3A4 substrates. Clearly, not all the curated mammalian CYP3 substrate compounds were positive hits, suggesting that zebrafish CYP3C and mammalian CYP3A function are distinct. Most of the substrates were pharmaceutically active compounds (Table 2). Many of the identified substrates, such as 2’6’-dihydroxy-4’-methoxy-chalcone, plumbagin, β-lapachone, lapachol, and antiarol were naturally occurring plant products. These data were not surprising as it is commonly believed that that the evolution of plant metabolites contributed to the evolution and diversification of CYP function, particularly for the CYP1-4 families (Gonzalez & Nebert 1990). Interestingly, plant products are commonly mammalian CYP2 and CYP3A substrates; it is this interaction that provides the bases for food-drug interactions (Fujita 2004).

Metabolism of Pharmacologically Active Compounds

Many of the identified CYP3C1 substrates are established or developing pharmaceutical compounds (ie, plumbagin, menadione, idebenone, primaquine diphosphate, cloxyquin and others). No direct data exist for the ability of zebrafish CYP3A65 to metabolize pharmaceuticals, but several lines of data suggest that fish CYP3A responds to pharmaceutical exposures (Baron et al 2017, Burkina et al 2013, Christen et al 2009, Corcoran et al 2012, Thibaut et al 2006) and that pharmaceuticals that are substrates of mammalian CYP3A are also metabolized in fish species (Tanoue et al 2017, Wassmur et al 2010). In mammals, however, it is well established that members of the CYP3 family, specifically CYP3A4, are responsible for the biotransformation of many pharmaceuticals (as reviewed by Zanger & Schwab 2013). It was likely that many of the identified substrates would have pharmacological properties given the nature of the chosen libraries. The LOPAC library is made solely of drug-like molecules that are involved in cell signalling and neuroscience, the Microsource library is 60% drugs with known pharmacological action, and Prestwick is solely composed from FDA approved drugs. It would be interesting to investigate whether pharmacological molecules would remain the top category of substrates if other libraries were used for the screen.

Metabolism of Structurally Diverse Compounds

Of the 200 compounds metabolized by fish CYP3C1, there is a high structural diversity amongst the identified substrates (Table 2). For example, compounds with similar catalytic activity, K_M and IC_{50} values, such as GW2974, a pyridopyrimidine, duloxetine hydrochloride, a thiophene derivative, and menadione, a 1,4-nathoquinone, have very different structures (Table 2). This is in line with current knowledge of the CYP3 enzymes, which are capable of metabolizing diverse compounds without a strong structure-activity relationship (as reviewed by Zanger & Schwab 2013). The human CYP3A4 enzyme has a highly promiscuous active site with the ability to metabolize more than 50% of known pharmaceuticals, most of which are not structurally related (for reviews see: Guengerich 1999, Johnson et al 2014, Kuehl et al 2001, Zanger & Schwab 2013). It is likely that CYP3C active site is also flexible, but this hypothesis remains to be tested.

Metabolism of Structurally Diverse Quinone Based Substrates

Quinones are a group of organic compounds that are naturally occurring and usually derived from plants (Barr & Crane 1971). Though quinones themselves are not aromatic, they are the result of aromatic compound metabolism such as benzenes, phenols or other polycyclic aromatic compounds (Talalay & Dinkova-Kostova 2004). The compounds with the larger rates of NADPH depletion and lower IC_{50} values, contained a quinone moiety, and some of those compounds, such as plumbagin, menadione, NSC 95397 and β-lapachone, were classified as 1,4 naphthoquinones. Quinones are good antifungal, antimicrobial and anticancer therapeutants (Bolton et al 2000). In channel catfish, naphthoquinones were acutely toxic, resulting in mortality and a reduction in hemoglobin concentration (Andaya & Di Giulio 1987). From the data presented in Chapter 3, it is not clear if the activity we observed with quinone compounds is CYP3C1 dependent, but previous work has implicated quinones as CYP substrates (Mueller et al 1998). Quinone compounds can interact with reductases, such as cytochrome P450 reductase, to consume an electron, produce a reactive semiquinones and superoxides, which can result in redox cycling (Segura-Aguilar et al 1998). Future experiments to rule out reductase mediated NADPH consumption with quinones can include: 1) test quinone reactions in the absence of CYP3C1 enzyme but in the presence of reductase (reductase only control); 2) determine whether quinones are competitive inhibitors of CYP3C1 activity; and 3) measure parent compound loss over-time. Parent loss would only be expected if CYP mediated metabolism occurred; redox cycling would regenerate the parent compound. Pending the confirmation of quinone-based compounds as CYP3C1 substrates, it is interesting to speculate structure-activity relationships for CYP3C1

Plumbagin is 1,4-naphthoquinone derived from leadwort plants *(Plumbago*). Plumbagin has anticancer, antifungal, antibacterial (Krishnaswamy & Purushothaman 1980) and antimicrobial (Paiva et al 2003) properties. However, plumbagin can also be cytotoxic and damaging to the skin (Sugie et al 1998). Despite its medicinal importance, little information is known about plumbagin and CYP3 interactions. Some studies suggest that plumbagin is a mixed inhibitor of human CYP3A4 (Chen et al 2016). Other studies suggest that plumbagin can modify the protein expression level of CYP3A (Sukkasem et al 2018). Our study identified plumbagin as a potential high affinity substrate of zebrafish CYP3C1 (Table 3).

Menadione (also known as Vitamin K_3) is as a synthetic compound and a 1, 4 naphthoquinone that contains a methyl group (Table 3). Traditionally, menadione was used in animal feed as a vitamin K supplement, but it is also noted for having anticancer properties (Tetef et al 1995), specifically in lung (Verrax et al 2004) and pancreatic (Tetef et al 1995) cancer. Metabolism of menadione in mammals is not well understood. In our study, we found that menadione is potentially a CYP3C1 substrate with high affinity (Table 3). Menadione is known to produce toxicity in zebrafish (Song et al 2010) and other aquatic invertebrates (Raikow et al 2006); the role of CYP3C1 in the toxicity or detoxification of menadione is worthy of further study.

β-lapachone is an ortho-naphthoquinone compound derived from lapacho (*Tabebuia avellandedae)* tree bark. β-lapachone is studied for ovarian, breast (Dubin et al 2001), prostate, colon (Huang & Pardee 1999), and pancreatic (Ough et al 2005) anticancer properties. Some studies suggest that β-lapachone also has antiparasitic (Lopes et al 1978, Teixeira et al 2001) and antifungal (Medeiros et al 2010) properties. One study linked β-lapachone to abnormal morphological defects in embryonic zebrafish hearts (Wu et al 2011). β-lapachone is potentially a high affinity CYP3C1 substrate (Table 3).

Interestingly, CYP3C1 is maternally deposited into the embryo and expressed in adult zebrafish hearts (Shaya et al 2014); our current data suggests that CYP3C1 may be involved in the biotransformation of β-lapachone in zebrafish. Furthermore, a compound related to β-lapachone, lapachol (a phenolic 1, 4- naphthoquinone) was also a substrate of CYP3C1 (Table 2). Despite the very similar structure between the two compounds, the affinity of CYP3C1 to lapachol was much less than for β-lapachone (Table 3).

Idebenone, sometimes referred to as Coenzyme Q10, is a synthetic benzoquinone compound used in treatment of cognitive diseases, such as Alzheimer's (Gutzmann & Hadler 1998) and Huntington's (Ranen et al 1996). In Canada, idebenone (Catena®) was authorized, with conditions, to be used in patients with Friedrich's ataxia, a genetic disease that affects the nervous system (Rustin et al 1999). In 2013, the drug developer and Health Canada withdrew Catena® due to a failure to meet the conditions specified for the authorization. This study identified idebenone as a potential high affinity substrate of CYP3C1 (Table 2). Idebenone had the most unique structure of the quinones, containing one ring and a 10-hydroxydecyl in the 6 position (Table 2). This unique compound speaks to the ability of CYP3C1 to potentially metabolize structurally diverse quinones.

Developing a Profile of CYP3C1 Substrates

This study is the first step in developing a thorough profile of CYP3C1 substrates and to determine the function of this orphan CYP enzyme. The functionality of heterologously expressed CYP3C1 was confirmed by a P450 peak in the CO reduction spectral assay and measurable fluorescent product for several fluorogenic probe substrates (Table 1). There was a large overlap in substrate profile for CYP1A and CYP3C, but

CYP1A provides higher rates of metabolism of the alkoxy-resorufin and BFC substrates. Considering that CYP1, CYP3C1 and CYP3A65 genes are all expressed in the liver and are individually capable of the metabolism of resorufin substrate and BFC, *in vivo* AROD and BFCOD activity may need some consideration. The basal expression of each enzyme in each tissue, the potential for gene induction through compound exposures, and the relative rate of metabolism (as indicated *in vitro*) will ultimately determine whether CYP1 or CYP3 enzymes are most important for metabolism. *In-vivo* testing would be beneficial to understand the potential contribution of CYP3C1 to AROD or BFCOD activity.

The high throughput screen identified 200 substrates of CYP3C1 from the selected libraries and very few of the substrates were removed as false positives. Of the identified compounds, we can conclude that CYP3C1 can metabolize several pharmacologically active compounds, most of which are plant based. Interestingly, many of the top hits had a quinone moiety. The K_M and IC_{50} values were determined for the top 48 substrates, but not all hits, leaving a possibility that several of the identified compounds in Table 3 are potentially high affinity CYP3C1 substrates and warrant further attention.

Developing a profile of CYP3C1 substrates will not only provide the ability to infer the CY3C1 function in zebrafish, but it will inform studies using zebrafish in toxicology and medicine. Despite the lack of understanding of fish pharmaceutical metabolism, the zebrafish is a commonly used tool to develop drugs for human diseases. For example, a recent study implanted human non-small lung cancer cells into zebrafish and found that plumbagin reduced tumour growth (Vinothkumar et al 2017) to develop plumbagin for cancer treatment in humans. Our study identified plumbagin as a high affinity substrate of zebrafish CYP3C1 (Table 3), providing novel data that can may allow for better translation of zebrafish research. Interestingly, we identified that many of the top CYP3C1 substrates contain a quinone moiety which suggests that there may be some structure-activity relationships for CYP3C1 substrates. This hypothesis warrants further investigation, specifically by ruling out the potential contribution of reductase contributing to NADPH consumption independent of the CYP enzyme

ACKNOWLEDGEMENT

This research was supported by the Natural Science and Engineering Council of Canada. We thank Dr. Derek Alsop for technical support and advice, and for the McMaster Centre for Microbial Chemical Biology, specifically Cecelia Murphy, for support running high throughput bioassays.

TABLES

TABLE 3.1 K_M and V_{max} of the metabolism of alkyloxy-resorufin substrates, BFC and DBF by heterologously expressed zebrafish CYP3C1. Values were calculated from curve fitting Michaelis-Menten Curves using the online tool: http://www.ic50.tk/kmvmax.html. All alkyloxy-resorufin substrates were run in EROD buffer; 7-benzyloxy-4-(trifluoromethyl)coumarin (BFC) and dibenzylfluorescein (DBF) were run in $KP0_4$ buffer. benzyloxyresorufin (7-BR), 7-ethoxyresorufin (7-ER), 7-methoxyresorufin (7-MR) and 7-pentoxyresorufin (7-PR) were run at 0.5% DMSO. BFC and DBF were run at 0.25%. Concentration ranges tested are indicated in brackets next to each substrate. All reactions were 200 µL total volume.

Substrate	Km	Vmax
	(μM) ± SEM	(pmol nmol P450^{-1} min^{-1}) ± SEM
7-ethoxyresorufin (7-ER; 5 – 25 μM)	14.18 ± 6.08	274.12 ± 56.85
7-methoxyresorufin (7-MR; 10 – 28 μM)	12.40 ± 17.58	1384.87 ± 765.20
7-benzyloxyresorufin (7-BR; 0.06 – 1 μM)	0.38 ± 0.17	95.35 ± 18.94
7-pentoxyresorufin (7-PR; 0.09 – 3 μM)	0.51 ± 0.27	490.69 ± 89.28
7-benzyloxy-4-(trifluoromethyl)coumarin (BFC; 5-60 μM)	9.25 ± 2.18	1331.38 ± 88.86
Dibenzylfluorescein (DBF; 0.05 – 2.5 μM)	1.29 ± 0.49	323.17 ± 45.41

TABLE 3.2 NADPH depletion, reactive oxygen species (ROS) formation, and NADPH depletion in the absence of enzyme for the 132 top hit compounds of heterologously expression zebrafish CYP3C1. Structure, molecular weight and name of each compound are provided. The rates of NADPH depletion, NADPH depletion in the absence of enzyme, and ROS formation were normalized for total P450 content. Values obtained for each individual replicate are displayed in the table, along with an average of the two replicates. Due to technical error, some samples were run with double the concentration of substrate and DMSO (see materials and methods for more detail) and are highlighted in grey. Compounds that were identified to be CYP3A4 substrates through DataBank.ca (Wishart et al 2018) are identified by an asterisk after the compound name. <LOD (limit of detection) indicates wells where the value was below the limit of detection. The LOD value was substituted when calculating the average for a group of wells that had value(s) below the LOD.

			Rate of NADPH Depletion % Positive Control			Rate of ROS Formation % Positive Control			Rate of NADPH Depletion (No Enzyme) % Postive Control			Rate of NADPH Depletion nmol nmol p450^{-1} min^{-1}			Rate of ROS Formation pmol nmol p450^{-1} min^{-1}			Rate of NADPH Depletion (No Enzyme) nmol nmol p450^{-1} min^{-1}		
Compound name	**Structure**	**Weight**	**Rep 1**	**Rep 2**	**Average**	**Rep 1**	**Rep 2**	**Average**	**Rep 1**	**Rep 2**	**Average**	**Rep 1**	**Rep 2**	**Average**	**Rep 1**	**Rep 2**	**Average**	**Rep 1**	**Rep 2**	**Average**
UVAOL	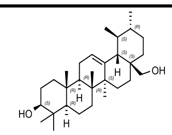	442.728	81.08	153.73	117.40	<LOD	<LOD	30.00	<LOD	<LOD	12.90	1080.37	2287.01	1683.69	<LOD	<LOD	954.32	<LOD	<LOD	231.80
2',6'-DIHYDROXY-4'-METHOXY-CHALCONE	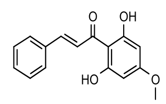	270.284	55.81	127.32	91.56	<LOD	<LOD	30.00	<LOD	<LOD	12.90	743.63	1894.15	1318.89	<LOD	<LOD	954.32	<LOD	<LOD	231.80
PLUMBAGIN	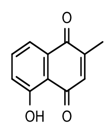	188.182	78.59	73.81	76.20	47.19	51.78	49.49	<LOD	<LOD	12.90	1332.92	1234.70	1283.81	1509.99	1656.89	1583.44	<LOD	<LOD	231.80
MENADIONE	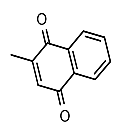	172.183	70.32	78.85	74.58	32.55	32.09	32.32	<LOD	<LOD	12.90	1192.61	1318.89	1255.75	1041.44	1026.90	1034.17	<LOD	<LOD	231.80
ISOCORYDINE	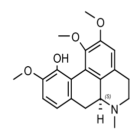	341.407	58.97	62.25	60.61	<LOD	<LOD	30.00	<LOD	<LOD	12.90	785.72	926.03	855.87	<LOD	<LOD	954.32	<LOD	<LOD	231.80
APOMORPHINE HYDROCHLORIDE HEMIHYDRATE*	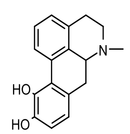	303.788	46.33	74.51	60.42	<LOD	<LOD	30.00	<LOD	<LOD	12.90	617.35	1108.43	862.89	<LOD	<LOD	954.32	<LOD	<LOD	231.80
GW2974	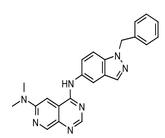	395.470	59.82	59.00	59.41	<LOD	<LOD	30.00	<LOD	<LOD	12.90	855.87	940.06	897.97	<LOD	<LOD	954.32	<LOD	<LOD	231.80
BTO-1	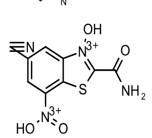	266.230	60.13	57.58	58.86	<LOD	<LOD	30.00	<LOD	<LOD	12.90	982.15	926.03	954.09	<LOD	<LOD	954.32	<LOD	<LOD	231.80
DULOXETINE HYDROCHLORIDE*	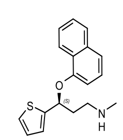	333.880	53.92	62.59	58.25	<LOD	<LOD	30.00		<LOD	12.90	883.94	1010.21	947.07	<LOD	<LOD	954.32	<LOD	<LOD	231.80
PRIMAQUINE DIPHOSPHATE*	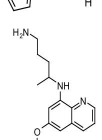	455.341	54.44	58.54	56.49	31.85	32.37	32.11	<LOD	<LOD	12.90	897.97	912.00	904.98	1018.96	1035.78	1027.37	<LOD	<LOD	231.80

NSC 95397	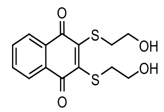	310.380	58.84	53.71	56.28	39.67	39.18	39.42	<LOD	<LOD	12.90	841.84	855.87	848.86	1269.26	1253.50	1261.38	<LOD	<LOD	231.80
IDEBENONE	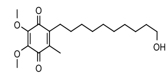	338.444	62.25	46.40	54.32	<LOD	<LOD	30.00	<LOD	<LOD	12.90	926.03	757.66	841.84	<LOD	<LOD	954.32	<LOD	<LOD	231.80
CLOXYQUIN	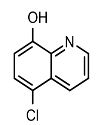	179.600	54.56	52.26	53.41	<LOD	<LOD	30.00	<LOD	<LOD	12.90	771.69	841.84	806.77	<LOD	<LOD	954.32	<LOD	<LOD	231.80
5, 6 -DEHYDROKAWAIN	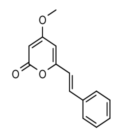	228.247	17.90	87.71	52.81	<LOD	<LOD	30.00	<LOD	<LOD	12.90	238.52	1304.86	771.69	<LOD	<LOD	954.32	<LOD	<LOD	231.80
OXYQUINOLINE HEMISULFATE	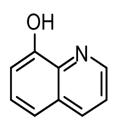	243.231	49.34	54.94	52.14	<LOD	<LOD	30.00	<LOD	<LOD	12.90	813.78	855.87	834.83	<LOD	<LOD	954.32	<LOD	<LOD	231.80
3,4-DIMETHOXY-DALBERGIONE	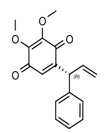	284.311	52.15	47.17	49.66	<LOD	<LOD	30.00	<LOD	<LOD	12.90	771.69	729.60	750.64	<LOD	<LOD	954.32	<LOD	<LOD	231.80
CHLORANIL	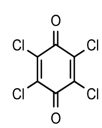	245.860	51.58	47.03	49.31	<LOD	<LOD	30.00	15.53	16.40	15.97	729.60	757.66	743.63	<LOD	<LOD	954.32	252.55	266.58	259.57
VULPINIC ACID	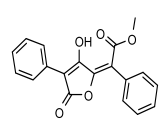	322.316	44.23	50.93	47.58	<LOD	<LOD	30.00	<LOD	<LOD	12.90	589.29	757.66	673.47	<LOD	<LOD	954.32	<LOD	<LOD	231.80
HYCANTHONE	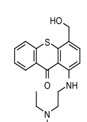	356.480	42.79	50.42	46.61	<LOD	<LOD	30.00	<LOD	<LOD	12.90	701.54	813.78	757.66	<LOD	<LOD	954.32	<LOD	<LOD	231.80
R(-)-APOCODEINE HYDROCHLORIDE	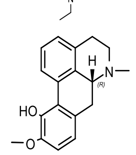	317.815	50.68	41.00	45.84	<LOD	<LOD	30.00	<LOD	<LOD	12.90	827.81	659.44	743.63	<LOD	<LOD	954.32	<LOD	<LOD	231.80
ANTIAROL	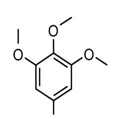	184.191	45.51	45.35	45.43	<LOD	<LOD	30.00	<LOD	<LOD	12.90	673.47	701.54	687.51	<LOD	<LOD	954.32	<LOD	<LOD	231.80
FLAVOKAWAIN A	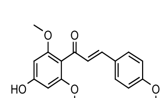	314.337	36.85	53.76	45.31	<LOD	<LOD	30.00	12.94	<LOD	12.92	491.08	799.75	645.41	<LOD	<LOD	954.32	<LOD	<LOD	231.80

PRAZOSIN HYDROCHLORIDE*	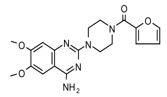	419.868	44.26	45.85	45.06	<LOD	<LOD	30.00	<LOD	<LOD	12.90	645.41	729.60	687.51	<LOD	<LOD	954.32	<LOD	<LOD	231.80
NITROMIDE	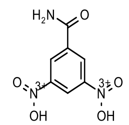	213.146	43.38	44.13	43.76	<LOD	<LOD	30.00	<LOD	<LOD	12.90	715.57	687.51	701.54	<LOD	<LOD	954.32	<LOD	<LOD	231.80
R(-)-2,10,11-TRIHYDROXY-N-PROPYLNORAPORPHINE HYDROBROMIDE*	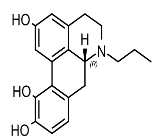	392.293	42.95	42.75	42.85	<LOD	<LOD	30.00	<LOD	<LOD	12.90	701.54	687.51	694.52	<LOD	<LOD	954.32	<LOD	<LOD	231.80
β-LAPACHONE	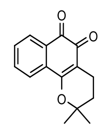	242.274	<LOD	78.01	45.65	<LOD	<LOD	30.00	<LOD	<LOD	12.90	<LOD	1304.86	756.18	<LOD	<LOD	954.32	<LOD	<LOD	231.80
AZOMYCIN	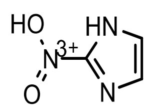	114.082	46.33	38.67	42.50	<LOD	<LOD	30.00	<LOD	<LOD	12.90	617.35	575.26	596.31	<LOD	<LOD	954.32	<LOD	<LOD	231.80
LAPACHOL	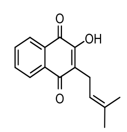	242.274	47.59	35.22	41.41	<LOD	<LOD	30.00	<LOD	<LOD	12.90	687.51	547.20	617.35	<LOD	<LOD	954.32	<LOD	<LOD	231.80
DOXAZOSIN MESYLATE*	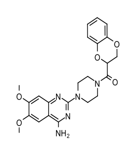	547.583	41.19	41.39	41.29	<LOD	<LOD	30.00	<LOD	<LOD	12.90	589.29	659.44	624.37	<LOD	<LOD	954.32	<LOD	<LOD	231.80
CORALYNE CHLORIDE HYDRATE	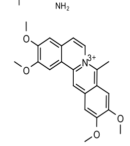	415.870	30.43	52.11	41.27	63.42	62.91	63.16	<LOD	<LOD	12.90	463.01	869.90	666.46	2029.11	2012.82	2020.96	<LOD	<LOD	231.80
ACETOSYRINGONE	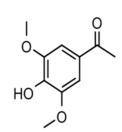	196.202	48.56	33.42	40.99	<LOD	<LOD	30.00	13.81	13.81	13.81	701.54	519.14	610.34	<LOD	<LOD	954.32	224.49	224.49	224.49
HYPOCRELLIN A	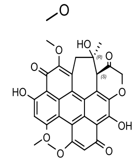	546.528	36.85	44.33	40.59	<LOD	<LOD	30.00	<LOD	<LOD	12.90	491.08	659.44	575.26	<LOD	<LOD	954.32	<LOD	<LOD	231.80
GOSSYPETIN	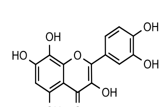	318.237	43.70	37.03	40.37	<LOD	<LOD	30.00	<LOD	<LOD	12.90	631.38	575.26	603.32	<LOD	<LOD	954.32	<LOD	<LOD	231.80
CORALYNE CHLORIDE	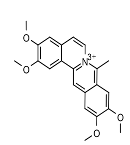	397.855	35.93	40.64	38.29	<LOD	<LOD	30.00	<LOD	<LOD	12.90	519.14	631.38	575.26	<LOD	<LOD	954.32	<LOD	<LOD	231.80

SANGUINARINE SULFATE	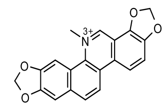	427.379	39.98	36.03	38.00	32.64	31.31	31.97	<LOD	<LOD	12.90	659.44	561.23	610.34	1044.30	1001.80	1023.05	<LOD	<LOD	231.80
R(-)-2,10,11-TRIHYDROXY APORPHINE HYBROBROMIDE*	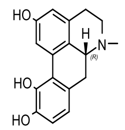	364.239	37.80	36.64	37.22	<LOD	<LOD	30.00	<LOD	<LOD	12.90	617.35	589.29	603.32	<LOD	<LOD	954.32	<LOD	<LOD	231.80
ZM 39923 HYDROCHLORIDE	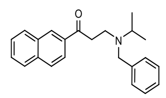	367.919	36.56	37.03	36.80	<LOD	<LOD	30.00	<LOD	<LOD	12.90	533.17	589.29	561.23	<LOD	<LOD	954.32	<LOD	<LOD	231.80
ISORESERPINE, (-)	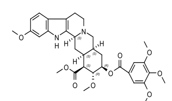	608.688	31.59	41.50	36.54	<LOD	<LOD	30.00	<LOD	<LOD	12.90	420.92	617.35	519.14	<LOD	<LOD	954.32	<LOD	<LOD	231.80
1-(1-NAPHTHYL) PIPERAZINE HYDROCHLORIDE	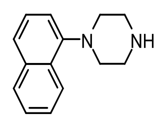	248.756	35.08	37.19	36.13	<LOD	<LOD	30.00	<LOD	<LOD	12.90	519.14	575.26	547.20	<LOD	<LOD	954.32	<LOD	<LOD	231.80
FLUPIRTINE MALEATE	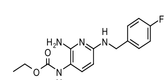	420.397	33.34	38.75	36.04	<LOD	<LOD	30.00	<LOD	<LOD	12.90	477.04	617.35	547.20	<LOD	<LOD	954.32	<LOD	<LOD	231.80
DAPH	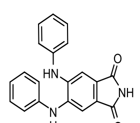	329.359	33.50	38.39	35.94	<LOD	<LOD	30.00	<LOD	<LOD	12.90	869.90	617.35	743.63	<LOD	<LOD	954.32	<LOD	<LOD	231.80
OSTHOLE	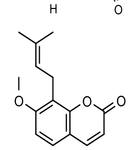	244.290	<LOD	62.25	37.77	<LOD	<LOD	30.00	<LOD	<LOD	12.90	<LOD	926.03	566.77	<LOD	<LOD	954.32	<LOD	<LOD	231.80
TETRAHYDROALSTONINE	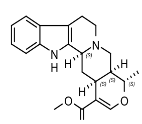	352.434	33.09	37.75	35.42	<LOD	<LOD	30.00	<LOD	<LOD	12.90	561.29	631.38	596.34	<LOD	<LOD	954.32	<LOD	<LOD	231.80
MYRICETIN	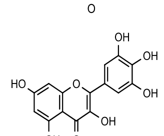	318.237	23.16	46.97	35.07	<LOD	<LOD	30.00	17.26	18.99	18.12	392.86	785.72	589.29	<LOD	<LOD	954.32	280.61	308.68	294.65
DEPHOSTATIN	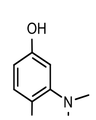	168.152	36.94	33.15	35.05	<LOD	<LOD	30.00	<LOD	<LOD	12.90	603.32	533.17	568.24	<LOD	<LOD	954.32	<LOD	<LOD	231.80
YANGONIN	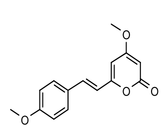	258.273	<LOD	62.25	37.77	<LOD	<LOD	30.00	<LOD	<LOD	12.90	<LOD	926.03	566.77	<LOD	<LOD	954.32	<LOD	<LOD	231.80

BERBERINE*	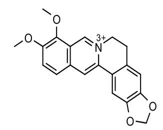	336.365	29.48	39.61	34.55	<LOD	<LOD	30.00	<LOD	<LOD	12.90	392.86	589.29	491.08	<LOD	<LOD	954.32	<LOD	<LOD	231.80
METHYLENE BLUE	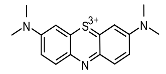	335.851	30.75	36.58	33.67	117.35	121.61	119.48	<LOD	<LOD	12.90	434.95	589.29	512.12	3754.89	3890.93	3822.91	<LOD	<LOD	231.80
HOMIDIUM BROMIDE	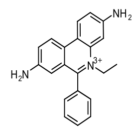	392.298	39.68	26.13	32.90	43.82	38.86	41.34	12.94	<LOD	12.92	561.23	420.92	491.08	1402.15	1243.52	1322.83	<LOD	<LOD	231.80
TETRA-HYDROPAPAVERINE*	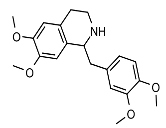	343.423	26.32	36.78	31.55	<LOD	<LOD	30.00	<LOD	<LOD	12.90	350.77	547.20	448.98	<LOD	<LOD	954.32	<LOD	<LOD	231.80
ATOVAQUONE*	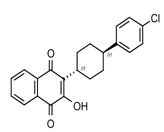	366.840	34.23	27.82	31.03	<LOD	<LOD	30.00	<LOD	<LOD	12.90	561.23	448.98	505.11	<LOD	<LOD	954.32	<LOD	<LOD	231.80
CORYNANTHINE	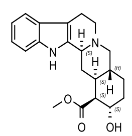	354.450	24.22	37.72	30.97	<LOD	<LOD	30.00	<LOD	<LOD	12.90	322.71	561.23	441.97	<LOD	<LOD	954.32	<LOD	<LOD	231.80
CI-976	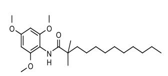	393.568	30.79	30.86	30.83	<LOD	<LOD	30.00	<LOD	<LOD	12.90	448.98	491.08	470.03	<LOD	<LOD	954.32	<LOD	<LOD	231.80
R(-) APOMORPHINE HYDROCHLORIDE HEMIHYDRATE*	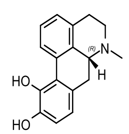	312.796	35.84	25.78	30.81	<LOD	<LOD	30.00	<LOD	<LOD	12.90	533.17	420.92	477.04	<LOD	<LOD	954.32	<LOD	<LOD	231.80
PROPIDIUM IODIDE*	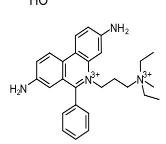	664.370	28.59	32.78	30.68	42.77	41.43	42.10	<LOD	<LOD	12.90	434.95	547.20	491.08	1368.58	1325.61	1347.09	<LOD	<LOD	231.80
NF 023	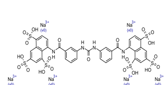	1,168.890	<LOD	57.32	35.31	<LOD	<LOD	30.00	<LOD	<LOD	12.90	<LOD	912.00	559.75	<LOD	<LOD	954.32	<LOD	<LOD	231.80
CHELERYTHRINE CHLORIDE	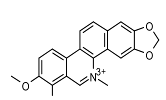	381.812	34.36	26.17	30.27	<LOD	<LOD	30.00	<LOD	<LOD	12.90	561.23	420.92	491.08	<LOD	<LOD	954.32	<LOD	<LOD	231.80
LYSERGOL	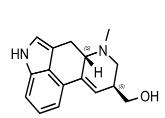	254.333	19.03	41.10	30.06	<LOD	<LOD	30.00	<LOD	<LOD	12.90	1192.61	687.51	940.06	<LOD	<LOD	954.32	<LOD	<LOD	231.80

IODOQUINOL	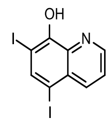	396.954	28.07	31.52	29.80	<LOD	<LOD	30.00	<LOD	<LOD	12.90	322.71	491.08	406.89	<LOD	<LOD	954.32	<LOD	<LOD	231.80
EUGENYL BENZOATE	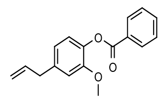	268.312	32.32	27.02	29.67	<LOD	<LOD	30.00	<LOD	<LOD	12.90	533.17	420.92	477.04	<LOD	<LOD	954.32	<LOD	<LOD	231.80
PAPAVERINE*	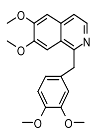	339.391	28.43	30.18	29.31	<LOD	<LOD	30.00	<LOD	<LOD	12.90	378.83	448.98	413.91	<LOD	<LOD	954.32	<LOD	<LOD	231.80
LAWSONE	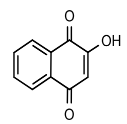	174.155	32.05	26.19	29.12	<LOD	<LOD	30.00	<LOD	<LOD	12.90	463.01	406.89	434.95	<LOD	<LOD	954.32	<LOD	<LOD	231.80
3-BROMO-7-NITROINDAZOLE	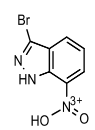	243.038	30.07	27.92	28.99	<LOD	<LOD	30.00	<LOD	<LOD	12.90	491.08	448.98	470.03	<LOD	<LOD	954.32	<LOD	<LOD	231.80
CHRYSOERIOL	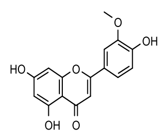	300.266	<LOD	57.88	35.59	<LOD	<LOD	30.00	<LOD	<LOD	12.90	<LOD	968.12	587.81	<LOD	<LOD	954.32	<LOD	<LOD	231.80
KAEMPFEROL-7-NEOHESPERIDOSIDE	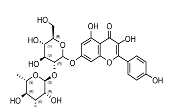	594.522	<LOD	56.20	34.75	<LOD	<LOD	30.00	<LOD	<LOD	12.90	<LOD	940.06	573.78	<LOD	<LOD	954.32	<LOD	<LOD	231.80
PYRVINIUM PAMOATE	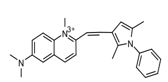	508.964	26.99	28.12	27.56	<LOD	<LOD	30.00	<LOD	<LOD	12.90	420.92	463.01	441.97	<LOD	<LOD	954.32	<LOD	<LOD	231.80
SCOULERINE	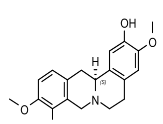	327.380	20.68	34.39	27.54	<LOD	<LOD	30.00	<LOD	<LOD	12.90	350.77	575.26	463.01	<LOD	<LOD	954.32	<LOD	<LOD	231.80
2,6-DIMETHOXYQUINONE	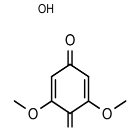	168.148	25.60	29.02	27.31	<LOD	<LOD	30.00	<LOD	<LOD	12.90	378.83	448.98	413.91	<LOD	<LOD	954.32	<LOD	<LOD	231.80
PELLITORINE	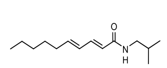	223.360	<LOD	50.33	31.81	<LOD	<LOD	30.00	<LOD	<LOD	12.90	<LOD	841.84	524.68	<LOD	<LOD	954.32	<LOD	<LOD	231.80
AMRINONE	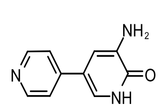	187.202	25.46	27.50	26.48	<LOD	<LOD	30.00	<LOD	<LOD	12.90	378.83	448.98	413.91	<LOD	<LOD	954.32	<LOD	<LOD	231.80

ISOQUERCITRINE	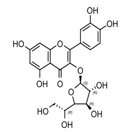	464.379	15.79	35.84	25.82	<LOD	<LOD	30.00	<LOD	<LOD	12.90	210.46	533.17	371.81	<LOD	<LOD	954.32	<LOD	<LOD	231.80
DIHYDROTANSHINONE	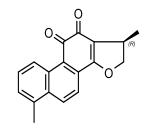	278.307	18.95	31.12	25.04	<LOD	<LOD	30.00	<LOD	<LOD	12.90	252.55	463.01	357.78	<LOD	<LOD	954.32	<LOD	<LOD	231.80
ROBINETINE	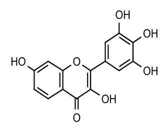	302.238	<LOD	39.42	26.36	<LOD	<LOD	30.00	18.12	19.85	18.99	<LOD	659.44	433.48	<LOD	<LOD	954.32	294.65	322.71	308.68
NORFLUOROCURARINE	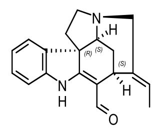	292.382	19.86	29.36	24.61	<LOD	<LOD	30.00	<LOD	<LOD	12.90	336.74	491.08	413.91	<LOD	<LOD	954.32	<LOD	<LOD	231.80
DALBERGIONE	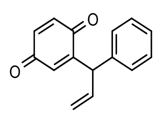	224.259	23.70	25.40	24.55	<LOD	<LOD	30.00	<LOD	<LOD	12.90	350.77	392.86	371.81	<LOD	<LOD	954.32	<LOD	<LOD	231.80
ATOVAQUONE*	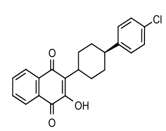	366.840	29.51	19.33	24.42	<LOD	<LOD	30.00	<LOD	<LOD	12.90	448.98	322.71	385.84	<LOD	<LOD	954.32	<LOD	<LOD	231.80
ALPHA-CYANO-4-HYDROXYCINNAMIC ACID	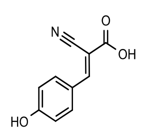	189.170	20.83	27.87	24.35	<LOD	<LOD	30.00	<LOD	12.94	12.92	294.65	448.98	371.81	<LOD	<LOD	954.32	<LOD	<LOD	231.80
PALMATINE	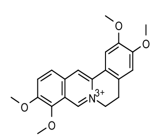	352.408	18.95	29.24	24.10	<LOD	<LOD	30.00	<LOD	<LOD	12.90	252.55	434.95	343.75	<LOD	<LOD	954.32	<LOD	<LOD	231.80
PYRVINIUM PAMOATE	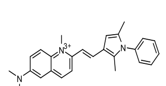	767.880	23.11	24.34	23.72	<LOD	<LOD	30.00	<LOD	<LOD	12.90	378.83	392.86	385.84	<LOD	<LOD	954.32	<LOD	<LOD	231.80
PPNDS TETRASODIUM	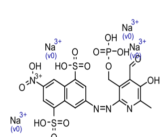	699.380	24.05	22.93	23.49	<LOD	<LOD	30.00	<LOD	<LOD	12.90	350.77	364.80	357.78	<LOD	<LOD	954.32	<LOD	<LOD	231.80
SB-215505	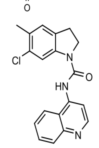	337.810	33.67	<LOD	23.49	<LOD	<LOD	30.00	<LOD	<LOD	12.90	491.08	210.46	350.77	<LOD	<LOD	954.32	<LOD	<LOD	231.80
LYSERGOL*	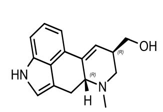	254.333	25.82	21.01	23.42	<LOD	<LOD	30.00	<LOD	<LOD	12.90	392.86	350.77	371.81	<LOD	<LOD	954.32	<LOD	<LOD	231.80

A-77636 HYDROCHLORIDE	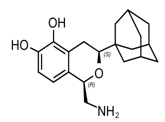	365.900	17.90	28.29	23.10	<LOD	<LOD	30.00	<LOD	<LOD	12.90	238.52	420.92	329.72	<LOD	<LOD	954.32	<LOD	<LOD	231.80
P-MPPF DIHYDROCHLORIDE	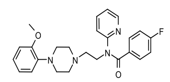	507.435	<LOD	41.44	27.37	<LOD	<LOD	30.00	<LOD	<LOD	12.90	<LOD	659.44	433.48	<LOD	<LOD	954.32	<LOD	<LOD	231.80
ST-148	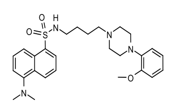	612.742	20.20	23.81	22.01	<LOD	<LOD	30.00	<LOD	<LOD	12.90	294.65	378.83	336.74	<LOD	<LOD	954.32	<LOD	<LOD	231.80
ERGOTAMINE TARTRATE*	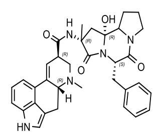	729.787	23.81	20.03	21.92	<LOD	<LOD	30.00	<LOD	<LOD	12.90	336.74	322.71	329.72	<LOD	<LOD	954.32	<LOD	<LOD	231.80
1,1-DIMETHYL-4-PHENYL-PIPERAZINIUM IODIDE	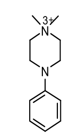	316.184	53.26	<LOD	33.28	<LOD	<LOD	30.00	<LOD	<LOD	12.90	869.90	<LOD	869.90	<LOD	<LOD	954.32	<LOD	<LOD	231.80
CPNQ	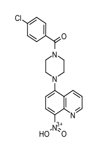	397.840	21.58	22.01	21.79	<LOD	<LOD	30.00	<LOD	<LOD	12.90	308.68	350.77	329.72	<LOD	<LOD	954.32	<LOD	<LOD	231.80
()-OCTOCLOTHEPIN MALEATE	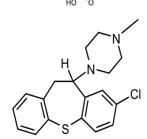	460.972	<LOD	37.03	25.17	<LOD	<LOD	30.00	<LOD	<LOD	12.90	<LOD	589.29	398.40	<LOD	<LOD	954.32	<LOD	<LOD	231.80
BENZO[A]PYRENE*	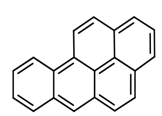	252.316	20.83	21.77	21.30	<LOD	<LOD	30.00	<LOD	<LOD	12.90	294.65	350.77	322.71	<LOD	<LOD	954.32	<LOD	<LOD	231.80
STREPTONIGRIN	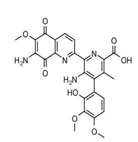	506.471	16.85	25.46	21.16	<LOD	<LOD	30.00	<LOD	<LOD	12.90	224.49	378.83	301.66	<LOD	<LOD	954.32	<LOD	<LOD	231.80
DIOSMIN	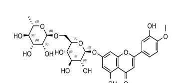	608.549	<LOD	37.72	25.51	<LOD	<LOD	30.00	<LOD	<LOD	12.90	<LOD	561.23	384.37	<LOD	<LOD	954.32	<LOD	<LOD	231.80
7-HYDROXYFLAVONE,	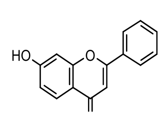	238.242	<LOD	31.87	22.59	<LOD	<LOD	30.00	<LOD	<LOD	12.90	<LOD	533.17	370.34	<LOD	<LOD	954.32	<LOD	<LOD	231.80
TYRPHOSTIN 51	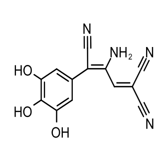	268.232	20.86	20.86	20.86	<LOD	<LOD	30.00	<LOD	<LOD	12.90	308.68	322.71	315.69	<LOD	<LOD	954.32	<LOD	<LOD	231.80

R(-)-PROPYLNOR APOMORPHINE HYDROCHLORIDE*	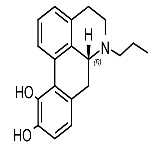	331.842	18.04	23.56	20.80	<LOD	<LOD	30.00	<LOD	<LOD	12.90	294.65	378.83	336.74	<LOD	<LOD	954.32	<LOD	<LOD	231.80
THYMOQUINONE	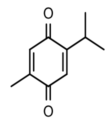	164.204	17.90	23.58	20.74	<LOD	<LOD	30.00	<LOD	<LOD	12.90	238.52	350.77	294.65	<LOD	<LOD	954.32	<LOD	<LOD	231.80
DIHYDROROBINETINE	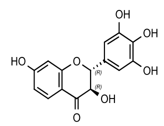	304.254	15.79	25.46	20.63	<LOD	<LOD	30.00	<LOD	<LOD	12.90	210.46	378.83	294.65	<LOD	<LOD	954.32	<LOD	<LOD	231.80
KOPARIN	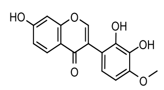	300.266	20.86	19.95	20.41	<LOD	<LOD	30.00	<LOD	<LOD	12.90	308.68	308.68	308.68	<LOD	<LOD	954.32	<LOD	<LOD	231.80
SALMETEROL XINAFOATE*	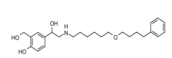	603.756	21.17	19.40	20.28	<LOD	<LOD	30.00	<LOD	<LOD	12.90	308.68	308.68	308.68	<LOD	<LOD	954.32	<LOD	<LOD	231.80
4-AMINO-1,8-NAPHTHALIMIDE	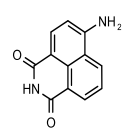	212.208	15.79	24.52	20.16	<LOD	<LOD	30.00	<LOD	<LOD	12.90	210.46	364.80	287.63	<LOD	<LOD	954.32	<LOD	<LOD	231.80
BU99006	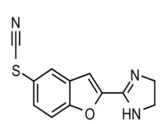	243.280	19.61	20.25	19.93	<LOD	<LOD	30.00	<LOD	<LOD	12.90	280.61	322.71	301.66	<LOD	<LOD	954.32	<LOD	<LOD	231.80
R(-)-N-ALLYLNORAPOMORPHINE HYDROBROMIDE*	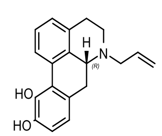	374.278	18.90	20.94	19.92	<LOD	<LOD	30.00	<LOD	<LOD	12.90	308.68	336.74	322.71	<LOD	<LOD	954.32	<LOD	<LOD	231.80
RESERPINE*	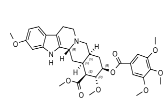	608.688	<LOD	31.12	22.21	<LOD	<LOD	30.00	<LOD	<LOD	12.90	<LOD	463.01	335.26	<LOD	<LOD	954.32	<LOD	<LOD	231.80
METHYLERGONOVINE*	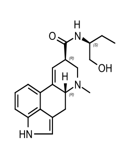	339.439	13.69	25.46	19.58	<LOD	<LOD	30.00	<LOD	<LOD	12.90	<LOD	378.83	293.17	<LOD	<LOD	954.32	<LOD	<LOD	231.80
4-METHOXYDALBERGIONE	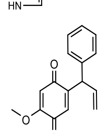	254.285	16.12	22.68	19.40	<LOD	<LOD	30.00	<LOD	<LOD	12.90	238.52	350.77	294.65	<LOD	<LOD	954.32	<LOD	<LOD	231.80
SB 218795	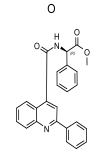	396.446	23.54	14.97	19.25	<LOD	<LOD	30.00	<LOD	<LOD	12.90	336.74	238.52	287.63	<LOD	<LOD	954.32	<LOD	<LOD	231.80

GENISTEIN	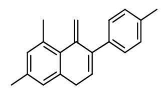	260.380	<LOD	31.04	22.17	<LOD	<LOD	30.00	<LOD	<LOD	12.90	<LOD	519.14	363.32	<LOD	<LOD	954.32	<LOD	<LOD	231.80
CNQX DISODIUM	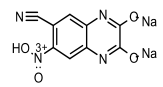	277.125	18.04	20.07	19.05	38.98	48.90	43.94	<LOD	<LOD	12.90	294.65	322.71	308.68	1247.31	1564.70	1406.00	<LOD	<LOD	231.80
RUTIN	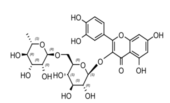	610.521	<LOD	26.41	19.85	<LOD	<LOD	30.00	<LOD	<LOD	12.90	<LOD	392.86	300.19	<LOD	<LOD	954.32	<LOD	<LOD	231.80
PTAEROXYLIN	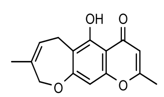	258.273	<LOD	31.75	22.52	<LOD	<LOD	30.00	<LOD	<LOD	12.90	<LOD	491.08	349.29	<LOD	<LOD	954.32	<LOD	<LOD	231.80
ETHOXYQUIN	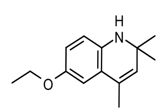	217.312	23.05	13.45	18.25	<LOD	<LOD	30.00	<LOD	<LOD	12.90	350.77	224.49	287.63	<LOD	<LOD	954.32	<LOD	<LOD	231.80
SCH-28080	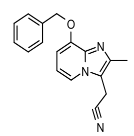	277.327	16.32	20.07	18.19	<LOD	<LOD	30.00	<LOD	<LOD	12.90	266.58	322.71	294.65	<LOD	<LOD	954.32	<LOD	<LOD	231.80
CHRYSINE	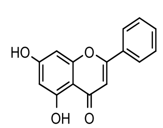	254.241	<LOD	31.04	22.17	<LOD	<LOD	30.00	<LOD	<LOD	12.90	<LOD	519.14	363.32	<LOD	<LOD	954.32	<LOD	<LOD	231.80
MOLINDONE HYDROCHLORIDE*	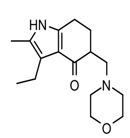	312.840	14.71	21.13	17.92	<LOD	<LOD	30.00	<LOD	<LOD	12.90	210.46	336.74	273.60	<LOD	<LOD	954.32	<LOD	<LOD	231.80
FLAVOKAWAIN B	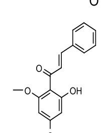	284.311	<LOD	29.36	21.33	<LOD	<LOD	30.00	15.53	18.12	16.83	<LOD	491.08	349.29	<LOD	<LOD	954.32	252.55	294.65	273.60
OXANTEL PAMOATE	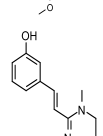	604.659	20.83	13.94	17.38	<LOD	<LOD	30.00	<LOD	<LOD	12.90	294.65	224.49	259.57	<LOD	<LOD	954.32	<LOD	<LOD	231.80
PRATOL	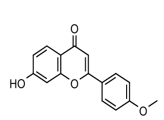	268.268	<LOD	30.20	21.75	<LOD	<LOD	30.00	<LOD	<LOD	12.90	<LOD	505.12	356.32	<LOD	<LOD	954.32	<LOD	<LOD	231.80
PD 98,059	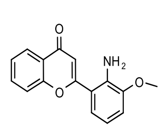	267.284	<LOD	21.16	17.23	<LOD	<LOD	30.00	<LOD	<LOD	12.90	<LOD	336.74	272.12	<LOD	<LOD	954.32	<LOD	<LOD	231.80

VIOLASTYRENE	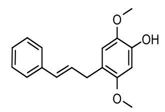	270.328	22.76	<LOD	18.03	<LOD	<LOD	30.00	<LOD	<LOD	12.90	336.74	<LOD	272.12	<LOD	<LOD	954.32	<LOD	<LOD	231.80
THONZONIUM BROMIDE	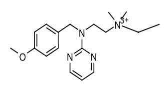	589.705	23.05	<LOD	18.18	<LOD	<LOD	30.00	<LOD	226.97	119.93	350.77	<LOD	279.14	<LOD	<LOD	954.32	<LOD	3690.08	1960.94
VITEXIN	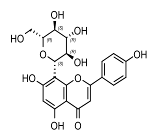	432.381	<LOD	25.46	19.38	<LOD	<LOD	30.00	<LOD	<LOD	12.90	<LOD	378.83	293.17	<LOD	<LOD	954.32	<LOD	<LOD	231.80
7,8-DIHYDROXYFLAVONE	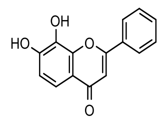	254.241	20.86	<LOD	17.08	<LOD	<LOD	30.00	<LOD	<LOD	12.90	308.68	<LOD	258.09	<LOD	<LOD	954.32	<LOD	<LOD	231.80
AJMALICINE HYDROCHLORIDE	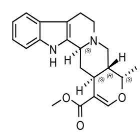	388.894	<LOD	26.90	20.10	<LOD	<LOD	30.00	<LOD	<LOD	12.90	<LOD	448.98	328.25	<LOD	<LOD	954.32	<LOD	<LOD	231.80
SANGUINARINE	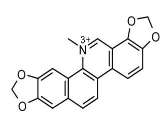	332.333	<LOD	21.81	17.55	<LOD	<LOD	30.00	<LOD	<LOD	12.90	<LOD	364.80	286.15	<LOD	<LOD	954.32	<LOD	<LOD	231.80
PHOSPHORAMIDON DISODIUM*	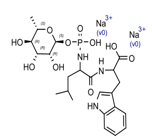	589.486	<LOD	27.34	20.32	<LOD	<LOD	30.00	<LOD	<LOD	12.90	<LOD	434.95	321.23	<LOD	<LOD	954.32	<LOD	<LOD	231.80
10-HYDROXYCAMPTOTHECIN	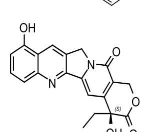	364.357	<LOD	28.52	20.91	<LOD	<LOD	30.00	<LOD	<LOD	12.90	<LOD	477.04	342.28	<LOD	<LOD	954.32	<LOD	<LOD	231.80
ACETYLPHENYLALANINE	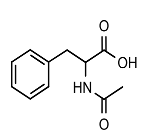	207.229	<LOD	20.62	16.96	<LOD	<LOD	30.00	<LOD	<LOD	12.90	<LOD	336.74	272.12	<LOD	<LOD	954.32	<LOD	<LOD	231.80
TERBINAFINE HYDROCHLORIDE*	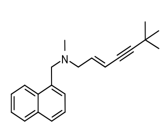	327.898	<LOD	21.77	17.54	<LOD	<LOD	30.00	<LOD	<LOD	12.90	<LOD	350.77	279.14	<LOD	<LOD	954.32	<LOD	<LOD	231.80
CARNOSIC ACID	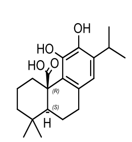	332.440	<LOD	26.41	19.85	<LOD	<LOD	30.00	<LOD	<LOD	12.90	<LOD	392.86	300.19	<LOD	<LOD	954.32	<LOD	<LOD	231.80
GAMBOGIC ACID	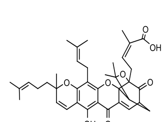	628.762	26.55	<LOD	19.92	<LOD	<LOD	30.00	<LOD	<LOD	12.90	392.86	<LOD	300.19	<LOD	<LOD	954.32	<LOD	<LOD	231.80

SCHISANDRIN B, S(-)-	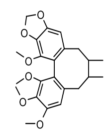	400.471	<LOD	31.12	22.21	<LOD	<LOD	30.00	<LOD	<LOD	12.90	<LOD	463.01	335.26	<LOD	<LOD	954.32	<LOD	<LOD	231.80
SPIRAMYCIN*	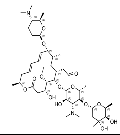	843.065	22.12	<LOD	17.71	<LOD	<LOD	30.00	<LOD	<LOD	12.90	364.80	<LOD	286.15	<LOD	<LOD	954.32	<LOD	<LOD	231.80

TABLE 3.3 K_M and IC_{50} of the top 48 hit substrates of CYP3C1. Compound name and structure are given. K_M was determined for rates of NADPH depletion and IC_{50} was based on the inhibition of BFC metabolism. Data are given with their respective standard error of the mean (SEM) developed from Michaelis-Menten curves, fitted using online tool: http://www.ic50.tk/. NA is denoted in places where the curve did not follow typical Michaelis-Menten kinetics and K_M and IC_{50} values could not be computed. Grey highlighted cells indicate K_M and IC_{50} where maximum inhibition or fluorescence was not reached. Compounds that were identified to be CYP3A4 substrates through DataBank.ca (Wishart et al 2018) are identified by an asterisk beside the compound name.

		K_M		IC_{50}	
Compound Name	**Structure**	**(µM) ± SEM**		**(µM) ± SEM**	
2',6'-DIHYDROXY-4'-METHOXY-CHALCONE	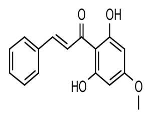	NA	NA	1.6150	0.8495
OSTHOLE	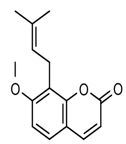	NA	NA	2.4418	1.0290
PLUMBAGIN	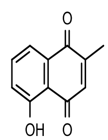	6.8772	1.1400	4.1209	0.1477
β-LAPACHONE	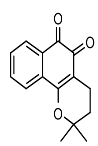	20.7236	4.6820	5.5259	0.3569
MENADIONE	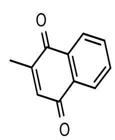	12.6968	1.4420	6.2638	0.3540
NSC 95397	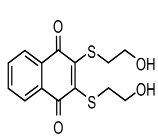	7.3095	2.0700	8.1779	0.4796
NITROMIDE	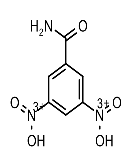	35.0379	18.2500	8.3350	1.6600
IDEBENONE	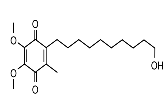	7.7752	1.7360	8.4574	2.7090

GW2974	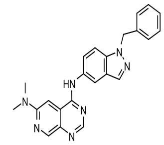	15.8155	6.5470	9.7430	0.8502
ZM 39923 HYDROCHLORIDE	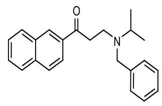	100.7420	54.4800	9.8863	2.1690
HYCANTHONE	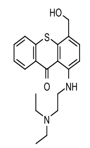	NA	NA	10.3374	1.5870
DULOXETINE HYDROCHLORIDE	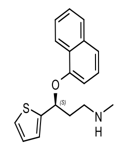	15.8898	6.6720	11.8316	2.6450
CLOXYQUIN	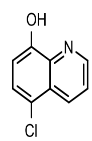	36.9614	19.7400	12.1016	0.9303
PRIMAQUINE DIPHOSPHATE	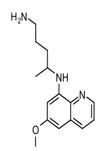	40.2012	9.4040	12.3988	1.7570
HYPOCRELLIN A	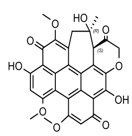	0.0071	0.0096	13.3154	5.0420
HOMIDIUM BROMIDE	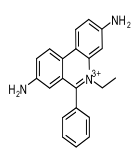	12.1734	4.5690	14.5438	7.5850
3,4-DIMETHOXY-DALBERGIONE	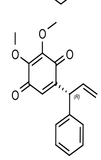	13.2500	13.2500	15.7604	1.0010
DAPH	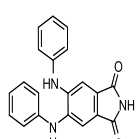	21.4603	20.6500	16.4600	1.9459

MYRICETIN	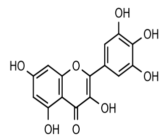	235.554*	480.7000	16.5310	4.1980
GOSSYPETIN	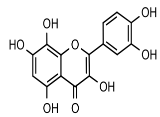	79.4538*	39.3900	16.5316	2.1880
SANGUINARINE SULFATE	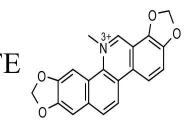	44.9685	14.6300	17.1769	2.0550
1-(1-NAPHTHYL) PIPERAZINE HYDROCHLORIDE	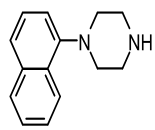	417.006*	1386.0000	21.1889	1.7370
FLUPIRTINE MALEATE	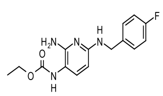	20.2897	7.1630	21.9072	10.8100
APOMORPHINE HYDROCHLORIDE HEMIHYDRATE	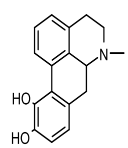	245.9990	475.9000	26.3179	29.8300
DEPHOSTATIN	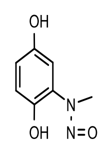	81.6966*	60.4000	27.5166	9.4460
ISORESERPINE, (-)	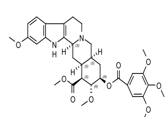	NA	NA	32.1931	12.4000
DOXAZOSIN MESYLATE	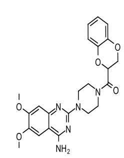	128.5130	106.9000	33.5833	11.5700
BTO-1	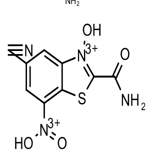	107.0810	52.1500	34.0822	5.2250

ANTIAROL	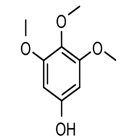	41.6904	15.6000	34.3012	14.9300
AZOMYCIN	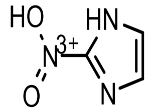	0.0025	0.0020	34.6889*	101.9*
ISOCORYDINE	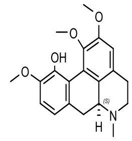	86.5106	85.8900	43.8828	14.9700
LAPACHOL	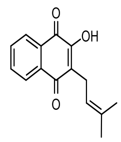	29.0373	8.5210	46.4123	10.9500
TETRAHYDROALSTONIN E	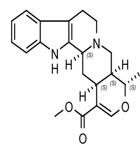	0.0172	0.0248	48.0535	26.5400
R(-)-2,10,11-TRIHYDROXY-N-PROPYLNORAPORPHINE HYDROBROMIDE	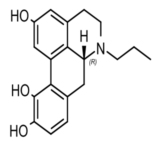	125.7790	98.1600	84.4824	4.2130
R(-)-APOCODEINE HYDROCHLORIDE	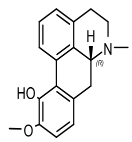	75.2378	67.0700	129.8590	218.1000
OXYQUINOLINE HEMISULFATE	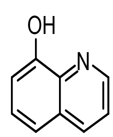	62.4385	23.0400	459.2320	1367.0000
ACETOSYRINGONE	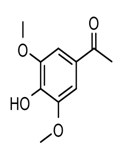	5264.2300	86600	482.787*	18070*
BERBERINE	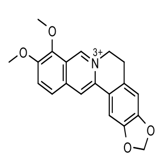	0.0010	0.0014	1048.6500	248000.0000

CHLORANIL	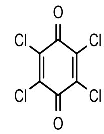	129.2190	58.8900	11842.2000	203500
FLAVOKAWAIN A	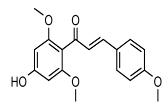	90.5152	144.4000	49730.0000	102200000
R(-)-2,10,11-TRIHYDROXY-APORPHINE HYBROBROMIDE	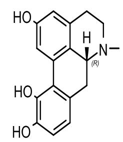	782.2340	2681.0000	112569	28960000
5,6-DEHYDROKAWAIN	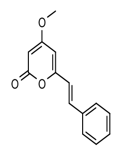	NA	NA	NA	NA
UVAOL	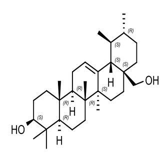	NA	NA	NA	NA
VULPINIC ACID	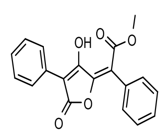	0.0008	0.0011	NA	NA
CORALYNE CHLORIDE	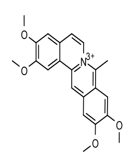	16.0050	6.1230	NA	NA
CORALYNE CHLORIDE HYDRATE	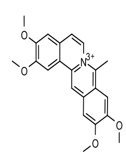	22.8694	4.5340	NA	NA
YANGONIN	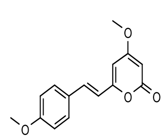	NA	NA	NA	NA
PRAZOSIN HYDROCHLORIDE	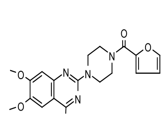	0.00377*	0.002012*	NA	NA

FIGURES

FIGURE 3.1 The effects of increasing concentrations of DMSO (%v/v) on the rates of CYP3C1 mediated **A)** NADPH depletion with 20 μM 7-methoxyresorufin (7-MR) and **B)** 7-hydroxy-4-(trifluoromethyl)coumarin (HFC) formation at 20 μM 7-benxyloxy-4-(trifluoromethyl) coumarin (BFC). All reactions were performed in 50 μL reactions in EROD buffer. Catalytic rates are normalized to P450 content.

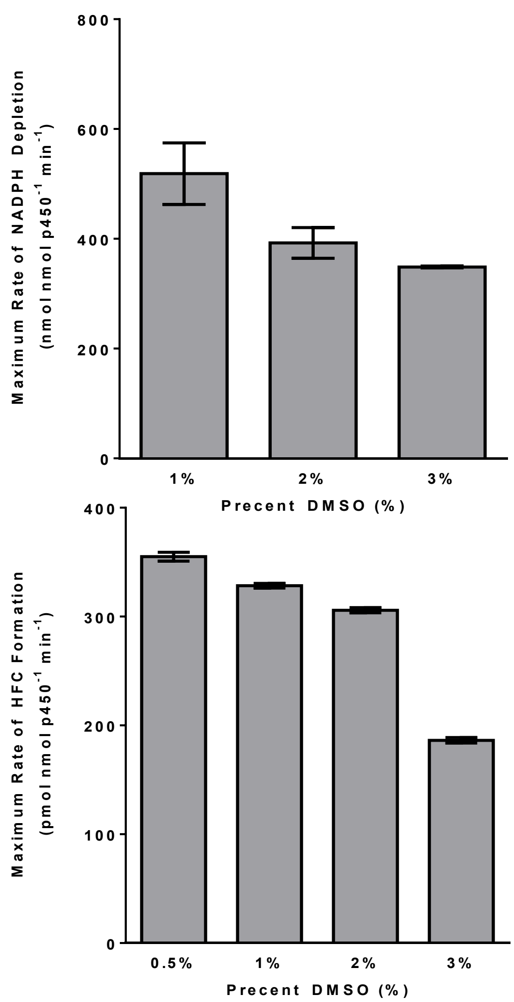

FIGURE 3.2 The maximum catalytic activity of CYP3C1 mediated metabolism for alkyloxy-resorufin substrates. Data are shown for reactions with 1 μM 7-benzyloxyresorufin (7-BR), 25 μM 7-ethoxyresorufin (7-ER), 15 μM 7-methoxyresorufin (7-MR) and 3 μM 7-pentoxyresorufin (7-PR). All reactions were performed in 200 μL reactions, initiated with 1.33 mM NADPH and contained 0.5% DMSO in EROD buffer.

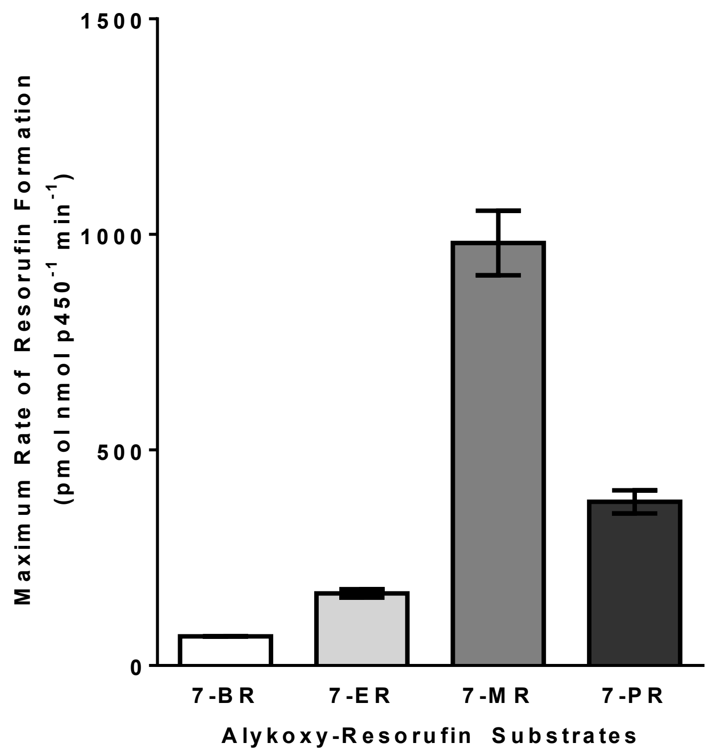

FIGURE 3.3 The maximum catalytic activity of CYP3C1 mediated metabolism of 7-benxyloxy-4-(trifluoromethyl) coumarin (BFC) and dibenzylfluorescein (DBF). All reactions were performed in 200 µL reactions, initiated with 1.33 mM NADPH and contained 0.25% DMSO in KPO_4 buffer with either 60 µM BFC or 3 µM DBF

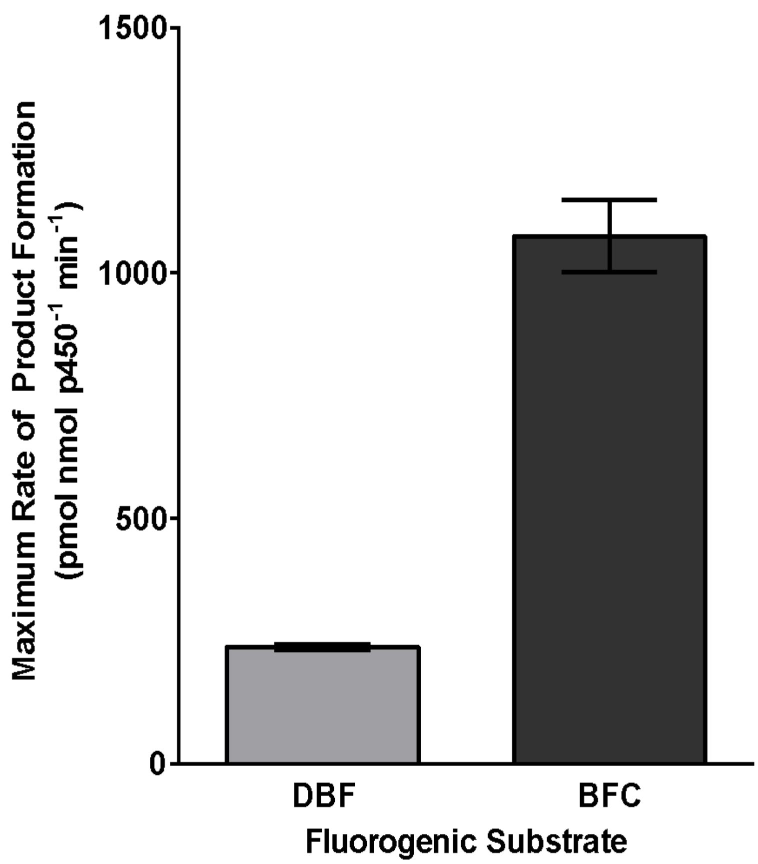

FIGURE 3.4 Michaelis-Menten curves of 7-methoyxresorufin (7-MR) and B) 7-benxyloxy-4-(trifluoromethyl)coumarin (BFC) metabolism. All reactions were performed in 200 µL reactions, initiated with 1.33 mM NADPH; BFC contained 0.25% DMSO in KPO_4 buffer and 7-MR contained 0.5% DMSO in EROD buffer.

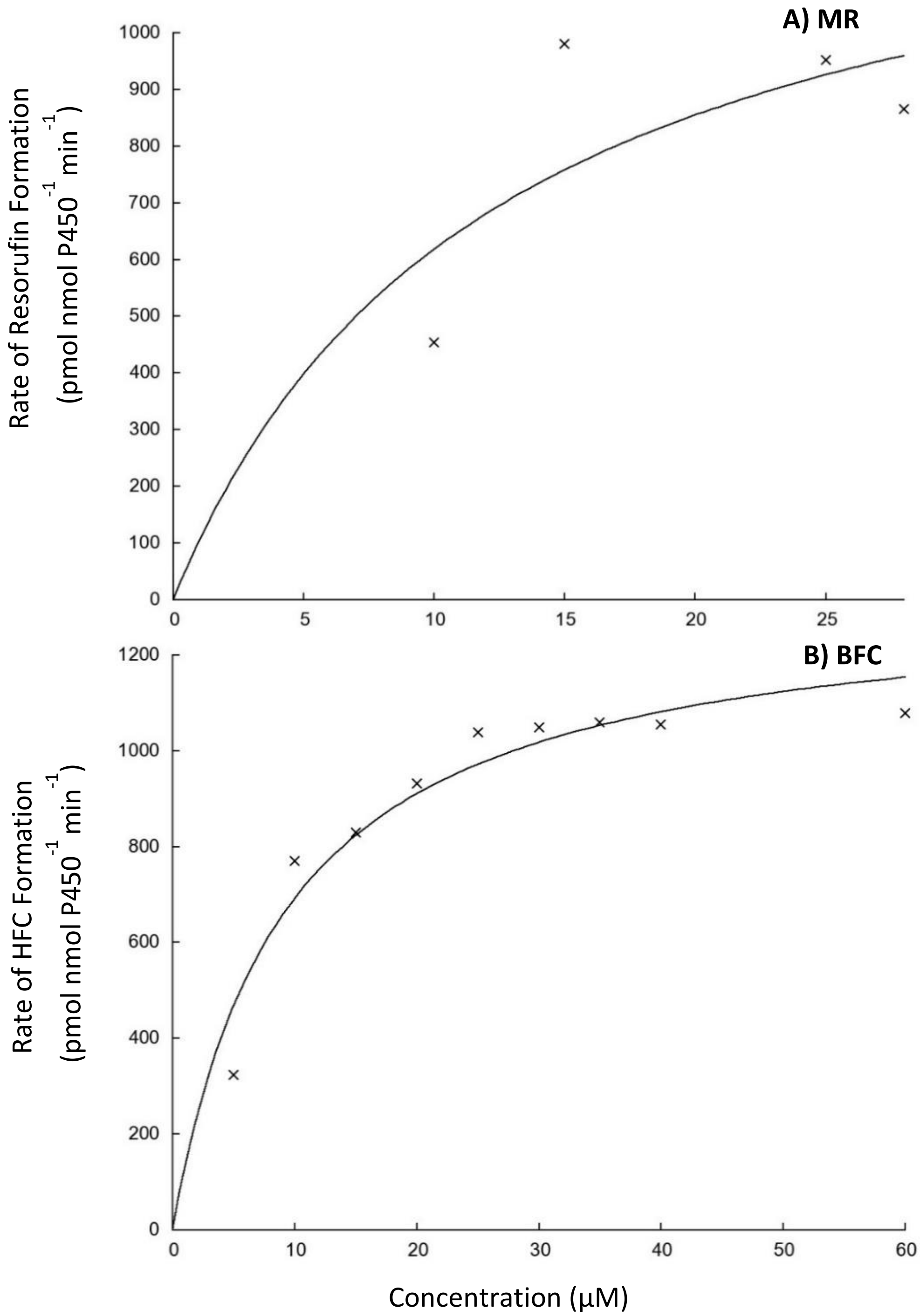
A) MR
Rate of Resorufin Formation
(pmol nmol P450^{-1} min^{-1})
0
100
200
300
400
500
600
700
800
900
1000
0
5
10
15
20
25
B) BFC
Rate of HFC Formation
(pmol nmol P450^{-1} min^{-1})
0
200
400
600
800
1000
1200
0
10
20
30
40
50
60
Concentration (µM)

FIGURE 3.5 Rate of NADPH depletion for ~4000 compounds, reported as a percent of the positive control (CYP3C1 + 7-methoxyresorufin; 7-MR). Catalytic activity of replicate two is graphed as a function of replicate one. The solid and dashed black lines denotes the limit of detection, determined as 3-standard deviation above the mean rate of NADPH depletion in the negative control (No substrate; CYP3C1 + 2% DMSO; 13% of the positive control), and the cut off for compounds to be included in the initial follow up (20% of the positive control), respectively.

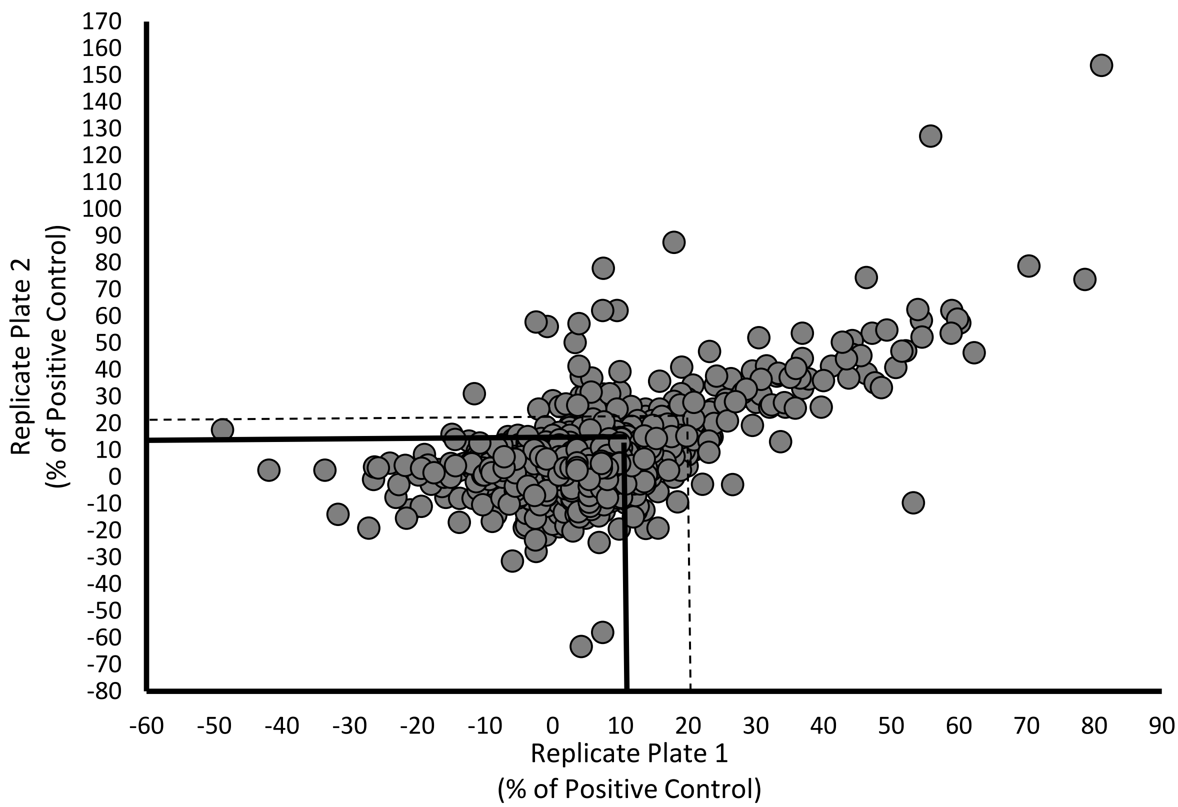
170
160
150
140
130
120
110
100
90
80
70
60
50
40
30
20
10
0
-10
-20
-30
-40
-50
-60
-70
-80
Replicate Plate 2
(% of Positive Control)
-60
-50
-40
-30
-20
-10
0
10
20
30
40
50
60
70
80
90
Replicate Plate 1
(% of Positive Control)

REFERENCES

Baron MG, Mintram KS, Owen SF, Hetheridge MJ, Moody AJ, et al. 2017. Pharmaceutical Metabolism in Fish: Using a 3-D Hepatic In Vitro Model to Assess Clearance. *PloS One* 12: e0168837-e37

Burke MD, Thompson S, Weaver RJ, Wolf CR, Mayers RT. 1994. Cytochrome P450 specificities of alkoxy-resorufin O-dealkylation in human and rat liver. *Biochemical Pharmacology* 48: 923-36

Burkina V, Zlabek V, Zamaratskaia G. 2013. Clotrimazole, but not dexamethasone, is a potent in vitro inhibitor of cytochrome P450 isoforms CYP1A and CYP3A in rainbow trout. *Chemosphere* 92: 1099-104

Chen A, Zhou X, Tang S, Liu M, Wang X. 2016. Evaluation of the inhibition potential of plumbagin against cytochrome P450 using LC-MS/MS and cocktail approach. *Scientific Reports* 6: 28482

Christen V, Oggier DM, Fent K. 2009. A microtiter-plate-based cytochrome P450 3A activity assay in fish cell lines. *Environmental Toxicology and Chemistry* 28: 2632-2638

Corcoran J, Lange A, Winter MJ, Tyler CR. 2012. Effects of Pharmaceuticals on the Expression of Genes Involved in Detoxification in a Carp Primary Hepatocyte Model. *Environmental Science and Technology* 46: 6306-14

Corley-Smith GE, Su HT, Wang-Buhler JL, Tseng HP, Hu CH, et al. 2006. CYP3C1, the first member of a new cytochrome P450 subfamily found in zebrafish (*Danio rerio*). *Biochemical and Biophysical Research Communications* 340: 1039-46

Crespi CL, Stresser DM. 2000. Fluorometric screening for metabolism-based drug–drug interactions. *Journal of Pharmacological and Toxicological Methods* 44: 325-31

Dai YJ, Jia YF, Chen N, Bian WP, Li QK, et al. 2014. Zebrafish as a model system to study toxicology. *Environmental Toxicology and Chemistry* 33: 11-17

Denisov IG, Makris TM, Sligar SG, Schlichting I. 2005. Structure and Chemistry of Cytochrome P450. *Chemical Reviews* 105: 2253-78

Dooley K, Zon LI. 2000. Zebrafish: a model system for the study of human disease. *Current Opinion in Genetics and Development* 10: 252-56

Dubin M, Fernandez SV, Stoppani A. 2001. Cytotoxicity of beta-lapachone, an naphthoquinone with possible therapeutic use. *Medicina* 61: 343-50

Ekroos M, Sjögren T. 2006. Structural basis for ligand promiscuity in cytochrome P450 3A4. *Proceedings of the National Academy of Sciences* 103: 13682-87

Fujita K-i. 2004. Food-drug interactions Via human Cytochrome P450 3A (CYP3A). *Drug Metabolism and Drug Interactions* 20: 195-217

Gonzalez FJ, Nebert DW. 1990. Evolution of the P450 gene superfamily: animal-plant 'warfare', molecular drive and human genetic differences in drug oxidation. *Trends in Genetics : TIG* 6: 182-6

Guengerich FP. 1999. Cytochrome P-450 3A4: regulation and role in drug metabolism. *Annual Review of Pharmacology and Toxicology* 39: 1-17

Guengerich FP. 2001. Common and uncommon cytochrome P450 reactions related to metabolism and chemical toxicity. *Chemical Research in Toxicology* 14: 611-50

Guengerich FP, Cheng Q. 2011. Orphans in the human cytochrome P450 superfamily: approaches to discovering functions and relevance in pharmacology. *Pharmacological Reviews* 63: 684-99

Gutzmann H, Hadler D. 1998. Sustained efficacy and safety of idebenone in the treatment of Alzheimer’s disease: update on a 2-year double-blind multicentre study In *Alzheimer’s Disease—From Basic Research to Clinical Applications*, pp. 301-10: Springer

Harskamp J, Britz-McKibbin P, Wilson JY. 2012. Functional screening of cytochrome P450 activity and uncoupling by capillary electrophoresis. *Analytical Chemistry* 84: 862-6

Hartl MGJ, Kilemade M, Sheehan D, Mothersill C, O’Halloran J, et al. 2007. Hepatic biomarkers of sediment-associated pollution in juvenile turbot, *Scophthalmus maximus L*. *Marine Environmental Research* 64: 191-208

Hegelund T, Ottosson K, Rådinger M, Tomberg P, Celander MC. 2004. Effects of the antifungal imidazole ketoconazole on CYP1A and CYP3A in rainbow trout and killifish. *Environmental Toxicology and Chemistry* 23: 1326-34

Hill AJ, Teraoka H, Heideman W, Peterson RE. 2005. Zebrafish as a model vertebrate for investigating chemical toxicity. *Toxicological Sciences : An Official Journal of the Society of Toxicology* 86: 6-19

Huang L, Pardee AB. 1999. beta-lapachone induces cell cycle arrest and apoptosis in human colon cancer cells. *Molecular Medicine* 5: 711

Johnson EF, Connick JP, Reed JR, Backes WL, Desai MC, et al. 2014. Correlating structure and function of drug-metabolizing enzymes: progress and ongoing challenges. *Drug Metabolism and Disposition* 42: 9-22

Kobayashi K, Urashima K, Shimada N, Chiba K. 2002. Substrate specificity for rat cytochrome P450 (CYP) isoforms: screening with cDNA-expressed systems of the rat. *Biochemical Pharmacology* 63: 889-96

Koenig S, Fernández P, Solé M. 2012. Differences in cytochrome P450 enzyme activities between fish and crustacea: Relationship with the bioaccumulation patterns of polychlorobiphenyls (PCBs). *Aquatic Toxicology* 108: 11-17

Krishnaswamy M, Purushothaman K. 1980. Plumbagin: a study of its anticancer, antibacterial and antifungal properties. *Indian Journal of Experimental Biology* 18: 876-77

Kubota A, Goldstone JV, Lemaire B, Takata M, Woodin BR, Stegeman JJ. 2015. Role of pregnane X receptor and aryl hydrocarbon receptor in transcriptional regulation of pxr, CYP2, and CYP3 genes in developing zebrafish. *Toxicological Sciences* 143: 398-407

Kuehl P, Zhang J, Lin Y, Lamba J, Assem M, et al. 2001. Sequence diversity in CYP3A promoters and characterization of the genetic basis of polymorphic CYP3A5 expression. *Nature Genetics* 27: 383

LeBel CP, Ischiropoulos H, Bondy SC. 1992. Evaluation of the probe 2',7'-dichlorofluorescin as an indicator of reactive oxygen species formation and oxidative stress. *Chemical Research in Toxicology* 5: 227-31

Lopes J, Cruz F, Docampo R, Vasconcellos M, Sampaio M, et al. 1978. In vitro and in vivo evaluation of the toxicity of 1, 4-naphthoquinone and 1, 2-naphthoquinone derivatives against *Trypanosoma cruzi. Annals of Tropical Medicine & Parasitology* 72: 523-31

Massey V. 1959. The microestimation of succinate and the extinction coefficient of cytochrome c. *Biochimica et biophysica acta* 34: 255-6

Medeiros C, Pontes-Filho N, Camara C, Lima-Filho J, Oliveira P, et al. 2010. Antifungal activity of the naphthoquinone beta-lapachone against disseminated infection with Cryptococcus neoformans var. neoformans in dexamethasone-immunosuppressed Swiss mice. *Brazilian Journal of Medical and Biological Research* 43: 345-49

Mueller SO, Stopper H, Dekant W. 1998. Biotransformation of the anthraquinones emodin and chrysophanol by cytochrome P450 enzymes. Bioactivation to genotoxic metabolites. *Drug Metabolism and Disposition: the Biological Fate of Chemicals* 26: 540-6

Murray GI, Melvin WT, Greenlee WF, Burke MD. 2001. Regulation, function, and tissue-specific expression of cytochrome P450 CYP1B1. *Annual Review of Pharmacology and Toxicology* 41: 297-316

Nelson DR. 2006. Cytochrome P450 nomenclature, 2004. *Methods in Molecular Biology (Clifton, N.J.)* 320: 1-10

Nelson DR, Goldstone JV, Stegeman JJ. 2013. The cytochrome P450 genesis locus: the origin and evolution of animal cytochrome P450s. *Philosophical Transactions of the Royal Society of London. Series B, Biological Sciences* 368: 20120474-74

Nelson DR, Nebert DW. 2018. Cytochrome P450 (*CYP*) Gene Superfamily In *eLS*, pp. 1-19: John Wiley & Sons, Ltd (Ed). doi:10.1002/9780470015902.a0005667.pub3

Nerurkar PV, Park SS, Thomas PE, Nims RW, Lubet RA. 1993. Methoxyresorufin and benzyloxyresorufin: substrates preferentially metabolized by cytochromes P4501A2 and 2B, respectively, in the rat and mouse. *Biochemical Pharmacology* 46: 933-43

Omura T, Sato R. 1964. The carbon monoxide-binding pigment of liver microsomes. I. Evidence for its hemoprotein nature. *The Journal of Biological Chemistry* 239: 2370-8

Ough M, Lewis A, Bey EA, Gao J, Ritchie JM, et al. 2005. Efficacy of beta-lapachone in pancreatic cancer treatment: exploiting the novel, therapeutic target NQO1. *Cancer Biology and Therapy* 4: 102-09

Paiva SRd, Figueiredo MR, Aragão TV, Kaplan MAC. 2003. Antimicrobial activity in vitro of plumbagin isolated from Plumbago species. *Memorias do Instituto Oswaldo Cruz* 98: 959-61

Pritchard MP, McLaughlin L, Friedberg T. 2006. Establishment of functional human cytochrome P450 monooxygenase systems in *Escherichia coli. Methods in Molecular Biology* 320: 19-29

Pritchard MP, Ossetian R, Li DN, Henderson CJ, Burchell B, et al. 1997. A general strategy for the expression of recombinant human cytochrome P450s in *Escherichia coli* using bacterial signal peptides: Expression of CYP3A4, CYP2A6, and CYP2E1. *Archives of Biochemistry and Biophysics* 345: 342-54

Raikow DF, Reid DF, Maynard EE, Landrum PF. 2006. Sensitivity of aquatic invertebrate resting eggs to SeaKleen®(menadione): A test of potential ballast tank treatment options. *Environmental Toxicology and Chemistry* 25: 552-59

Ranen NG, Peyser CE, Coyle JT, Bylsma FW, Sherr M, et al. 1996. A controlled trial of idebenone in Huntington's disease. *Movement disorders : Official Journal of The Movement Disorder Society* 11: 549-54

Rustin P, von Kleist-Retzow J-C, Chantrel-Groussard K, Sidi D, Munnich A, Rötig A. 1999. Effect of idebenone on cardiomyopathy in Friedreich's ataxia: a preliminary study. *The Lancet* 354: 477-79

Scornaienchi ML, Thornton C, Willett KL, Wilson JY. 2010a. Cytochrome P450-mediated 17β-estradiol metabolism in zebrafish (*Danio rerio*). *Journal of Endocrinology* 206: 317-25

Scornaienchi ML, Thornton C, Willett KL, Wilson JY. 2010b. Functional differences in the cytochrome P450 1 family enzymes from zebrafish (*Danio rerio*) using heterologously expressed proteins. *Archives of Biochemistry and Biophysics* 502: 17-22

Segura-Aguilar J, Metodiewa D, Welch CJ. 1998. Metabolic activation of dopamine o-quinones to o-semiquinones by NADPH cytochrome P450 reductase may play an important role in oxidative stress and apoptotic effects. *Biochimica et Biophysica Acta (BBA) - General Subjects* 1381: 1-6

Shaya L, Dejong C, Wilson JY. 2014. Expression patterns of cytochrome P450 3B and 3C genes in model fish species. *Comparative Biochemistry and Physiology. Toxicology and Pharmacology : CBP* 166: 115-25

Shaya L, Jones DE, Wilson JY. 2019. CYP3C gene regulation by the aryl hydrocarbon and estrogen receptors in zebrafish. *Toxicology and Applied Pharmacology* 362: 77-85

Song WH, Ding F, Guo J, Li LY, Zhang JH, et al. 2010. Study on acute toxicity and structure-activity relationship of zebrafish (*Danio rerio*) exposed to naphthoquinones. *Journal of Environmental Science and Health Part B* 45: 601-05

Stegeman JJ, Behrendt L, Woodin BR, Kubota A, Lemaire B, et al. 2015. Functional characterization of zebrafish cytochrome P450 1 family proteins expressed in yeast. *Biochimica et biophysica acta* 1850: 2340-52

Stresser DM, Turner SD, Blanchard AP, Miller VP, Crespi CL. 2002. Cytochrome P450 fluorometric substrates: identification of isoform-selective probes for rat CYP2D2 and human CYP3A4. *Drug Metabolism and Disposition* 30: 845-52

Sugie S, Okamoto K, Rahman KW, Tanaka T, Kawai K, et al. 1998. Inhibitory effects of plumbagin and juglone on azoxymethane-induced intestinal carcinogenesis in rats. *Cancer Letters* 127: 177-83

Sukkasem N, Chatuphonprasert W, Jarukamjorn K. 2018. Altered cytochrome P450 profiles by Plumbago indica Linn. and plumbagin after oral administration in mice. *Pharmacognosy Magazine* 14: 507

Talalay P, Dinkova-Kostova AT. 2004. Role of Nicotinamide Quinone Oxidoreductase 1 (NQO1) in Protection against Toxicity of Electrophiles and Reactive Oxygen Intermediates In *Methods in Enzymology*, pp. 355-64: Academic Press

Tanoue R, Margiotta-Casaluci L, Huerta B, Runnalls TJ, Nomiyama K, et al. 2017. Uptake and Metabolism of Human Pharmaceuticals by Fish: A Case Study with the Opioid Analgesic Tramadol. *Environmental Science and Technology* 51: 12825-35

Teixeira MJ, de Almeida YM, Viana JR, Holanda Filha JG, Rodrigues TP, et al. 2001. In vitro and in vivo Leishmanicidal activity of 2-hydroxy-3-(3-methyl-2-butenyl)-1, 4-naphthoquinone (lapachol). *Phytotherapy Research:* 15: 44-48

Tetef M, Margolin K, Ahn C, Akman S, Chow W, et al. 1995. Mitomycin C and menadione for the treatment of lung cancer: a phase II trial. *Investigational New drugs* 13: 157-62

Thibaut R, Schnell S, Porte C. 2006. The interference of pharmaceuticals with endogenous and xenobiotic metabolizing enzymes in carp liver: An In-Vitro Study. *Environmental Science & Technology* 40: 5154-60

Verrax J, Cadrobbi J, Marques C, Taper H, Habraken Y, et al. 2004. Ascorbate potentiates the cytotoxicity of menadione leading to an oxidative stress that kills cancer cells by a non-apoptotic caspase-3 independent form of cell death. *Apoptosis* 9: 223-33

Vinothkumar R, Ceasar SA, Divyarupa A. 2017. Chemosuppressive effect of plumbagin on human non-small lung cancer cell xenotransplanted zebrafish. *Indian Journal of Cancer* 54: 253-56

Wassmur B, Grans J, Kling P, Celander MC. 2010. Interactions of pharmaceuticals and other xenobiotics on hepatic pregnane X receptor and cytochrome P450 3A signaling pathway in rainbow trout (*Oncorhynchus mykiss*). *Aquatic Toxicology* 100: 91-100

White RD, Shea D, Stegeman JJ. 1997. Metabolism of the aryl hydrocarbon receptor agonist 3,3',4,4'-tetrachlorobiphenyl by the marine fish scup (*Stenotomus chrysops*) in vivo and in vitro. *Drug Metabolism and Disposition: the Biological Fate of Chemicals* 25: 564-72

Wishart DS, Feunang YD, Guo AC, Lo EJ, Marcu A, et al. 2018. DrugBank 5.0: a major update to the DrugBank database for 2018. *Nucleic Acids Research* 46: D1074-D1082

Wu Y-T, Lin CY, Tsai M-Y, Chen Y-H, Lu Y-F, et al. 2011. β-Lapachone induces heart morphogenetic and functional defects by promoting the death of erythrocytes and the endocardium in zebrafish embryos. *Journal of Biomedical Science* 18: 70

Yan J, Cai Z. 2010. Molecular evolution and functional divergence of the cytochrome P450 3 (CYP3) Family in Actinopterygii (ray-finned fish). *PloS one* 5: e14276

Zanger UM, Schwab M. 2013. Cytochrome P450 enzymes in drug metabolism: regulation of gene expression, enzyme activities, and impact of genetic variation. *Pharmacology and Therapeutics* 138: 103-41

CHAPTER 4

HIGH THROUGHPUT SCREENING OF SMALL BIOACTIVE COMPOUNDS FOR SUBSTRATES OF ZEBRAFISH (*DANIO RERIO*) CYP3A65

ABSTRACT

Cytochrome P450 monooxygenases play a critical role in detoxification processes. Human CYP3A4 is clinically important and metabolizes more than 50% of all known pharmaceuticals. Zebrafish have one CYP3A enzyme (CYP3A65) and it is commonly thought to have a similar function to human CYP3A4, however, there have been few functional assessments of CYP3A65. From an evolutionary standpoint, CYP3A65 is not an ortholog of CYP3A4 but is more closely related to the fish specific CYP3 enzymes from CYP3B, CYP3C, and CYP3D subfamilies, raising questions about functional overlap of fish and mammalian CYP3A enzymes. This study investigated the function of heterologously expressed zebrafish CYP3A65 by determining the catalytic activity for mammalian CYP specific fluorogenic substrates and in a high throughput screen of ~4000 biologically and pharmacologically active compounds. CYP3A65 metabolized all the tested alkyloxy-resorufin substrates but the catalytic activity was the greatest for 7-methyoxyresorufin (7-MR) and 7-ethoxyresorufin (7-ER), and the lowest for 7-benzyloxyresorufin (7-BR). CYP3A65 was capable of 7-benzyloxy-4-trifluoromethylcoumarin (BFC) and dibenzylfluorescein (DBF) metabolism, two mammalian CYP3A substrates, at similar rates but the rates were much less than those reported for human CYP3A4 and zebrafish CYP3C1 and CYP1A. These data suggest that CYP3A65 in fish is functionally different than mammalian CYP3A and that multiple fish CYP families and subfamilies are capable of metabolism of mammalian CYP3A specific

fluorogenic substrates. The high throughput screen was based on NADPH co-factor depletion and identified 320 compounds with activity above background; many were pharmacologically active compounds. The top 139 compounds had at least 20% of the activity found with 7-MR, but only 24 of these were human CYP3A4 substrates, suggesting a small overlap between mammalian and fish CYP3A. A large number (111/139) of top hits were overlapping with positive hits from a screen of zebrafish CYP3C1. The top substrates with the highest affinity for CYP3A65 included plumbagin, menadione, β-lapachone, and primaquine diphosphate. Despite structural diversity of the top 139 compounds, the best CYP3A65 substrates appeared biased to quinone-based structures. Further research is required to confirm quinone compounds as CYP3A65 substrates. Collectively, this data suggests that CYP3A65 differs in function from mammalian CYP3A enzymes. More catalytic data from fish CYP3A enzymes is needed to establish a substrate profile and function for CYP3A enzymes in fish.

INTRODUCTION

Cytochrome P450 (CYP) enzymes are monooxygenase enzymes found in all domains of life. To date, there are >55 000 cytochrome P450s that are categorized, based on amino acid sequence identity, into families and subfamilies (Nelson 2006, Nelson & Nebert 2018). Enzymes that have a sequence similarity of > 40% and 55% are placed in the same family and subfamily, respectively. CYP families 1, 2, 3 and 4 are predominantly involved in xenobiotic metabolism (as reviewed by Zanger & Schwab 2013). In mammals, CYP3A is the most abundantly expressed CYP enzyme in the liver and intestine (as reviewed by Zhou et al 2005). In humans, the CYP3A subfamily has high clinical value and is of biomedical interest due to the ability to metabolize more than 50% of pharmaceuticals, many environmental contaminants, xenobiotics and steroids (As reviewed by Zanger & Schwab 2013). There is some evidence to suggest that CYP3A enzymes can metabolize mycotoxins (Delaforge et al 1997, Shimada & Guengerich 1989) and bioactivate environmental procarcinogens, such as polycyclic aromatic hydrocarbons (Shimada et al 1989). The metabolism of steroids in mammals is an important process that is well established and mediated by several CYP enzymes including CYP3A (as reviewed by Tsuchiya et al 2005). Mammalian CYP3A enzymes in the brain and liver are important for the hydroxylation of testosterone, androstenedione, progesterone, dehydroepiandrosterone (Wang et al 2000) and estradiol (Lee et al 2001). Overall, the physiological role of CYP3A in mammals is important for detoxification and homeostasis.

Teleosts, such as zebrafish, have become an increasingly popular model system in toxicology (as reviewed by Dai et al 2014, and Hill et al 2005), disease research (as reviewed by Dooley & Zon 2000), and drug research and development (as reviewed by Zon & Peterson 2005). Zebrafish contain one CYP3A enzyme (CYP3A65) that was originally thought to share a close evolutionary relationship with mammalian CYP3A4, based on the phylogenetic clustering of fish CYP3A genes with mammalian, reptilian, and amphibian CYP3A genes (Goldstone et al 2010) until whole genome sequencing identified the unique teleost CYP3 subfamilies CYP3B, CYP3C, and CYP3D (Yan & Cai 2010). Phylogenies with all of the teleost CYP3 subfamilies clearly cluster teleost CYP3A genes in a clade with the other teleost CYP3 subfamilies and not with other vertebrate CYP3A genes (Yan and Cai 2010), supporting the notion that CYP3A genes in fish are not orthologs of mammalian CYP3A.

Like human CYP3A4, zebrafish CYP3A65 is highly expressed in detoxification organs like the intestine and liver (Tseng et al 2005). Several studies described an induction of CYP3A65 gene (Al-Habsi et al 2016, Jackson & Kennedy 2017, Liu et al 2018) and protein (Tseng et al 2005) expression with various pharmaceuticals suggesting that CYP3A65 may have the capacity to metabolize pharmacological compounds. Fish have shown the capacity to metabolize the synthetic mammalian CYP3A4 prototypical substrate, 7-benzyloxy-5-(trifluoromethyl) coumarin (BFC), in fish hepatocytes and microsomes (Hasselberg et al 2005, Hegelund et al 2004), supporting functional similarity between CYP3A65 and CYP3A4. Yet, heterologously expressed zebrafish CYP1s and CYP3A65 have been assessed *in vitro* for the metabolism of the mammalian

CYP3A substrates 17β-estradiol (E_2), BFC, 7-benzyloxyquinoline (BQ), and dibenzylfluorescein (DBF) with surprising results (Scornaienchi et al 2010b). Unlike in mammals, BFC and DBF metabolism was higher with zebrafish CYP1A and BQ metabolism was not detected with CYP3A65 (Scornaienchi et al 2010b). While in mammals E_2 is metabolized to a large extent by CYP1B1 and CYP3A4 (Lee et al 2003), fish CYP1A had higher catalytic activity for E_2 than CYP3A65 in vitro (Scornaienchi et al 2010b). Collectively, this suggests that some mammalian CYP3A substrates are not selective or specific for CYP3A65 and that CYP1 and CYP3 enzymes in fish may have some overlapping substrates.

Regulation of zebrafish CYP3A65 has been poorly characterized but may provide some clues on the function of the enzyme because it is common that ligands of receptors that regulate CYP expression are also substrates of that CYP. For examples, human CYP3A4 is regulated by the pregnane-x-receptor (PXR; Goodwin et al 2002), and the ligand of PXR, dexamethasone is also metabolised by CYP3A4 (Tomlinson et al 1997). The involvement of PXR in fish CYP regulation is not clear. Ligands that typically bind to the mammalian PXR do not always induce CYP3A protein or enzymatic activity in fish microsomes (Bainy et al 2013). Surprisingly, while mammalian CYP3A is not regulated by the aryl hydrocarbon receptor (AHR), zebrafish CYP3A65 was induced by a proto-typical AHR ligand (TCDD) and by mammalian PXR ligands (dexamethasone, rifampicin, pregnenolone), suggesting an involvement of both PXR and AhR in the regulatory pathway of zebrafish CYP3A65 (Chang et al 2013, Kubota et al 2014, Tseng et al 2005). Very little information is available on the regulation of other fish CYP3 subfamilies. Studies suggest that the AHR (Kubota et al 2014, Shaya et al 2019) and the ER (Shaya et al 2019) are involved in the regulation of CYP3C1.

Collectively, the current research provides evidence for both similarities and differences in the regulation and function between zebrafish CYP3A65 and human CYP3A4. The objective of this study was to provide significant catalytic data to identify CYP3A65 substrates and help clarify the function of this enzyme. We determined the catalytic activity of CYP3A65 for several fluorogenic CYP probe substrates and in a high throughput screen with 4000 pharmacologically and biologically active compounds from commercially available libraries. Substrate docking in the CYP active site triggers the reduction of nicotinoamide adenine dinucleotide phosphate hydrogen (NADPH) by cytochrome P450 reductase (as reviewed by Guengerich 2001) and two serial electron donations to the catalytic reaction (as reviewed by Denisov et al 2005). The high throughput screen capitalizes on this aspect of the CYP catalytic cycle and uses the depletion of the co-factor NADPH as an indirect measure of CYP activity. If reactions are not tightly coupled, CYP enzymes can consume NADPH but produce reactive oxygen species (ROS), with little to no product formation (as reviewed by Denison et al 2005). The catalytic reactions that result in the formation of significant ROS are considered uncoupled reactions and are more common with CYPs that are involved in detoxification (as reviewed by Denison et al 2005). Thus, we have determined ROS production in our positive hits to assess how well coupled the catalytic reactions were for CYP3A65 and remove false positives from highly uncoupled reactions. The mammalian CYP3A active site is known to be very promiscuous and can accommodate many structurally un-related compounds (Ekroos and Sjorgen 2006). Assuming this might also be true of CYP3A65, testing individual compounds would not provide enough data to infer CYP3A65 function. This screen provided significant data to determine substrates of CYP3A65, to provide a robust assessment of function, and to contrast with mammalian CYP3A and zebrafish CYP3C1 enzymes. We expected to identify many structurally diverse substrates of CYP3A65. Based on the close evolutionary relationship between CYP3A65 and CYP3C1, and prior data that suggests some overlap in function of CYP3A65 and CYP3A4, we predicted that we would identify common substrates between CYP3A65 and CYP3C1 and hit compounds known to be substrates for CYP3A4.

MATERIALS AND METHODS

CYP3A65 Heterologous Expression

CYP3A65 was previously heterologously expressed (Scornaienchi et al 2010). A sample of glycerol stocks of JM109 competent *Escherichia coli* (*E.Coli)* cells containing OmpA(2+)-CYP3A65 constructs and human cytochrome P450 reductase (CPR) were grown overnight at 37°C on Luria-Bertani (LB) agar plates supplemented with ampicillin (50 μg/mL) and chloramphenicol (25 μg/mL). A single colony was grown overnight in supplemented LB-broth. The sample was purified by PureLink Quick Plasmid Miniprep Kit (Invitrogen, Carlsbad, CA) and the presence of CYP3A65 and CPR were confirmed using sanger sequencing by Mobix Laboratory (McMaster University, Hamilton, ON).

Cultures of the bacteria were grown in Terrific Broth (TB) supplemented with ampicillin (50 μg/mL), chloramphenicol (25 μg/mL), and thiamine (1mM). Once the culture had reached an appropriate density (OD600 of ~0.8) it was supplemented with isopropyl B-D-1-thiogalactopyranoside (IPTG; 1mM; Fisher Scientific, Pittsburgh, PA) and δ-aminolevulinic acid (ALA, 0.1mM; MP Biomedicals, Solon, OH). ALA was used to maximize the incorporation of the heme to ensure active enzyme. The cultures were incubated for 22 hours before cells were harvested and the membranes were purified as previously described (Pritchard et al 2006). Total protein content was determined using a bicinchoninic acid protein assay kit as per manufacturer's protocol (Thermo Scientific, Rockford, IL).

Total P450 Analysis and Cytochrome P450 Reductase Activity

Total P450 content was measured using a carbon monoxide (CO) difference spectral assay (Pritchard et al 2006) and calculated based on the extinction coefficient of 92/mM/cM (Omura & Sato 1964). Cytochrome P450 reductase activity was measured using NADH (5 mg/ mL; Sigma Aldrich, St Louis, MO) and cytochrome c (1 mg/mL from bovine; Sigma Aldrich, St Louis, MO) in 0.2 M potassium phosphate buffer (KPO_4) at 37°C by determining increasing absorbance at 550nM over time (Pritchard et al 2006). Cytochrome P450 reductase activity was normalized for total protein content and calculated based on the extinction coefficient of 21/mM/cm (Massey 1959).

Fluorescent Catalytic Assays

CYP3A65 catalytic activity, K_M and V_{max} was determined for 10 synthetic fluorogenic probe substrates with known specificity for mammalian CYPs (Table 1; Murray et al 2001, Stresser et al 2002, Scornaienchi et al 2010a). All fluorogenic substrates were purchased from Sigma Aldrich (St Louis, MO). 7-ethoxyresorufin (7-ER), 7-methyoxyresorufin (7-MR), 7-benzyloxyresorufin (7-BR) and 7-pentoxyresorufin (7-

PR) substrates were resuspended in dimethysulfoxide (DMSO). 3-[2-(N,N-diethyl-Nmethylamino)ethyl]-7-methoxy-4-methylcoumarin (AMMC), 7-methoxy-4-(aminomethyl)-coumarin (MAMC), 7-benzyloxy-4(trifluoromethyl)coumarin (BFC), 7-benzyoxyquinoline (BQ), dibenzylfluorescein (DBF), and 7-methyoxy-trifluoromethylcoumarin (MFC) were resuspended in acetonitrile and sonicated for 30 seconds on ice. The resorufin substrates reactions were run at 30°C in 40mM Tris HCl, 80mM NaCl; pH 7.8. All other substrates were run at 30ºC in 0.4M $KP0_4$ buffer at pH 7.4. All reactions were performed in 200uL in 96 well plates and initiated with 1.33mM NADPH. DMSO concentration was maintained at the lowest possible concentration to obtain maximum enzymatic activity. A Michaelis-Menten curve was generated by measuring the catalytic activity on a Synergy 2 fluorimeter (BioTek, Winooski, VT), at various concentrations of substrate, over 15 minutes, and at appropriate excitation and emission wavelengths for each fluorogenic substrate. Catalytic activity was normalized to the total P450 content in each reaction. K_M and V_{max} values and respective standard error values were generated from fitting the Michaelis-Menten curve using an online tool (http://www.ic50.tk/kmvmax.html).

High Throughput Screening Assay Design: NADPH Depletion

The rate of NADPH depletion by CYP3A65 was used to assess catalytic activity for bioactive substrates from commercially available libraries including Prestwick, Microsource Spectrum, Library of Pharmacologically Active Compounds (LOPAC) and BioMol Natural Products Library (BioMol). Screens were performed at the Centre for Microbial Chemical Biology (McMaster University, Hamilton, ON). Prior to high throughput screening, the NADPH depletion assay was optimized for CYP3A65 with 7-MR using 1-3% DMSO (Figure 1A), various concentrations of enzyme, temperature, light sensitivity and miniaturization of reaction volume. The Michaelis-Menten curve was developed for CYP3A65 catalytic activity with 7-MR (Figure 2A) to determine an appropriate substrate concentration for the high throughput reactions. 50 µL reactions were run in 384 well plates, containing 41.5mM Tris-HCL, 83mM NaCl, 20 µM substrate in DMSO (2% v/v), 150 µM NADPH, and initiated with 3.85µg of purified CYP3A65 membranes. Prior to high throughput screening, a Z-prime (Z') was calculated to assess the quality of the assay conditions chosen. The Z' is a statistical tool that measures the signal window by taking into consideration the mean and standard deviations of the positive control and negative controls. In this case, the positive and negative controls were the rate of NADPH depletion for CYP3A65 and 2% DMSO, with or without 20µM 7-MR, respectively. An acceptable Z' for a high throughput assay must be between 0.5 – 1; the closer to 1, the better the quality of the assay. The Z' prime was calculated at 0.75 from a single 384 well plate where half the wells contained the positive control and the other half contained negative controls (data not shown).

For the primary high throughput screen, each reaction was run twice, on replicate plates. Reactions were plated by Biomek® FXP Integrated Liquid Handler (Beckman Coulter, Indianapolis, IN). All experimental plates contained 32 positive controls (7-MR) and 32 negative controls (DMSO only) to ensure assay quality throughout the duration of the screen. For all assay plates, the change in absorbance at 355 nM was measured, using EnVision Multilabel Plate Reader (Perkin Elmer, Hopkinton, MA), every 2 minutes for a

10-minute duration, providing an 8-point curve. A rate was obtained from the curve for each of the wells in the 384 well plate. Rates of NADPH depletion in each well were calculated and normalized for total P450. The background was measured from the negative control wells (no substrate) and hits were defined as those whose rate of NADPH depletion was 3 times the standard deviations above the mean rate of NADPH depletion of the negative control (lowest limit of detection; LOD). Data for NADPH depletion are normalized for P450 content and presented either as catalytic rate (nmol/nmol P450/min) or as a percent of the activity in the positive control (Table 2).

Due to a technical error, 9 compound plates (containing 2880 compounds) had one of the replicate plates run with double the concentration of substrate and DMSO (40 μM; 4% v/v DMSO). To account for differences in NADPH depletion at different substrate and DMSO concentrations across replicates, compounds were considered a hit if the rate of NADPH in either replicate 1 or replicate 2 met the cut-off (>LOD). Replicates are reported separately (Table 2).

The top 139 hits, based on the highest rate of NADPH depletion, were selected for a secondary screen to determine if the catalytic activity was protein dependent and to quantify the reactive oxygen species generation (described below) to detect highly uncoupled reactions. Reactions were assessed for enzyme independent NADPH depletion by repeating reactions as described above but in the absence of the enzyme; the enzyme was replaced with an equal volume of buffer. Those reactions with significant NADPH depletion in absence of protein were considered false positives.

Reacting Oxygen Species (ROS) 2’7’ Dichlorofluorescin Probe Assay

The top 139 hits were assessed for reactive oxygen species (ROS) generation using the fluorogenic probe dichlorofluorescein (DCF). In the presence of ROS, DCF is converted to the product, fluorescein, and can be measured fluorometrically. The DCF assay was done following previously described methods (LeBel et al 1992) but optimized for a 50 µL reaction. In this assay, 1 mM of 2’7’-dichlorofluorescin diacetate (DCFH-DA; Sigma Aldrich, St Louis, MO) underwent deesterification to DCFH. Deesterfication was performed daily for use in the ROS assay. Reactions were plated into 384 well plates by BiomekFXP Integrated Liquid Handler (Bechman Coulter, Indianapolis, IN) and all assay conditions were as previously described for NADPH depletion except that reactions were initiated with CYP3A65 purified membranes in buffer containing DCFH. Each 384 well plate contained 32 positive controls. The rate of ROS formation between CYP1A and 7-PR, reactions that have been established as highly uncoupled (Harskamp et al 2012), served as a positive control. Plates contained negative controls of CYP1A with 2% DMSO to provide a measure of background rates of fluorescence. Fluorescent activity was monitored for 15 minutes using a Synergy 4 fluorimeter (Synergy4, BioTek, Winooski, VT) with excitation wavelength at 485/20 nm and emission at 528/20 nm. The rate of ROS production was normalized for the total P450 and expressed either as a catalytic rate (pmol nmol $P450^{-1}$ min^{-1}) or as a percent of the positive control. Reactions that had a rate of ROS formation more than 3 standard deviations above the mean rate of ROS formation in the negative control were considered above background. These hits were not considered false positives because it is common to see some ROS production in

CYP reactions that result in product. Reactions with ROS formation that were >50% of the positive control (CYP1A and 7-PR) and if the NADPH depletion was <30% of the positive control (CYP3A65 and 7-MR) were considered highly uncoupled and suggestive of a false positive.

Determining K_M and IC_{50} in the top hits

The top hits were defined as those with low ROS production and high rates of NADPH depletion that were protein dependent. K_M values for NADPH depletion were determined for the top 32 hits. Each substrate was serially diluted half a log from the highest concentration giving 11 final concentrations, ranging from of 0 μM (no substrate control) to 100 μM. Each substrate concentration was run in duplicate in a 50 μL reactions as described above. NADPH depletion was monitored every 2 minutes for 10 minutes. The rate of NADPH depletion was normalized for total P450 content and a Michaelis-Menten curve was generated from the dilution series for each substrate. K_M values were obtained from curve fitting nonlinear regression models using on online tool (http://www.ic50.tk/kmvmax.html)

IC_{50} values were determined for the top 32 hits, assessing the inhibition of fluorescent product produced from the catalytic reaction between CYP3A65 purified membranes and 75 μM BFC. The batch of CYP3A65 purified membranes used for the IC_{50} assay was different than the one used for initial screen and follow up, however, data was normalized for CYP content and optimization steps for protein content, CO difference, and activity levels were assessed to consider and remove any potential effects on the data from batch to batch variation in protein expression. The inhibition assay was optimized for BFC concentration and DMSO (Figure 1B). The Michaelis-Menten curve for BFC was developed to determine appropriate BFC concentration (Figure 2B). Each substrate was serially diluted half a log from the highest concentration giving 11 final concentrations, including a no substrate control (0 µM) and ranging from 0.01 - 100 µM. Other reactions components were as described above, except each reaction was initiated with purified membranes and 75 µM of BFC. Fluorescent activity was monitored every 2 minutes, for 15 minutes on a Synergy 4 fluorimeter (BioTek, Winooski, VT) with excitation wavelength/bandwidth at 400/30 nm and emission wavelength/bandwidth at 528/20 nm. The rate of inhibition was normalized for the total P450 content. IC_{50} values were obtained from curve fitting nonlinear regression models using Sigma Plot (Systat Software, San Jose, CA).

RESULTS

Expression of CYP3C1 Protein and Catalytic Activity

The CO-difference spectrum was used to assess the presence of functional P450 and P450 content was 0.21 nmol/mg. Cytochrome P450 reductase activity was 14.76 nmol/mg/min indicating appropriate expression of a functional reductase. CYP3A65 catalytic activity was confirmed by measuring the rate of reaction of CYP3A65 for 10 synthetic fluorogenic probe substrates: 7-ER, 7-MR, 7-PR, 7-BR, DBF, BFC, MFC, AMMC, MAMC, BQ. CYP3A65 was able to metabolize all resorufin substrates to some extent but had the highest activity for 7-ER (Figure 3). 7-ER had the highest K_M and V_{max} (Table 1) while 7-BR had the lowest V_{max} and the second highest K_M. Rates of resorufin production by CYP3A65 mediated 7-MR metabolism following traditional Michaelis-

Menten kinetics (Figure 1A) with some level of variation at V_{max} that was due to poor solubility of 7-MR at higher concentrations.

CYP3A65 did not metabolize many of the coumarin and the one quinoline fluorogenic substrates (MFC, AMMC, MAMC and BQ) under the tested conditions (data not shown). CYP3A65 did metabolize both BFC and DBF (Figure 4). DBF had a lower K_M and thus, higher affinity for CYP3A65 (Table 1), but the maximum rate of reaction for CYP3A65 was similar with BFC and DBF (Figure 4). Rates of fluorescent product formation by CYP3A65 mediated BFC metabolism followed Mechaelis-Menten kinetics (Figure 2B). The V_{max} for 7-MR was half the V_{max} values for BFC, but 7-MR had a lower K_M than BFC (Table1).

<u>High Throughput Screening for NADPH Depletion With and Without Enzyme</u>

The high throughput assay was optimized for rate of NADPH depletion by CYP3A65 and 7-MR. BFC absorbs light at 340 nm (data not shown), interfering with the ability to read the rate of NADPH depletion in this assay and so could not be used as a positive control or to optimize the high throughput assay. The effects of temperature and light had little effect on rate of NADPH depletion. DMSO had no effect on the rate of NADPH depletion by CYP3A65 and 7-MR (Figure 1A) but there was a 4-fold decrease in the rate of BFC formation at 2-3% DMSO (Figure 1B); the lower DMSO percent of 2% was used for subsequent experiments. The limit of detection (LOD) for NADPH depletion was 151 nmol nmol $P450^{-1}min^{-1}$. The LOD was 13% of the rate of NADPH depletion in the positive control (with 7-MR substrate). Following the primary screen, 310 compounds had a rate of NADPH depletion that was greater than the limit of detection (Figure 5). Of those hits, 139 substrates had a rate of NADPH depletion that was 20% of the rate of NADPH depletion for the positive control. Plumbagin, menadione, idebenone and β-lapachone had the highest rates of NADPH depletion of all the tested compounds, all of which were >80% of the positive control (Table 2).

A secondary screen assessed 139 top hits for protein independent NADPH depletion. Overall, little NADPH depletion was detected in the absence of the enzyme for all the top substrates (Table 2). Plumbagin, menadione, idebenone and β-lapachone had a rate of NADPH depletion similar to controls in the absence of enzyme compared to the rate of NADPH depletion in the presence of an enzyme, indicating that the reaction was enzyme dependent (Table 2). For epinephrine hydrochloride and demethylnobiletin, the rate of NADPH depletion in the presence and absence of the enzyme were approximately equal, suggesting that these are false positives (Table 2).

Reactive Oxygen Species (ROS) 2'7'Dichlorofluorescin Probe Assay, K_m and IC_{50}

The 139 top hits were assessed for rates of ROS formation. The rate of ROS formation between the positive control, CYP1A and 7-PR, was 5944±822 pmol nmol $P450^{-1}$ min^{-1}. There was detectable background fluorescence in wells containing CYP1A and 2% DMSO but no substrate (1286±263 pmol nmol $P450^{-1}$ min^{-1}), equivalent to 22% of the positive control. Of the 139 hits, 123 substrates interacted with CYP3A65 to produce fluorescence equivalent to the negative control, suggesting low or insignificant ROS production (Table 2). The highest rate of ROS formation was seen for methylene blue (129% of the positive control) and coralyne chloride hydrate (60% of the positive control), suggesting highly uncoupled reactions with CYPA65 (Table 2). Compounds with a high rate of NADPH depletion, such plumbagin and menadione also had higher rates of ROS formation but only slightly above background (Table 2). β-lapachone had a very low rate of ROS formation and a higher rate of NADPH depletion (Table 2), which suggests a highly coupled reaction between CYP3A65 and this compound.

32 compounds were selected from the top 139 hits to assess enzyme kinetics; kinetics were assessed by determining the K_M for NADPH consumption and the IC_{50} for the inhibition of BFC metabolism. Of the 32 compounds, 9 substrates had K_M and IC_{50} values that were less than 26 μM and reactions closely followed Michaelis-Menten kinetics as tested by curve-fitting tools; 6 compounds had one of the values (K_M or IC_{50}) that was < 20 μM (Table 3). 12 compounds had NADPH depletion and fluorescence inhibition, but the highest concentration tested was not high enough to successfully obtain maximum depletion or inhibition (Table 3), which in some case led to higher error values associated with the calculated K_M or IC_{50}. We could not calculate K_M and IC_{50} values for 5 compounds because reactions had limited NADPH depletion or fluorescence inhibition, respectively (Table 3). Plumbagin; idebenone; menadione; 3',4-dimethoxydalbergione; and β-lapachone had large rates of NADPH depletion (≥50% the rate of the positive control) along with the smallest K_M values (4 μM - 20 μM) and IC50 values (1 μM - 10 μM; Table 3). These compounds are high affinity CYP3A65 substrates. Compounds such as primaquine diphosphate, GW2974, flupirtine maleate, duloxetine hydrochloride, doxasin mesylate and lapachol had IC_{50} values that were less than 20 μM but had K_M values that were greater than 20 μM (Table 3); thus, the screen has identified at least 10-15 high affinity substrates for CYP3A65.

DISCUSSION

The zebrafish is an increasingly popular model species; it is small, cheap and very easy to culture in a laboratory. A high fecundity coupled with continuous reproduction, fast development, and transparent embryos increases throughput for developmental, reproductive, and multi-generational studies. The zebrafish genome has been sequenced and shares a close similarity to the human genome, making it an affordable vertebrate research tool in genetics, toxicology (as reviewed by Dai et al 2013), pharmacology, and biomedical research (as reviewed by Zon & Peterson 2005). A major limitation of the zebrafish model is a lack of understanding of the capacity of this fish for xenobiotic metabolism. While it is commonly thought that CYP3A65 is functionally like mammalian CYP3A4, little functional data exists to support this notion. That evolutionary studies have clearly identified that CYP3A65 is not orthologous to mammalian CYP3A genes calls into question whether it is reasonable to assume similar function across these species. In this study, we assessed the catalytic function of heterologously expressed zebrafish CYP3A65 by fluorogenic probes that are commonly used to test mammalian CYP catalytic activity. We screened approximately 4000 pharmacologically active compounds, based on rates of NADPH depletion, to better understand the function of CYP3A65 and the potential overlap in function with mammalian CYP3A4. Zebrafish CYP3A65 had low catalytic activity for substrates that are prototypical mammalian CYP3A substrates (Table 1) and of the 139 top CYP3A65 hits from the screen, only 24 were known mammalian CYP3A4 substrates (Table 2). Many of the top hits were pharmacologically active compounds that contained a quinone moiety. Furthermore, there was a large overlap between substrates of zebrafish CYP3A65 and CYP3C1 indicating a higher functional similarity across zebrafish CYP3 subfamilies than between mammalian and fish CYP3A enzymes.

Zebrafish CYP3A65 and Mammalian CYP3A4 Substrate Profiles

CYP3A65 catalytic activity was assessed with 7-BR, 7-ER, 7-MR and 7-PR probe substrates whose metabolism is commonly used to assess the catalytic activity of CYP1s in mammals (Murray et al 2001) and fish (Scornaienchi et al 2010b, Whyte et al 2000). 7-ER, 7-BR, and 7-MR are regularly used to assess CYP1A protein induction in fish. 7-BR is more commonly used to assess catalytic activity of CYP1A1 and CYP1B in fish (Scornaienchi et al 2010b, Murray et al 2001), CYP1A2 and CYP2B in mammals (Kobayashi et al 2002, Nerurkar et al 1993) but has also been used as a biomarker for CYP3A induction in mammals (Hagemeyer et al 2010) and in fish (Hartl et al 2007). In mammals, 7-PR activity is traditionally used to assess CYP2 activity (Burke et al 1994); it is not clear what enzymes are responsible for 7-PR metabolism in fish. CYP3A65 metabolized all the resorufin substrates to some extent (Table 1; Figure 3). We expected the highest catalytic activity between CYP3A65 and 7-BR, but 7-BR metabolism by CYP3A65 was minor (Table 1; Figure 3). Unlike mammalian CYP3A enzymes, CYP3A65 metabolized both 7-ER and 7-MR (Figure 3), although the catalytic activity of CYP3A65 for the alkoxy-resorufin substrates was much less than that seen with zebrafish CYP1 proteins (Scornaienchi et al 2010b). Traditionally, the alkoxy-resorufins (except 7-PR) are considered markers of CYP1 activity; our data does not dispute this use but does indicate that fish CYP3A enzymes are capable of alkoxy-resorufin metabolism and may partially contribute in tissues where CYP3A expression is high. In mammals, 7-ER, 7-MR and 7-PR substrates are not associated with human CYP3A activity and the main metabolizers of 7-BR vary depending on what CYP is induced (Burke et al 1994).

BFC, DBF and BQ are mammalian CYP3A substrates (Ghosal et al 2003, Stresser et al 2002); DBF is also a substrate of mammalian CYP2C8, CYP2C9 and CYP2C19 (Koenig et al 2012). While zebrafish CYP3A65 was not capable of BQ metabolism, it was able to metabolize both DBF and BFC at similar rates. However, the catalytic rates were much less than what has been reported for mammalian CYP3A proteins (Stresser et al 2002). In fact, heterologously expressed CYP1A metabolized BFC ~25 times faster than CYP3A65 and DBF metabolism was at similar rates for CYP3A65 and CYP1A (CYP3A65 activity from this study; CYP1A activity from Scornaienchi et al 2010a). These data were in line with previous studies using heterologously expressed CYP3A65 (Scornaienchi et al 2010a). Unlike human CYP3A4, CYP3A65 was not selective for nor had the highest rates of metabolism of BFC and DBF and it could be predicted that CYP1A may contribute significantly to the metabolism of these substrates in tissues. Collectively, these data illustrate differences in the specificity and function of zebrafish CYP3A65 and mammalian CYP3A enzymes for fluorogenic probe substrate metabolism and argues that there is some overlap in teleost CYP1 and CYP3 substrates that might not be expected based on data in mammalian systems.

Considering that fluorogenic substrates are few and mammalian CYP3A enzymes are highly promiscuous enzymes with structurally diverse substrates, we determined the catalytic activity of heterologously expressed CYP3A65 against ~4000 biologically and pharmacology active compounds in a high throughput screen based on NADPH depletion. Given the importance of mammalian CYP3A4 in pharmaceutical metabolism, we selected from commercially available libraries to screen ~4000 non-redundant compounds that include biologically and pharmacologically active small molecules, off patent and FDA approved pharmaceuticals, and natural plant products. We performed a non-exhaustive preliminary curation of the libraries to ensure they contained significant numbers of mammalian CYP3A4 substrates. We identified approximately 400 mammalian CYP3A4 substrates in the compound library, many of which were pharmaceutically relevant compounds, supporting its use to assess CYP3A65 function and the potential functional overlap with mammalian CYP3A enzymes. The selected libraries contained both structurally diverse compounds and structurally similar compounds allowing for the inference of structure function relationships.

From the 4000 screened compounds, 310 compounds were positive hits with NADPH depletion rates above the limit of detection based on the LOD (Figure 5). 139 of the top hits were selected for follow up to remove false positives, based on assessing the rate of NADPH depletion in the absence of enzyme and identification of highly uncoupled reactions via measurement of ROS production (Table 2). Of the compounds selected for follow up, only 24 compounds were known mammalian CYP3A4 substrates, and of the 32 compounds that were further assessed to determine the K_M (for NADPH depletion) and IC_{50} (for BFC inhibition), only 2 were CYP3A4 substrates; primaquine diphosphate (antimalarial drug) and duloxetine hydrochloride (depressive disorder drug). While many of the top hits did have pharmacological significance and are being developed to treat human disease, their metabolism by mammalian CYP enzymes was unknown or they were substrates or inhibitors of various other CYPs. For example, menadione is an inhibitor of CYP1A2 and CYP2 enzymes but not a substrate of CYP3A4 (Wishart et al 2018). From this, we can conclude that the screen identified unique CYP3A65 substrates and there was little overlap of the top hits for CYP3A65 and those that are known mammalian CYP3A4 substrates. This strongly argues that zebrafish CYP3A65 does share high functional similarity to mammalian CYP3A4.

The top 139 CYP3A65 substrate compounds were structurally diverse (Table 2). For example, compounds with similar catalytic activity, K_M and IC_{50} values have very different structures, such as GW2974, a pyridopyrimidine; duloxetine hydrochloride, a thiophene derivative; and β-lapachone, a 1,2-nathoquinone (Table 3). This is in line with current knowledge of the mammalian CYP3 enzymes, which are capable of metabolizing diverse compounds without a strong structure activity relationship (as reviewed by Zanger & Schwab 2013). The human CYP3A4 enzyme has a highly promiscuous active site with the ability to metabolize more than 50% of known pharmaceuticals, most of which are not structurally related (for reviews see: Guengerich 1999, Johnson et al 2014, Kuehl et al 2001, Zanger & Schwab 2013). It is likely that fish CYP3A65 active site is also flexible, but this hypothesis remains to be specifically tested.

Despite the high structural diversity, one interesting characteristics of CYP3A65 substrates was that many contained a quinone moiety. Quinones are a group of organic compounds that are naturally occurring and usually derived from plants (Barr & Crane 1971). Though quinones themselves are not aromatic, they are the result of aromatic compound metabolism such as benzenes, phenols or other polycyclic aromatic compounds (Talalay & Dinkova-Kostova 2004). Quinones are good antifungal, antimicrobial and anticancer therapeutants (Bolton et al 2000). The highest activity hits, with lower IC_{50} values, contained a quinone moiety; 7 of the top 32 hits were structurally diverse quinone-based compounds, five of which were 1,4-naphthoquinones, one was an ortho-naphthoquinone, and one was a 1,4 benzoquinone (Table 3). From these data, is not clear if CYP3A65 has a bias for quinone substrates or if the quinone reactions we observed are CYP3A65 dependent reactions. Quinone compounds are known to interact with reductases, such as cytochrome P450 reductase, to consume an electron and produce a reactive semiquinone and superoxide, which eventually results in redox cycling (Segura-Aguilar et al 1998). Future experiments to determine if quinones are substrates of CYP3A65 can include:1) testing quinone reactions in the absence of CYP3A65 enzyme and in the presence of reductase alone; 2) determining whether quinones are competitive, un-competitive or non-competitive inhibitors of CYP3A65 activity; and 3) measure parent compound loss over-time. It is interestingly to consider the involvement of CYP3A65 in the mechanisms of toxicity and metabolism of naphthoquinones, and the potential for structure-activity relationships.

Overlap between CYP3A65 and CYP3C1 Substrate Profiles

Interestingly, fluorogenic substrate profiles for CYP3A65 were largely similar to those for zebrafish CYP3C1 (Chapter 3). Like the CYP3A65 enzyme, CYP3C1 had the capacity to metabolize the alkoxy-resorufin substrates (Chapter 3, Table 1, Figure 2). Zebrafish CYP3A65 metabolized 7-ER and 7-MR at rates that are about 2 folds less

(Table 1; Figure 3) than the rate of CYP3C1 metabolism of 7-MR and 7-ER (Chapter 3, Table 1, Figure 2). Like CYP3A65 (Table 1; Figure 3), 7-BR metabolism by CYP3C1 was minor relative to other resorufin substrates (Chapter 3, Table 1, Figure 2). It is likely that fish CYP3 subfamilies have limited capacity for the metabolism of 7-BR. Zebrafish CYP3C1 metabolized DBF (Chapter 3, Table 1, Figure 1) at approximately the same rate as zebrafish CYP3A65 (Table 1, Figure 4) but had higher catalytic activity with BFC than with CYP3A65. CYP3C1 metabolized BFC (Chapter 3, Figure 1) at rates that were ~7 fold more than rates observed for zebrafish CYP3A65 (Figure 4) but these rates were still ~ 4-fold less than rates of metabolism by CYP1A (Scornaienchi et al 2010a). BFC metabolism is commonly used to determine CYP3A induction and catalytic activity in mammals (Crespi & Stresser 2000) and fish (Burkina et al 2013, Hegelund et al 2004); these data demonstrates that multiple teleost CYP enzymes are capable of BFC metabolism *in vitro*, with CYP3A65 having lower metabolic capacity for BFC than CYP3C1 and CYP1A. Overall, compared to CYP3A65, CYP3C1 had a higher catalytic activity for most of the tested fluorogenic substrates but substrate profiles and rank order were similar.

Following the high throughput screening of the 4000 compounds, we found that CYP3A65 and CYP3C1 substrate profiles largely overlapped. From the 139 top CYP3A65 hits, 111 of those were top hits from screening CYP3C1. In fact, of the 32 compounds that we determined IC_{50} and K_M, 7,2-dihydroxflavone was the only compound that was unique to CYP3A65 (Table 3), and no IC_{50} and K_M values could be computed for this compound, thus further investigation is required to confirm that it is a substrate. The similarities between CYP3C1 and CYP3A65 were not overly surprising due to the close evolutionary relationship between the two genes (Yan & Cai, 2010). Recent phylogenetic analysis reveals that fish, unlike mammals, contain several CYP3 subfamilies: CYP3A, CYP3B, CYP3C and CYP3D (Yan & Cai 2010). Zebrafish contain CYP3A65 and 4 CYP3C genes: CYP3C1, CYP3C2, CYP3C3 and CYP3C4. Fish CYP3A genes are more closely related to other fish CYP3 subfamilies, rather than to human CYP3A4. The large functional similarity between CYP3A65 and CYP3C1 suggests that these paralogs may perform a similar function. Because CYP3C1 is ubiquitously expressed in organs (Shaya et al 2014), while CYP3A65 is more localized to intestine and liver (Tseng et al 2005), CYP3A65 may provide an important role in primary detoxification while CYP3C1 may metabolize similar compounds in other organs including heart, brain, gonads, eye and olfactory rosette (Shaya et al 2014). This hypothesis warrants further investigation.

Developing a Profile of CYP3A65 Substrates

The high throughput screen identified 310 substrates of CYP3A65 from the selected libraries and very few of the substrates were removed as false positives. We were only able to investigate the K_M and IC_{50} of 32 of the top hits, leaving a large quantity of potential CYP3A65 substrates that can be further investigated (Table 3). Of the identified compounds, we can conclude that CYP3A65 can metabolize several pharmacologically active compounds. Only 24 of the top 139 compounds were also mammalian CYP3A4 substrates, while 111 were also CYP3C1 substrates, indicating a larger functional similarity between CYP3C1 and CYP3A65 than for CYP3A4 and CYP3A65.

Interestingly, many of the top hits of CYP3A65 contained a quinone moiety and could provide some information any whether any structure-activity relationship exists for CYP3A65 substrates, however further follow up is required to establish quinones as CYP3A65 substrates.

Developing a profile of CYP3A65 substrates will not only provide the ability to infer the CY3A65 function in zebrafish and better characterize detoxification capacities of fish, but it will inform studies using zebrafish in pharmacology and biomedical sciences. The zebrafish has become an increasingly popular animal model in pharmaceutical studies (as reviewed by Fleming & Alderton, 2013) and drug development research at the validation, efficacy and safety screening, and drug toxicity screening stages (as reviewed by Fleming & Alderton, 2013). Zebrafish have been used to test seizure-liability of human pharmaceuticals in early-stage drug development (Winter et al, 2008), and is a good model species for drug-induced cardiotoxicity, a leading cause for drug withdrawals from the market (as reviewed by Zakaria et al 2018). Despite this important use, little effort has so far been made to understand zebrafish drug metabolism. Historical data from rodents and humans indicate that there are important differences in drug response across species. Even for well establish human-alternative models, such mice and rats, results from 30% of animal studies used to predict human toxicity lack concordance with what is seen in humans (Lillly et al 2000). Zebrafish have been used to investigate the side effects of pharmaceuticals on humans, such as citalopram (Prasad et al 2015), triadimefon (Zoupa et al 2017), and gabapentin (Benote et al 2013). The translation of zebrafish pharmaceutical research to humans relies, to a certain extent, on conservation of drug metabolism between fish and humans or at least a thorough understanding of where drug metabolism may be significantly different. This study suggests that translation of zebrafish research to humans would be better informed by a thorough profile of CYP3 enzyme function in fish.

ACKNOWLEDGEMENT

This research was supported by the Natural Science and Engineering Council of Canada. We thank Marcus Scornaienchi for design of the CYP3A65 construct, Dr. Derek Alsop for technical support and advice, and for the McMaster Centre for Microbial Chemical Biology, specifically Cecelia Murphy, for support running high throughput put bioassays.

TABLES

TABLE 4.1 K_M and V_{max} of the metabolism of alkyloxy-resorufin substrates, BFC and DBF by heterologously expressed zebrafish CYP3A65. Values were calculated from curve fitting Michaelis-Menten Curves using the online tool: http://www.ic50.tk/kmvmax.html. All alkyloxy-resorufin substrates were run in EROD buffer; 7-benzyloxy-4-(trifluoromethyl)coumarin (BFC) and dibenzylfluorescein (DBF) were run in $KP0_4$ buffer. 7-ethoxyresorufin (7-ER), 7-benzyloxyresorufin (7-BR) and 7-pentoxyresorufin (7-PR) and BFC were run at 0.5% DMSO. 7-methoxyresorufin (7-MR) was run at 1% DMSO and DBF was run at 0.25%. Concentration ranges tested are indicated in brackets next to each substrate. All reactions were 200 µL total volume.

Substrate	Km	Vmax
	(μM) ± SEM	(pmol nmol P450^{-1} min^{-1}) ± SEM
7-ethoxyresorufin (7-ER; 4 - 30 μM)	17.04 ± 14.18	391.08 ± 168.60
7-methoxyresorufin (7-MR; 2.5 - 20 μM)	6.03 ± 12.96	258.13 ± 260.1
7-benzyloxyresorufin (7-BR; 8 - 18 μM)	10.67 ± 7.59	7.50 ± 2.27
7-pentoxyresorufin (7-PR; 0.8 - 12.5 μM)	0.759 ± 4.258	91.98 ± 4.26
7-benzyloxy-4-(trifluoromethyl)coumarin (BFC; 0 - 200 μM)	34.58 ± 17.71	471.14 ± 84.35
Dibenzylfluorescein (DBF; 0.05 - 2.5 μM)	0.378 ± 0.15	445.79 ± 59.85

TABLE 4.2 NADPH depletion, reactive oxygen species (ROS) formation, and NADPH depletion in the absence of enzyme for the 139 top hit compounds of heterologously expression zebrafish CYP3A65. Structure, molecular weight and name of each compound are provided. The rates of NADPH depletion, NADPH depletion in the absence of enzyme, and ROS formation were normalized for total P450 content. Values obtained for each individual replicate are displayed in the table, along with an average of the two replicates. Due to technical error, some samples were run with double the concentration of substrate and DMSO (see materials and methods for more detail) and are highlighted in grey. Compounds that were identified to be CYP3A4 substrates through DataBank.ca (Wishart et al 2018) are identified by an asterisk after the compound name. <LOD (limit of detection) indicates wells where the value was below the limit of detection. The LOD value was substituted when calculating the average for a group of wells that had value(s) both below and/or above the LOD.

			Rate of NADPH Depletion % Positive Control			Rate of ROS Formation % Positive Control			Rate of NADPH Depletion (No Enzyme) % Postive Control			Rate of NADPH Depletion nmol nmol p450^{-1} min^{-1}			Rate of ROS Formation pmol nmol p450^{-1} min^{-1}			Rate of NADPH Depletion (No Enzyme) nmol nmol p450^{-1} min^{-1}		
Compound name	**Structure**	**Weight**	**Rep 1**	**Rep 2**	**Average**	**Rep 1**	**Rep 2**	**Average**	**Rep 1**	**Rep 2**	**Average**	**Rep 1**	**Rep 2**	**Average**	**Rep 1**	**Rep 2**	**Average**	**Rep 1**	**Rep 2**	**Average**
PLUMBAGIN	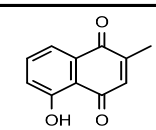	188.182	82.9	86.0	84.4	41.3	56.2	48.8	<LOD	<LOD	13.0	1129.3	1148.0	1138.7	952.5	1298.6	1125.6	<LOD	<LOD	154.0
MENADIONE	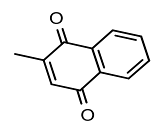	172.183	83.6	81.1	82.3	<LOD	<LOD	34.9	<LOD	<LOD	13.0	1138.7	1082.7	1110.7	<LOD	<LOD	805.5	<LOD	<LOD	154.0
IDEBENONE	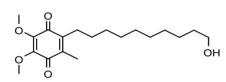	338.444	81.6	82.0	81.8	<LOD	<LOD	34.9	<LOD	<LOD	13.0	821.3	1026.7	924.0	<LOD	<LOD	805.5	<LOD	<LOD	154.0
β-LAPACHONE	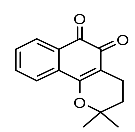	242.274	76.7	86.0	81.4	<LOD	<LOD	34.9	<LOD	<LOD	13.0	1045.3	1148.0	1096.7	<LOD	<LOD	805.5	<LOD	<LOD	154.0
GW2974	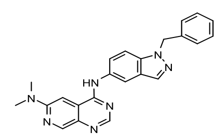	395.470	80.5	62.1	71.3	<LOD	<LOD	34.9	<LOD	<LOD	13.0	821.3	644.0	732.7	<LOD	<LOD	805.5	<LOD	<LOD	154.0
ISOCORYDINE	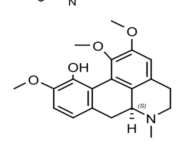	341.407	73.2	68.5	70.8	<LOD	<LOD	34.9	<LOD	<LOD	13.0	802.7	840.0	821.3	<LOD	<LOD	805.5	<LOD	<LOD	154.0
DPO-1	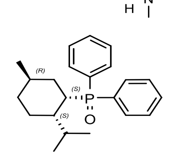	340.447	127.2	<LOD	70.1	<LOD	<LOD	34.9	<LOD	<LOD	13.0	1297.3	<LOD	724.2	<LOD	<LOD	805.5	<LOD	<LOD	154.0
PRIMAQUINE DIPHOSPHATE*	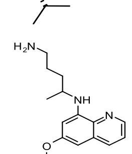	455.341	74.1	59.0	66.5	<LOD	<LOD	34.9	<LOD	<LOD	13.0	905.3	737.3	821.3	<LOD	<LOD	805.5	<LOD	<LOD	154.0
OXYQUINOLINE HEMISULFATE	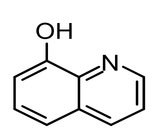	243.231	77.1	51.5	64.3	<LOD	<LOD	34.9	<LOD	<LOD	13.0	942.7	644.0	793.3	<LOD	<LOD	805.5	<LOD	<LOD	154.0
DULOXETINE HYDROCHLORIDE*	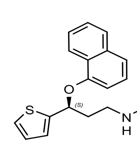	333.880	72.3	55.0	63.6	<LOD	<LOD	34.9	<LOD	<LOD	13.0	886.7	700.0	793.3	<LOD	<LOD	805.5	<LOD	<LOD	154.0

BTO-1	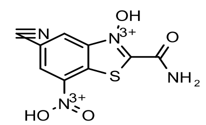	266.230	56.9	69.7	63.3	<LOD	<LOD	34.9	<LOD	<LOD	13.0	812.0	952.0	882.0	<LOD	<LOD	805.5	<LOD	<LOD	154.0
CLOXYQUIN	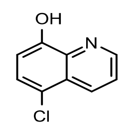	179.600	63.9	61.3	62.6	<LOD	<LOD	34.9	<LOD	<LOD	13.0	746.7	756.0	751.3	<LOD	<LOD	805.5	<LOD	<LOD	154.0
PRAZOSIN HYDROCHLORIDE*	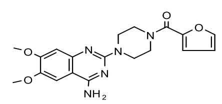	419.868	56.4	68.3	62.3	<LOD	<LOD	34.9	<LOD	<LOD	13.0	718.7	830.7	774.7	<LOD	<LOD	805.5	<LOD	<LOD	154.0
VULPINIC ACID	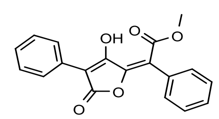	322.316	39.2	76.8	58.0	<LOD	<LOD	34.9	<LOD	<LOD	13.0	429.3	942.7	686.0	<LOD	<LOD	805.5	<LOD	<LOD	154.0
3,4-DIMETHOXY-DALBERGIONE	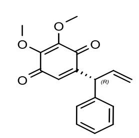	284.311	63.4	51.1	57.2	<LOD	<LOD	34.9	<LOD	<LOD	13.0	774.7	588.0	681.3	<LOD	<LOD	805.5	<LOD	<LOD	154.0
R(-)-APOCODEINE HYDROCHLORIDE*	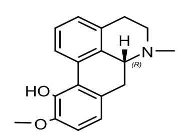	317.815	55.0	57.4	56.2	<LOD	<LOD	34.9	<LOD	<LOD	13.0	784.0	784.0	784.0	<LOD	<LOD	805.5	<LOD	<LOD	154.0
APOMORPHINE HYDROCHLORIDE HEMIHYDRATE*	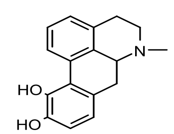	303.788	46.0	66.2	56.1	<LOD	<LOD	34.9	<LOD	<LOD	13.0	504.0	812.0	658.0	<LOD	<LOD	805.5	<LOD	<LOD	154.0
UVAOL	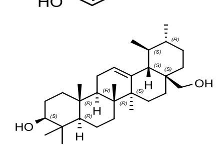	442.728	<LOD	108.0	60.5	<LOD	<LOD	34.9	<LOD	<LOD	13.0	<LOD	1325.3	738.2	<LOD	<LOD	805.5	<LOD	<LOD	154.0
1-(1-NAPHTHYL)-PIPERAZINE HYDROCHLORIDE	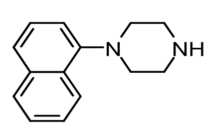	248.756	52.0	58.4	55.2	<LOD	<LOD	34.9	<LOD	<LOD	13.0	634.7	672.0	653.3	<LOD	<LOD	805.5	<LOD	<LOD	154.0
HYCANTHONE	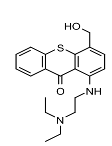	356.480	46.4	62.3	54.4	<LOD	<LOD	34.9	<LOD	<LOD	13.0	569.3	793.3	681.3	<LOD	<LOD	805.5	<LOD	<LOD	154.0
NITROMIDE	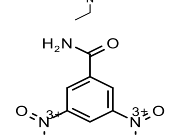	213.146	52.7	53.7	53.2	<LOD	<LOD	34.9	<LOD	<LOD	13.0	644.0	672.0	658.0	<LOD	<LOD	805.5	<LOD	<LOD	154.0
FLUPIRTINE MALEATE	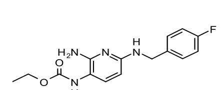	420.397	56.7	49.5	53.1	<LOD	<LOD	34.9	<LOD	<LOD	13.0	578.7	513.3	546.0	<LOD	<LOD	805.5	<LOD	<LOD	154.0

DOXAZOSIN MESYLATE*	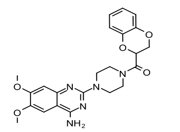	547.583	49.4	56.7	53.1	<LOD	<LOD	34.9	<LOD	<LOD	13.0	504.0	588.0	546.0	<LOD	<LOD	805.5	<LOD	<LOD	154.0
7,2'-DIHYDROXY-FLAVONE	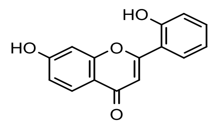	254.241	17.3	87.7	52.5	<LOD	<LOD	34.9	<LOD	<LOD	13.0	186.7	989.3	588.0	<LOD	<LOD	805.5	<LOD	<LOD	154.0
R(-)-2,10,11-TRIHYDROXY-N-PROPYLNOR APORPHINE HYDROBROMIDE	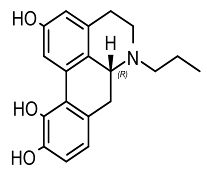	392.293	44.5	59.4	52.0	<LOD	<LOD	34.9	<LOD	<LOD	13.0	634.7	812.0	723.3	<LOD	<LOD	805.5	<LOD	<LOD	154.0
2',6'-DIHYDROXY-4'-METHOXY-CHALCONE	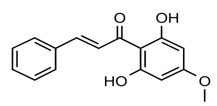	270.284	<LOD	98.9	56.0	<LOD	<LOD	34.9	<LOD	<LOD	13.0	<LOD	1213.3	682.2	<LOD	<LOD	805.5	<LOD	<LOD	154.0
DAPH	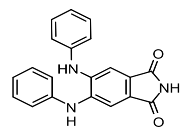	329.359	41.9	60.8	51.3	<LOD	<LOD	34.9	<LOD	<LOD	13.0	597.3	830.7	714.0	<LOD	<LOD	805.5	<LOD	<LOD	154.0
LAPACHOL	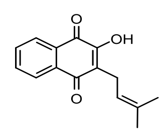	242.274	61.3	38.9	50.1	<LOD	<LOD	34.9	<LOD	<LOD	13.0	662.7	438.7	550.7	<LOD	<LOD	805.5	<LOD	<LOD	154.0
CI-976	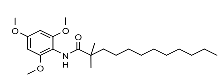	393.568	42.5	57.5	50.0	<LOD	<LOD	34.9	<LOD	<LOD	13.0	541.3	700.0	620.7	<LOD	<LOD	805.5	<LOD	<LOD	154.0
HOMIDIUM BROMIDE	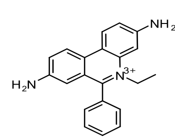	392.298	44.7	50.7	47.7	<LOD	<LOD	34.9	<LOD	<LOD	13.0	522.7	625.3	574.0	<LOD	<LOD	805.5	<LOD	<LOD	154.0
SANGUINARINE SULFATE	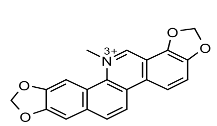	427.379	46.6	47.0	46.8	<LOD	<LOD	34.9	<LOD	<LOD	13.0	569.3	588.0	578.7	<LOD	<LOD	805.5	<LOD	<LOD	154.0
CORALYNE CHLORIDE	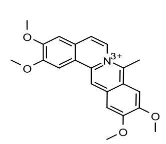	397.855	46.7	44.7	45.7	<LOD	<LOD	34.9	<LOD	<LOD	13.0	504.0	504.0	504.0	<LOD	<LOD	805.5	<LOD	<LOD	154.0
NSC 95397	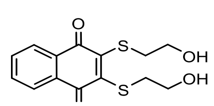	310.380	58.5	31.5	45.0	44.0	42.5	43.2	<LOD	<LOD	13.0	597.3	326.7	462.0	1015.6	980.1	997.9	<LOD	<LOD	154.0

CORALYNE CHLORIDE HYDRATE	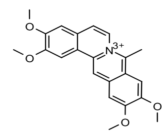	415.870	27.8	61.3	44.6	59.7	59.6	59.6	<LOD	<LOD	13.0	298.7	756.0	527.3	1379.3	1375.0	1377.1	<LOD	<LOD	154.0
HYPOCRELLIN A	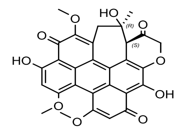	546.528	44.3	44.1	44.2	<LOD	<LOD	34.9	<LOD	<LOD	13.0	485.3	541.3	513.3	<LOD	<LOD	805.5	<LOD	<LOD	154.0
3,4'-DIHYDROXY-FLAVONE	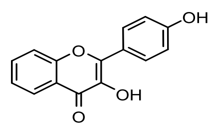	254.241	<LOD	77.0	45.0	<LOD	<LOD	34.9	<LOD	<LOD	13.0	<LOD	868.0	509.5	<LOD	<LOD	805.5	<LOD	<LOD	154.0
TETRA-HYDROALSTONINE	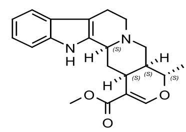	352.434	39.7	48.2	44.0	<LOD	<LOD	34.9	<LOD	<LOD	13.0	541.3	644.0	592.7	<LOD	<LOD	805.5	<LOD	<LOD	154.0
R(-)-2,10,11-TRI-HYDROXYAPORPHINE HYBROBROMIDE	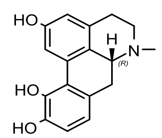	364.239	30.8	56.7	43.7	<LOD	<LOD	34.9	<LOD	<LOD	13.0	438.7	774.7	606.7	<LOD	<LOD	805.5	<LOD	<LOD	154.0
ZM 39923 HYDROCHLORIDE	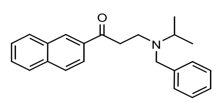	367.919	36.6	50.6	43.6	<LOD	<LOD	34.9	<LOD	<LOD	13.0	466.7	616.0	541.3	<LOD	<LOD	805.5	<LOD	<LOD	154.0
ANTIAROL	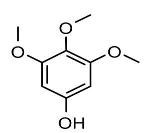	184.191	46.6	40.5	43.6	<LOD	<LOD	34.9	<LOD	<LOD	13.0	569.3	466.7	518.0	<LOD	<LOD	805.5	<LOD	<LOD	154.0
GOSSYPETIN	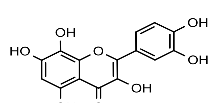	318.237	40.6	46.4	43.5	<LOD	<LOD	34.9	<LOD	<LOD	13.0	438.7	522.7	480.7	<LOD	<LOD	805.5	<LOD	<LOD	154.0
ATOVAQUONE*	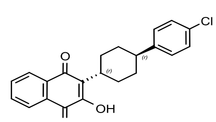	366.840	38.8	46.2	42.5	<LOD	<LOD	34.9	<LOD	<LOD	13.0	476.0	588.0	532.0	<LOD	<LOD	805.5	<LOD	<LOD	154.0
METHYLENE BLUE	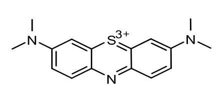	335.851	39.1	45.4	42.3	126.2	131.9	34.9	<LOD	<LOD	13.0	457.3	560.0	508.7	2913.3	3044.4	2978.8	<LOD	<LOD	154.0
R(-) APOMORPHINE HYDROCHLORIDE HEMIHYDRATE*	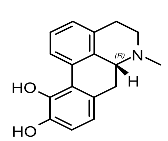	312.796	47.3	36.5	41.9	<LOD	<LOD	34.9	<LOD	<LOD	13.0	476.0	457.3	466.7	<LOD	<LOD	805.5	<LOD	<LOD	154.0
2',5'-DIHYDROXY-4-METHOXYCHALCONE	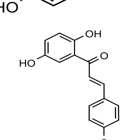	270.284	<LOD	75.3	44.2	<LOD	<LOD	34.9	<LOD	<LOD	13.0	<LOD	849.3	500.2	<LOD	<LOD	805.5	<LOD	<LOD	154.0

DECOQUINATE	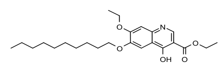	417.546	75.8	<LOD	44.4	<LOD	<LOD	34.9	<LOD	<LOD	13.0	886.7	<LOD	518.8	<LOD	<LOD	805.5	<LOD	<LOD	154.0
SB-215505	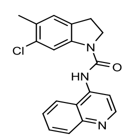	337.810	32.2	49.9	41.0	<LOD	<LOD	34.9	<LOD	<LOD	13.0	410.7	606.7	508.7	<LOD	<LOD	805.5	<LOD	<LOD	154.0
5, 6-DEHYDROKAWAIN	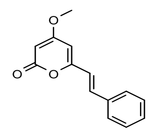	228.247	16.2	65.4	40.8	<LOD	<LOD	34.9	<LOD	<LOD	13.0	177.3	802.7	490.0	<LOD	<LOD	805.5	<LOD	<LOD	154.0
PYRVINIUM PAMOATE	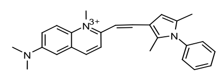	508.964	51.0	29.7	40.3	<LOD	<LOD	34.9	<LOD	<LOD	13.0	457.3	364.0	410.7	<LOD	<LOD	805.5	<LOD	<LOD	154.0
CORYNANTHINE	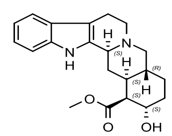	354.450	34.1	45.6	39.9	<LOD	<LOD	34.9	<LOD	<LOD	13.0	373.3	560.0	466.7	<LOD	<LOD	805.5	<LOD	<LOD	154.0
PROPIDIUM IODIDE*	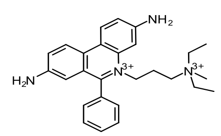	664.370	40.0	39.3	39.7	39.4	46.2	42.8	<LOD	<LOD	13.0	429.3	485.3	457.3	908.9	1065.9	987.4	<LOD	<LOD	154.0
ATOVAQUONE*	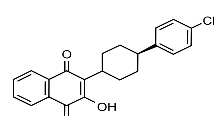	366.840	45.2	34.1	39.6	<LOD	<LOD	34.9	<LOD	<LOD	13.0	485.3	420.0	452.7	<LOD	<LOD	805.5	<LOD	<LOD	154.0
3-BROMO-7-NITROINDAZOLE	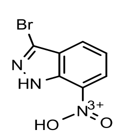	243.038	32.1	47.1	39.6	<LOD	<LOD	34.9	<LOD	<LOD	13.0	457.3	644.0	550.7	<LOD	<LOD	805.5	<LOD	<LOD	154.0
PAPAVERINE*	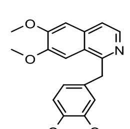	339.391	35.8	42.6	39.2	<LOD	<LOD	34.9	<LOD	<LOD	13.0	392.0	522.7	457.3	<LOD	<LOD	805.5	<LOD	<LOD	154.0
LYSERGOL*	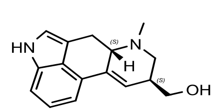	254.333	33.6	44.7	39.2	<LOD	<LOD	34.9	<LOD	<LOD	13.0	457.3	597.3	527.3	<LOD	<LOD	805.5	<LOD	<LOD	154.0
DEPHOSTATIN	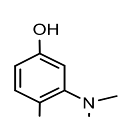	168.152	38.0	40.3	39.1	<LOD	<LOD	34.9	<LOD	<LOD	13.0	541.3	550.7	546.0	<LOD	<LOD	805.5	<LOD	<LOD	154.0
CHELERYTHRINE CHLORIDE	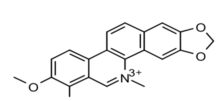	381.812	35.3	42.3	38.8	<LOD	<LOD	34.9	<LOD	<LOD	13.0	504.0	578.7	541.3	<LOD	<LOD	805.5	<LOD	<LOD	154.0

BERBERINE*	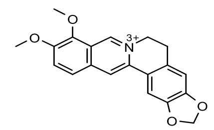	336.365	34.1	43.4	38.7	<LOD	<LOD	34.9	<LOD	<LOD	13.0	373.3	532.0	452.7	<LOD	<LOD	805.5	<LOD	<LOD	154.0
AZOMYCIN	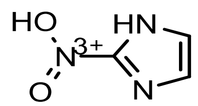	114.082	38.3	38.0	38.2	<LOD	<LOD	34.9	<LOD	<LOD	13.0	420.0	466.7	443.3	<LOD	<LOD	805.5	<LOD	<LOD	154.0
LAWSONE	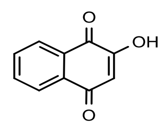	174.155	47.5	28.1	37.8	<LOD	<LOD	34.9	<LOD	<LOD	13.0	513.3	317.3	415.3	<LOD	<LOD	805.5	<LOD	<LOD	154.0
PD 98,059	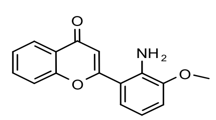	267.284	30.0	45.3	37.6	<LOD	<LOD	34.9	<LOD	<LOD	13.0	382.7	550.7	466.7	<LOD	<LOD	805.5	<LOD	<LOD	154.0
SCOULERINE	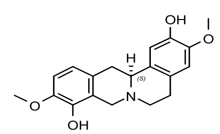	327.380	32.2	41.2	36.7	<LOD	<LOD	34.9	<LOD	<LOD	13.0	438.7	550.7	494.7	<LOD	<LOD	805.5	<LOD	<LOD	154.0
ST-148	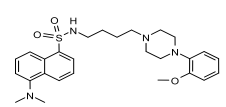	612.742	29.3	43.0	36.1	<LOD	<LOD	34.9	<LOD	<LOD	13.0	373.3	522.7	448.0	<LOD	<LOD	805.5	<LOD	<LOD	154.0
ISORESERPINE, (-)	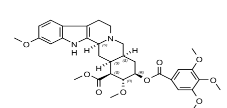	608.688	26.4	44.9	35.6	<LOD	<LOD	34.9	<LOD	<LOD	13.0	289.3	550.7	420.0	<LOD	<LOD	805.5	<LOD	<LOD	154.0
BU99006	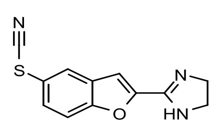	243.280	40.3	30.6	35.4	<LOD	<LOD	34.9	<LOD	<LOD	13.0	410.7	317.3	364.0	<LOD	<LOD	805.5	<LOD	<LOD	154.0
NORFLUOROCURARINE	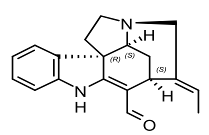	292.382	29.5	41.2	35.4	<LOD	<LOD	34.9	<LOD	<LOD	13.0	401.3	550.7	476.0	<LOD	<LOD	805.5	<LOD	<LOD	154.0
OSTHOLE	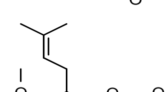	244.290	13.6	57.1	35.3	<LOD	<LOD	34.9	<LOD	<LOD	13.0	<LOD	700.0	425.5	<LOD	<LOD	805.5	<LOD	<LOD	154.0
CHLORANIL	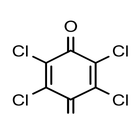	245.860	35.9	32.5	34.2	<LOD	<LOD	34.9	13.0	13.6	13.3	420.0	401.3	410.7	<LOD	<LOD	805.5	168.0	177.3	172.7
VINDOLINE	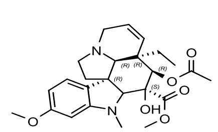	456.539	<LOD	77.8	45.4	<LOD	<LOD	34.9	<LOD	<LOD	13.0	<LOD	877.3	514.2	<LOD	<LOD	805.5	<LOD	<LOD	154.0

CPNQ	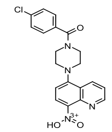	397.840	24.7	43.2	34.0	<LOD	<LOD	34.9	<LOD	<LOD	13.0	252.0	448.0	350.0	<LOD	<LOD	805.5	<LOD	<LOD	154.0
IODOQUINOL	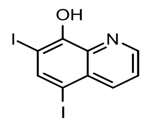	396.954	31.3	35.8	33.6	<LOD	<LOD	34.9	<LOD	<LOD	13.0	382.7	448.0	415.3	<LOD	<LOD	805.5	<LOD	<LOD	154.0
PYRVINIUM PAMOATE	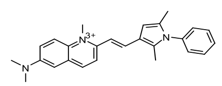	767.880	26.6	40.3	33.5	<LOD	<LOD	34.9	<LOD	<LOD	13.0	326.7	513.3	420.0	<LOD	<LOD	805.5	<LOD	<LOD	154.0
DEOXYSAPPANONE B 7,3'-DIMETHYL ETHER	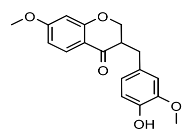	314.337	<LOD	54.3	33.7	<LOD	<LOD	34.9	<LOD	<LOD	13.0	<LOD	625.3	388.2	<LOD	<LOD	805.5	<LOD	<LOD	154.0
NARINGENIN	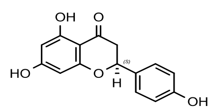	272.256	60.3	<LOD	36.6	<LOD	<LOD	34.9	<LOD	<LOD	13.0	821.3	<LOD	486.2	<LOD	<LOD	805.5	<LOD	<LOD	154.0
TETRAHYDROPAPAVERI NE	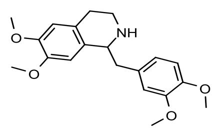	343.423	27.2	37.3	32.3	<LOD	<LOD	34.9	<LOD	<LOD	13.0	298.7	457.3	378.0	<LOD	<LOD	805.5	<LOD	<LOD	154.0
SCOPOLOMINE N-BUTYLBROMIDE	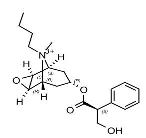	438.360	<LOD	58.0	35.5	<LOD	<LOD	34.9	<LOD	<LOD	13.0	<LOD	774.7	462.8	<LOD	<LOD	805.5	<LOD	<LOD	154.0
2',3-DIHYDROXY-4,4',6'-TRI-METHOXYCHALCONE	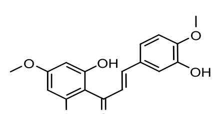	330.336	16.4	46.4	31.4	<LOD	<LOD	34.9	22.8	13.6	18.2	177.3	522.7	350.0	<LOD	<LOD	805.5	298.7	177.3	154.0
RO 90-7501	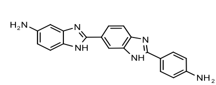	340.390	22.0	40.5	31.2	<LOD	<LOD	34.9	<LOD	<LOD	13.0	224.0	420.0	322.0	<LOD	<LOD	805.5	<LOD	<LOD	154.0
β-ECDYSONE	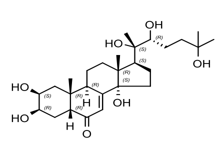	480.642	<LOD	50.2	50.2	<LOD	<LOD	34.9	<LOD	<LOD	13.0	<LOD	616.0	383.5	<LOD	<LOD	805.5	<LOD	<LOD	154.0
R(-)-PROPYLNOR APOMORPHINE HYDROCHLORIDE*	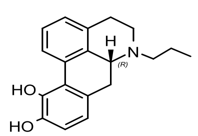	331.842	17.0	45.1	31.0	<LOD	<LOD	34.9	<LOD	<LOD	13.0	242.7	616.0	429.3	<LOD	<LOD	805.5	<LOD	<LOD	154.0
DALBERGIONE	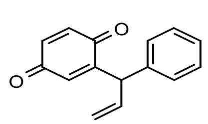	224.259	30.6	30.8	30.7	<LOD	<LOD	34.9	<LOD	<LOD	13.0	373.3	354.7	364.0	<LOD	<LOD	805.5	<LOD	<LOD	154.0

2,6-DIMETHOXYQUINONE	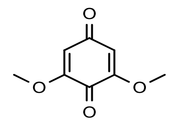	168.148	32.1	29.2	30.6	<LOD	<LOD	34.9	<LOD	<LOD	13.0	392.0	336.0	364.0	<LOD	<LOD	805.5	<LOD	<LOD	154.0
METHYLERGONOVINE MALEATE*	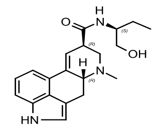	455.511	32.9	27.9	30.4	<LOD	<LOD	34.9	<LOD	<LOD	13.0	336.0	289.3	312.7	<LOD	<LOD	805.5	<LOD	<LOD	154.0
ACETOSYRINGONE	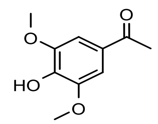	196.202	24.2	35.6	29.9	<LOD	<LOD	34.9	<LOD	<LOD	13.0	261.3	401.3	331.3	<LOD	<LOD	805.5	<LOD	<LOD	154.0
ERGOSTEROL ACETATE*	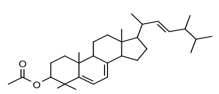	466.750	<LOD	56.8	34.9	<LOD	<LOD	34.9	<LOD	<LOD	13.0	<LOD	653.3	402.2	<LOD	<LOD	805.5	<LOD	<LOD	154.0
DEMETHYLNOBILETIN	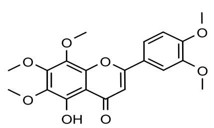	388.372	<LOD	53.8	33.4	<LOD	<LOD	34.9	24.3	25.7	25.0	<LOD	606.7	378.8	<LOD	<LOD	805.5	317.3	336.0	326.7
SALMETEROL XINAFOATE*	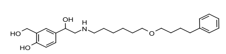	603.756	24.2	34.5	29.3	<LOD	<LOD	34.9	<LOD	<LOD	13.0	308.0	420.0	364.0	<LOD	<LOD	805.5	<LOD	<LOD	154.0
LYSERGOL*	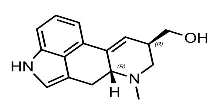	254.333	26.1	32.5	29.3	<LOD	<LOD	34.9	<LOD	<LOD	13.0	280.0	401.3	340.7	<LOD	<LOD	805.5	<LOD	<LOD	154.0
VIOLASTYRENE	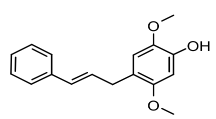	270.328	32.1	25.9	29.0	<LOD	<LOD	34.9	<LOD	<LOD	13.0	392.0	298.7	345.3	<LOD	<LOD	805.5	<LOD	<LOD	154.0
4-METHOXYDALBERGIONE	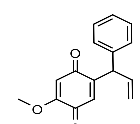	254.285	28.3	29.2	28.7	<LOD	<LOD	34.9	<LOD	<LOD	13.0	345.3	336.0	340.7	<LOD	<LOD	805.5	<LOD	<LOD	154.0
N-OMEGA-METHYL-5-HYDROXYTRYPTAMINE OXALATE SALT	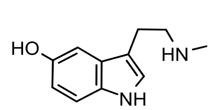	280.280	37.5	19.8	28.7	<LOD	<LOD	34.9	<LOD	<LOD	13.0	382.7	205.3	294.0	<LOD	<LOD	805.5	<LOD	<LOD	154.0
AMRINONE	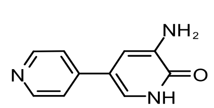	187.202	20.4	36.5	28.5	<LOD	<LOD	34.9	<LOD	<LOD	13.0	205.3	457.3	331.3	<LOD	<LOD	805.5	<LOD	<LOD	154.0
DIOSMIN	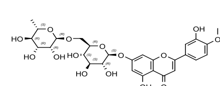	608.549	<LOD	63.1	38.1	<LOD	<LOD	34.9	<LOD	<LOD	13.0	<LOD	774.7	462.8	<LOD	<LOD	805.5	<LOD	<LOD	154.0

6-HYDROXYMELATONIN	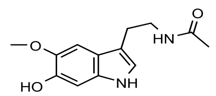	248.282	22.9	33.3	28.1	<LOD	<LOD	34.9	<LOD	<LOD	13.0	233.3	345.3	289.3	<LOD	<LOD	805.5	<LOD	<LOD	154.0
RESERPINE*	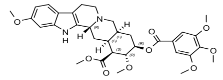	608.688	17.9	38.0	28.0	<LOD	<LOD	34.9	<LOD	<LOD	13.0	196.0	466.7	331.3	<LOD	<LOD	805.5	<LOD	<LOD	154.0
SEROTONIN HYDROCHLORIDE	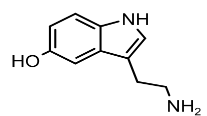	212.679	33.8	21.6	27.7	<LOD	<LOD	34.9	<LOD	<LOD	13.0	345.3	224.0	284.7	<LOD	<LOD	805.5	<LOD	<LOD	154.0
CNQX DISODIUM	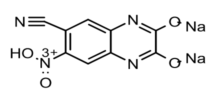	277.125	20.9	34.1	27.5	44.7	47.1	45.9	<LOD	<LOD	13.0	298.7	466.7	382.7	1031.3	1088.2	1059.8	<LOD	<LOD	154.0
MOLINDONE HYDROCHLORIDE*	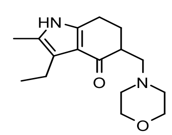	312.840	27.4	27.0	27.2	<LOD	<LOD	34.9	<LOD	<LOD	13.0	280.0	280.0	280.0	<LOD	<LOD	805.5	<LOD	<LOD	154.0
MYRICETIN	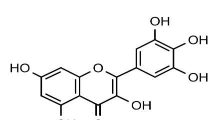	318.237	16.4	37.8	27.1	<LOD	<LOD	34.9	14.3	15.7	15.0	224.0	504.0	364.0	<LOD	<LOD	805.5	186.7	205.3	154.0
METHYLERGONOVINE*	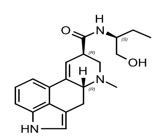	339.439	24.7	28.2	26.4	<LOD	<LOD	34.9	<LOD	<LOD	13.0	270.7	345.3	308.0	<LOD	<LOD	805.5	<LOD	<LOD	154.0
PPNDS TETRASODIUM	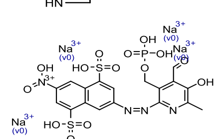	699.380	25.6	26.9	26.2	<LOD	<LOD	34.9	<LOD	<LOD	13.0	326.7	326.7	326.7	<LOD	<LOD	805.5	<LOD	<LOD	154.0
JWH-015	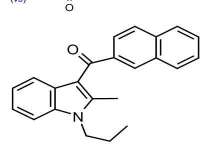	327.427	18.3	32.4	25.4	<LOD	<LOD	34.9	<LOD	<LOD	13.0	186.7	336.0	261.3	<LOD	<LOD	805.5	<LOD	158.7	156.3
MESALAMINE	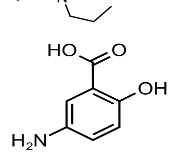	153.137	31.2	19.0	25.1	<LOD	<LOD	34.9	<LOD	<LOD	13.0	280.0	233.3	256.7	<LOD	<LOD	805.5	<LOD	<LOD	154.0
()-EPINEPHRINE HYDROCHLORIDE	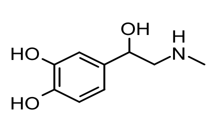	219.667	30.2	18.9	24.5	<LOD	<LOD	34.9	<LOD	42.1	27.6	308.0	196.0	252.0	<LOD	<LOD	805.5	<LOD	550.7	352.3
FLAVOKAWAIN A	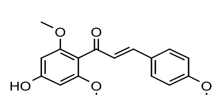	314.337	17.9	30.4	24.2	<LOD	<LOD	34.9	<LOD	<LOD	13.0	196.0	373.3	284.7	<LOD	<LOD	805.5	<LOD	<LOD	154.0

R(-)-N-ALLYLNORAPOMORPHINE HYDROBROMIDE*	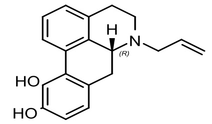	374.278	15.1	32.8	23.9	<LOD	<LOD	34.9	<LOD	<LOD	13.0	214.7	448.0	331.3	<LOD	<LOD	805.5	<LOD	<LOD	154.0
OBLIQUIN	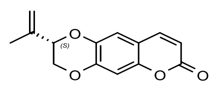	244.246	15.3	32.4	23.9	<LOD	<LOD	34.9	<LOD	<LOD	13.0	186.7	317.3	252.0	<LOD	<LOD	805.5	<LOD	<LOD	154.0
ROBINETINE	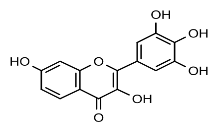	302.238	15.1	32.2	23.6	<LOD	<LOD	34.9	15.0	16.4	15.7	205.3	429.3	317.3	<LOD	<LOD	805.5	196.0	214.7	154.0
THYMOQUINONE	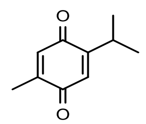	164.204	17.9	28.9	23.4	<LOD	<LOD	34.9	<LOD	<LOD	13.0	196.0	354.7	275.3	<LOD	<LOD	805.5	<LOD	<LOD	154.0
ALPHA-CYANO-4-HYDROXYCINNAMIC ACID	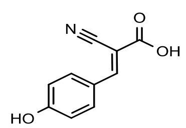	189.170	24.0	21.9	22.9	<LOD	<LOD	34.9	<LOD	<LOD	13.0	280.0	270.7	275.3	<LOD	<LOD	805.5	<LOD	<LOD	154.0
10-HYDROXY-CAMPTOTHECIN*	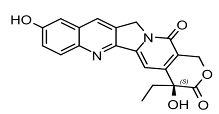	364.357	<LOD	33.6	23.3	<LOD	<LOD	34.9	<LOD	<LOD	13.0	<LOD	420.0	285.5	<LOD	<LOD	805.5	<LOD	<LOD	154.0
BENZO[A]PYRENE	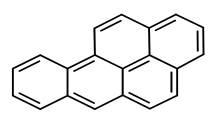	252.316	19.2	25.7	22.4	43.3	55.6	49.4	<LOD	<LOD	13.0	224.0	317.3	270.7	998.8	1284.0	1141.4	<LOD	<LOD	154.0
PALMATINE	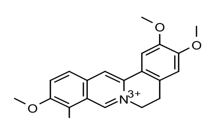	352.408	19.6	25.1	22.3	<LOD	<LOD	34.9	<LOD	<LOD	13.0	214.7	308.0	261.3	<LOD	<LOD	805.5	<LOD	<LOD	154.0
SCH-28080	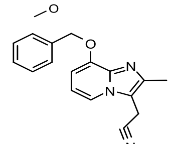	277.327	19.6	24.6	22.1	<LOD	<LOD	34.9	<LOD	<LOD	13.0	280.0	336.0	308.0	<LOD	<LOD	805.5	<LOD	<LOD	154.0
A-77636 HYDROCHLORIDE	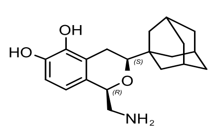	365.900	21.3	22.8	22.1	<LOD	<LOD	34.9	<LOD	<LOD	13.0	233.3	280.0	256.7	<LOD	<LOD	805.5	<LOD	<LOD	154.0
PRATOL	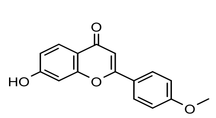	268.268	<LOD	36.4	24.7	<LOD	<LOD	34.9	<LOD	<LOD	13.0	<LOD	485.3	318.2	<LOD	<LOD	805.5	<LOD	<LOD	154.0
CARNOSIC ACID	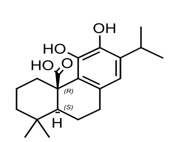	332.440	17.0	26.6	21.8	<LOD	<LOD	34.9	<LOD	<LOD	13.0	186.7	326.7	256.7	<LOD	<LOD	805.5	<LOD	<LOD	154.0

ERGOTAMINE TARTRATE*	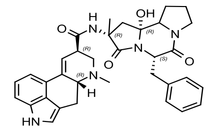	729.787	22.4	21.2	21.8	<LOD	<LOD	34.9	<LOD	<LOD	13.0	261.3	261.3	261.3	<LOD	<LOD	805.5	<LOD	<LOD	154.0
DIHYDROROBINETINE	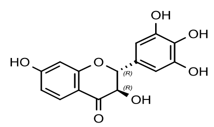	304.254	17.0	25.1	21.1	<LOD	<LOD	34.9	<LOD	<LOD	13.0	186.7	308.0	247.3	<LOD	<LOD	805.5	<LOD	<LOD	154.0
OXANTEL PAMOATE	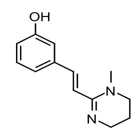	604.659	22.4	18.9	20.6	<LOD	<LOD	34.9	<LOD	<LOD	13.0	261.3	233.3	247.3	<LOD	<LOD	805.5	<LOD	<LOD	154.0
STREPTONIGRIN	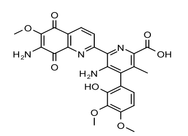	506.471	19.6	21.3	20.4	<LOD	<LOD	34.9	<LOD	<LOD	13.0	214.7	261.3	238.0	<LOD	<LOD	805.5	<LOD	<LOD	154.0
YANGONIN	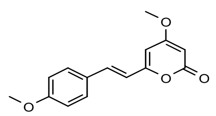	258.273	<LOD	36.5	24.8	<LOD	<LOD	34.9	<LOD	<LOD	13.0	<LOD	448.0	299.5	<LOD	<LOD	805.5	<LOD	<LOD	154.0
CHRYSOERIOL	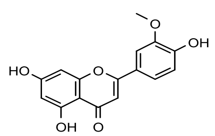	300.266	<LOD	48.2	30.6	<LOD	<LOD	34.9	<LOD	<LOD	13.0	<LOD	644.0	397.5	<LOD	<LOD	805.5	<LOD	<LOD	154.0
ETHOXYQUIN	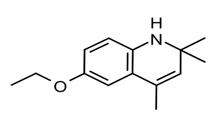	217.312	18.3	21.2	19.7	<LOD	<LOD	34.9	<LOD	<LOD	13.0	196.0	261.3	228.7	<LOD	<LOD	805.5	<LOD	<LOD	154.0
DIHYDROTANSHINONE	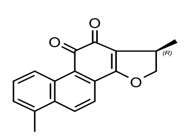	278.307	<LOD	28.2	20.6	<LOD	<LOD	34.9	<LOD	<LOD	13.0	<LOD	345.3	248.2	<LOD	<LOD	805.5	<LOD	<LOD	154.0
4-AMINO-1,8-NAPHTHALIMIDE	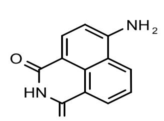	212.208	15.3	23.6	19.5	<LOD	<LOD	34.9	<LOD	<LOD	13.0	168.0	289.3	228.7	<LOD	<LOD	805.5	<LOD	<LOD	154.0
ISOQUERCITRINE	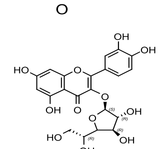	464.379	17.9	20.5	19.2	<LOD	<LOD	34.9	<LOD	<LOD	13.0	196.0	252.0	224.0	<LOD	<LOD	805.5	<LOD	<LOD	154.0
APRAMYCIN	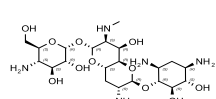	539.583	<LOD	42.5	27.8	<LOD	<LOD	34.9	<LOD	<LOD	13.0	<LOD	532.0	341.5	<LOD	<LOD	805.5	<LOD	<LOD	154.0
EUGENYL BENZOATE	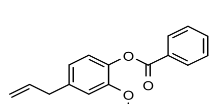	268.312	22.9	13.4	18.2	<LOD	<LOD	34.9	<LOD	<LOD	13.0	280.0	168.0	224.0	<LOD	<LOD	805.5	<LOD	<LOD	154.0

PELLITORINE	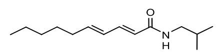	223.360	<LOD	31.5	22.2	<LOD	<LOD	34.9	<LOD	<LOD	13.0	<LOD	420.0	285.5	<LOD	<LOD	805.5	<LOD	<LOD	154.0
6,7-DIHYDROXYFLAVONE	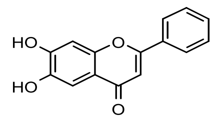	254.241	<LOD	30.1	21.5	<LOD	<LOD	34.9	<LOD	<LOD	13.0	<LOD	401.3	276.2	<LOD	<LOD	805.5	<LOD	<LOD	154.0
AVOCADYNE ACETATE	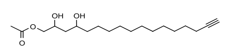	326.477	<LOD	39.7	26.4	<LOD	<LOD	34.9	19.3	21.4	20.3	<LOD	448.0	299.5	<LOD	<LOD	805.5	252.0	280.0	154.0
KOPARIN	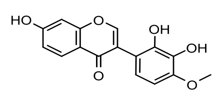	300.266	<LOD	24.3	18.7	<LOD	<LOD	34.9	<LOD	<LOD	13.0	<LOD	280.0	215.5	<LOD	<LOD	805.5	<LOD	<LOD	154.0
FLAVOKAWAIN B	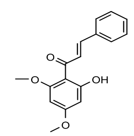	284.311	<LOD	26.6	19.8	<LOD	<LOD	34.9	<LOD	15.0	15.0	<LOD	354.7	252.8	<LOD	<LOD	805.5	168.0	196.0	182.0
CHRYSINE	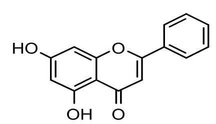	254.241	<LOD	23.1	18.0	<LOD	<LOD	34.9	<LOD	<LOD	13.0	<LOD	308.0	229.5	<LOD	<LOD	805.5	<LOD	<LOD	154.0
CRYPTOTANSHINONE	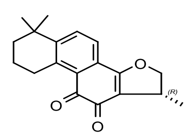	296.366	<LOD	43.4	28.2	<LOD	<LOD	34.9	<LOD	<LOD	13.0	<LOD	532.0	341.5	<LOD	<LOD	805.5	<LOD	<LOD	154.0
VITEXIN	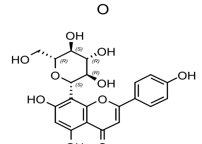	432.381	<LOD	21.3	17.2	<LOD	<LOD	34.9	<LOD	<LOD	13.0	<LOD	261.3	206.2	<LOD	<LOD	805.5	<LOD	<LOD	154.0
DIOSMETINE	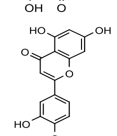	300.266	<LOD	48.7	30.8	<LOD	<LOD	34.9	<LOD	<LOD	13.0	<LOD	597.3	374.2	<LOD	<LOD	805.5	<LOD	<LOD	154.0

TABLE 4.3 K_M and IC_{50} of the top 32 hit substrates of CYP3A65. Compound name and structure are given. K_M was determined for rates of NADPH depletion and IC_{50} was based on the inhibition of BFC metabolism. Data are given with their respective standard error of the mean (SEM) developed from Michaelis-Menten curves, fitted using online tool: http://www.ic50.tk/. NA is denoted in places where the curve did not follow typical Michaelis-Menten kinetics and K_M and IC_{50} values could not be computed. Grey highlighted cells indicate K_M and IC_{50} where maximum inhibition or fluorescence was not reached. Compounds that were identified to be CYP3A4 substrates through DataBank.ca (Wishart et al 2018) are identified by an asterisk beside the compound name.

Compound Name	Structure	Km		IC_{50}	
		(µM) ± SEM		(µM) ± SEM	
PLUMBAGIN	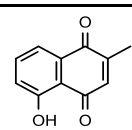	4.1294	0.4239	1.7123	0.1537
MENADIONE	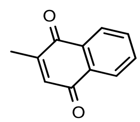	8.8477	1.5760	3.4184	0.4143
β-LAPACHONE	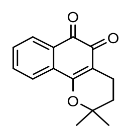	19.9361	6.4130	5.2911	1.3060
PRIMAQUINE DIPHOSPHATE*	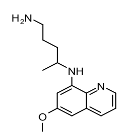	22.4417	5.8970	7.5310	1.2410
3,4-DIMETHOXY-DALBERGIONE	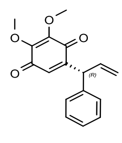	10.2851	1.8200	7.6016	1.6630
NSC 95397	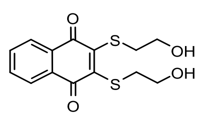	5.2481	1.8880	7.6986	0.8385
IDEBENONE	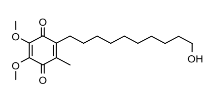	5.3559	1.3100	9.1429	1.6870
GW2974	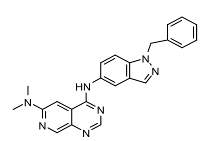	20.9696	6.0510	11.9755	1.1690
FLUPIRTINE MALEATE	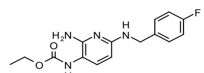	25.7201	9.8340	12.1380	4.3850
DULOXETINE HYDROCHLORIDE*	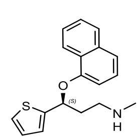	24.1250	10.1400	12.2464	1.1910

DOXAZOSIN MESYLATE*	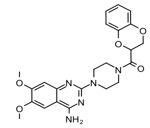	318.6150	448.2000	15.6952	3.9990
LAPACHOL	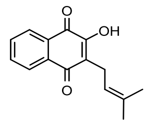	30.5046	10.1500	20.9284	2.5210
CI-976	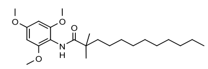	NA	NA	23.7218	2.9270
CLOXYQUIN	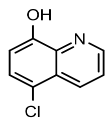	30.6403	16.1900	24.5180	4.2240
SANGUINARINE SULFATE	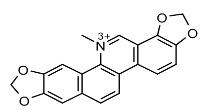	45.7001	15.1100	28.8556	8.8100
APOMORPHINE HYDROCHLORIDE HEMIHYDRATE*	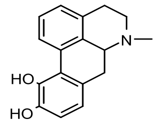	85.5779	97.5200	31.3532	12.2500
R(-)-2,10,11-TRIHYDROXY-N-PROPYLNORAPORPHINE HYDROBROMIDE*	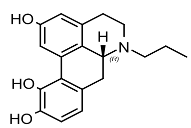	146.7720	127.9000	31.3542	23.0000
NITROMIDE	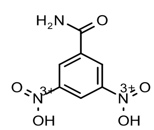	39.1341	19.6100	32.4862	9.5600
DAPH	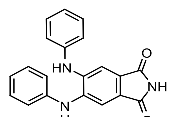	19.9163	14.5500	33.0599	8.1940
ISOCORYDINE	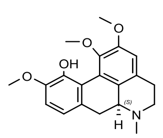	75.6221	72.2200	37.0759	16.1200
R(-)-APOCODEINE HYDROCHLORIDE	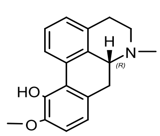	45.1329	48.9500	46.1323	30.6300
OXYQUINOLINE HEMISULFATE	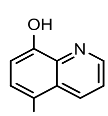	60.9661	24.9800	61.1294	24.0500

PRAZOSIN HYDROCHLORIDE*	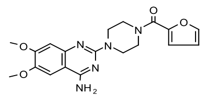	NA	NA	NA	NA
1-(1-NAPHTHYL)-PIPERAZINE HYDROCHLORIDE	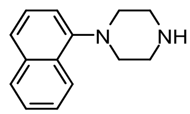	119.9530	122.2000	3493	611100
BTO-1	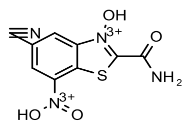	194.9200	147.3000	3957	394300
HYCANTHONE	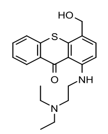	0.1062	0.0963	37.1006	1322
7,2'-DIHYDROXYFLAVONE	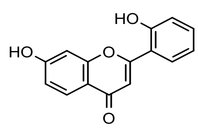	NA	NA	NA	NA
2',6'-DIHYDROXY-4'-METHOXY-CHALCONE	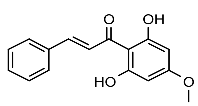	NA	NA	NA	NA
HOMIDIUM BROMIDE	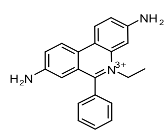	12.0298	3.4270	NA	NA
CORALYNE CHLORIDE	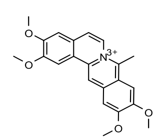	13.9413	5.0760	NA	NA
VULPINIC ACID	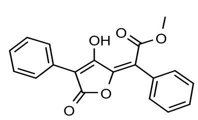	NA	NA	NA	NA
UVAOL	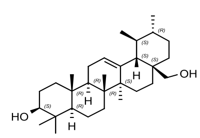	NA	NA	NA	NA

FIGURES

FIGURE 4.1 The effects of increasing concentrations of DMSO (%v/v) on the rates of CYP3A65 mediated **A)** NADPH depletion with 20 μM 7-methoxyresorufin (7-MR) and **B)** 7-hydroxy-4-(trifluoromethyl) coumarin (HFC) formation from 100 μM 7-benxyloxy-4-(trifluoromethyl)coumarin (BFC). All reactions were performed in 50 μL reactions in EROD buffer.

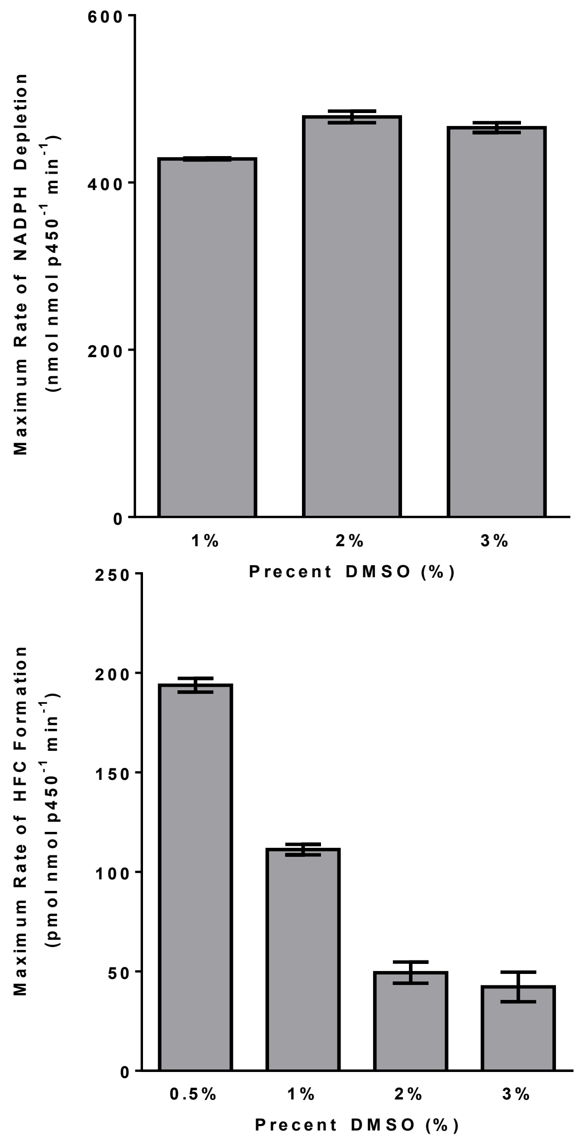

FIGURE 4.2 A) Michaelis-Menten curves of 7-methoyxresorufin (7-MR) and B) 7-benxyloxy-4-(trifluoromethyl)coumarin (BFC) metabolism. All reactions were performed in 200 µL reactions, initiated with 1.33 mM NADPH; BFC contained 0.25% DMSO in KPO_4 buffer and 7-MR contained 0.5% DMSO in EROD buffer.

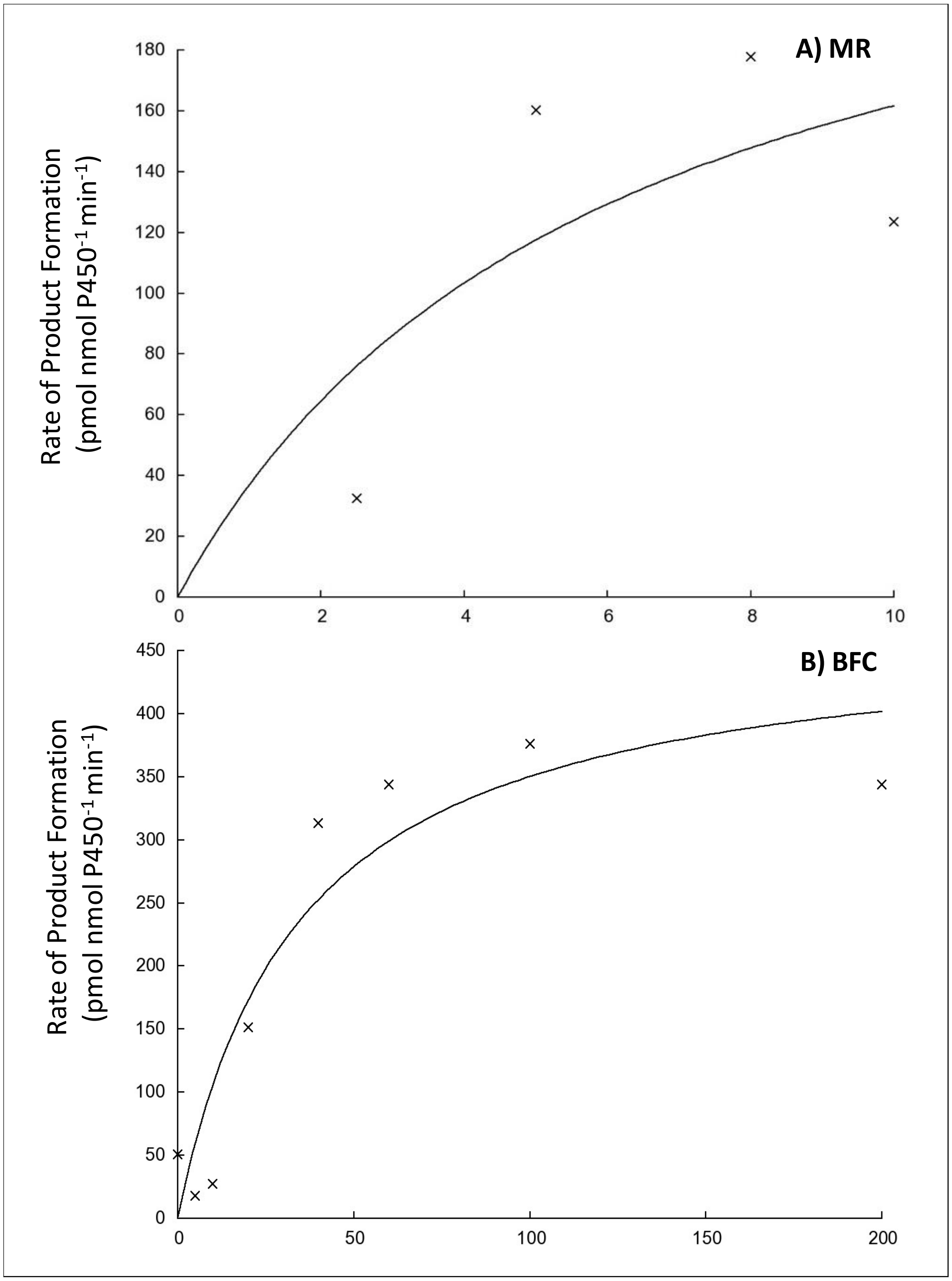
A) MR
Rate of Product Formation
(pmol nmol P450^{-1} min^{-1})
0
20
40
60
80
100
120
140
160
180
0
2
4
6
8
10
B) BFC
Rate of Product Formation
(pmol nmol P450^{-1} min^{-1})
0
50
100
150
200
250
300
350
400
450
0
50
100
150
200

FIGURE 4.3 The maximum catalytic activity of CYP3A65 mediated metabolism for alkyloxy-resorufin substrates. Data are shown for reactions with 5 µM 7-benzyloxyresorufin (7-BR), 25 µM 7-ethoxyresorufin (7-ER), 15 µM 7-methoxyresorufin (7-MR) and 12.5 µM 7-pentoxyresorufin (7-PR). All reactions were performed in 200 µL reactions, initiated with 1.33 mM NADPH and contained 0.5% DMSO in EROD buffer.

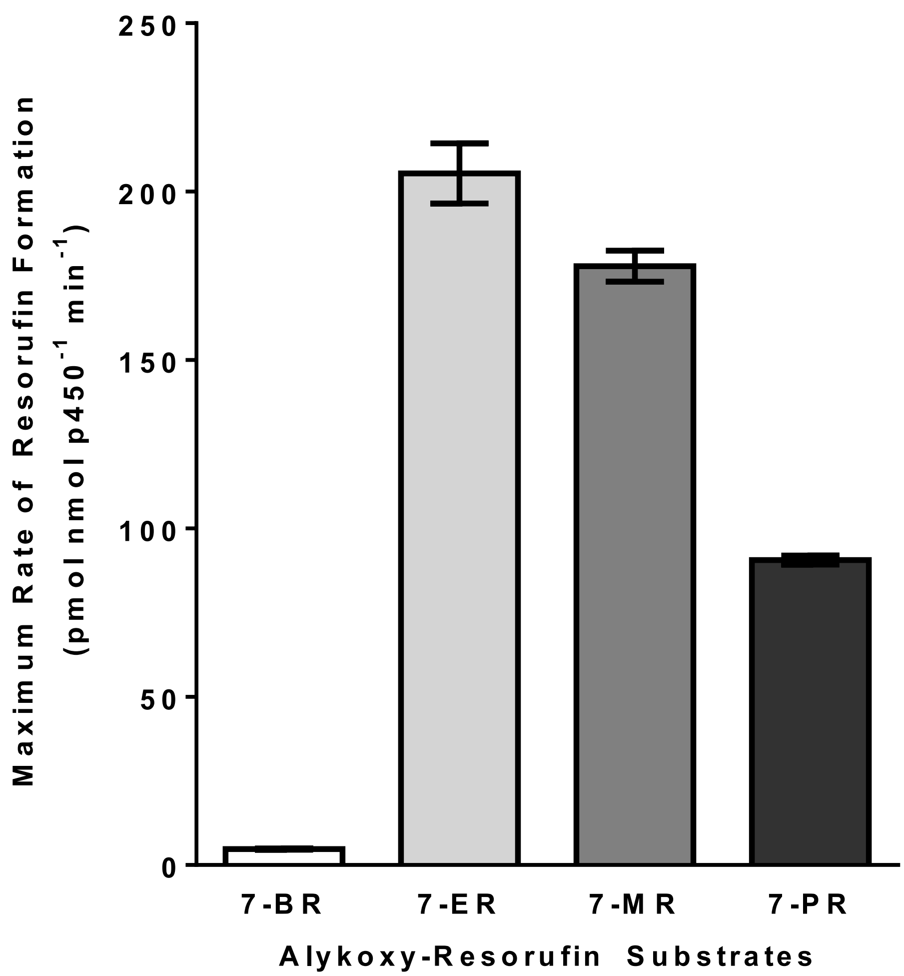

FIGURE 4.4 The maximum catalytic activity of CYP3A65 mediated metabolism of 7-benxyloxy-4-(trifluoromethyl) coumarin (BFC) and dibenzylfluorescein (DBF). All reactions were performed in 200 µL reactions, initiated with 1.33 mM NADPH and contained 0.25% DMSO in KPO_4 buffer with either 100 µM BFC or 2.5 µM DBF.

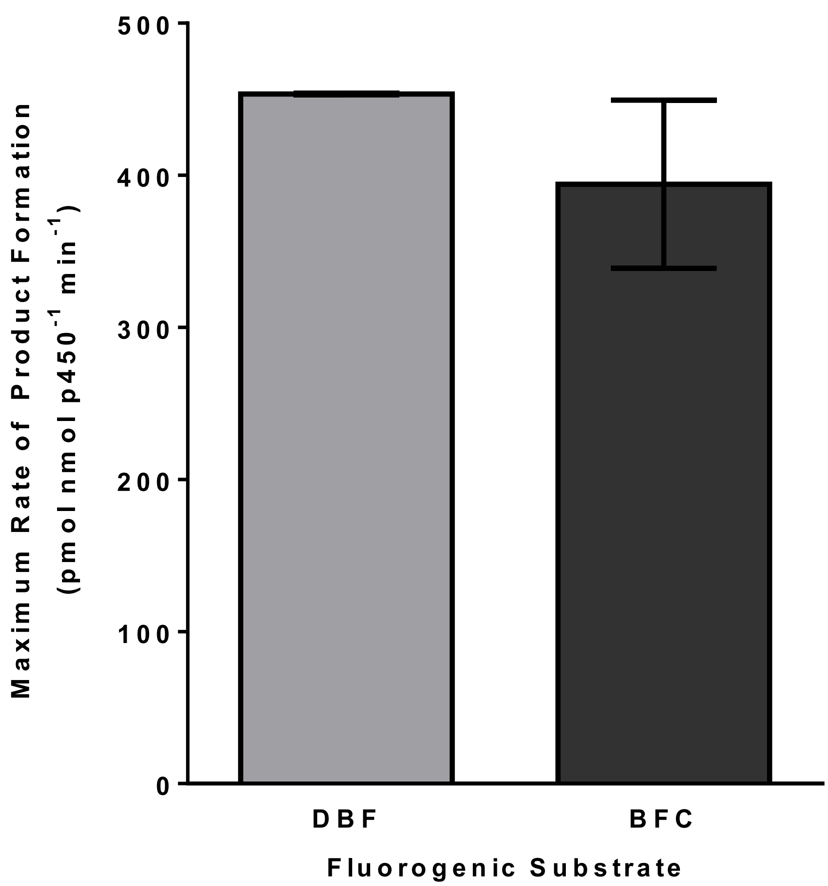

FIGURE 4.5 Rate of NADPH depletion for ~4000 compounds, reported as a percent of the positive control (CYP3A65 + 7-methoxyresorufin; 7-MR). Catalytic activity of replicate two is graphed as a function of replicate one. The solid and dashed black lines denotes the limit of detection, determined as 3-standard deviation above the mean rate of NADPH depletion in the negative control (No substrate; CYP3A65 + 2% DMSO; 13% of the positive control), and the cut off for compounds to be included in the initial follow up (20% of the positive control), respectively.

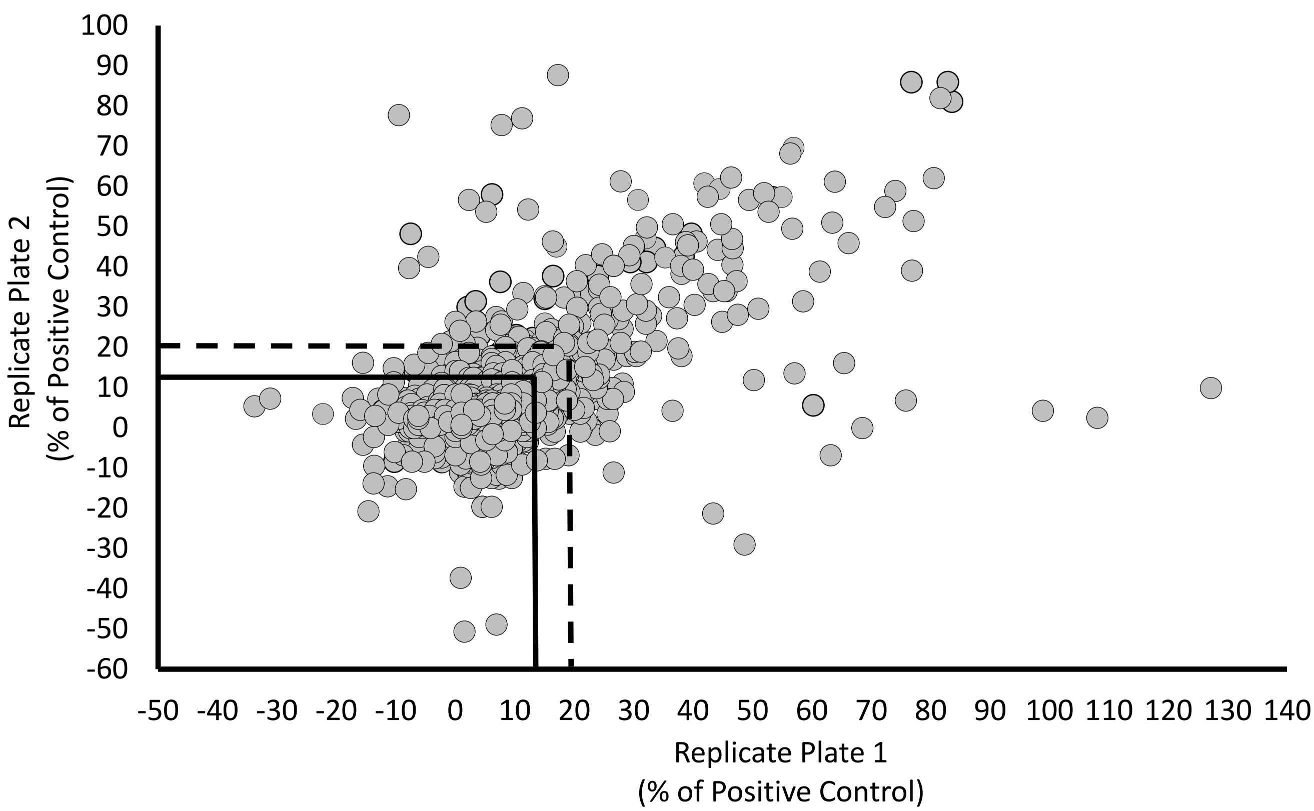

Replicate Plate 2
(% of Positive Control)
100
90
80
70
60
50
40
30
20
10
0
-10
-20
-30
-40
-50
-60
-50 -40 -30 -20 -10 0 10 20 30 40 50 60 70 80 90 100 110 120 130 140
Replicate Plate 1
(% of Positive Control)

REFERENCES

Al-Habsi AA, Massarsky A, Moon TW. 2016. Exposure to gemfibrozil and atorvastatin affects cholesterol metabolism and steroid production in zebrafish (*Danio rerio*). *Comparative biochemistry and physiology. Part B, Biochemistry and Molecular Biology* 199: 87-96

Baillie TA, Rettie AE. 2011. Role of biotransformation in drug-induced toxicity: influence of intra- and inter-species differences in drug metabolism. *Drug Metabolism and Pharmacokinetics* 26: 15-29

Bainy AC, Kubota A, Goldstone JV, Lille-Langøy R, Karchner SI, et al. 2013. Functional characterization of a full length pregnane X receptor, expression in vivo, and identification of PXR alleles, in zebrafish (*Danio rerio*). *Aquatic Toxicology* 142: 447-57

Barr R, Crane FL. 1971. [37] Quinones in algae and higher plants In *Methods in Enzymology*, pp. 372-408: Academic Press

Bolton JL, Trush MA, Penning TM, Dryhurst G, Monks TJ. 2000. Role of quinones in toxicology. *Chemical Research in Toxicology* 13: 135-60

Burke MD, Thompson S, Weaver RJ, Wolf CR, Mayers RT. 1994. Cytochrome P450 specificities of alkoxyresorufin O-dealkylation in human and rat liver. *Biochemical Pharmacology* 48: 923-36

Burkina V, Zlabek V, Zamaratskaia G. 2013. Clotrimazole, but not dexamethasone, is a potent in vitro inhibitor of cytochrome P450 isoforms CYP1A and CYP3A in rainbow trout. *Chemosphere* 92: 1099-104

Chang CT, Chung HY, Su HT, Tseng HP, Tzou WS, Hu CH. 2013. Regulation of zebrafish CYP3A65 transcription by AHR2. *Toxicology and Applied Pharmacology* 270: 174-84

Crespi CL, Stresser DM. 2000. Fluorometric screening for metabolism-based drug–drug interactions. *Journal of Pharmacological and Toxicological Methods* 44: 325-31

Dai YJ, Jia YF, Chen N, Bian WP, Li QK, et al. 2014. Zebrafish as a model system to study toxicology. *Environmental Toxicology and Chemistry* 33: 11-17

Delaforge M, Andre F, Jaouen M, Dolgos H, Benech H, et al. 1997. Metabolism of tentoxin by hepatic cytochrome P-450 3A isozymes. *European Journal of Biochemistry* 250: 150-57

Denisov IG, Makris TM, Sligar SG, Schlichting I. 2005. Structure and chemistry of cytochrome p450. *Chemical Reviews* 105: 2253-78

Dooley K, Zon LI. 2000. Zebrafish: a model system for the study of human disease. *Current Opinion in Genetics and Development* 10: 252-56

Ghosal A, Hapangama N, Yuan Y, Lu X, Horne D, et al. 2003. Rapid determination of enzyme activities of recombinant human cytochromes P450, human liver microsomes and hepatocytes. *Biopharmaceutics and Drug disposition* 24: 375-84

Goldstone JV, McArthur AG, Kubota A, Zanette J, Parente T, et al. 2010. Identification and developmental expression of the full complement of Cytochrome P450 genes in Zebrafish. *BMC Genomics* 11: 643

Goodwin B, Redinbo MR, Kliewer SA. 2002. Regulation of cyp3a gene transcription by the pregnane x receptor. *Annual Review of Pharmacology and Toxicology* 42: 1-23

Guengerich FP. 1999. Cytochrome P-450 3A4: regulation and role in drug metabolism. *Annual Review of Pharmacology and Toxicology* 39: 1-17

Guengerich FP. 2001. Common and uncommon cytochrome P450 reactions related to metabolism and chemical toxicity. *Chemical Research in Toxicology* 14: 611-50

Hagemeyer CE, Burck C, Schwab R, Knoth R, Meyer RP. 2010. 7-Benzyloxyresorufin-O-dealkylase activity as a marker for measuring cytochrome P450 CYP3A induction in mouse liver. *Analytical Biochemistry* 398: 104-11

Hartl MGJ, Kilemade M, Sheehan D, Mothersill C, O'Halloran J, et al. 2007. Hepatic biomarkers of sediment-associated pollution in juvenile turbot, *Scophthalmus maximus L. Marine Environmental Research* 64: 191-208

Hasselberg L, Grøsvik BE, Goksøyr A, Celander MC. 2005. Interactions between xenoestrogens and ketoconazole on hepatic CYP1A and CYP3A, in juvenile Atlantic cod (*Gadus morhua*). *Comparative Hepatology* 4: 2-2

Hegelund T, Ottosson K, Radinger M, Tomberg P, Celander MC. 2004. Effects of the antifungal imidazole ketoconazole on CYP1A and CYP3A in rainbow trout and killifish. *Environmental Toxicology and Chemistry* 23: 1326-34

Hill AJ, Teraoka H, Heideman W, Peterson RE. 2005. Zebrafish as a model vertebrate for investigating chemical toxicity. *Toxicological Sciences* 86: 6-19

Jackson JS, Kennedy CJ. 2017. Regulation of hepatic abcb4 and cyp3a65 gene expression and multidrug/multixenobiotic resistance (MDR/MXR) functional activity in the model teleost, *Danio rerio* (zebrafish). *Comparative Biochemistry and Physiology. Toxicology and Pharmacology: CBP* 200: 34-41

Johnson EF, Connick JP, Reed JR, Backes WL, Desai MC, et al. 2014. Correlating structure and function of drug-metabolizing enzymes: progress and ongoing challenges. *Drug Metabolism and Disposition* 42: 9-22

Kobayashi K, Urashima K, Shimada N, Chiba K. 2002. Substrate specificity for rat cytochrome P450 (CYP) isoforms: screening with cDNA-expressed systems of the rat. *Biochemical Pharmacology* 63: 889-96

Koenig S, Fernández P, Solé M. 2012. Differences in cytochrome P450 enzyme activities between fish and crustacea: Relationship with the bioaccumulation patterns of polychlorobiphenyls (PCBs). *Aquatic Toxicology* 108: 11-17

Kubota A, Goldstone JV, Lemaire B, Takata M, Woodin BR, Stegeman JJ. 2014. Role of pregnane X receptor and aryl hydrocarbon receptor in transcriptional regulation of pxr, CYP2, and CYP3 genes in developing zebrafish. *Toxicological Sciences* 143: 398-407

Kuehl P, Zhang J, Lin Y, Lamba J, Assem M, et al. 2001. Sequence diversity in CYP3A promoters and characterization of the genetic basis of polymorphic CYP3A5 expression. *Nature Genetics* 27: 383

Lee AJ, Kosh JW, Conney AH, Zhu BT. 2001. Characterization of the NADPH-dependent metabolism of 17β-estradiol to multiple metabolites by human liver microsomes and selectively expressed human cytochrome P450 3A4 and 3A5. *Journal of Pharmacology and Experimental Therapeutics* 298: 420-32

Liu Y, Junaid M, Wang Y, Tang Y-M, Bian W-P, et al. 2018. New toxicogenetic insights and ranking of the selected pharmaceuticals belong to the three different classes: A toxicity estimation to confirmation approach. *Aquatic Toxicology* 201: 151-61

Murray GI, Melvin WT, Greenlee WF, Burke MD. 2001. Regulation, function, and tissue-specific expression of cytochrome P450 CYP1B1. *Annual review of pharmacology and toxicology* 41: 297-316

Nebert DW, Russell DW. 2002. Clinical importance of the cytochromes P450. *The Lancet* 360: 1155-62

Nelson DR. 2006. Cytochrome P450 nomenclature, 2004. *Methods in Molecular Biology (Clifton, N.J.)* 320: 1-10

Nelson DR, Nebert DW. 2018. Cytochrome P450 (*CYP*) Gene Superfamily In *eLS*, pp. 1-19: John Wiley & Sons, Ltd (Ed). doi:10.1002/9780470015902.a0005667.pub3

Nerurkar PV, Park SS, Thomas PE, Nims RW, Lubet RA. 1993. Methoxyresorufin and benzyloxyresorufin: substrates preferentially metabolized by cytochromes P4501A2 and 2B, respectively, in the rat and mouse. *Biochemical Pharmacology* 46: 933-43

Patrinostro X, Carter ML, Kramer AC, Lund TC. 2013. A model of glucose-6-phosphate dehydrogenase deficiency in the zebrafish. *Experimental Hematology* 41: 697-710.e2

Scornaienchi ML, Thornton C, Willett KL, Wilson JY. 2010a. Cytochrome P450-mediated 17β-estradiol metabolism in zebrafish (*Danio rerio*). *Journal of Endocrinology* 206: 317-25

Scornaienchi ML, Thornton C, Willett KL, Wilson JY. 2010b. Functional differences in the cytochrome P450 1 family enzymes from zebrafish (*Danio rerio*) using heterologously expressed proteins. *Archives of Biochemistry and Biophysics* 502: 17-22

Segura-Aguilar J, Metodiewa D, Welch CJ. 1998. Metabolic activation of dopamine o-quinones to o-semiquinones by NADPH cytochrome P450 reductase may play an important role in oxidative stress and apoptotic effects. *Biochimica et Biophysica Acta (BBA) - General Subjects* 1381: 1-6

Shaya L, Dejong C, Wilson JY. 2014. Expression patterns of cytochrome P450 3B and 3C genes in model fish species. *Comparative Biochemistry and Physiology. Toxicology and Pharmacology: CBP* 166: 115-25

Shaya L, Jones DE, Wilson JY. 2019. CYP3C gene regulation by the aryl hydrocarbon and estrogen receptors in zebrafish. *Toxicology and Applied Pharmacology* 362: 77-85

Shimada T, Guengerich FP. 1989. Evidence for cytochrome P-450NF, the nifedipine oxidase, being the principal enzyme involved in the bioactivation of aflatoxins in human liver. *Proceedings of the National Academy of Sciences* 86: 462-65

Shimada T, Iwasaki M, Martin MV, Guengerich FP. 1989. Human liver microsomal cytochrome P-450 enzymes involved in the bioactivation of procarcinogens detected by umu gene response in *Salmonella typhimurium* TA 1535/pSK1002. *Cancer Research* 49: 3218-28

Stresser DM, Turner SD, Blanchard AP, Miller VP, Crespi CL. 2002. Cytochrome P450 fluorometric substrates: identification of isoform-selective probes for rat CYP2D2 and human CYP3A4. *Drug Metabolism and Disposition* 30: 845-52

Talalay P, Dinkova-Kostova AT. 2004. Role of Nicotinamide Quinone Oxidoreductase 1 (NQO1) in Protection against Toxicity of Electrophiles and Reactive Oxygen Intermediates In *Methods in Enzymology*, pp. 355-64: Academic Press

Tseng H-P, Hseu T-H, Buhler DR, Wang W-D, Hu C-H. 2005. Constitutive and xenobiotics-induced expression of a novel CYP3A gene from zebrafish larva. *Toxicology and Applied Pharmacology* 205: 247-58

Tsuchiya Y, Nakajima M, Yokoi T. 2005. Cytochrome P450-mediated metabolism of estrogens and its regulation in human. *Cancer letters* 227: 115-24

Wang H, Napoli KL, Strobel HW. 2000. Cytochrome P450 3A9 catalyzes the metabolism of progesterone and other steroid hormones. *Molecular and Cellular Biochemistry* 213: 127-35

Whyte JJ, Jung R, Schmitt C, Tillitt D. 2000. Ethoxyresorufin-O-deethylase (EROD) activity in fish as a biomarker of chemical exposure. *Critical Reviews in Toxicology* 30: 347-570

Wishart DS, Feunang YD, Guo AC, Lo EJ, Marcu A, et al. 2018. DrugBank 5.0: a major update to the DrugBank database for 2018. *Nucleic Acids Research* 46: D1074-d82

Yan J, Cai Z. 2010. Molecular evolution and functional divergence of the cytochrome P450 3 (CYP3) Family in Actinopterygii (ray-finned fish). *PloS one* 5: e14276

Zanger UM, Schwab M. 2013. Cytochrome P450 enzymes in drug metabolism: regulation of gene expression, enzyme activities, and impact of genetic variation. *Pharmacology and therapeutics* 138: 103-41

Zhou S, Chan E, Li X, Huang M. 2005. Clinical outcomes and management of mechanism-based inhibition of cytochrome P450 3A4. *Therapeutics and Clinical Risk Management* 1: 3-13

Zon LI, Peterson RT. 2005. In vivo drug discovery in the zebrafish. *Nature Reviews Drug Discovery* 4: 35

CHAPTER 5

GENERAL DISCUSSION

ORPHAN CYTOCHROME P450 GENES

Whole genome sequencing has resulted in the identification of more than 55,000 cytochrome P450 (CYP) genes (Nelson & Nebert 2018); only a handful of these genes have been tested for function, while the others are "orphans" with unknown expression patterns, regulation mechanisms, and/or function (Guengerich & Cheng 2011). CYP enzymes are especially interesting because of their functional diversity and their presence in all domains of life; most recently a CYP has been identified in viruses (Lamb et al 2019). CYPs are involved in various biochemical processes that lead to the production of primary and secondary metabolites. In plants, some of these metabolites are responsible for the smell and taste of agriculturally important products, such as wine (Ilc et al 2017), and others are important in defense mechanisms and development (Xu et al 2015). In insects, CYPs are expressed in the antennae and play a role in odour and pheromone detection and metabolism (Maïbèche-Coisne et al 2002, Wojtasek & Leal 1999). One critical function of CYP enzymes in all organisms is their ability to metabolize exogenous compounds to provide chemical defence. Specifically, CYP1, CYP2, CYP3 and CYP4 families are primarily responsible for exogenous compound (xenobiotic) metabolism (as reviewed by Zanger & Schwab 2013). In humans, the CYP3 family has considerable clinical value for its role in drug metabolism (as reviewed by Zanger & Schwab 2013).

The CYP3 family contains 4 subfamilies: CYP3A, CYP3B, CYP3C and CYP3D. While all organisms have one or more gene within the CYP3A subfamily, CYP3B, CYP3C and CYP3D subfamilies are unique to the teleost lineage (Goldstone et al 2010, McArthur et al 2003, Yan & Cai 2010). The members of the CYP3A subfamily are well characterized in mammalian systems and are responsible for the metabolism of >50% pharmaceuticals (as reviewed by Zanger and Schwab) and some steroids, such as estradiol (Tsuchiya et al 2005). In most other organisms, and specifically fish, members of CYP3A, CYP3B, CYP3C and CYP3D subfamilies are 'orphans' with unknown function and/or regulation. Fish, like the zebrafish, provide a valuable opportunity to study multiple CYP3 subfamilies where the CYP content of the genome has been established. Given the close evolutionary relationship of CYP3 genes in fish and other vertebrates (Goldstone et al 2010, McArthur et al 2003, Yan & Cai 2010) it is not unreasonable that fish CYP3 families play a critical role in detoxification and endogenous compound metabolism. Assigning function to orphan CYP3 genes will allow us to elucidate CYP3 evolution, and the possible roles of this family in endogenous and exogenous compound metabolism, providing several novel applications to the fields of physiology, toxicology, pharmacology and medicine, fields in which CYP3 enzymes have established and leading roles in mammals.

CYPs are functionally diverse enzymes and the assays that assess function must be catered specifically to each CYP studied, making it challenging to assign function to all the orphan enzymes. As reviewed by Guengerich et al (2005), traditional biochemistry relies on having an assay that led to the identification of a unique function, followed by the isolation, purification, cloning and sequencing of the gene to elucidate what mediated the identified function. In this method, a function is identified first, followed by characterizing the gene/protein responsible for that function. A more contemporary biochemistry approach, and similar to the one used in this thesis, makes use of the rapidly sequenced genome to identify novel and candidate CYP genes, followed by the development of specific assays to identify function (Guengerich et al 2005). The downside of this approach is that it is slow because the numbers of potential substrates are endless when both endogenous and exogenous compounds are considered. Overall, the number of novel CYP genes identified through genome sequencing is so large that the function of most orphan CYP enzyme remains unknown due to limitations in existing functional characterization strategies.

For CYP enzymes, one method to glean insight on function is to characterize the gene and/or protein expression (as reviewed by Albert et al 2002). For zebrafish, functional hypothesis have been made based on gene expression (Kubota et al 2019b, Shaya et al 2014). For example, in humans, the intestine and the liver are major sites of pharmaceutical absorption and metabolism, respectively, thus human CYP3A4 is highly expressed in these organs where it plays an important role in pharmaceutical biotransformation and detoxification (For reviews see: Guengerich 2008, Zanger & Schwab 2013). Like mammalian CYP3A4, zebrafish CYP3A65 is also highly expressed in the liver and intestine (Kubota et al 2019b, Tseng et al 2005). This specific expression profile is assumed to be indicative of xenobiotic metabolism and detoxification (Kubota et al 2019b, Shaya et al 2014, Verbueken et al 2018). Indeed, like CYP3A4 (Gautier et al 1996), CYP3A65 can metabolize xenobiotic compounds like benzo[a]pyrene (BaP; Scornaienchi 2009). It is important to note, that expression work for orphan CYP genes mostly relies on the quantification of mRNA transcripts, which does not always relate to protein expression. The challenge remains to be that characterizing expression profiles only provides information to shape hypothesis on function and is not actually data on function of CYP3 genes. Nonetheless, expression profiles can provide clues for potential future functional studies. Our laboratory has previously established the expression profiles of zebrafish CYP3C genes (Shaya et al 2014), and these data were used to inform the studies presented in this thesis.

Beyond simple expression patterns, understanding the regulation of the CYP genes of interest may provide insight on the function. For example, the mammalian CYP3A is regulated by the pregnane-x-receptor (PXR), a chemosensor in the nuclear receptor family that is activated by several classes of compounds, such as pharmaceuticals, environmental pollutants, steroids and others (as reviewed by Goodwin et al 2002). Ligand- activated PXR acts as a transcription factor to induce various proteins, including CYP3A enzymes, involved in xenobiotic metabolism and transport. Thus, many PXR ligands are CYP3A substrates (e.g. taxol (Cresteil et al 1994), ritonavir (Denissen et al 1997, Kumar et al 1996), dexamethasone (Tomlinson et al 1997), triol (Dussault et al 2003)). Identifying the receptor and ligands involved in CYP regulation could provide valuable clues for potential CYP substrates. Thus, I utilized the data in Chapter 2, on CYP3C gene regulation, to raise hypotheses tested in Chapter 3.

Promoter characterization data can be the first steps to identifying nuclear receptors involved in orphan CYP gene regulation (Callard et al 2001, Kubota et al 2015, Shaya et al 2014, Zhang et al 2012). We previously established that CYP3C genes contain various xenobiotic (XRE; Zeruth & Pollenz 2007) and estrogen response elements (ERE; Gruber et al 2004), which the AhR and ER, respectively, bind to activate gene transcription. Promoter data (Kubota et al 2015, Shaya et al 2014), differential expression in adult male and female zebrafish, and the expression of CYP3Cs in xenobiotic and steroid metabolizing organs (Corley-Smith et al 2006, Shaya et al 2014), suggested that the AhR and ER were involved in regulation. In Chapter 2, I characterized the role of the AhR and ER in regulation of the orphan zebrafish CYP3C1, CYP3C2, CYP3C3, and CYP3C4 genes using the xenobiotic AhR ligand, β-naphthoflavone (βNF) and the endogenous ER ligand, 17β-estradiol (E_2). While previous studies have investigated the regulatory mechanisms of CYP3C1 in embryonic zebrafish (Corley-Smith et al 2006, Kubota et al 2015) this is the first study to provide information on the regulation of the full suite of CYP3C enzymes in adult zebrafish (Shaya et al 2019). Characterizing the regulation of the orphan CYP3C genes in Chapter 2 provided insight on their function. AhR ligands are planar aromatic hydrocarbon (For reviews see: Denison & Nagy 2003, Hahn 2002), most of which are also CYP1A substrates (Kim & Guengerich 2005, Mescher & Haarmann-Stemmann 2018, Scornaienchi 2009, Shimada & Fujii-Kuriyama 2004). Regulation by AhR implicates the involvement of planar aromatic xenobiotic compounds as substrates that may be metabolized by CYP3C enzymes, and likewise, regulation by the ER implicates steroids as CYP3C substrates, as established for human CYP1B1 (Tsuchiya et al 2004). It is important to note, that regulatory data can be difficult to interpret when expression is tissue, gene, sex and time specific, as demonstrated in Chapter 2, and while the regulation provides insight on function, functional hypothesis made from regulation data require empirical testing.

CYP catalytic function has often been assessed with established fluorogenic or luminogenic substrates; several substrates are commercially available and their selectivity and specificity for the important xenobiotic metabolizing CYPs has been characterized in mammals (Cali et al 2006, Cali et al 2012, Stresser et al 2000, Stresser et al 2002). These assays are highly useful because they are fast, relatively cheap, and directly measure metabolite formation. The caveats are that there are relatively few of these CYP substrates available and their selectivity and specificity outside of mammals is not clear. Data from Scornaienchi et al (2010), Smith et al (2012), Chapter 3 and 4 suggest that they are not selective or specific to individual fish CYPs, limiting their usefulness to assess function in teleost species. Alternatively, it is possible to test individual substrates and monitor either parent compound loss or metabolite formation with time, for example, using liquid (LC-MS) and/or gas (GC-MS) chromatography – mass spectrometry (Cusinato et al 2019, Oh et al 2017). This method also serves as a direct method to study metabolism of potential substrates by CYP3 enzymes. However, standards for individual substrates or metabolites may not be available to perform robust LC-MS/GC-MS analysis and developing these assays for each compound is both time consuming and costly.

Mammalian CYP3A research has revealed that the active site is promiscuous, accommodating many structurally unrelated compounds (Ekroos & Sjogren 2006), thus it is likely that large data sets would be needed for a robust functional assessment of orphan CYP3 enzymes. In this thesis, we employed a high throughput screening (HTS) method that measured the consumption of NADPH as an indirect measure of substrate metabolism by CYP3C1 (Chapter 3) and CYP3A65 (Chapter 4). The advantage of this approach is that it can produce a large quantity of data in a short period of time, allows testing of any potential substrate, requires no knowledge of the metabolite formed, is useful to infer function, and can potentially establish structure – activity relationships. The challenge with our HTS approach is that it is an indirect measure of metabolism. NADPH consumption does not always result in substrate metabolism but can be the result of NADPH auto-oxidation or the formation of reactive oxygen species (ROS; as reviewed by Denisov 2005). Thus, this approach requires a series of follow-up screens and controls to verify the metabolism of the substrate, which may add time and cost to the screening. Nonetheless, this approach offered a great opportunity to identify substrates of CYP3A65 and CYP3C1 and is a great strategy to rapidly produce substrate data for a number of orphan CYP genes identified through genome sequencing.

REGULATORY CONTROL OF CYP3C ENZYMES IN ZEBRAFISH

In Chapter 2, we established CYP3C gene induction after exposure to βNF and E_2, which suggests that both the AhR and ER are involved in CYP3C gene regulation in a manner that is tissue, gene, and sex specific, and dependent on time of exposure. There were notable differences in CYP3C expression profiles between the liver, intestine and gonads (Chapter 2, Figure 1, 3, 4). Tissue specific induction of the CYP3C genes was likely the result of tissue distribution of the AhR and ER and of their dimerization partners, as well as the preference different subtypes have for different target genes. Zebrafish have three AhR (AhR1a (Andreasen et al 2002a), AhR1b (Karchner et al 2005) and AhR2 (Tanguay et al 1999)) and ARNT (ARNT2a, ARNT2b and ARNT2c) subtypes, each with various levels of activity and tissue distribution (Andreasen et al 2002a, Andreasen et al 2002b, Tanguay et al 2000). With the exception of liver, AhR1a is lowly expressed in many tissues and not inducible by typical AhR ligands (Andreasen et al 2002a). AhR1b is more widely expressed than AhR1a and binds TCDD with relatively high affinity (Andreasen et al 2002a). The AhR2 is highly inducible by TCDD and βNF and expressed in the adult zebrafish liver (Andreasen et al 2002b). Little data exists for the distribution of AhR2 in the adult intestine and gonads. Regulation of CYP1A, a hallmark gene in the AhR pathway, has previously been shown to be mediated through AhR2 in most tissues; AhR1b is thought to mediate CYP1A regulation in renal tubules and hematopoietic tissues (Karchner et al 2005). The interaction of AhR2 with ARNT2b is very important in regulating the CYP1 gene family, including CYP1A in zebrafish (Andreasen et al 2002b, Goodale et al 2012), thus the expression of AhR2 regulated genes would highly depend on the co-localization of both AhR2 and ARNT2b in each tissue.

Like the AhR, zebrafish have multiple ER subtypes: ERα, ERβ1, and ERβ2 (Menuet et al 2002). All ER subtypes are involved to some extent in regulating E_2 inducible genes such as CYP19 and vitellogenin (Griffin et al 2013, Menuet et al 2004, Menuet et al 2002). However, ERβ1 and ERβ2 are more highly expressed in the liver, intestines, and gonads of pre-ovulatory females than ERα, and in vitro luciferase assays demonstrated that E_2 activates ERα and ERβ2 more than ERβ1 (Griffin et al 2013, Menuet et al 2004, Menuet et al 2002). ERβ2 is more highly favoured for the induction of CYP19b in the brain and vitellogenin in the liver of larval zebrafish (Griffin et al 2013, Menuet et al 2004). Thus, ERβ2 is more likely involved in regulating E_2 responsive genes in liver, intestine, and gonads. Understanding which AhR and ER subtype is more likely to mediate CYP3C gene transcript regulation and the profile of regulatory co-factors in each tissue could be useful in understanding the differences seen in CYP3C expression profiles across the various tested tissues (Chapter 2, Figures 1, 3, 4).

Using pharmacological tools to manipulate gene expression and characterize regulation pathways can be very informative but challenging if there is no prior information on the system being tested. As reviewed by Honkakoski and Negishi (2000), there are several possible nuclear receptors that can be involved in regulating CYP genes, such as the AhR, ER, AR , PXR, constitutive androstane receptor (CAR), glucocorticoid receptor (GR), and Vitamin-D receptor. Existing data are required in order to identify a good receptor candidate for regulation studies, such as expression profiles and/or response element data. To pharmacologically test a receptor, a specific ligand is needed. Some ligands are problematic because they activate multiple receptors. For example, dexamethasone is both a good PXR (as reviewed by Goodwin et al 2002) and GR ligand (Frego & Davidson 2006). While selective and specific receptor ligands are well established for AhR and ER in fish, it is not always the case for other receptors, such as the PXR. Furthermore, for each potential ligand, dose-range experiments are required to establish an appropriate dosing regimen. This is key as it is possible that low doses can result in no effect and high doses may result in transcriptional inhibition. We suspect that this is the case with higher doses of E_2 where down regulation was observed at 10 μM (Chapter 2, Figure 3).

Beyond defining the appropriate dose, it is important to consider the exposure time for transcriptional gene induction. In Chapter 2, zebrafish adults were continuously exposed for 96 hours prior to sampling. Surprisingly, induction of CYP1A was apparent following βNF exposure in intestine, but not the liver (Chapter 2, Figure 1). These data prompted a second exposure to investigate the time-course of induction of CYP3C and CYP1A up to 96 hours (Chapter 2, Figure 2). In the time-course exposure, CYP3C and CYP1A were not consistently upregulated throughout the 96 hour of exposure (Chapter 2, Figure 2). CYP1A expression was abolished in the liver following 12 h (Chapter 2, Figure 2), thus sampling after 96 hours of exposure would lead to undetectable levels of CYP1A in the liver. The time-course of induction of CYP1A in the liver supported the dose response data in Chapter 2, Figure 1. Likewise, CYP3C1, CYP3C2 and CYP3C4 expression was no longer inducible past 12-48 hours of exposure to E_2 (Chapter 2, Figure 5), thus sampling following a 96 hour exposure may result in data that suggest that these genes are not regulated by βNF or E_2. Understanding the timing and the dosing component associated with gene induction is an important factor when using pharmacological tools to study regulation.

While pharmacological tools were an excellent way to characterize regulatory mechanisms involved in CYP3C regulation, morpholinos and CRISPR-Cas methods would be important next steps to confirm the involvement of the AhR and ER and clearly identify the receptor subtype. Morpholinos (MO), used with stringent controls and standards, are an excellent tool to study the effects receptor knockdown on gene regulation. Specifically, MOs are oligomers that are covalently bound to dendrimer moieties, allowing them to permeate cells, block translation or interfere with splicing of pre-mRNA to produce little or non-functional protein (Morcos et al 2008, Moulton & Jiang 2009). *Vivo* MOs can be used in adults as opposed to embryonic zebrafish; this would be necessary because some CYP3C genes are not constitutively expressed in embryonic stages (Shaya et al 2014). *Vivo* MOs have previously been utilized in adult fish and result in over 50% protein knockdown in several organs, including liver (Guo et al 2011, Kim et al 2010, Notch et al 2011). It is important to note that morpholinos provide only a transient knockdown, thus complete receptor knockout zebrafish would be a more accurate measure of AhR and ER involvement in regulation. To date, AhR2 (Garcia et al 2018, Goodale et al 2012) and all three ER subtype (Lu et al 2017) knockout zebrafish have been produced and used in toxicity studies. Comparing the gene expression and regulation in knockdown or knockout mutant with the wildtype would be effective for understanding the involvement of AhR and ER in regulation as each knockout or knockdown would target a specific receptor subtype, this would help clarify the exact receptor involved in gene regulation. We expect that that the mutants would have a lower basal expression of the CYP3C genes and no response to receptor ligand exposure.

Overall, the data presented in Chapter 2 suggest fish CYP3C genes are regulated differently than mammalian CYP3A and that multiple receptors are involved. In mammals, CYP3A is regulated by the PXR and CAR. To date, CAR has not been identified in fish (Hahn et al 2005) and is unlikely to be involved in regulating CYP3 genes in any fish species. However, there is some evidence to suggest that the PXR is involved in CYP3A65 and CYP3C1 regulation, as tested by the PXR ligand pregnenolone (Kubota et al 2015). Yet the data regarding the involvement of the PXR are not consistent and previous studies have found that embryonic zebrafish CYP3C1 expression was not inducible by other PXR ligands such as dexamethasone or rifampicin (Corley-Smith et al., 2006). Evidently, more studies are required in order to understand if fish CYP3 expression is regulated by PXR but this is difficult due to the differences in response to PXR ligands by different fish species, the potential that these compounds may not be specific ligands of PXR in fish, and the lack of a conserved PXR transcriptional response element in fish (Wassmur et al 2010).

Besides EREs and XREs, the promoter regions of CYP3C genes contain multiple androgen response elements, suggesting a possible role for androgen receptors (AR) in gene regulation (Shaya et al 2014). This is true for other CYPs involved in hormone synthesis and metabolism. CYP19 is involved in the biosynthesis of estrogens and generally regulated by E_2 (Callard et al 2001) but some evidence suggests CYP19 in the monkey brain is also regulated by androgens (as reviewed by Roselli & Resko 2001). CYP3A27 in juvenile rainbow trout was slightly induced with exposure to testosterone (Buhler et al 2000). Overall, differential expression of CYP3s between sexes has been seen in mammals (as reviewed by Waxman & Holloway 2009) and fish (Lee et al 1998, Shaya et al 2014), and suggests a sex specific role for CYP3s. Investigating the involvement of testosterone in regulation of CYP3Cs will better characterize the regulation of these enzymes and provide insight on the sex difference seen in the expression profile.

Future work can elucidate the involvement of other receptors in regulation of CYP3C genes; PXR and AR would be the most fruitful nuclear receptors to target for a role in CYP3C gene regulation. Use of non-pharmacological tools, such as CRISPR-Cas gene knockout lines or morpholino based gene knockdowns, may provide useful data to confirm regulatory roles of AhR and nuclear receptors in CYP3C expression, and the receptor subtypes responsible , particularly for nuclear receptors where proto-typical ligands have not been clearly defined (e.g. PXR).

CHARACTERIZING THE FUNCTION OF CYP3C1 AND CYP3A65

The metabolism of alkyloxy-resorufins (AROD; Murray et al 2001, Scornaienchi et al 2010b, Whyte et al 2000) and BFC (BFCOD; Burkina et al 2013, Hegelund et al 2004, Stresser et al 2000) is commonly used to indicate the expression of CYP1A and CYP3A, respectively. From the *in vitro* studies presented in Chapter 3 (CYP3C1) and 4 (CYP3A65), we have identified that CYP3A65 and CYP3C1 are able to metabolize the alkyloxy-resorufins and BFC. Together, these data indicate that in tissues, where there is co-expression of multiple CYP1s and/or CYP3s, AROD and BFCOD may not be specific to CYP1A and CYP3A activity in fish. However, predicting the *in vivo* capacity of CYP3A65 and CYP3C1 for a given substrate is highly dependent on a clear understanding of which CYPs are co-expressed in a given tissue, the basal protein expression of each enzyme, the exposure history of the animal (i.e. whether CYP induction is likely), and the induction/response of each CYP due to that exposure. For example, the zebrafish liver expresses CYP1A (Goldstone et al 2009), CYP3A65 (Tseng et al 2005) and CYP3C1 (Shaya et al 2014). Basal expression of CYP1A is sex dependent, and in males, it is generally very low compared to CYP3A65 (Kubota et al 2019a); previous studies have shown that uninduced animals have a basal level of AROD (Whyte et al 2000), which may be mediated by a combination of CYP3C1, CYP3A65 and CYP1A enzymes. However, exposure to AhR ligand induces CYP1A transcript by 35-folds (Jönsson et al 2007) and AROD activity by approximately 8-folds (Ortiz-Delgado et al 2008), suggesting that the contributions from CYP1A are likely more important than CYP3A65 and CYP3C1 in an animal exposed to AhR ligands. Likewise, even though CYP1A and CYP3C have an *in vitro* capacity to metabolize BFC (BFCOD; Chapter 3, Figure; Chapter 4, Figure), the high basal expression of CYP3A65 relative to the other genes suggests that it would contribute more to BFC metabolism than CYP1A in an uninduced liver. In a scenario where the liver has been exposed to an AhR ligand, all three enzymes will be upregulated, but because CYP1A (Scornaienchi et al 2010b) has the highest capacity for BFC metabolism *in vitro* compared to CYP3C1 (Chapter 3) and CYP3A65 (Chapter 4), and it is highly inducible by AhR (Goldstone et al 2009, Jönsson et al 2007, Ortiz-Delgado et al 2008), it may become the main CYP responsible for BFCOD activity. This hypothesis would have to be further investigated. As illustrated, interpreting the *in vivo* capacity of CYP3A65, CYP3C1 and CYP1A is difficult due to the overlap of the fluorogenic substrate profile of these fish genes *in vitro*. Unlike in mammals, Chapter 3 and 4 clearly demonstrates that the alkyloxy-resorufins and BFC are not specific to CYP1A and CYP3A enzymes in fish *in vitro*, and that *in vivo* interpretations are challenging and must consider CYP co-expression, basal expression and animal exposure history. The high throughput screen (HTS) employed in this thesis allows for the possibility to identify new selective substrates or probes to distinguish CYP isoforms *in vivo*. Producing catalytic data for all the orphan CYP3 enzymes in a given tissue would facilitate this. A query of the top hits would help identify substrates which overlap and substrates that are unique. Unique substrate may be developed as new probes or tools to distinguish CYP isoforms *in vivo*.

The HTS assay was developed based on indirectly measuring catalytic activity by monitoring NADPH depletion with follow-up to identify false positives. The follow up data largely supports that this was a successful approach; approximately 200 hits were identified in the initial screen and the follow up screens indicated only 2-5 were likely false positives. The HTS hits appear to well predict substrates. A proportion of the top hits that passed the initial follow up were further assessed to identify enzyme and substrate affinity by calculating K_M and IC_{50} values. IC_{50} calculations were only possible if the identified hit was capable of inhibiting the activity between CYP3C1 and BFC. We were successful in calculating IC50 values for 10-15 CYP3C1 (Chapter 3, Table 3) and CYP3A65 (Chapter 4, Table 3) substrates for the 32-48 that we tested, and most had low μM values, supporting the top hits as good substrates for the enzyme. Knowing the involvement of AhR in regulation, we identified BaP as a potential CYP3C1 substrate, and previous work had already established BaP as a CYP3A65 substrate (Scornaienchi 2009). Indeed, both the CYP3C1 (Chapter 3, Table 2) and CYP3A65 (Chapter 4, Table 2) HTS identified BaP as a hit, as had been predicted, indicating the effectiveness of HTS because the approach identified known substrates.

A technical error clearly demonstrated that screening at one concentration is a significant trade off and that caution is needed in interpreting compounds that are negative in the initial screen. A technical error resulted in the screening of some of the compounds at double the concentration in one of the two replicates (As described in Chapter 3 and 4, Materials and Methods). Some of the compounds screened at 20 and 40 μM had activity that was below and above the cut-off for follow up, respectively. In some cases, screening at the higher concentration led to the inhibition of activity. Screening at one substrate concentration is necessary but the concentration will not be optimal for all compounds and clearly leads to false negatives. For example, we had hypothesized that E_2 would be identified as a hit in the HTS of CYP3C1 and CYP3A65 because the estrogen receptor was involved in CYP3C1 regulation (Chapter 2) and previous work documented the metabolism of E_2 by CYP3A65 (Scornaienchi et al 2010a). Yet, neither HTS identified E_2 as a substrate for CYP3A65 or CYP3C1 with 20 μM E_2. CYP3A65 metabolized 50 μM E_2 at a rate of 25.6±5.3 pmol nmol P450^{-1} min^{-1} (Scornaienchi et al 2010a), suggesting that screening with non-optimal conditions may lead to false negatives if the concentration selected is sub-optimal. However, this is a necessary trade off with the HTS approach because it would be time consuming, utilize a very large amount of protein, and would be very costly to screen at multiple concentrations.

Some considerations are necessary when using NADPH consumption as a measure of CYP activity. NADPH is generally unstable and can autoxidize in light (Wu et al 1986), thus measuring NADPH consumption in the absence of enzyme was necessary to ensure that reactions were enzyme dependent. Secondly, many CYP enzymes are likely to undergo uncoupled reactions that result in the consumption of NADPH and the formation of reactive oxygen species (ROS; as reviewed by Denisov et al 2005). CYP enzymes with a flexible or promiscuous active site are more likely to undergo uncoupled reactions relative to enzymes that metabolize structurally similar compounds (as reviewed by Denisov et al 2005). The ROS production, as an indication of uncoupling, was measured for the top 132 and 139 hits for CYP3C1 and CYP3A65, respectively. Unsurprisingly, there was a background level of ROS in all our reactions, however the data suggest that the hits from the HTS did not undergo a high level of uncoupling for either CYP3C1 (Chapter 3, Table 2) or CYP3A65 (Chapter 4, Table 2). The reactions produced little ROS relative to what has previously been reported for fish CYP1A (Harskamp et al 2012, Schlezinger et al 2000). Whether this indicates that CYP3A65 and CYP3C1 are less prone to uncoupling overall, compared to CYP1A, is not yet clear but the HTS data clearly suggests this. Including a measure of ROS helped identify false positives from the HTS, but it also gave an understanding of the level of uncoupling between the enzyme and substrates in general.

Many of the identified hits of CYP3A65 (Chapter 4, Table 2) and CYP3C1 (Chapter 3, Table 2) contained a quinone moiety, several of which were further classified as 1,4 naphthoquinones. Though not as prominent, we also identified quinolines amongst the top substrates for CYP3C1 and CYP365. This data is contrary to what has previously been described for mammalian CYP3A4, which is well known to metabolize many structurally unrelated compounds (Ekroos & Sjogren 2006). Future directions should focus on understanding whether quinones and quinoline compounds are substrates of

CYP3A65 and CYP3C1 enzymes in general and whether there is a structure –activity relationship for compounds. The HTS assay in this thesis identified 3700-3800 compounds that were not hits of the CYP3A65 and CYP3C1 in zebrafish. Pending the confirmation of quinones as true CYP3A65 and CYP3C1 substrates, the next steps could include a query of the substrate list to identify whether there were quinones that were not hits. This could provide preliminary data to better elucidate whether a structure – activity relationship exists for CYP3A65 and CYP3C1 substrate. Future work could include *in silico* molecular docking approaches to robustly assess the potential bias for 1,4 naphthoquinones as substrates. Molecular docking analyses have been done for various CYP enzymes and their ligands in humans (Lewis et al 1996, Lill et al 2006, Mannu et al 2011) and fish (Leaver & George 2000, Prasad et al 2007). For example, modelling will allow for a computational assessment of the interaction between the substrates with a putative three-dimensional structure of the enzyme (as reviewed by Stegeman et al 2010). The binding mode of the non-quinone structures can be compared to those of the quinones to identify a structural explanation for the preference CYP3 enzymes may have for quinones. This approach has been employed previously to understand why fish CYP1A metabolizes the compound 3,3',4',4' tetrachlorobiphenyl more slowly than mammalian CYP1A1 (as reviewed by Stegeman et al 2010). Overall all this approach will be useful in identifying the binding modes of the CYP3C1 (Chapter 3) and CYP3A65 (Chapter 4) substrates we established in this thesis, possibly providing a framework for predicting some CYP3A65 and CYP3C1 substrates from their structure.

The hits identified from the HTS are strongly related to the library choice. For experiments in Chapter 3 and 4, the following libraries were selected because they contained ~4000 small biologically and pharmacologically active molecules: Prestwick, Microsource Spectrum, Library of Pharmacologically Active Compounds (LOPAC) and BioMol Natural Products Library. More specifically, the LOPAC library was solely composed of drug-like molecules involved in cell signalling and neuroscience; 60% of the compounds in Microsource were drugs with known pharmacological action; Prestwick was solely composed of 100% FDA approved drugs and BioMol contained natural products and steroids. These libraries provided a large and diverse list of xenobiotics and endogenous compounds to develop a substrate profile for fish CYP3 subfamilies. A non-exhaustive curation of the libraries revealed they contained at least ~400 known mammalian CYP3A4 pharmaceuticals for the screen providing plenty of data to identify unique and common substrates to contrast mammalian and fish CYP3 enzymes substrate profiles. Given the libraries selected, it was not surprising that many of the top hits were pharmaceuticals and natural plant products. Future studies can include screening CYP3A enzymes against other libraries. To better define whether regulation is related to function, it would be interesting to screen CYP3C1 with compound libraries that contained AhR and ER ligands. This information would allow us to better define the relationship between regulation and function. To investigate the structure-relationship activity, it would be also be beneficial to screen a library of quinone compounds for metabolism by CYP3C and CYP3A65.

EVOLUTION OF CYTOCHROME P450 FAMILY 3

Prior to fish genome sequencing, fish CYP3A was phylogenetically clustered with mammalian CYP3A genes and classified as a member of the CYP3A subfamily, making it appear to be a mammalian CYP3A homolog (Goldstone et al 2010). This instigated the assumption that fish CYP3A is functionally like mammalian CYP3A4 (McGrath & Li 2008, van Wijk et al 2016). As more fish genomes were sequenced, unique CYP3 subfamilies were established in the teleost lineage (e.g. CYP3B, CYP3C and CYP3D). Recent phylogenetic analyses show fish CYP3 genes cluster together, away from vertebrate CYP3A; interestingly the teleost CYP3A genes were placed in two clades, separated by the CYP3D genes (Yan & Cai 2010). Thus, the CYP3A genes in fish have incorrect nomenclature, are not orthologs of mammalian CYP3A, and are not monophyletic. Our current understanding of CYP3 evolution suggests that teleost CYP3A and CYP3D genes are more closely related while the CYP3B and CYP3C genes form a second clade (Yan & Cai 2010). While all fish have one or more CYP3A genes, CYP3B, CYP3C, and CYP3D have been identified in some (but not all) fish genomes. Seven CYP3B genes have been identified: CYP3B1 and CYP3B2 were identified in the green spotted and the Japanese pufferfish (*T. nigroviridis; F. rubripes*, respectively*)*, CYP3B3-CYP3B6 in medake (*O. latipes*), and CYP3B7 in stickleback (*G. aculeatus*; Yan & Cai 2010). There were 5 CYP3C genes identified: CYP3C1, CYP3C2, CYP3C3 and CYP3C4 were found in the zebrafish genome and CYP3C5 was identified in channel catfish (*I. punctatus*; (Zhang et al 2014). CYP3D genes appear in sablefish (*A. fimbri*), gilt-head sea bream (*S.aurata*), Atlantic Halibut (*H. hippoglossus*), stickleback, largemouth bass (*M.*

salmoides), green spotted and Japanese pufferfish (Yan & Cai 2010). Functionally, it is more likely that teleost CYP3 subfamilies are more similar than they are with mammalian CYP3As. Our functional date supports this perspective; of the 400 compounds that we had identified as human CYP3A4 substrates in the compound library, only 6% of those were top hits for zebrafish CYP3A65, indicating a functional divergence between mammalian and fish CYP3A genes. Conversely, approximately 80% of the CYP3A65 substrates were also CYP3C1 substrates, suggesting a stronger functional similarity across teleost fish CYP3 subfamilies. Expression patterns of fish CYP3 enzymes are distinct, with CYP3A65 highly expressed in intestine and liver (Tseng et al 2005) and CYP3C1 more ubiquitously expressed in tissues (Shaya et al 2014). Thus, these enzymes may have a large overlap in function but contribute to metabolism in different organs. This may true for the other CYP3C genes, given their unique expression profiles that does not always overlap with CYP3C1 and CYP3A65 expression (Shaya et al 2014). The high sequence identity across CYP3C genes (>75%) is a strong indication that CYP3C enzymes share a similar function (Shaya et al 2014). However, given the limitations of assuming function from sequence similarity alone, it is important to experimentally test the function of CYP3C2, CYP3C3 and CYP3C4 to understand their capacity for exogenous compound metabolism.

It is not clear if the data gathered from CYP3A65 well represents the function of other CYP3A enzymes in various fish species or whether the function of CYP3A65 is more similar to CYP3D function than CYP3B and CYP3C. Medaka and stickleback offer the opportunity to study at least three of the four identified CYP3 subfamilies. Medaka contain three CYP3A, four CYP3B genes and one CYP3D gene (Yan & Cai 2010). The medaka is a small, easy to culture fish that is quickly emerging as model fish species and an alternative to mammalian models (Kelly et al 1998, Lin et al 2016). Stickleback offer an interesting perspective on CYP3A evolution; the species contains 3 CYP3A genes that appear in the CYP3A clade closest to CYP3D clade, and 1 CYP3A that appears in the second CYP3A clade, clustered further from CYP3D (Yan & Cai 2010). Understanding the functional difference between these CYP3A genes can provide insight on the difference between the two CYP3A clades. Like medaka, stickleback contains a CYP3D gene and CYP3B7, which would allow for a comparison between CYP3A, CYP3D and CYP3B genes in the same species (Yan & Cai, 2010). Compiling more information on various CYP3 enzymes in fish species will provide a more holistic understanding of the teleost CYP3 family evolution and the biological functions of these enzymes.

REFERENCES

Albert B, Johnson A, Lewis J, Martin R, Keith R, Walter P. 2002. Studying Gene Expression and Function In *Molecular Biology of the Cell*. New York: Garland Science

Andreasen EA, Hahn ME, Heideman W, Peterson RE, Tanguay RL. 2002a. The zebrafish (*Danio rerio*) aryl hydrocarbon receptor type 1 is a novel vertebrate receptor. *Molecular Pharmacology* 62: 234-49

Andreasen EA, Spitsbergen JM, Tanguay RL, Stegeman JJ, Heideman W, Peterson RE. 2002b. Tissue-specific expression of AHR2, ARNT2, and CYP1A in zebrafish embryos and larvae: effects of developmental stage and 2, 3, 7, 8-tetrachlorodibenzo-p-dioxin exposure. *Toxicological Sciences* 68: 403-19

Buhler DR, Miranda CL, Henderson MC, Yang Y-H, Lee S-J, Wang-Buhler J-L. 2000. Effects of 17β-estradiol and testosterone on hepatic mRNA/protein levels and catalytic activities of CYP2M1, CYP2K1, and CYP3A27 in rainbow trout (*Oncorhynchus mykiss*). *Toxicology and Applied Pharmacology* 168: 91-101

Burkina V, Zlabek V, Zamaratskaia G. 2013. Clotrimazole, but not dexamethasone, is a potent in vitro inhibitor of cytochrome P450 isoforms CYP1A and CYP3A in rainbow trout. *Chemosphere* 92: 1099-104

Cali JJ, Ma D, Sobol M, Simpson DJ, Frackman S, et al. 2006. Luminogenic cytochrome P450 assays. *Expert opinion on Drug Metabolism and Toxicology* 2: 629-45

Cali JJ, Ma D, Wood MG, Meisenheimer PL, Klaubert DH. 2012. Bioluminescent assays for ADME evaluation: dialing in CYP selectivity with luminogenic substrates. *Expert Opinion on Drug Metabolism and Toxicology* 8: 1115-30

Callard GV, Tchoudakova AV, Kishida M, Wood E. 2001. Differential tissue distribution, developmental programming, estrogen regulation and promoter characteristics of cyp19 genes in teleost fish. *The Journal of Steroid Biochemistry and Molecular Biology* 79: 305-14

Corley-Smith GE, Su HT, Wang-Buhler JL, Tseng HP, Hu CH, et al. 2006. CYP3C1, the first member of a new cytochrome P450 subfamily found in zebrafish (*Danio rerio*). *Biochemical and Biophysical Research Communications* 340: 1039-46

Cresteil T, Monsarrat B, Alvinerie P, Treluyer JM, Vieira I, Wright M. 1994. Taxol metabolism by human liver microsomes: identification of cytochrome P450 isozymes involved in its biotransformation. *Cancer Research* 54: 386-92

Cusinato DAC, Filgueira GCO, Rocha A, Cintra M, Lanchote VL, Coelho EB. 2019. LC-MS/MS analysis of the plasma concentrations of a cocktail of 5 cytochrome P450 and P-glycoprotein probe substrates and their metabolites using subtherapeutic doses. *Journal of Pharmaceutical and Biomedical Analysis* 164: 430-41

Denison MS, Nagy SR. 2003. Activation of the aryl hydrocarbon receptor by structurally diverse exogenous and endogenous chemicals. *Annual Review of Pharmacology and Toxicology* 43: 309-34

Denisov IG, Makris TM, Sligar SG, Schlichting I. 2005. Structure and Chemistry of Cytochrome P450. *Chemical Reviews* 105: 2253-78

Denissen JF, Grabowski BA, Johnson MK, Buko AM, Kempf DJ, et al. 1997. Metabolism and disposition of the HIV-1 protease inhibitor ritonavir (ABT-538) in rats, dogs, and humans. *Drug Metabolism and Disposition* 25: 489-89

Dussault I, Yoo H-D, Lin M, Wang E, Fan M, et al. 2003. Identification of an endogenous ligand that activates pregnane X receptor-mediated sterol clearance. *Proceedings of the National Academy of Sciences* 100: 833-38

Ekroos M, Sjogren T. 2006. Structural basis for ligand promiscuity in cytochrome P450 3A4. *Proceedings of the National Academy of Sciences of the United States of America* 103: 13682-7

Frego L, Davidson W. 2006. Conformational changes of the glucocorticoid receptor ligand binding domain induced by ligand and cofactor binding, and the location of cofactor binding sites determined by hydrogen/deuterium exchange mass spectrometry. *Protein Science* 15: 722-30

Garcia GR, Bugel SM, Truong L, Spagnoli S, Tanguay RL. 2018. AHR2 required for normal behavioral responses and proper development of the skeletal and reproductive systems in zebrafish. *PLoS One* 13: e0193484

Gautier JC, Lecoeur S, Cosme J, Perret A, Urban P, et al. 1996. Contribution of human cytochrome P450 to benzo[a]pyrene and benzo[a]pyrene-7,8-

dihydrodiol metabolism, as predicted from heterologous expression in yeast. *Pharmacogenetics* 6: 489-99

Goldstone JV, Jönsson ME, Behrendt L, Woodin BR, Jenny MJ, et al. 2009. Cytochrome P450 1D1: a novel CYP1A-related gene that is not transcriptionally activated by PCB126 or TCDD. *Archives of Biochemistry and Biophysics* 482: 7-16

Goldstone JV, McArthur AG, Kubota A, Zanette J, Parente T, et al. 2010. Identification and developmental expression of the full complement of Cytochrome P450 genes in Zebrafish. *BMC Genomics* 11: 643

Goodale BC, La Du JK, Bisson WH, Janszen DB, Waters KM, Tanguay RL. 2012. AHR2 Mutant Reveals Functional Diversity of Aryl Hydrocarbon Receptors in Zebrafish. *PLos One* 7: e29346

Goodwin B, Redinbo MR, Kliewer SA. 2002. Regulation of CYP3A Gene Transcription by the Pregnane X Receptor. *Annual Review of Pharmacology and Toxicology* 42: 1-23

Griffin LB, January KE, Ho KW, Cotter KA, Callard GV. 2013. Morpholino-mediated knockdown of ERα, ERβa, and ERβb mRNAs in zebrafish (*Danio rerio*) embryos reveals differential regulation of estrogen-inducible genes. *Endocrinology* 154: 4158-69

Gruber CJ, Gruber DM, Gruber IM, Wieser F, Huber JC. 2004. Anatomy of the estrogen response element. *Trends in Endocrinology and Metabolism:* 15: 73-8

Guengerich FP. 2008. Cytochrome p450 and chemical toxicology. *Chemical Research in Toxicology* 21: 70-83

Guengerich FP, Cheng Q. 2011. Orphans in the human cytochrome P450 superfamily: approaches to discovering functions and relevance in pharmacology. *Pharmacological Reviews* 63: 684-99

Guengerich FP, Wu Z-L, Bartleson CJ. 2005. Function of human cytochrome P450s: Characterization of the orphans. *Biochemical and Biophysical Research Communications* 338: 465-69

Guo Y, Ma L, Cristofanilli M, Hart RP, Hao A, Schachner M. 2011. Transcription factor Sox11b is involved in spinal cord regeneration in adult zebrafish. *Neuroscience* 172: 329-41

Hahn ME. 2002. Aryl hydrocarbon receptors: diversity and evolution. *Chemico-Biological Interactions* 141: 131-60

Harskamp J, Britz-McKibbin P, Wilson JY. 2012. Functional Screening of Cytochrome P450 Activity and Uncoupling by Capillary Electrophoresis. *Analytical Chemistry* 84: 862-66

Hegelund T, Ottosson K, Rådinger M, Tomberg P, Celander MC. 2004. Effects of the antifungal imidazole ketoconazole on CYP1A and CYP3A in rainbow trout and killifish. *Environmental Toxicology and Chemistry: An International Journal* 23: 1326-34

Honkakoski P, Negishi M. 2000. Regulation of cytochrome P450 (CYP) genes by nuclear receptors. *Biochemical Journal* 347: 321-37

Ilc T, Halter D, Miesch L, Lauvoisard F, Kriegshauser L, et al. 2017. A grapevine cytochrome P450 generates the precursor of wine lactone, a key odorant in wine. *New Phytologist* 213: 264-74

Jönsson ME, Orrego R, Woodin BR, Goldstone JV, Stegeman JJ. 2007. Basal and 3, 3′, 4, 4′, 5-pentachlorobiphenyl-induced expression of cytochrome P450 1A, 1B and 1C genes in zebrafish. *Toxicology and Applied Pharmacology* 221: 29-41

Karchner SI, Franks DG, Hahn ME. 2005. AHR1B, a new functional aryl hydrocarbon receptor in zebrafish: tandem arrangement of ahr1b and ahr2 genes. *Biochemical Journal* 392: 153-61

Kelly KA, Havrilla CM, Brady TC, Abramo KH, Levin ED. 1998. Oxidative stress in toxicology: established mammalian and emerging piscine model systems. *Environmental Health Perspectives* 106: 375-84

Kim D, Guengerich FP. 2005. Cytochrome P450 activation of arylamines and heterocyclic amines. *Annual Review of Pharmacology and Toxicology* 45: 27-49

Kim S, Radhakrishnan UP, Rajpurohit SK, Kulkarni V, Jagadeeswaran P. 2010. Vivo-Morpholino knockdown of alphaIIb: A novel approach to inhibit thrombocyte function in adult zebrafish. *Blood cells, Molecules and Diseases* 44: 169-74

Kubota A, Goldstone JV, Lemaire B, Takata M, Woodin BR, Stegeman JJ. 2015. Role of pregnane X receptor and aryl hydrocarbon receptor in transcriptional regulation of pxr, CYP2, and CYP3 genes in developing zebrafish. *Toxicological Sciences:* 143: 398-407

Kubota A, Kawai YK, Yamashita N, Lee JS, Kondoh D, et al. 2019b. Transcriptional profiling of cytochrome P450 genes in the liver of adult zebrafish, *Danio rerio*. *The Journal of Toxicological Sciences* 44: 347-56

Kumar GN, Rodrigues AD, Buko AM, Denissen JF. 1996. Cytochrome P450-mediated metabolism of the HIV-1 protease inhibitor ritonavir (ABT-538) in human liver microsomes. *The Journal of Pharmacology and Experimental Therapeutics* 277: 423-31

Lamb DC, Follmer AH, Goldstone JV, Nelson DR, Warrilow AG, et al. 2019. On the occurrence of cytochrome P450 in viruses. *Proceedings of the National Academy of Sciences of the United States of America* 116: 12343-52

Leaver MJ, George SG. 2000. A cytochrome P4501B gene from a fish, Pleuronectes platessa. *Gene* 256: 83-91

Lee S-J, Wang-Buhler J-L, Cok I, Yu T-S, Yang Y-H, et al. 1998. Cloning, sequencing, and tissue expression of CYP3A27, a new member of the CYP3A subfamily from embryonic and adult rainbow trout livers. *Archives of biochemistry and biophysics* 360: 53-61

Lewis DFV, Eddershaw PJ, Goldfarb PS, Tarbit MH. 1996. Molecular modelling of CYP3A4 from an alignment with CYP102: Identification of key interactions between putative active site residues and CYP3A-specific chemicals. *Xenobiotica* 26: 1067-86

Lill MA, Dobler M, Vedani A. 2006. Prediction of Small-Molecule Binding to Cytochrome P450 3A4: Flexible Docking Combined with Multidimensional QSAR. *ChemMedChem* 1: 73-81

Lin C-Y, Chiang C-Y, Tsai H-J. 2016. Zebrafish and Medaka: new model organisms for modern biomedical research. *Journal of Biomedical Science* 23: 19-19

Lu H, Cui Y, Jiang L, Ge W. 2017. Functional Analysis of Nuclear Estrogen Receptors in Zebrafish Reproduction by Genome Editing Approach. *Endocrinology* 158: 2292-308

Maïbèche-Coisne M, Jacquin-Joly E, François MC, Nagnan-Le Meillour P. 2002. cDNA cloning of biotransformation enzymes belonging to the cytochrome

P450 family in the antennae of the noctuid moth Mamestra brassicae. *Insect Molecular Biology* 11: 273-81

Mannu J, Jenardhanan P, Mathur PP. 2011. A computational study of CYP3A4 mediated drug interaction profiles for anti-HIV drugs. *Journal of Molecular Modeling* 17: 1847-54

McArthur AG, Hegelund T, Cox RL, Stegeman JJ, Liljenberg M, et al. 2003. Phylogenetic analysis of the cytochrome P450 3 (CYP3) gene family. *Journal of Molecular Evolution* 57: 200-11

McGrath P, Li CQ. 2008. Zebrafish: a predictive model for assessing drug-induced toxicity. *Drug Discovery Today* 13: 394-401

Menuet A, Le Page Y, Torres O, Kern L, Kah O, Pakdel F. 2004. Analysis of the estrogen regulation of the zebrafish estrogen receptor (ER) reveals distinct effects of ERalpha, ERbeta1 and ERbeta2. *Journal of Molecular Endocrinology* 32: 975-86

Menuet A, Pellegrini E, Anglade I, Blaise O, Laudet V, et al. 2002. Molecular characterization of three estrogen receptor forms in zebrafish: binding characteristics, transactivation properties, and tissue distributions. *Biology of Reproduction* 66: 1881-92

Mescher M, Haarmann-Stemmann T. 2018. Modulation of CYP1A1 metabolism: From adverse health effects to chemoprevention and therapeutic options. *Pharmacology and Therapeutics* 187: 71-87

Morcos PA, Li Y, Jiang S. 2008. Vivo-Morpholinos: a non-peptide transporter delivers Morpholinos into a wide array of mouse tissues. *BioTechniques* 45: 613-4, 16, 18 passim

Moulton JD, Jiang S. 2009. Gene knockdowns in adult animals: PPMOs and vivo-morpholinos. *Molecules (Basel, Switzerland)* 14: 1304-23

Murray GI, Melvin WT, Greenlee WF, Burke MD. 2001. Regulation, function, and tissue-specific expression of cytochrome P450 CYP1B1. *Annual Review of Pharmacology and Toxicology* 41: 297-316

Nelson DR, Nebert DW. 2018. Cytochrome P450 (*CYP*) Gene Superfamily In *eLS*, pp. 1-19: John Wiley & Sons, Ltd (Ed). doi:10.1002/9780470015902.a0005667.pub3

Notch EG, Shaw JR, Coutermarsh BA, Dzioba M, Stanton BA. 2011. Morpholino gene knockdown in adult Fundulus heteroclitus: role of SGK1 in seawater acclimation. *PLoS One* 6: e29462

Oh H-A, Lee H, Kim D, Jung BH. 2017. Development of GC-MS based cytochrome P450 assay for the investigation of multi-herb interaction. *Analytical Biochemistry* 519: 71-83

Ortiz-Delgado JB, Behrens A, Segner H, Sarasquete C. 2008. Tissue-specific induction of EROD activity and CYP1A protein in Sparus aurata exposed to B(a)P and TCDD. *Ecotoxicology and Environmental Safety* 69: 80-88

Prasad JC, Goldstone JV, Camacho CJ, Vajda S, Stegeman JJ. 2007. Ensemble modeling of substrate binding to cytochromes P450: analysis of catalytic differences between CYP1A orthologs. *Biochemistry* 46: 2640-54

Roselli CE, Resko JA. 2001. Cytochrome P450 aromatase (CYP19) in the non-human primate brain: distribution, regulation, and functional significance. *The Journal of Steroid Biochemistry and Molecular Biology* 79: 247-53

Schlezinger JJ, Keller J, Verbrugge LA, Stegeman JJ. 2000. 3,3',4,4'-Tetrachlorobiphenyl oxidation in fish, bird and reptile species: relationship to cytochrome P450 1A inactivation and reactive oxygen production. *Comparative Biochemistry and Physiology. Toxicology and Pharmacology : CBP* 125: 273-86

Scornaienchi ML. 2009. *Functional Characterization of Zebrafish Cytochrome P450 1 and 3A Genes Using Heterologously Expressed Proteins*. McMaster University Hamilton, Ontario

Scornaienchi ML, Thornton C, Willett KL, Wilson JY. 2010a. Cytochrome P450-mediated 17beta-estradiol metabolism in zebrafish (*Danio rerio*). *The Journal of Endocrinology* 206: 317-25

Scornaienchi ML, Thornton C, Willett KL, Wilson JY. 2010b. Functional differences in the cytochrome P450 1 family enzymes from zebrafish (*Danio rerio*) using heterologously expressed proteins. *Archives of Biochemistry and Biophysics* 502: 17-22

Shaya L, Dejong C, Wilson JY. 2014. Expression patterns of cytochrome P450 3B and 3C genes in model fish species. *Comparative Biochemistry and Physiology. Toxicology and Pharmacology : CBP* 166: 115-25

Shaya L, Jones DE, Wilson JY. 2019. CYP3C gene regulation by the aryl hydrocarbon and estrogen receptors in zebrafish. *Toxicology and Applied Pharmacology* 362: 77-85

Shimada T, Fujii-Kuriyama Y. 2004. Metabolic activation of polycyclic aromatic hydrocarbons to carcinogens by cytochromes P450 1A1 and 1B1. *Cancer Science* 95: 1-6

Smith EM, Iftikar FI, Higgins S, Irshad A, Jandoc R, et al. 2012. In vitro inhibition of cytochrome P450-mediated reactions by gemfibrozil, erythromycin, ciprofloxacin and fluoxetine in fish liver microsomes. *Aquatic Toxicology (Amsterdam, Netherlands)* 109: 259-66

Stegeman JJ, Goldstone JV, Hahn ME. 2010. Perspectives on zebrafish as a model in environmental toxicology In *Fish Physiology*, pp. 367-439: Elsevier

Stresser DM, Blanchard AP, Turner SD, Erve JCL, Dandeneau AA, et al. 2000. Substrate-Dependent Modulation of CYP3A4 Catalytic Activity: Analysis of 27 Test Compounds with Four Fluorometric Substrates. *Drug Metabolism and Disposition* 28: 1440-48

Stresser DM, Turner SD, Blanchard AP, Miller VP, Crespi CL. 2002. Cytochrome P450 fluorometric substrates: identification of isoform-selective probes for rat CYP2D2 and human CYP3A4. *Drug Metabolism and Disposition: the Biological Fate of Chemicals* 30: 845-52

Tanguay RL, Abnet CC, Heideman W, Peterson RE. 1999. Cloning and characterization of the zebrafish (*Danio rerio*) aryl hydrocarbon receptor. *Biochimica et Biophysica Acta (BBA)-Gene Structure and Expression* 1444: 35-48

Tanguay RL, Andreasen E, Heideman W, Peterson RE. 2000. Identification and expression of alternatively spliced aryl hydrocarbon nuclear translocator 2 (ARNT2) cDNAs from zebrafish with distinct functions. *Biochimica et Biophysica Acta* 1494: 117-28

Tomlinson ES, Maggs JL, Park BK, Back DJ. 1997. Dexamethasone metabolism in vitro: species differences. *The Journal of Steroid Biochemistry and Molecular Biology* 62: 345-52

Tseng HP, Hseu TH, Buhler DR, Wang WD, Hu CH. 2005. Constitutive and xenobiotics-induced expression of a novel CYP3A gene from zebrafish larva. *Toxicology and Applied Pharmacology* 205: 247-58

Tsuchiya Y, Nakajima M, Kyo S, Kanaya T, Inoue M, Yokoi T. 2004. Human CYP1B1 is regulated by estradiol via estrogen receptor. *Cancer Research* 64: 3119-25

Tsuchiya Y, Nakajima M, Yokoi T. 2005. Cytochrome P450-mediated metabolism of estrogens and its regulation in human. *Cancer Letters* 227: 115-24

Van Wijk RC, Krekels EHJ, Hankemeier T, Spaink HP, van der Graaf PH. 2016. Systems pharmacology of hepatic metabolism in zebrafish larvae. *Drug Discovery Today: Disease Models* 22: 27-34

Verbueken E, Bars C, Ball JS, Periz-Stanacev J, Marei WFA, et al. 2018. From mRNA Expression of Drug Disposition Genes to In Vivo Assessment of CYP-Mediated Biotransformation during Zebrafish Embryonic and Larval Development. *International Journal of Molecular Sciences* 19: E3979

Wassmur B, Grans J, Kling P, Celander MC. 2010. Interactions of pharmaceuticals and other xenobiotics on hepatic pregnane X receptor and cytochrome P450 3A signaling pathway in rainbow trout (Oncorhynchus mykiss). *Aquatic Toxicology* 100: 91-100

Waxman DJ, Holloway MG. 2009. Sex differences in the expression of hepatic drug metabolizing enzymes. *Molecular Pharmacology* 76: 215-28

Whyte JJ, Jung RE, Schmitt CJ, Tillitt DE. 2000. Ethoxyresorufin-O-deethylase (EROD) activity in fish as a biomarker of chemical exposure. *Critical Reviews in Toxicology* 30: 347-570

Wojtasek H, Leal WS. 1999. Degradation of an alkaloid pheromone from the pale-brown chafer, Phyllopertha diversa (*Coleoptera: Scarabaeidae*), by an insect olfactory cytochrome P450. *FEBS Letters* 458: 333-36

Wu JT, Wu LH, Knight JA. 1986. Stability of NADPH: effect of various factors on the kinetics of degradation. *Clinical Chemistry* 32: 314-9

Xu J, Wang X-y, Guo W-z. 2015. The cytochrome P450 superfamily: Key players in plant development and defense. *Journal of Integrative Agriculture* 14: 1673-86

Yan J, Cai Z. 2010. Molecular evolution and functional divergence of the cytochrome P450 3 (CYP3) Family in Actinopterygii (ray-finned fish). *PLoS One* 5: e14276

Zanger UM, Schwab M. 2013. Cytochrome P450 enzymes in drug metabolism: regulation of gene expression, enzyme activities, and impact of genetic variation. *Pharmacology and Therapeautics* 138: 103-41

Zeruth G, Pollenz RS. 2007. Functional analysis of cis-regulatory regions within the dioxin-inducible CYP1A promoter/enhancer region from zebrafish (*Danio rerio*). *Chemico-Biological Interactions* 170: 100-13

Zhang J, Yao J, Wang R, Zhang Y, Liu S, et al. 2014. The cytochrome P450 genes of channel catfish: their involvement in disease defense responses as revealed by meta-analysis of RNA-Seq datasets. *Biochimica et Biophysica acta* 1840: 2813-28

Zhang W, Lu H, Jiang H, Li M, Zhang S, et al. 2012. Isolation and characterization of cyp19a1a and cyp19a1b promoters in the protogynous hermaphrodite orange-spotted grouper (*Epinephelus coioides*). *General and Comparative Endocrinology* 175: 473-87